2012

DEVELOPMENT OF MOLECULAR DIAGNOSTIC ASSAYS FOR EQUINE RESPIRATORY VIRUSES AND ANALYSIS OF THE ROLE OF EQUINE ARTERITIS VIRUS ENVELOPE PROTEINS IN THE EARLY EVENTS OF VIRUS ENTRY

Zhengchun Lu
University of Kentucky, zlu2@uky.edu

STUDENT AGREEMENT:

I represent that my thesis or dissertation and abstract are my original work. Proper attribution has been given to all outside sources. I understand that I am solely responsible for obtaining any needed copyright permissions. I have obtained and attached hereto needed written permission statements(s) from the owner(s) of each third-party copyrighted matter to be included in my work, allowing electronic distribution (if such use is not permitted by the fair use doctrine).

I hereby grant to The University of Kentucky and its agents the non-exclusive license to archive and make accessible my work in whole or in part in all forms of media, now or hereafter known. I agree that the document mentioned above may be made available immediately for worldwide access unless a preapproved embargo applies.

I retain all other ownership rights to the copyright of my work. I also retain the right to use in future works (such as articles or books) all or part of my work. I understand that I am free to register the copyright to my work.

REVIEW, APPROVAL AND ACCEPTANCE

The document mentioned above has been reviewed and accepted by the student's advisor, on behalf of the advisory committee, and by the Director of Graduate Studies (DGS), on behalf of the program; we verify that this is the final, approved version of the student's dissertation including all changes required by the advisory committee. The undersigned agree to abide by the statements above.

Zhengchun Lu, Student

Dr. Udeni B. R. Balasuriya, Major Professor

Dr. Daniel Howe, Director of Graduate Studies

DEVELOPMENT OF MOLECULAR DIAGNOSTIC ASSAYS FOR EQUINE RESPIRATORY VIRUSES AND ANALYSIS OF THE ROLE OF EQUINE ARTERITIS VIRUS ENVELOPE PROTEINS IN THE EARLY EVENTS OF VIRUS ENTRY

DISSERTATION

A dissertation submitted in partial fulfillment of the
requirements for the degree of Doctor of Philosophy in the
College of Agriculture
at the University of Kentucky

By

Zhengchun Lu

Lexington, Kentucky

Director: Dr. Udeni B. R. Balasuriya, Professor of Virology

Lexington, Kentucky

2012

ABSTRACT OF DISSERTATION

DEVELOPMENT OF MOLECULAR DIAGNOSTIC ASSAYS FOR EQUINE RESPIRATORY VIRUSES AND ANALYSIS OF THE ROLE OF EQUINE ARTERITIS VIRUS ENVELOPE PROTEINS IN THE EARLY EVENTS OF VIRUS ENTRY

There is an urgent need for detection of viral respiratory pathogens to identify the causal agent(s) involved and to prevent the spread of related diseases. The first part of this dissertation focuses on development, optimization and validation of Real-time reverse transcription polymerase chain reaction (rRT-PCR) assays for the detection of several common equine viral pathogens: equine arteritis virus (EAV), equine influenza virus and equine rhinitis viruses A and B. Emphasis of the second part of this dissertation is on studying the role of EAV envelope proteins in virus attachment and entry. Using an infectious cDNA clone of EAV and reverse genetics, a panel of chimeric viruses was generated by swapping the N-terminal ectodomains and full-lengths of the two major envelope proteins (GP5 and M) from porcine reproductive and respiratory syndrome virus (PRRSV). The recombinant viruses expressing the N-terminal ectodomain of PRRSV GP5 or M or both (GP5ecto, Mecto, and GP5&Mecto, respectively) in an EAV backbone were viable and genetically stable. Compared to the parental virus, these three chimeric viruses produced lower titers and smaller plaque sizes indicating that they have a crippled phenotype. Interestingly, the three chimeric viruses could only infect EAV susceptible cell lines but not the PRRSV susceptible cell line. Therefore, the exchange of GP5 and/or M protein N-terminal ectodomains from PRRSV did not alter the cellular tropism of the chimeric viruses. We also investigated the role of one of the minor envelope proteins (E) of EAV in virus attachment and entry. The results showed that EAV infection of equine endothelial cells is heparin-dependent and the C-terminus of the E protein contains a putative heparin-binding domain. We generated a panel of arginine to glycine mutations in the conserved region of both the full-length EAV infectious cDNA clone and individual E protein expression vectors. The triple mutation R52,60,65G construct grew significantly slower and produced much smaller plaques. The double mutant R52,60G completely blocked the interaction between E protein and heparin. Taken together, these data indicated that E protein interacts with heparin to facilitate virus attachment and plays a major role in EAV infection.

KEYWORDS: Molecular Diagnostics, Real-time RT-PCR, Equine Viral Respiratory Disease, Equine Arteritis Virus, Viral Envelope Protein

Zhengchun Lu

June 22, 2012

DEVELOPMENT OF MOLECULAR DIAGNOSTIC ASSAYS FOR EQUINE RESPIRATORY VIRUSES AND ANALYSIS OF THE ROLE OF EQUINE ARTERITIS VIRUS ENVELOPE PROTEINS IN THE EARLY EVENTS OF VIRUS ENTRY

By

Zhengchun Lu

Udeni B.R. Balasuriya
Director of Dissertation

Daniel Howe
Director of Graduate Studies

June 22, 2012

This doctoral dissertation is dedicated to my beloved family members:

Father Zhikang Lu

Mother Guizhu Liu

Brother Zhengning Lu

Husband Bing Hu

Daughters Sophia Hu
&
Victoria Hu

Nephew Yunpeng Lu

ACKNOWLEDGMENTS

The completion of my doctorate would not have been possible without the support, patience and guidance of many people that I have met and worked with during my graduate studies. It is a pleasure to convey my gratitude to everyone in my humble acknowledgment.

I owe my deepest gratitude to Dr. Udeni B. R. Balasuriya for his advice, supervision, and generous support throughout my studies. He opened the doors for me to join the program and provided support and care for me the entire time. His encouragement inspired me and enriched my growth as a student, a researcher and a scientist. I am indebted for all his contributions of time and ideas which helped to make my graduate experience productive and stimulating. I sincerely appreciate his friendship and the years spent under his guidance.

I am most grateful to Dr. Peter J. Timoney for being so supportive throughout my studies. He brought me to the program and made sure I was taken care of in every aspect he could think of.

I would like to express my sincere gratitude to my other Ph.D dissertation committee members, Drs. Frank Cook, Thomas Chambers, Rebecca Dutch, and the outside examiner, Dr. Robert Coleman, for their time, insightful questions and valuable discussions during my exam as well as the committee meetings. Without the support of Dr. Chambers, the influenza real-time PCR projects would not have been completed.

Thank you to all my collaborators: Dr. Adam Branscum (University of Kentucky) for conducting the statistical analysis for the equine arteritis virus (EAV) real-time PCR paper; Drs. Stephen Sells and Mary Lynn Vickers (UKVDL) for providing samples for

the equine influenza virus (EIV) and canine influenza virus (CIV) real-time PCR projects; Dr. Edward Dubovi (Cornell University) for providing strains of EAV, EIV and CIV for the respective real-time PCR assays which we used in all four real-time PCR publications; Drs. Kay Faaberg (USDA, ARS) and Raymond Rowland (Kansas State University) for providing reagents for the EAV-PRRSV chimeric virus project; and Dr. Hans Heidner (University of Texas at San Antonio) for making plasmid constructs for the heparin project.

I also appreciate the support received from the all of the EAV and EHV lab members. Particularly, I am indebted to Dr. Jianqiang Zhang for his friendship and scientific contribution. Without his valuable EAV-PRRSV chimeric constructs, I could not have completed the project. I would like to thank Dr. Yun Young Go for always being a good friend and I'm sure this friendship will last forever. I thank Pam Henney for so many things. I especially enjoyed her company on the"road trips" to the UKVDL. I am grateful to Kathy Shuck for patiently correcting and proof-reading my manuscripts. It was an honor to work with Yanqiu Li, Bora Nam and Fabien Miszczak. Everyone was great!

I would especially like to thank Dr. Daniel Howe for his support as the Director of Graduate Studies. I extend my appreciation to the faculty and staff in the deparment; particularly to the members of Drs. Chambers, Cook, Horohov, Howe, MacLeod, and Lear's laboratories for allowing me use their equipment and instructing me on how to operate everything.

I would also like to thank all of the administrative staff in the Department of Veterinary Science, especially Diane Furry, Patsy Garrett, Roy Leach, Debbie Mollet,

and Gail Watkins who were always ready to help and made being a graduate student in the department pleasant.

I gratefully acknowledge the funding sources that made my Ph.D. work possible: American Quarter Horse Association, Fort Dodge Animal Health Laboratories, Fort Dodge, IA (now Pfizer Animal Health Inc, Kalamazoo, MI), gifts and contracts to Dr. Udeni B. R. Balasuriya and intramural funding from the College of Agriculture, University of Kentucky that made my Ph.D. work possible. The Geoffrey C. Hughes Foundation Fellowship program is greatly acknowledged for providing my personal financial stipend.

Last, but not the least, I would like to thank all of my family members for their unconditional love, trust, and encouragement. Thanks to my dad, Zhikang Lu; my mom, Guizhu Liu; and my brother Zhengning Lu, for all the support and love since I was little. I am sure you are all proud of me! Thanks to my dearest husband Bing and lovely daughters Sophia and Victoria. You are the driving force that makes me always want to move forward and reach higher.

TABLE OF CONTENTS

LIST OF TABLES

LIST OF FIGURES

CHAPTER ONE

Literature Review

1.1 Application of molecular diagnostic assays for the detection of equine respiratory viruses

Respiratory diseases can be costly for the horse owner and equine industry in many ways. Infectious diseases involving the respiratory tract of horses have been identified as one of the most common clinical conditions encountered by equine veterinarians in the USA and worldwide.[1] Clinical diagnosis of respiratory disease is difficult because most of the infectious agents and non-infectious disease conditions give rise to similar clinical presentations. Some of the viral respiratory pathogens also cause abortion and this can result in severe economic loss for the equine industry. Rapid detection and identification of viral pathogens causing respiratory tract infections are critical in selecting appropriate treatment strategies and very important to minimize days lost in training, racing, showing or poor performance, which is often the greatest cost to the owner.[2] The major challenge encountered by equine veterinarians when confronted with a case of respiratory tract infection is to determine the contagious nature of the disease in order to properly manage the affected animal and to reduce the risk of exposure of other horses. This requires the availability of fast and reliable diagnostic tests.

The invention of the polymerase chain reaction (PCR) by Kary Mullis and colleagues in 1983 set the stage for a scientific revolution.[3] The PCR assay established a base technology from which many specific and diverse applications have been developed; these have dramatically impacted the advancement of medicine and the basic science. After the invention of PCR, the detection of amplification products has undergone, and continues to undergo, pronounced changes that have taken the technology into new contexts and uses. The most dramatic innovation has been the invention of real-time

quantitative PCR, which has addressed many of the practical limitations associated with gel-based PCR.[4] This adaptation allows detection of the accumulation of amplified DNA in real time after each amplification cycle. There are several real-time PCR protocols available to investigate a respiratory tract infection. The short turnaround time and accuracy of real-time PCR make it an ideal method for the detection of infectious respiratory viruses.[5]

A good understanding of these diseases and diagnostic options will help us to choose the most appropriate diagnostic method and to facilitate disease prevention and control. In this section, a general introduction is provided to provide to the most common equine respiratory viruses; that is followed by a description of the diagnostic methods used to detect these pathogens.

1.1.1 Common equine viral respiratory pathogens

The most important viral respiratory diseases affecting horses are equine influenza virus (EIV), equine arteritis virus (EAV), equine herpesvirus type 1 and 4 (EHV-1,-4), equine rhinitis virus A and B (ERAV and ERBV), and equine adenovirus 1 (EAdV1). [6-7] A recent surveillance study investigated the prevalence and epidemiology of the presence of EIV, EHV-1, and EHV-4 in horses with upper respiratory tract signs and/or acute febrile infection with neurological signs.[8] In this study, a total of 761 horses, mules and donkeys were enrolled in the surveillance program over a 24-month study period in the USA. In total, 201 (26.4%) cases tested PCR-positive for one or more of the four viral pathogens. The highest detection rate was for EHV-4 (82 cases, 10.8%), followed by EIV (60 cases, 7.9%), and EHV-1 (23 cases, 3.0%). There were 15 horses with double infections (six EHV-4/EIV, five EHV-4/*Streptococcus equi* subspecies *equi*, two EHV-1/EHV-4, one EHV-1/ *Streptococcus equi* subspecies *equi*, one EIV/ *Streptococcus equi* subspecies *equi*), and one horse with a triple infection (EHV-1/EHV-4/*Streptococcus equi* subspecies *equi*). The detection rate for the different pathogens varied by season and with the age, breed, sex, and use of the animal.[8] A similar epidmiological study of equine respiratory disease was conducted in Ontario from October 2003 to October 2005.[9] Nasopharyngeal swabs and acute and convalescent

serum samples were collected from 115 client-owned horses in 23 outbreaks of respiratory disease in Ontario and sera were tested for EIV, EHV-1, EHV-4, ERAV, and ERBV. EIV H3N8 subtype was isolated from 15 horses in 5 outbreaks and contributed to 56.5% of the case-specific morbidity rate. A 4-fold increase in antibody levels or the presence of a high titer against ERAV or ERBV was observed in 10 out of 13 outbreaks.[9] These data indicate that EHV and EIV probably cause the majority of the viral respiratory disease, but other viruses may also be a problem for the equine industry.

RNA Viruses

Equine influenza virus

Equine influenza (EI; family *Orthomyxoviridae*, genus *Influenzavirus*) is an acute, highly contagious viral respiratory disease of equids (horses, donkeys, mules, and zebras) caused by infection with type A influenza virus.[10] Equine influenza virus (EIV) is highly pleomorphic, spherical, or filamentous with a diameter of 80-120 nm and a segmented (8 segments), single-stranded RNA genome of negative sense. The eight gene segments encode for eleven polypeptides: two envelope glycoproteins (hemagglutinin [HA] and neuraminidase [NA]), two matrix proteins (M1 and M2), two nonstructural proteins (NS1 and NS2/NEP), three proteins that make up the viral RNA polymerase (PB1, PB2 and PA), and the nucleocapsid protein (NP), as well as a recently discovered PB1-F2 mitochondrial protein [11-12] Equine influenza virus was first isolated in Hungary in 1956 following a widespread epidemic of respiratory disease in horses in Eastern Europe and the virus was subsequently isolated in the United States. The initial strain of EIV, was characterized as subtype H7N7 and designated influenza virus A/equine/Praque/56 [equine influenza subtype-1 or A/equine-1;[13-14]]. Minor antigenic drift was identified within the H7N7 subtype. The last confirmed outbreak caused by this virus was recorded in 1979. A second EIV subtype, H3N8 prototype (influenza A/equine/Miami/63 [equine influenza subtype-2 or A/equine-2]) was first isolated in Miami, Florida, USA in 1963[15-16] Subtype H3N8 viruses have been identified with all recorded outbreaks of equine influenza in the past 25-30 years. Extensive antigenic drift has been detected in this virus over the years.[17-20] Phylogenetic analysis based on the nucleotide sequencing of the hemagglutinin gene has led to categorization of EIV isolates from around the world into

two lineages: American and Eurasian lineages.[21] Currently, equine H3N8 influenza virus continues to be the single most important equine respiratory pathogen of the horse in many countries around the world. Equine influenza is considered endemic in the USA, UK, and many European countries. Australia, a country previously free of EI, suffered an outbreak in 2007. The virus was apparently brought into Australia with horses imported from Japan[22], despite the fact that Japan itself had not experienced an outbreak of EI for 35 years prior to 2007.[23] In 2005, inter-species transmission of EIV H3N8 subtype from horse to dog was reported for the first time.[24]

Cases of influenza occur most commonly in the spring and fall. EI has a short incubation period of only one to three days. Therefore, the disease can spread rapidly through a group of susceptible horses and cause very high morbidity by 24-48 hours after exposure to the virus. The virus attacks and damages the respiratory tract lining and normally, it takes three weeks for the lining to regenerate, which predisposes the respiratory tract to secondary bacterial infection or to recurrent airway obstructive disease.[25] The clinical signs of influenza usually include a high fever, depression, and anorexia. In uncomplicated influenza cases, most clinical signs last from 2 to 10 days, but affected horses often develop a dry, nonproductive cough that can last for weeks. Intermandibular lymph nodes may become enlarged and some horses may experience muscle soreness. Horses can develop a generalized vasculitis, which is manifested as dependent swelling of the limbs, inflammation of the heart resulting in a high heart rate, and inflammation of the eye resulting in tearing and squinting of the eye.[16]

Equine rhinitis virus

Equine rhinitis A virus (ERAV; family *Picornaviridae*, genus *Aphthovirus*) and equine rhinitis B viruses 1 and 2 (ERBV 1 and ERBV 2; family *Picornaviridae*, genus *Erbovius*) are recognized as the causes of an acute respiratory disease with systemic clinical signs in horses.[26-27] Seroprevalence data reported in different studies indicated that neutralizing antibodies to ERAV and ERBV can be found in from 50% to 80% of horses worldwide and the presence of antibodies seems to be correlated with the age of the animals.[28-31] Most of ERAV, ERBV1, and ERBV2 isolates have been recovered from horses with acute febrile respiratory disease with clinical signs of fever, nasal discharge,

anorexia, leg edema, and enlarged lymph nodes. However, horses may carry and shed virus in their urine for a long time. Subclinical infection and subsequent seroconversion were also reported.[32-33] Due to difficulty in isolation of these viruses in cell culture, ERAV is relatively infrequently isolated, and hence was rarely diagnosed prior to the validation of molecular diagnostic methods. Epidemiologic studies have shown that ERAV is a primary cause of respiratory disease in horses, although it might have been underestimated when evaluating equine respiratory outbreaks.[9,27]

Equine arteritis virus

Equine arteritis virus (EAV; family *Arteriviridae,* genus *Arterivirus*) is the causative agent of equine viral arteritis (EVA), which can cause respiratory disease and abortions.[34] Stallions infected with EAV may shed the virus in their semen for months to years and are capable of transmitting the infection to mares during artificial insemination or natual breeding. Equine arteritis virus is spread by respiratory and venereal routes, and the persistently infected carrier stallion is the essential natural reservoir of the virus.[34-35] The clinical signs associated with EAV infection are similar to other viral respiratory diseases and can vary from severe to subclinical infections. This disease should be suspected if the following clinical signs are present: 1) pronounced discharges from the eyes, 2) dependent limb edema, 3) edema of the periorbital or supraorbital areas, midventral regions, scrotum, prepucec and mammary gland, and 4) abortion in the later acute or early convalescent phase of the infection.[36] A detailed introduction to EAV and EVA will be provided in the second part of this chapter.

DNA viruses

Alphaherpesvirus

Equine herpesvirus-1 and equine herpesvirus-4 (family *Herpesviridae*, subfamily *Alphaherpesvirinae*, genus *Varicellovirus)* are the major viral causes of reproductive and respiratory disease in equine populations worldwide.[37] Both viruses cause upper respiratory tract infection in horses, and EHV-1 is also the single most significant cause of viral abortion in pregnant mares. Acute, naturally occurring respiratory disease due to

EHV-1 or EHV-4 is characterized by fever, anorexia, nasal discharge of varying severity, and sometimes as ocular discharge. Clinical signs of the respiratory form of EHV-1 and EHV-4 are typically seen in young horses and frequently weanlings less than two years of age. Certain neuropathogenic strains of EHV-1 can cause myeloencephalopathy in horses of any age.[38] EHV-1 and EHV-4 establish life-long latent infections in lymphoid as well as in neural tissues in a high percentage of infected animals. The $CD5^+/CD8^+$ T lymphocytes are believed to be a significant site of EHV-1 latency, which is independently and indirectly activated by both IL-2 and equine chorionic gonadotrophin.[39] Reactivated EHV-4 is predominantly shed in nasal secretions from natually-infected horses following corticosteroid treatment.[40] The reactivation of latent virus results in virus shedding and the risk of transmission to susceptible horses.[37,41]

Gammaherpesvirus

Gammaherpesvirus includes EHV-2 and EHV-5.[42] Equine herpesvirus-2 (family *Herpesviridae*, subfamily *Gammaherpesvirinae*, genus *Rhadinovirus)* is ubiquitous in equine populations worldwide and has been associated with a variety of clinical disorders including respiratory tract disease, generalized malaise, fever, pharyngeal lymphoid hyperplasia, enlarged lymph nodes, keratoconjunctivitis, granulomatous dermatitis, and abortion.[43-50] EHV-2 shares many similarities with Epstein-Barr virus, the causative agent of human infectious mononucleosis, which is characterized by fever, persistant sore throat, and generalized lymphadenopathy.[51]

Equine herpesvirus-5 (family *Herpesviridae*, subfamily *Gammaherpesvirinae*, genus *Percavirus*) has been linked to multinodular pulmonary fibrosis (EMPF), a fibrotic interstitial lung disease of horses older than four years.[52-53] The virus has been detected in nasal swabs and peripheral blood leukocytes in young and adult horses with or without clinical signs of respiratory disease.[53-55]

Equine adenovirus

The earliest reports of equine adenovirus (EAdV; family *Adenoviridae,* Genus *Mastadenovirus*) isolation were obtained from pneumonic lungs of Arab foals in the United States in 1969 and in Germany in 1971. [56-58] Two serotypes of EAdV designated

EAdV-1 and EAdV-2 have been isolated to date. Studies have shown that EAdV-1 is predominantly associated with upper respiratory tract infections, conjunctivitis, and bronchopneumonia, while EAdV-2 has mainly been isolated from horses with gastrointestinal tract infections.[59] Clinical signs exhibited by adult horses with serological evidence of infection included mild respiratory signs and soft feces. Signs persisted in individual horses for four to eight weeks over a period of three to four months, although not all infections were associated with clinical disease. The possible association of soft feces with adenovirus infection may be important in the differential diagnosis of infectious respiratory disease.[6] Equine adenovirus-1 is primarily associated with the uniformly fatal, inherited disease syndrome, primary severe combined immunodeficiency disease (PSCID). When PSCID was first recognized in the early 1970s, it was estimated that it caused the death of about 3% of all purebred Arabian foals. Foals are born with a total absence of T and B lymphocytes. The disease is inherited as an autosomal recessive gene.[60-61]

1.1.2 Diagnosis of equine respiratory viruses

1.1.2.1 Conventional diagnostic methods for equine respiratory viruses

There are essentially four approaches which can be utilized in attempting a diagnosis by conventional laboratory methods:

1. Isolation and identification of the infectious agent.
2. Demonstration of the presence of or a significant rise in specific antibodies during the course of disease (serologic diagnosis).
3. Histopathological examination of infected tissues for characterization and determination of specific viral pathogens.
4. Electron microscopy to visualize and characterize a viral pathogen.

It is not always possible or necessary to follow all these suggested diagnostic approaches in each case. The decision on which approach to follow is largely determined by the nature of the infection encountered, the stage of the illness in which the horse is first seen, and the amount of information the method will yield in relation to the time and effort involved.

Virus isolation

It was the discovery that poliovirus could replicate in nonneural tissue culture that revolutionized diagnostic virology.[62] Generally, three main types of cell cultures are used: primary cell cultures, diploid cell lines, and continuous cell lines. Primary cell cultures are made directly from animal or human tissues and can be passaged for only a few times. Diploid cell strains are generally derived from embryonic tissues, particularly embryonic lung, and in some cases can be passaged up to 50 times. Continuous cell lines are usually derived from human or animal tumors and can divide indefinitely.[63] After inoculation into cell culture, viruses can induce changes, such as rounded refractile cells or grape-like clusters called cytopathic effect (CPE). Some viruses such as respiratory syncytial virus and parainfluenza virus, can induce characteristic syncytial formation while others, such as some strains of ERAV or ERBV and bovine viral diarrhea virus (BVDV), may produce no visible changes. These require other tests to identify their presence.[27,64] Preliminary identification of a virus isolate can be made based on the type of cell culture where the virus growing and the characteristic of CPE. For instance, cytomegalovirus induces CPE only in human fibroblast cells, while herpes simplex virus induces CPE in both human fibroblast and rabbit kidney cells.[63] However, the final confirmation usually requires a neutralization test using virus-specific antiserum. Ability to isolate virus in cell culture greatly facilitates the study and characterization of viruses, allows antigen production, and development of vaccines.

The three primary benefits of virus isolation in tissue culture include:

(1). It has the ability to propagate a number of animal and human viruses, the generation of infectious virus particles for biological characterization, and potential production of killed and modified live vaccine.[65] By inoculating several cell lines, it is possible to isolate known and unknown viruses. Because there are no virus-specific reagents required, cell culture allows clinicians to amplify any virus that has the ability to replicate in a particular cell line. This is a big difference compared to molecular diagnostic methods which requires the pathogen's genome sequence be known prior to diagnosis.

(2). Live virus particles can be used to characterize certain viral biological features such as cytopathic effect and size of the viral particles which cannot be obtained

through use of a nucleic acid assay. Oseltamivir (Tamiflu), an influenza virus neuraminidase (NA) inhibitor, is characterized by a NA enzyme inhibition assay.[66-67] Recently, some genetic markers indicative of antiviral resistance to this drug have been identified.[68] Without actually testing the biological response of each virus to each antiviral drug/gene, the resistance pattern is only a deduction.

(3). The cost of cell culture is relatively inexpensive because it does not require expensive modern diagnostic equipment.

While the advantages are beneficial, these are often outweighed by distinct disadvantages. It can take 5-14 days to get results from virus isolation. Often, the sick horse has already recovered by that time, rendering the diagnosis of little value in guiding treatment. Virus isolation also requires expertise to interpret results, particularly the capability of differentiating CPE caused by one virus from that of another. Finally, because tissue culture relies on inoculation of a virus from a specimen, sample selection, collection, handling, and storage are critical to insure that infectious virus is not inactivated before the specimen can be inoculated into cell culture.

Immunologic diagnostic methods

Immunologic diagnostic methods are a group of rapid techniques based on a specific reaction between antigen and antibody. The reaction must be labeled with a marker which can be a fluorescent dye, a radioisotype, or an enzyme such as peroxidase. Immunofluorescence (IF) techniques have long been used for the diagnosis of viral infections. The method was introduced by Albert Coons and colleagues in 1941,[69] and was first applied to the direct detection of influenza A virus in nasal smears in 1956.[70] In the 1980s, IF was applied to the diagnosis of RSV,[71] parainfluenza,[72-73] and adenovirus,[74] and recently to human metapneumovirus (HMPV).[75] Immunofluorescence is labor intensive; yet when done well, it is the most sensitive and specific immunoassay and able to detect just one infected cell. Immunofluorescence is also the only current immunologic method that can screen for 7 to 8 viruses in a single assay.[76]

The enzyme-linked immunosorbent assay (ELISA) is another commonly used immunologic method for viral diagnosis. Whereas IF detects only viral proteins in infected cells, ELISA can also detect cell-free viral proteins. In the 1980s, a microwell

ELISA was first applied to the detection of respiratory viruses, RSV[77-78] and influenza A virus.[79] In veterinary diagnostic laboratories, ELISA has been developed for the detection of EHV-1, EHV-4[80], ERAV,[81] and ERBV.[82] Membrane ELISA is a type of ELISA using individual cassettes and requiring no equipment. It only takes 20-30 minutes to complete and is considered a first generation rapid test for RSV and influenza. Current examples include Directigen RSV and Directigen Flu A+B kits. The latter can also be used in detection of equine influenza viruses. A successful ELISA test requires high titers of virus shed because no amplification step is involved in the process. Therefore, in clinical practice, it may not be sensitive. Careful and thorough washing is critical to avoid false positive results. For membrane assays, viscous samples such as nasopharyngeal aspirates can trap reagents and give rise to false positive results.

The virus neutralization (VN) assay is one of the most trusted and widely used methods employed for the detection of virus-specific neutralizing antibodies.[83] The power of the neutralization assay lies in its ability to detect biologically active antibodies. It is the most sensitive and accurate method for identifying a virus isolate. VN is considered the "gold standard" for detection and determination of antibodies to EAV.[84] Currently, the VN is the only validated test accepted for international trade. Although the VN is highly sensitive and accurate, it has several disadvantages: it is expensive, labor-intensive, and time-consuming to perform. In addition, results can vary among laboratories when adequate attention is not paid to standardization of both test reagents and procedure. Moreover, serum cytotoxicity caused by anti-cellular antibodies directed against cells can be mistaken for viral CPE and give rise to difficulties in test interpretation at lower serum dilutions. Also, the VN cannot differentiate an antibody response of vaccinated from naturally infected horses.

Electron microscope

The electron microscope (EM) has been used in the diagnosis of viral diseases for decades. This is the only method that allows a virus to be directly visualized. Virus size and shape can be easily identified. Although it may take there or more days to prepare a specimen, it is still a reliable diagnostic method since the fine structure of the virus particles and cells are very likely to be preserved. The recognition of a human

papovavirus in the brain cells of a patient with progressive multifocal leukoencephalopathy and the identification of Epstein-Barr virus in cultured lymphoblastic cells derived from a Burkitt's lymphoma patient would have been missed had not EM been used.[85-86] In the 1970s, the application of EM and immune EM (IEM) contributed to the identification of a number of new viruses which could not be isolated in cultures, e.g.hepatitis A and B viruses, enteric adenoviruses, rotavirus, and the Norwalk agent.[87-91] However, despite the many contributions of EM and IEM to virus diagnosis, it is still too expensive and cumbersome for routine viral diagnosis.

Currently there is tremendous interest in the development of rapid diagnostic techniques. However, conventional diagnostic methods remain the most widely used and are critical in confirming the usefulness of newer techniques.[63]

1.1.2.2 Molecular diagnostic methods

Nucleic acid amplification technology has opened new avenues of microbial detection and characterization, such that growth in cell culture is no longer required for microbial identification. Over the past decades, the focus of rapid diagnosis of infectious disease has shifted towards the nucleic acid amplification-based techniques, primarily PCR at the expense of traditional methods of clinical microbiology.[92]

1.1.2.2.1 Standard PCR technology

The application of PCR as a diagnosic method was first developed in 1985 for the prenatal diagnosis of sickle cell anemia.[93] It was based on the remarkable insight of Kary Mullis, who realized that repetition of a DNA extension reaction bounded by two synthetic oligonucleotide primers would generate a large quantity of any specified DNA sequence.[94] The basic technique of PCR includes repeated cycles of amplifying selected nucleic acid sequences. Each cycle consists of three steps: 1) a DNA denaturation step, in which the double strands of the target DNA are separated; 2) a primer annealing step, performed at a lower temperature, in which primers anneal to their complementary target sequences; and 3) an extension step, in which DNA polymerase extends the sequence between the primers. At the end of each cycle, the amount of PCR product is doubled.

Therefore, performance of 30 to 50 thermal cycles results in an exponetial increase in the total number of DNA copies amplified.[95-96]

Initially, PCR required the addition of thermolabile *Escherchia coli* DNA polymerase at each cycle, limiting its applications, although one of the earliest papers describing the detection of human papilloma virus (HPV) DNA by PCR used an automated pipetting device for the addition of the polymerase.[97] Two unique innovation that made PCR available to scientists were the purification of a thermostable polymerase from *Thermus aquaticus (Taq)* which is heat stable and the invention of thermal cycling heating blocks, both of which came from Mullis and other scientists at the Cetus and PerkinElmer corporations. Although *Taq* polymerase is the most widely used polymerase; it lacks a 3'-5' exonuclease activity. There are other enzymes available, some of which have properties that make them better suited than *Taq* for certain purposes. For example, *Pfu* from *Pyrococcus furiosus* has a higher copying fidelity than *Taq* and is a better choice for sequencing or protein expression studies where nucleotide misincorporation is not acceptable.[98]

Reverse transcriptase -PCR

Numerous modifications of the standard PCR procedure have been developed.[99-101] Some of these modifications greatly expand the diagnostic capabilities of PCR. Reverse transcriptase-PCR (RT-PCR) was developed to target RNA molecules. The RNA is first reverse transcribed into complementary DNA (cDNA) using the reverse transcriptase (RTase). The cDNA is further amplified using DNA polymerase. MMLV reverse transcriptase from the Moloney murine leukemia virus and AMV reverse transcriptase from the avian myeloblastosis virus are the commonly used reverse transcriptases. However, with the technolgy development, more RTases were generated using recombinant technology. For instance, the SuperScript II and SuperScript III RTases are engineered version of MMLV RTase with reduced RNase H activity and increased thermal stability. The PowerScript RTase is a point mutant of MMLV RTase which lacks the RNase H enzyme and retains wild-type polymerase activity, thus being able to synthesize longer cDNA fragments.[102] The conventional RT reactions are fastidious because the enzyme can not tolerate higher temperatures. Accordingly, the RT

and PCR steps are normally separate which limits wide application of this method in clinical diagnosis. Nowadays, many companies provide commercial RTase and DNA polymerase mixtures which make the single-tube one-step RT-PCR possible. After the reverse transcription step, reactions are heated to a high temperature (normally 95 ºC) to activate heat-stable DNA polymerase and to simultaneously inactivate the reverse transcriptase. The single-step RT-PCR dramatically enhances the diagnostic capability of detect RNA viral pathogens. [103-104]

Nested PCR

Nested PCR was developed mainly to increase the sensitivity of the assay using two sets of primers.[105-106] One set of primers is used for first round of amplification and the amplification product of the first reaction is then subjected to a second round of amplification with another set of primers that are specific for an internal sequence that was amplified by the first primer pair. The sensitivity of the nested PCR is extremely high due to the dual amplification process. The DNA product from the first round contains the hybridization sites for the second primer pair. Therefore, the second primer set further verifies the specificity of the first-round product. However, the major disadvantage of the nested PCR is the high risk of cross-contamination during transfer of the first-round amplification products to a second reaction tube. This can be overcome if the inner and outer primers are all present in the initial reaction mix and the primer sets use substantially different annealing temperatures.[99]

Semi-nested PCR is a modification of nested PCR. Instead of using two primer pairs (a total of four primers) in nested PCR, semi-nested PCR uses the same one primer for both rounds (a total of three primers).[107-110] Semi-nested PCR is also highly sensitive as compared to nested PCR, but the potential chance of cross-contamination is still a big disadvantage.

Multiplex PCR

Multiplex PCR is an amplification process in which two or more sets of primer pairs specific for different targets are introduced into the same tube.[111] Therefore, more than one DNA target in a specimen can be detected simultaneously.[112] It is critical to

design primers that have similar annealing temperatures, which often requires extensive optimization. Multiplex PCR can be used to detect multiple pathogens in a single specimen for diagnostic purposes.[113-116] The amount of target DNA or RNA in a specimen can also be quantified using a quantitative competitive PCR, which is a variation of the multiplex PCR.[117-118]

Broad-range PCR

Another important technical modification is the development of the broad-range PCR, in which a conserved sequence within phylogenetically informative genetic targets is used to diagnosis microbial infection. A universal primer set designed to target herpesvirus DNA polymerase might be useful to detect different types of herpesvirus infection in one reaction.[119] Broad-range ribosomal RNA (rRNA) PCR techniques offer the possibility of rapid bacterial identification through use of a single pair of primers targeting bacterial small-subunit 16S rRNA or DNA.[120-122]

Overall PCR technology has distinct advantages as a diagnostic tool over conventional microbology, especially in the detection of slow-growing, difficult-to-cultivate, or noncultivatable microorganisms. It can be used successfully in situations where inhibitory substances, such as antimicrobials, are present. Due to the stability of DNA, pathogens can be detected in a variety of specimen types, even in formalin-fixed tissue. The PCR also has inherent disadvantages. The risk of amplicon contamination is very high. Specifically, as the PCR amplifies the target, any contamination will also be amplified. Plus it is difficult to set up a quantitative assay. In addition, PCR requires laborious post-PCR handling steps to visualize the amplified end products. These problems are being addressed by the development of commercial automated systems such as the Roch Cobas Amplicor which requires minimum handling. The use of synthetic internal competitive targets in these commercial assays has facilitated the accurate quantification of the results. However, these assays are very expensive which is a hurdle to their application for routine diagnostic purposes.

1.1.2.2.2 Real-time PCR technology

Technological advances in PCR thermocycler performance and fluorescent signal detection in the early 1990s allowed introduction of a second-generation real-time PCR method in 1996 employing TaqMan® chemistry.[123] This method uses a fluorescent dual-labeled probe added to the PCR reaction mix. The 5 prime exonuclease activity of the DNA polymerase displaces and digests the probe upon primer extension. This causes the release of the quenched fluorescent signal, which is measured during each PCR cycle in a closed-tube detection system, hence the term real-time. A digital camera collects fluorescence signal in real-time and the data are stored on a computer. All post-PCR analysis is computer-based and does not require any agarose-gel analysis. The development of rPCR has revolutionized the way clinical microbiology laboratories diagnose human and animal pathogens.[124-127] This approach is a highly sensitive technique enabling simultaneous amplification and quantification of specific nucleic acid sequences. In addition to enhanced sensitivity, the benefits of real-time PCR assays over conventional detection methods include their large dynamic range, a low risk of cross-contamination due to its close-tube format, high-throughput applications, and the potential for accurate target quantifications.[128-130] Real-time PCR is suitable for a wide range of applications such as gene expression analysis, determination of viral load, detection of genetically modified organisms, single nucleotide polymorphism genotyping, and allelic discrimination. Detection of target sequences occurs by monitoring the fluorescence generated by intercalating dyes, fluorophore-labelled primers, or sequence-specific probes. There are many probe chemistries other than TaqMan® and those will be dicussed in detail in the following section.

1.1.2.2.2.1 Detection formats

1.1.2.2.2.1.1 Detection formats without sequence confirmation of the PCR product

Fluorescent dyes such as ethidium bromide (EtBr) that are specific for double-stranded DNA (dsDNA) were the first systems applied in real-time PCR assays in the early 1990s.[131] They used a video camera to detect the accumulation of dsDNA in each

PCR using the increase in fluorescence of EtBr that results from its binding to duplex DNA. Other intercalating dyes such as YO-PRO-1 have also been used.[132-133] Nowadays, SYBR Green I is the most commonly used intercalating dye in real-time PCR (Fig 1.1).

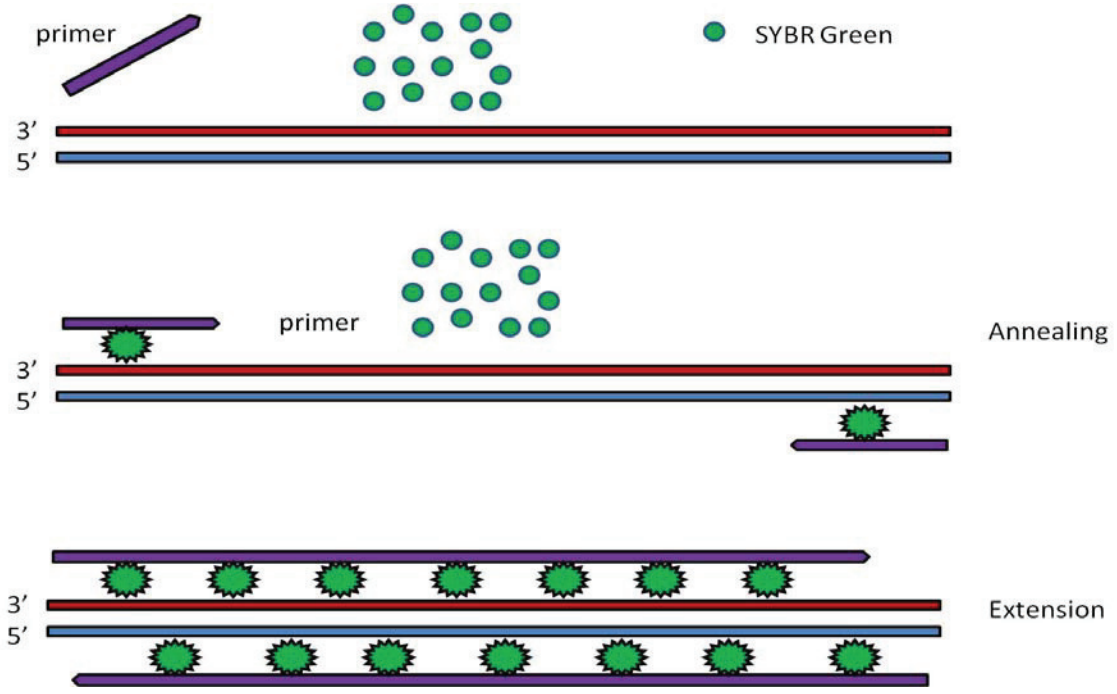

Fig 1.1. Principle of SYBR Green I technique. SYBR Green I fluorescence increases enormously upon binding to double-stranded DNA. During the extension phase, more and more SYBR Green I will bind to the PCR product, resulting in increased fluorescence. Consequently, during each subsequent PCR cycle more fluorescent signal will be detected. Modified from Van der Velden *et al* (2003)[134] with permission.

It has a 100 times higher binding affinity than ethidium bromide, and the fluorescence of bound dye is more than 1000-fold higher than that of free dye. These features make SYBR Green I highly suitable for monitoring product accumulation during PCR.[135-136] The biggest disadvantage using intercalating dyes is that non-specific dsDNA products, such as primer dimers can interfere with the assay signal and yield false positive results. Therefore, it is important to optimize the assay prior to use in clinical diagnosis to avoid non-specific amplification products. To solve this problem, specific PCR products can be discriminated from these potential artifacts by using melting curve

analysis, in which the melting temperature (*Tm*) of the product is determined.[137] Different melting curves can be easily distinguished from each other, indicating that the PCR products were not all identical in sequence. Another detection technology known as "LUX (Light Upon eXtention)" utilizes self-quenched fluorogenic primers which are labeled with a single fluorophore on a base close to the 3′-end with no quencher required. A tail of 5-7 nucleotides is added to the 5'-end of the primer to form a blunt-end hairpin when the primer is not incorporated into a PCR product. This design provides a low initial fluorescence of the primers that increases upon formation of the PCR product.[138-139] A similar approach called Amplifluor Quantitative PCR detection system uses both labeled and unlabeled primers. The PCR primers contain hairpin structures on their 5′-ends with donor and acceptor moieties located in close proximity on the hairpin stem. The primers are designed in such a way that a fluorescent signal is generated only when the primers are incorporated into an amplification product.[128,140-141] Both of these systems are highly flexible but have not been used frequently for diagnostic tests.

1.1.2.2.2.1.2 Detection formats with increased target specificity

Sensitive and specific detection is possible with real-time PCR by using novel fluorescent probe technology. The incorporation of a probe confirms the specificity of the amplicon. Fluorophore-labelled oligonucleotide probes are most commonly used for the specific detection of target sequences.[142-144] Three types of nucleic acid detection chemistries have been used most frequently with real-time PCR formats in clinical microbiology: 5' nuclease (TaqMan® probes), molecular beacons, and fluorescence resonance energy transfer (FRET) hybridization probes.[125] Collectively, these 3 types of probes are frequently referred to as FRET probes. However, when specifically referring to each of these three probes in the following section, only FRET appears in the name of FRET hybridization probes. In these assays, an increase in fluorescent signal proportional to the accumulation of PCR product arises as a consequence of FRET between two separate fluorogenic labels (reporter and quencher) conjugated to the probe. FRET is a spectroscopic process by which energy is passed over a maximum distance of 70Å

between reporter and acceptor molecules possessing overlapping emission and absorption spectra.[145]

For all types of FRET probes, FRET decreases as the distance between adjacent dye molecules increases. For TaqMan® probes or molecular beacons, the reporter and quencher dyes are attached to a single probe. In contrast, for FRET hybridization probes, dyes are attached separately to two probes that align in a head-to-tail configuration on target nucleic acids. The first dye is a fluorescent dye and the second is either a quencher dye or another fluorescent dye which can absorb fluorescent light transferred from the first dye and reemit light at a different wavelength. The most widely used detection chemistries are briefly reviewed below.

FRET hybridization probes

Hybridization probes use a pair of adjacent, fluorogenic hybridization oligos and are the only detection format that directly measures FRET.[142] FRET probes are labeled with different fluorescent dyes and are designed to anneal in a head-to-tail orientation to the target DNA between the PCR primers (Fig 1.2).

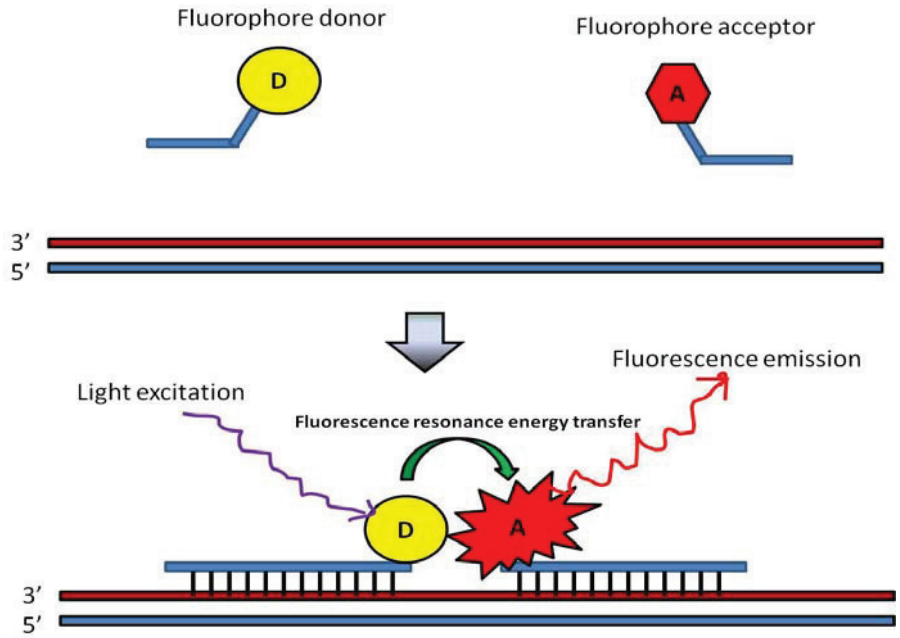

Fig 1.2. Principle of hybridization probes technique. In this technique one probe is labeled with a donor fluorochrome at the 3' end and a second probe is labeled with an

acceptor fluorochrome. When the two fluorochromes are in close vicinity (i.e. within 1–5 nucleotides), the emitted light of the donor fluorochrome will excite the acceptor fluorochrome. This results in the emission of fluorescence, which subsequently can be detected during the annealing phase and first part of the extension phase of the PCR reaction. After each subsequent PCR cycle more hybridization probes can anneal, resulting in higher fluorescence signals. Modified from Cardullo *et al* (1988)[142] with permission.

The upstream probe contains a donor fluorophore at the 3′-end; the downstream probe contains an acceptor fluorophore at the 5′-end. When the probes hybridize next to each other, fluorescence energy is transferred from the donor to the acceptor fluorophor, causing it to emit a unique fluorescent signal that can then be measured. If the two probes do not anneal adjacent to each other, a signal is not generated; therefore, nonspecific events do not contribute to the fluorescent signal. The requirement that a second probe bind before a signal is generated increases the number of specific events required for signal generation. Theoretically, this additional requirement enhances specificity beyond single fluorescent probe formats, like those that use TaqMan® probes.

TaqMan® probes

The first real-time fluorescent probes developed were 5' nuclease probes, which are commonly referred to by their proprietary name, TaqMan® probes (Fig 1.3).

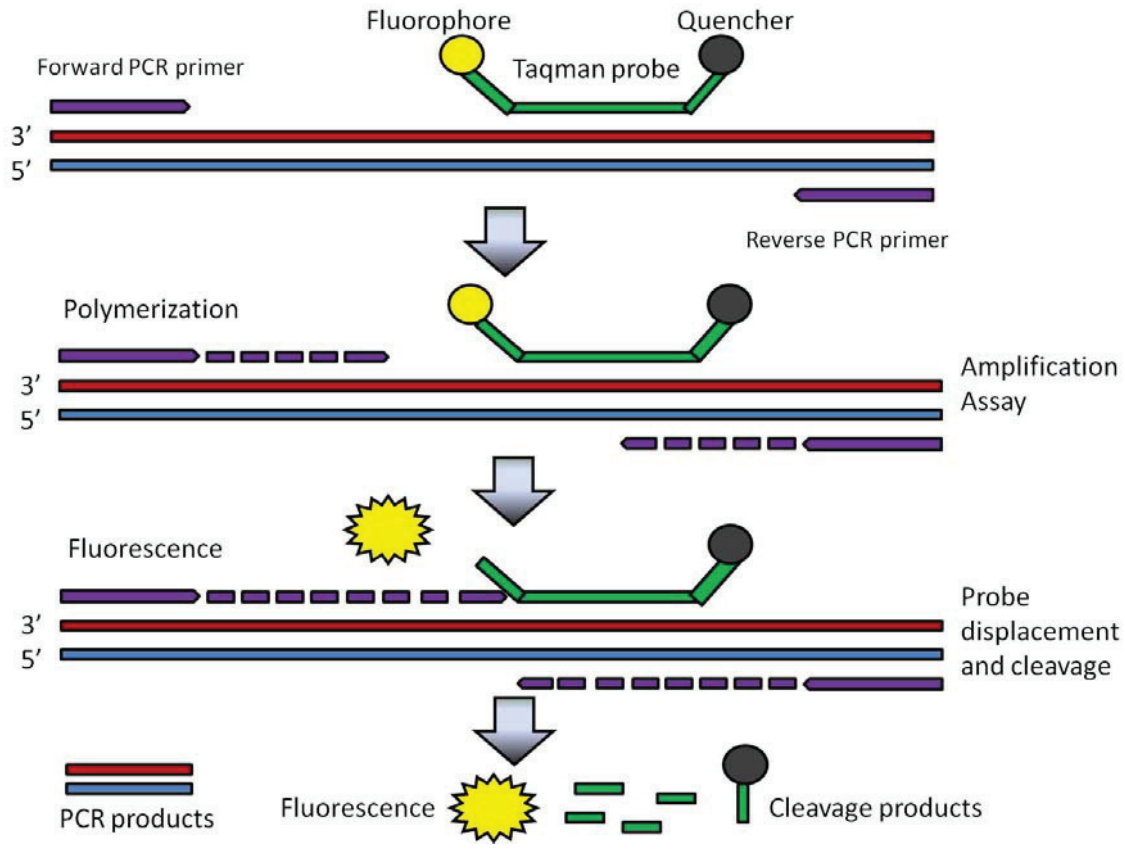

Fig 1.3. Principle of TaqMan® hydrolysis probe technique. The hydrolysis probe is conjugated with a quencher fluorochrome, which absorbs the fluorescence of the reporter fluorochrome as long as the probe is intact. However, upon amplification of the target sequence, the hydrolysis probe is displaced and subsequently hydrolyzed by the *Taq* polymerase. This results in the separation of the reporter and quencher fluorochrome and consequently the fluorescence of the reporter fluorochrome becomes detectable. During each consecutive PCR cycle this fluorescence will further increase because of the progressive and exponential accumulation of free reporter fluorochromes. Modified from Livak *et al* (1995)[146] with permission.

A TaqMan® probe is a short dual-fluorophore-labelled oligonucleotide (DNA) that contains a 5'-terminal reporter dye (e.g. FAM) and a 3'-terminal quencher dye (e.g. TAMRA). To generate a light signal, two events must occur. First, the probe must bind to a complementary strand of DNA at 60 ºC. Second, at this temperature, *Taq* polymerase,

the same enzyme used for the PCR, must cleave the 5' end of the TaqMan probe, separating the fluorescent dye from the quenching dye. Once the dyes are separated by destroying the TaqMan probe based on the 5' exonuclease activity of the DNA polymerase, the increase in reporter fluorescence caused by the removal of the adjacent quencher dye is monitored by a real-time PCR instrument.[146-148]

One important point is that the *Tm* of the probes should be higher (usually 5-10 ºC) than that of the primers to ensure strong binding of the probes during annealing. Therefore, the probes are normally between 20 and 30 nucleotides long. The design of this relatively long nucleotide may sometimes be difficult to optimize because of a particular AT-rich region in the sequence or becaue of sequence variability.[149]

A modification of this strategy exploits the so-called minor groove binding (MGB) probes. MGB probes form extremely stable duplexes with single-stranded DNA targets mediated mainly by van der Waals forces, and as a result, shorter-length probes are required for hybridization. A/T rich duplexes are stabilized more than G/C rich duplexes, therefore increasing *Tm* and simplifying design.[150] The shorter MGB probes are ideal for allele discrimination studies or for detection of single-nucleotide polymorphisms (SNPs) because they are more significantly destabilized by nucleotide changes within the hybridization site compared with probes of long of length.[151-153]

In the TaqMan® assay, the requirement that 5'-3' hydrolysis be performed between the fluorophore and quencher dye can be met only when these two moieties are not too close to each other.[154] This is a serious drawback of the assay since the efficiency of the energy transfer decreases with the inverse sixth power of the distance between the reporter and quencher dye.[155]

Molecular beacons

Molecular beacons are similar to Taqman probes but are not designed to be cleaved by the 5' nuclease activity of *Taq* polymerase. These beacons are hairpin-shaped oligonucleotides with a fluorescent dye on the 5'-end and a quencher dye on the 3'-end (Fig 1.4).[156-158]

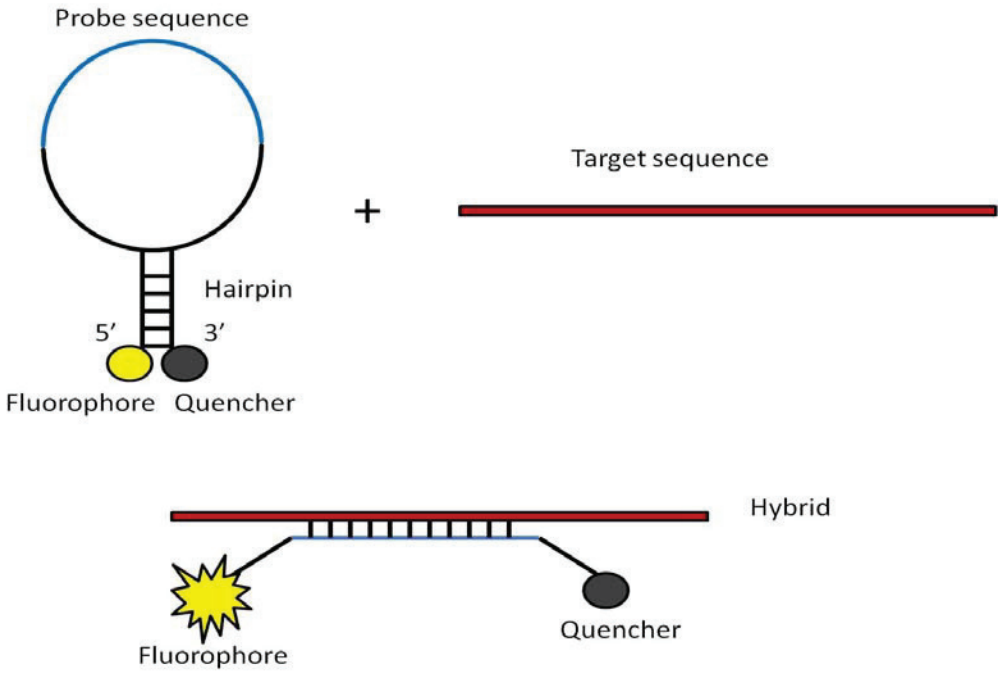

Fig 1.4. Principle of molecular beacons. The beacons are hairpin-shaped oligonucleotides with a fluorescent dye on the 5' end and a quencher dye on the 3' end. The central part of the probe is designed to be complementary to the PCR amplification target sequence. At high temperatures, both the PCR amplification product and probe are single stranded. When the temperature decreases, the central part of the molecular beacon probe binds to the target sequence and forces the separation of the fluorescent reporter dye from the quenching dye. Therefore the effects of the quencher dye are obviated and the light signal from the reporter dye can be detected. Modified from Tyagi *et al* (1998)[157] with permission.

A region at each end of the molecular beacon probe is designed to be complementary to itself, so at low temperature, the ends anneal forming the hairpin structure. This integral annealing property puts the two dyes in close proximity, quenching the fluorescence from the reporter dye. The central part of the probe is designed to be complementary to the PCR amplification target sequence. At high temperatures, both the PCR amplification product and probe are single stranded. When the temperature decreases, the central part of the molecular beacon probe binds to the

target sequence and forces the separation of the fluorescent reporter dye from the quenching dye. Therefore the effects of the quencher dye are obviated and the light signal from the reporter dye can be detected. If no PCR amplification product is available for binding, the probe reanneals to itself, forcing the reporter dye and quencher dye to move together, preventing a fluorescent signal.[125]

Typically, a single molecular beacon is used for detection of a PCR amplification product and multiple beacon probes with different reporter dyes are used for single nucleotide polymorphism detection. By choosing appropriate PCR temperatures and/or extension of the probe length, molecular beacons will bind to the target product when an unknown nucleotide polymorphism is present but at a slight cost of reduced specificity.

The advantage of molecular beacons is that no specific temperature thermocycling machine is required so that the temperature optimization of the PCR is simplified. Molecular beacons have been used to detect viral pathogens such as SARS virus and hepatitis B virus.[159-160]

Scorpion primer

Scorpions are bi-functional molecules that carry both primer and probes together on the same oligonucleotide construct (Fig 1.5).[161]

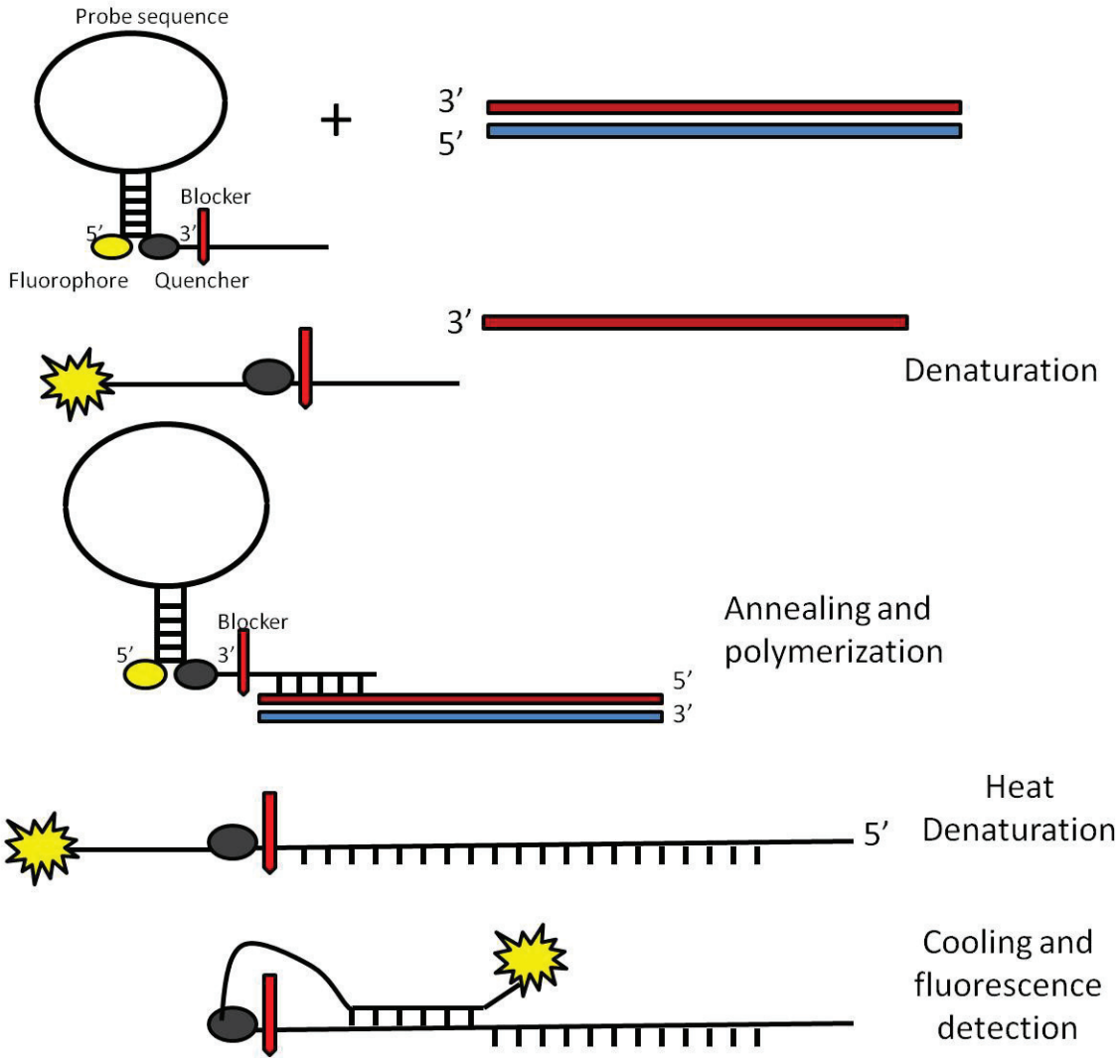

Fig 1.5. Principle of scorpion primers. Scorpion contains primer, probe sections, and a blocker. After annealing, the primer section is extended by the DNA polymerase. After strand separation, the probe section of the Scorpion oligodeoxynucleotide hybridizes to a region downstream from the primer sequence during the annealing step of the PCR reaction. The hairpin structure of the Scorpion primer is blocked from extension to ensure that the reporter dye and quencher are only separated by specific hybridization of the probe section to the target sequence. Modified from Whitcombe *et al* (1999)[161] with permission.

The probe is attached as a tail to the primer element through a PCR blocker that ensures the probe element does not get incorporated into the double-stranded product.[162] The Scorpion construct is arranged such that the probe element is complementary to the anticipated extension product of the primer element. The probe carries a reporter fluorphore that is quenched with a non-fluorescent quencher through a collisional mechanism. The quencher is held in close proximity to the fluorophore by base pairing which can be achieved by introduction of a stem-loop in the probe or through a second molecule, substantially complementary to the probe element.[161]

There are several advantages of a Scorpion probe. The appearance of signal is rapid and reliable, because probe-target binding is kinetically favored over duplex reannealing and thermodynamically favored over intrastrand secondary structures.[161] Scorpion probe's unimolecular binding events makes this technology faster and more efficient than the bimolecular mechanism because it does not depend on enzymatic cleavage of the probe.[163] This method works very well for the detection of amplicon and the detection is highly specific, down to the level of single base changes. The use of stems in the probe element offers two advantages: first, background signals are minimal because signals from unincorporated Scorpion primers are switched off; second, the stem can be designed to be thermodynamically favored over the binding of probe to mismatch target.[161] Therefore, a Scorpion probe is commonly used in allelic discrimination.[161,163] Development of a cystic fibrosis mutation detection assay shows that Scorpion primers are selective enough to detect single base mutations and give good sensitivity in all cases. Simultaneous detection of both normal and mutant alleles in a single reaction is possible by combining two Scorpions in a multiplex reaction.[163] Single nucleotide polymorphism (SNP) genotyping is another important application for Scorpion primers.[164]

Locked nucleic acid (LNA) probes

Locked nucleic acids (LNA) are a novel class of bicyclic DNA analogs in which the 2′ and 4′ positions in the furanose ring are joined via an O-methylene (oxy-LNA), S-methylene (thio-LNA), or amino-methylene (amino-LNA) moiety (Fig 1.6).[165-166]

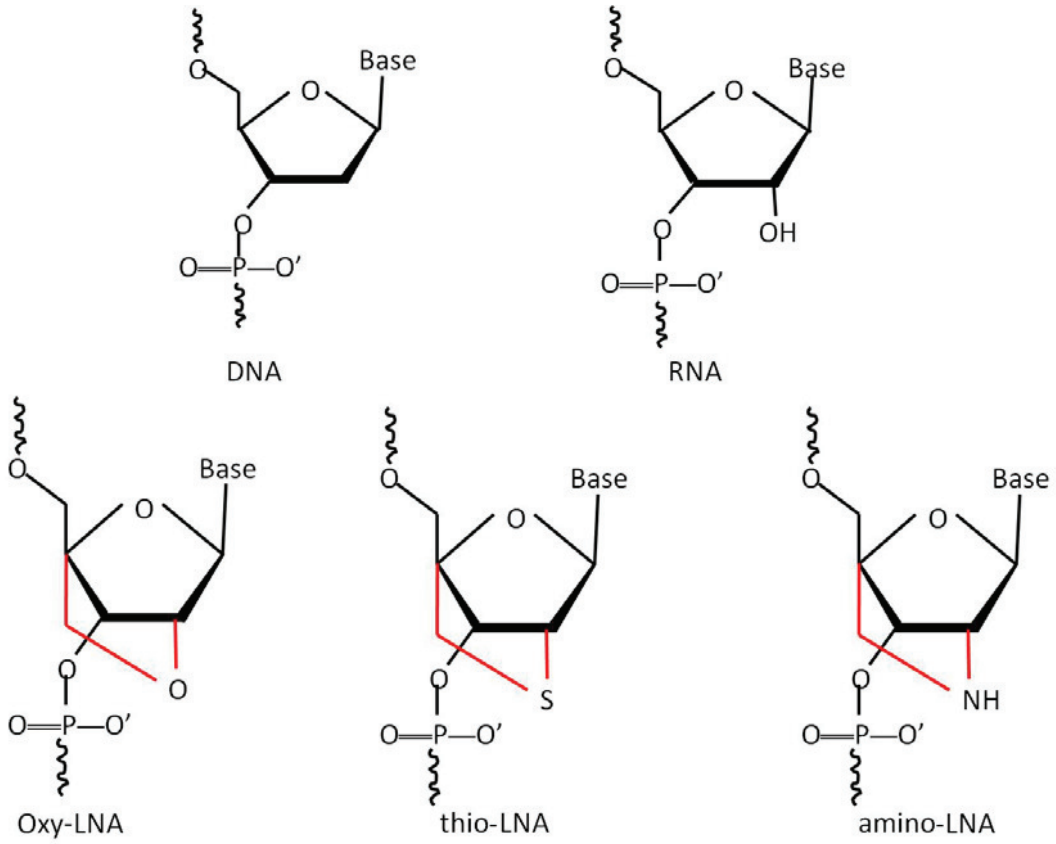

Fig 1.6. Chemical structures of DNA, RNA and LNA. LNA forms stable hybrid duplexes with DNA and RNA. Duplexes formed between two LNA oligonucleotides exhibit unparalleled affinity and specificity. LNA units can be incorporated into normal DNA or RNA oligonucleotides to increase the stability of probe-target hybrids. This is manifested as an increased melting temperature (T_m) of the hybrid duplex. Modified from Kumar *et al* (1998)[166] with permission.

The characteristics of LNA include: unprecedented thermal stabilities of duplexes towards complementary DNA and RNA; stability towards 3′-exonucleolytic degradation; efficient automated oligomerization, and good aqueous solubility.[166] The affinity between LNA toward complementary nucleic acids is by far the highest reported for a DNA analog.[166] The very high affinity allows the design of small probes because the specificity of a probe is inversely related to its size. These markedly shorter probes are used as allele-specific tools in genotyping assays.[149,167-169]

1.1.2.2.2.2 Multiplexing

Multiplex PCR is the simultaneous amplification of more than one target sequence in a single reaction.[170] The ability to multiplex PCR by probe color and *Tm* greatly expands the power of real-time PCR application. Each PCR probe has a unique *Tm* which can distinguish between different PCR products. This allows PCR multiplexing by *Tm*, a powerful tool with a multiplexing potential similar to that of fluorescence emission spectra. Simple hybridization probes with only a single fluorescent dye can be used for quantification and allele typing. Different probes are labeled with dyes that have unique emission spectra. Spectral data are collected with discrete optics or dispersed onto an array for detection.[171]

Many different fluorescence techniques are available for real-time PCR. Dyes like SYBR Green I can be used in any amplification, but they are not sequence-specific and not feasible for multiplexing by color.

Color multiplexing is possible with oligonucleotide probes that are labeled with different fluorescent groups. Real-time PCR instruments can discriminate between the different dyes. The signal from each dye is used to separately quantitate the amount of each target (Fig. 1.7). The multiplex PCR assays must be validated and often require optimization, which can be a challenge. It is necessary to keep in mind that since both assays are amplified in the same tube, they compete for the same reagents. This competition needs to be minimized. The two assays can also inhibit each other through interactions among the primers and probes, amplicons, or any combination of these. The goal is to accurately quantitate the amount of individual target without interference from competition or inhibition between assays. It is common to have duplex dyes depending on the application. More than three dyes can be used at the same time. TaqMan probe, MGB probe, or Scorpion probe are commonly used probes for multiplex real-time PCR.[172-176]

Fluor	5'	I	3'	Abs	Em
Alexa Fluor 350	•	•	•	346	442
Tide Fluor TF1	•	•	•	341	447
Oregon Green 488	•	•	•	490	514
Alexa Fluor 488	•	•	•	494	517
6-FAM	•		•	495	519
Fluorescein	•	•		495	520
Tide Fluor TF2	•	•	•	499	522
Rhodamine Green-X				504	531
TET	•			521	536
JOE	•	•	•	520	548
VIC				538	554
Alexa Fluor 532	•	•	•	530	555
HEX	•			535	556
Cy3	•			552	570
NED				546	570
Alexa Fluor 546	•	•	•	554	570
Alexa Fluor 555	•	•	•	555	572
TAMRA	•	•	•	544	576
Tide Fluor TF3	•	•	•	554	578
Rhodamine Red-X				574	594
PET				558	595
Cy3.5	•			581	596
ROX	•	•	•	575	602
Alexa Fluor 568	•	•	•	578	602
Texas Red-X	•	•	•	583	603
Tide Fluor TF4	•	•	•	588	610
Alexa Fluor 594	•	•	•	590	614
Alexa Fluor 633	•	•	•	621	639
Cy5	•			643	667
Tide Fluor TF5	•	•	•	656	670
Alexa Fluor 647	•	•	•	651	672
Cy5.5	•			675	694
Alexa Fluor 660	•	•	•	668	698
IRDye 700				689	700
Tide Fluor TF6	•	•	•	686	702
Alexa Fluor 680	•	•	•	684	707
DY-682				690	709
ATTO 700				700	719
Alexa Fluor 700	•	•	•	702	723
Tide Fluor TF7	•	•	•	756	775
Alexa Fluor 750	•	•	•	753	782
IRDye 800				767	786
DY782				783	800
Tide Fluor TF8	•	•	•	787	808

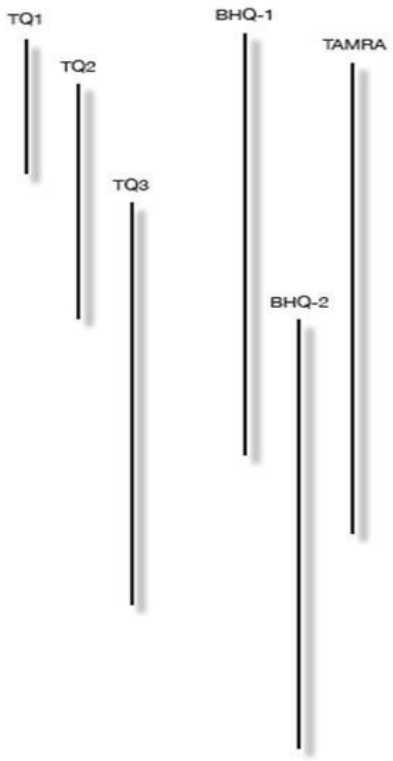

Fig 1.7. Common reporter fluors and quenchers used in multiplex real-time PCR. Modified from www.operon.com with permission.

For duplex real-time PCR testing, there are three possible scenarios for the relative expression level of the two targets:

1. One target (typically the endogenous control) is always abundant. In such cases, the greater starting quantity of the more abundant target causes the assay for that target to perform better than the other from the start, using up the reagents, and leaving little for the other assay. This problem can be solved by limiting the amount of primer for the more abundantly expressed target. As a result, the primers for that assay are used up

quickly, leading the reaction to plateau early and leaving sufficient reagents for the amplification of the less abundant target.

2. The two targets are expressed at similar levels. In this situation, neither assay needs to be primer-limited. The assays can simply be run as single or duplex reactions. If validations fail, it might require a primer-limit in one or both assays to ensure the duplexing performs better.

3. Either target may be more abundant. If either target could be more abundant than the other, depending on the samples being investigated, then both assays need to be primer-limited.[171]

Multiplexing PCR can be used in detection of common respiratory viruses such as influenza A and B viruses and respiratory syncytial virus from nasophayngeal specimens.[177-180] They can also be used to detect and determine different genotypes or serotypes of the target virus.[181-182]

1.1.2.2.2.3 Quality control in real-time PCR technology

Quality control allows the laboratory to minimize the reporting of inaccurate results, to report results with a high degree of confidence, and to decrease costs by detecting errors prior to reporting results. The ultimate goal of quality control is to reduce the number of controls needed for reporting reliable results.

Lab settings

The appropriate arrangement or design of a PCR laboratory is of great importance in maintaining a high standard of performance. As a minimum requirement, three dedicated areas are necessary: the reagent preparation area which is mainly to prepare the PCR master mix, the specimen preparation area which refers to the DNA/RNA extraction area, and the PCR detection area. If more space is available, it may be used to good advantage. This one-way workflow will significantly reduce the chance of cross-contamination.

Positive and negative controls

The ideal positive control is a specimen containing the target nucleic acid, but this is often not practical or feasible. An acceptable positive control is pooled negative specimens spiked with the infectious organism, or a representative sample of the nucleic acid to be detected. The positive control should be at the concentration near the lower limit of detection of the assay to challenge the detection system but still high enough to provide consistent positive results.[125]

Water or buffer is commonly used as a negative control. However, an ideal negative control is a sample containing non-target nucleic acid to determine that the nonspecific PCR amplification and detection of amplified product is not happening. Additionally, the negative control is used to demonstrate that the reagents are not contaminated and can be used to compensate for background signal generated by the reagents.[183] A carryover contamination due to PCR products from previous PCR runs is a major source of PCR contamination. This problem can be reduced by adding enzyme uracil-N-glycosylase to remove uracil from dUMP incorporated into any contamination molecules, leaving apyrimidinic sites which will be destroyed by cleavage at the abasic sites at a later PCR amplification step.[184]

Internal and inhibition controls

The use of an internal control is an important aspect of quality control. The internal control is necessary for ensuring adequate efficiency of RNA extraction and confirming the absence of PCR-inhibitors in each sample, therefore reducing false negative results.[183] It is a valuable tool when testing nucleic acid extracted from difficult biological matrices such as degraded samples where the presence of PCR-inhibitors could cause big problems. In such cases, co-amplification of an internal control increases the reliability of the results and is used to validate negative results.

There are different formats of internal controls. One approach is to detect an endogenous gene that is present naturally in the test specimen. The selected gene should be present as a constant, basal cell cycle-independent level of transcription that is not influenced by the cellular pathology associated with the disease tested by the real-time PCR. Genes fulfilling these criteria are commonly known as housekeeping genes such as

glyceraldehydes-3-phosphate, β-actin, 18S ribosomal RNA, glutamate decarboxylase (GAD), and β_2-microglobulin.[185-192] In contrast to an endogenous internal control, an exogenous internal control does not occur naturally within the nucleic acid preparation. This type of internal control can be designed to contain an all-purpose heterologous target sequence or a complete heterologous viral genome which is unrelated to the sequence to be tested.[193-197] The exogenous internal control can be added to each test sample before either the template extraction step or prior to real-time PCR amplification testing. Depending on the particular design of the internal controls, amplification of the control sequences may require an extra set of primer pairs in the reaction. Alternatively, *in vitro* transcripts, plasmids, or chimeric viruses can be generated containing homologous target sequences for the same primer pair as the diagnostic test. These "mimic" internal controls can contain internal sequences not present in the target amplicon to yield an amplification[198] product with a different length, which can be differentiated a from wild-type amplicon by a second, internal control-specific probe.[183,198-200] The advantage of this type of control is that it directly monitors the performance of diagnostic primer sets ensuring that the appropriate PCR components have been added.

1.1.2.2.2.4 Application of real-time PCR in detecting equine respiratory viruses

Many techniques discussed in this section have been used in veterinary diagnostic laboratories to detect common equine respiratory viruses. Our lab has taken leadership in developing several TaqMan® real-time PCR assays for the detection of EIV, EAV, equine rhinitis viruses A and B, and EHV-1.[201-203] The development and evaluation of the real-time PCR assays for the detection of EIV, EAV, and equine rhinitis viruses will be discussed in the following chapters in detail. Several real-time assays developed by other groups are also available for the detection of these common viral pathogens. For instance, Quinlivan *et al* (2005) developed a real-time PCR targeting equine influenza virus using SYBR Green I and evaluated the assay with conventional virus isolation and Directigen Flu A test.[204] There was a significant positive correlation ($P< 0.05$) between the quantitative RT-PCR and both of these assays. Mori *et al* (2009) developed a duplex real-time PCR for the detection of equine rhinitis A and B viruses.[205] Quinlivan *et al* (2010) developed two single real-time PCR for the detection of equine rhinitis A and

B.[206] All of these molecular assays have tremendously increased the detection capability of equine viral pathogens which has been beneficial to the equine industry.

1.2 Introduction to equine arteritis virus attachment and entry

1.2.1 Equine viral arteritis

Equine viral arteritis (EVA) is a contagious disease caused by equine arteritis virus (EAV) infection. EVA was first described perhaps 450 years ago with clinical descriptions of "pinkeye", "infectious or epizootic cellulitis", "influenza erysipelatosa", "Pferdestaupe", "Rotlaufseuche", and "equine influenza" in the European veterinary literature.[207-211] However, the virus was first isolated during an outbreak of respiratory disease and abortion on a Standardbred breeding farm in Bucyrus, Ohio, in 1953.[212] Serologic surveys have confirmed EAV is present in many horse populations throughout the world; Japan and Iceland are notable exceptions.[34,213-219] The consequences of EAV infection range from subclinical infection to a flu-like illness in adult horses, abortion in pregnant mares, and interstitial pneumonia in neonatal foals.[34,215,220-222] A variable percentage (from 10-70%) of acutely infected stallions can become persistently infected carriers after natural infection and continue to shed virus in their semen for periods that range from several weeks to the lifespan of individual stallions.[34,223-225] Carrier stallions are the natural reservoir of EAV; they ensure the virus is maintained in equine populations between breeding seasons.[34] Furthermore, EAV behaves as a quasispecies in the reproductive tract of the carrier stallion and novel genotypic and phenotypic variants arise during persistent infection.[35,226-227]

Transmission of EAV can occur either by respiratory or venereal routes. Aerosol transmission of EAV occurs after aerosolization of infected respiratory tract secretions from acutely infected horses. Venereal transmission of EAV occurs during natural or artificial breeding of a carrier stallion to susceptible mares.[228-231] Mares that become infected can then acutely transmit the virus by the respiratory route to susceptible cohorts in close proximity. EAV persists only in the reproductive tract of carrier stallions, mainly in the ampulla of the vas deferens. It has been demonstrated that testosterone plays a

critical role in the establishment and maintenance of the EAV carrier state in the stallion. Persistently infected stallions eliminate the virus following castration, whereas those that receive sufficient testosterone after castration continue to shed virus in their semen.[223,231] Persistent EAV infection does not occur in geldings, mares, fetuses, or in colts infected by the virus prior to their puberty. [34,223-224,232-233] The shedding of virus in carrier stallions is not related to the titer of neutralizing antibody in the serum, indicating that the humoral immunity alone does not prevent the virus persistence in the male reproductive system.[231]

Following respiratory infection, the virus initially replicates in endothelial cells and pulmonary macrophages, from which it rapidly spreads into the regional lymph nodes, especially in the lung and the bronchial lymph nodes, and from where it is disseminated throughout the body. In addition to the primarily infected macrophages and endothelial cells, EAV can also replicate in other cell types such as epithelial cells, mesothelium, and smooth muscle cells of small blood vessels and myometrium.[36,234-235]

The immune response to EAV infection can be divided into two categories: innate immunity and adaptive immunity. The innate immune response of the mucosal lining of the respiratory and genital tracts is the first line of defense after natural exposure to EAV. Equine arteritis virus infection of equine macrophages results in increased transcription of genes encoding proinflammatory mediators, including IL-1β, IL-6, IL-8, and TNF-α, with the release of substantial quantities of TNF-α into the culture medium.[236] Furthermore, virulent and avirulent strains of EAV induced different quantities of TNF-α and other proinflammatory cytokines (IL-1β, IL-6, IL-8), and the magnitude of the cytokine response of macrophage to EAV infection reflected the virulence of the infecting virus strain.[236] These studies clearly show that cytokine mediators are produced by EAV infected equine cells and, presumably, play an important role in determining the nature and severity of the outcome of infection. The humoral immune response to EAV includes the development of both complement-fixing (CF) and virus-specific neutralizing (VN) antibodies. [237-238] The CF antibodies appear between 1-2 weeks and peak 2-3 weeks after EAV infection in adult horses and ponies.[238] Neutralization of EAV is complement dependent and is associated with the IgG fraction of the late antiserum, but not the early antisera or their IgG and IgM fractions.[239-242] The requirement of complement for

efficient virus neutralization is also virus strain dependent.[243-244] The humoral immune response to EAV is mainly directed to the major envelope proteins, GP5, M, and N proteins [245-251]. The neutralization determinants of EAV are located in the GP5 protein and at least four potential neutralization sites on the N-terminal hydrophilic ectodomain of the GP5 protein, including aa 49 (site A), 61 (site B), 67-90 (site C), and 99-106 (site D) have been characterized.[252] It is speculated that the aa changes in the GP5 n-terminal ectodomain, especially if they occur during persistent infection in carrier stallions, contribute to the emergence of EAV strains with different neutralization phenotypes.[253] Besides neutralizing antibodies recognizing GP5 protein, horses also produce non-neutralizing anti-GP5 antibodies in response to EAV infection or immunization with an inactivated whole-virus vaccine.[247,254] Non-neutralizing antibodies against N and M proteins [249,251,254] were detected as early as 14 days post-infection and lasted at least 145 days in sequential sera from horses experimentally infected with EAV.[250]

1.2.2 Equine arteritis virus

1.2.2.1 Genome properties and organization

Because of the similarities in genome organization and protein expression strategies, the *Arteriviridae* (genus *Arterivirus*), *Coronaviridae* (genera *Coronavirus* and *Torovirus*) and *Roniviridae* (genus *Okavirus*) were grouped together in the order *Nidovirales*.[255] The name *Nidovirales*, derived from the Latin *nidus* for nest, reflects the nested-set arrangement of the subgenomic mRNAs (sg mRNAs) produced by this order of viruses during their replication cycle. The *Nidovirales* are grouped based on their phylogenetic relationships and genome organization. There are four members in the arterivirus genus: equine arteritis virus (EAV), porcine respiratory and reproductive syndrome virus (PRRSV), lactate dehydrogenase-elevating virus (LDV), and simian hemorrhagic fever virus (SHFV).[256]

Equine arteritis virus (EAV) is a single-stranded, positive sense RNA virus. It is the causative agent of equine viral arteritis (EVA) in horses and other equids.[212,255,257] The virion of EAV is spherical with a diameter of 40 to 60 nm. The isometric core particle (25 to 35 nm in diameter) is surrounded by a relatively smooth envelope that lacks large projections. EAV genome length varies between 12,704 to 12,731 bp among

different strains.[255,258-259] The EAV genome includes a 5′ leader sequence and at least nine ORFs (Fig 1.8). [260-261]

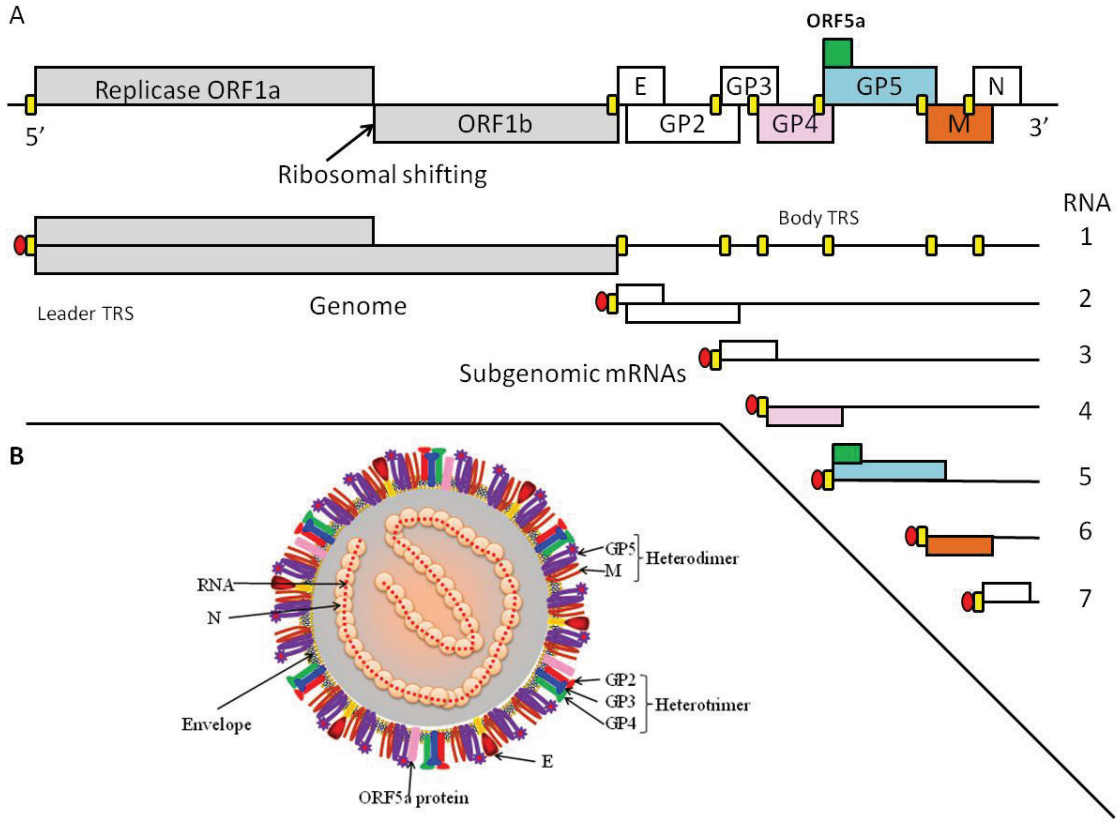

Fig 1.8. The EAV particle and genome organization. A. Overview of the polycistronic nature of EAV genome. The leader sequence and leader TRS (transcription regulating sequence) located at the 5′-end of genome are indicated as a red circle and a yellow box, respectively. Translation of E and GP2 genes occurs by leaky scanning of the 5'-proximal end of sg mRNA2.[262] The green square indicates the newly identified open reading frame, ORF5a, and the protein is likely to be expressed from the same sg mRNA.[263] B. Schematic representation of the EAV particle. The viral RNA is encapsidated by the nucleocapsid protein (N; encoded by ORF7) into an isometric core which is surrounded by an envelope containing eight structural proteins.

The two most 5′-proximal ORFs (1a and 1b) occupy approximately three-quarters of the genome and encode two replicase polyproteins (pp1a and pp1ab). The two

precursor proteins are extensively processed after translation into at least 13 nsps (nsp1-12, including nsp7 α/β) by three viral proteases (nsp1, nsp2 and nsp4).[258,264-265] The structural proteins of EAV are expressed from a 3′-coterminal nested set of sg mRNAs and not from the genomic RNA. Three of the minor envelope proteins (GP2, GP3, and GP4) form a heterotrimer in the EAV particle, which may also interact with another minor envelope protein E.[256,262] The two major envelope proteins (M and GP5) form a disulfide-linked heterodimer in the EAV virion.[266-268] The GP5 protein expresses the known major neutralization determinants of EAV.[252-253,269-273] Although there is considerable variation in the sequence of the GP5 protein of field strains of the virus, there is only one known major serotype of EAV and all strains evaluated thus far are neutralized by polyclonal equine antiserum raised against the Bucyrus strain of EAV.[34,229] However, field strains differ both in their neutralization and virulence phenotypes and not all strains are neutralized to the same degree.[227-228,252,259,274]

EAV is stable at -70 °C for years without significant loss of infectivity. Virus infectivity is lost within six months at room temperature, and after a month at 37 °C.[275] It has been reported that tissue culture fluid containing the experimentally derived virulent Bucyrus strain of EAV survived more than 75 days at 4 °C, 2~3 days at 37 °C, and 20~30 min at 56 °C.[276] Lyophilized virus is highly stable at -20 °C and moderately stable at 4 °C.[277]

1.2.2.2 Equine arteritis virus life cycle

Equine arteritis virus can be propagated in a variety of primary cell cultures such as equine macrophages, equine endothelial cells, equine kidney cells, and hamster kidney cells.[236,276,278-279] Many other continuous cell lines such as rabbit kidney (RK-13), baby hamster kidney (BHK-21), African green monkey kidney (Vero), human cervix cells (Hela), and mouse connective tissue (L-M) are also susceptible to EAV infection.[280-282] Equine arteritis virus infection of primary cells and continuous cell lines is highly cytocidal. The appearance of cytopathic effect (CPE) in EAV-infected cells is characterized by rounding of cells and cell dissociation from the culture plate surface.[276,281] The appearance of CPE varies among different cell lines.

The EAV life cycle starts with virus interaction with an unknown cellular receptor, entrance into the cells via clathrin-dependent endocytosis and delivery to acidic endosomal compartments.[283] Following entry and release into the cytosol, the RNA genome is uncoated and translated into two large replicase polyproteins (pp1a and pp1ab) from which at least 13 nsps are released by autoproteolytic processing mediated by the viral proteases.[265,284] The nsps interact and form a membrane-bound replication/transcription complex (RTC) which provides a scaffold for genome replication and subgenomic mRNA transcription.[285-288] The subgenomic mRNAs are further translated into the viral structural proteins. The newly synthesized genome is encapsidated into the N proteins forming the nucleocapsid (N), which becomes enveloped by budding through the ER-Golgi intermediate compartment (ERGIC) that contains membranes with viral envelope proteins. Newly formed virions mature in the Golgi complex during their exocytic pathway and are ultimately released from infected cells (Fig 1.9).

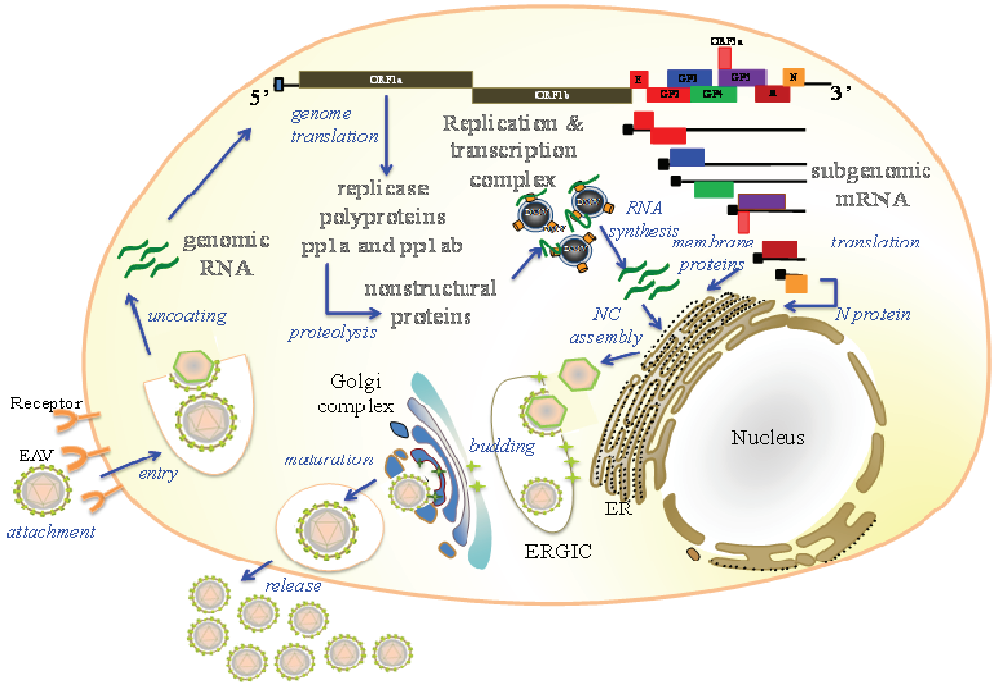

Fig 1.9. Schematic overview of EAV life cycle. ER: endoplasmic reticulum; ERGIC: ER-Golgi intermediate compartment; NC: nucleocapsid.

(I) Virus attachment and entry

The initial events in a viral infection consist of attachment of the virus to the surface of the host cell, followed by penetration of the virus particle into the cytoplasm of the cell. The success of these events depends on the recognition of specific molecules (receptors) on the cell surface by the virus. The replication cycle of EAV has been studied extensively. However, there is very limited information on EAV receptor binding and virus entry. Previous studies have shown that heparin treatment of EAV can reduce plaque formation by 14% as compared to untreated control virus.[289] The hemagglutination caused by EAV was also inhibited by heparin.[290] Mouse erythrocytes treated with heparinase can dramatically reduce the agglutination activity of EAV.[290] Therefore, all the data suggest that a heparin-like molecule plays an important role in EAV infection, probably in the attachment and entry step. But the precise mechanism of this aspect of EAV infection is not yet known.

The viral protein involved in receptor attachment and binding is still a mystery. By analogy with many other animal RNA viruses and in view of its recognition by neutralizing antibodies, it has been speculated for many years that the ectodomain of the arterivirus major glycoprotein GP5 is involved in receptor recognition. However, direct experimental studies by exchanging the ectodomain of the EAV GP5 protein with that of PRRSV or LDV in the context of an infectious EAV cDNA clone did not alter the cell tropism of the virus.[291] Similarly, PRRSV mutants in which the ectodomain of the M protein was replaced by that of EAV or LDV retained the ability to infect porcine alveolar macrophages and did not aquire tropism to cells susceptible to the respective viruses from which the foreign ectodomains were derived.[292] These results indicate that neither GP5 nor M proteins are responsible for receptor binding of EAV although they are the main neutralization antibody recognition sites. It is anticipated that the EAV minor envelope glycoproteins GP2, GP3, and GP4 together with minor structural protein E are likely to mediate the initial virus attachment to the host cell surface based on the fact that the E, GP2, GP3, and GP4 proteins are not required for the formation of EAV particles, although these proteins are believed essential for ensuring that the virus particles are infectious, however detailed experiments have not been performed.[262,268,293] A very recent publication by Tian *et al* used a PRRSV infectious cDNA clone to replace

its own minor structural protein genes encoding E, GP2, GP3, and GP4 with those of EAV. The chimeric virus expressing EAV ORF2ab34 gained the broad *in vitro* cell tropism of EAV, indicating that the minor envelope proteins (GP2, GP3, GP4, and E) play a critical role as viral attachment proteins.[294] This is direct evidence that minor envelope structural proteins are involved in cellular tropism determination.

The entry of EAV into BHK cells is mediated via clathrin-dependent endocytosis and delivery to acidic endosomal compartments.[283] The plaque formation is strongly inhibited by substances which interfere with clathrin-dependent endocytosis and by lysosomotropic compounds. The infection of BHK cells is suppressed when antisense RNA against clathrin-heavy chain is used. Other members of the family *Arteriviridae*, such as PRRSV use a similar receptor-mediated, low pH-dependent pathway to enter host cells.[295-296]

The process of EAV attachment and entry still needs further investigation. The virus attachment molecules and/or receptors need to be identified. It is not clear whether EAV uses the same receptors in different cell lines or whether different EAV strains use the same or different receptors.

(II) Biosynthesis: genome translation and replication, mRNA transcription, and viral protein synthesis

A. Genome translation and post-translational processing of replicase polyproteins

The EAV replication cycle starts with the expression of the replicase gene from the genome. Replicase ORF1a and ORF1b, generated from -1 ribosomal reading frameshift, are both expressed from the genomic mRNA. The ORF1b ribosomal frameshift is located just before ORF1a.[260] There are two signals assumed to promote this event: a "slippery signal" 5' GUUAAAC 3' and a downstream RNA pseudoknot structure.[256]

Translation of the EAV replicase gene yields two large polyproteins: the polyprotein (pp) 1a and pp1ab. The EAV pp1a and pp1ab are cleaved by three ORF 1a-encoded proteases: nsp 1, nsp 2, and nsp4.[264,288,297-299] The nsp1 protease is a papain-like cysteine protease (PCP) which directs an autoproteolytic cleavage at C terminus (Gly-260 | Gly-261) of pp1a resulting in the rapid release of nsp1.[298] The EAV PCP mediates

probably exclusively *in cis* cleavage, and attempts to achieve cleavage *in trans* were unsuccessful.[298,300] The nsp2 protease is a cysteine protease which cleaves nsp2 at position Gly-831 | Gly-832.[298] The nsp2|3 cleavage can be performed *in cis* or *in trans*, although *trans*-cleavage activity is relatively low.[265,299] The nsp4 protease is the major viral protease which contains several unique characteristics. It utilizes the His-Asp-Ser (His-1103, Asp 1129, and Ser-1184) catalytic triad, a typical characteristic of classical chymotrypsin-like protease.[301] The putative substrate-binding region of nsp4 protease also contains Thr and His residues (Thr-1179 and His-1198) which are conserved in viral 3C-like cysteine proteases and determine the specificity of cleavage sites containing a (Glu/Gln) | (Gly-Ser) dipeptide.[301] Therefore, the nsp4 protease was defined as the prototype of a novel group of chymotrypsin-like enzymes, the 3C-like serine proteases (3CLSP). It mediates five cleavages in pp1a and three in ORF1b-encoded polypeptides. But these sites are not equally sensitive to the nsp4 protease. The C-terminal half of the EAV pp1a can be cleaved via two alternative pathways.[302](Fig 1.10)

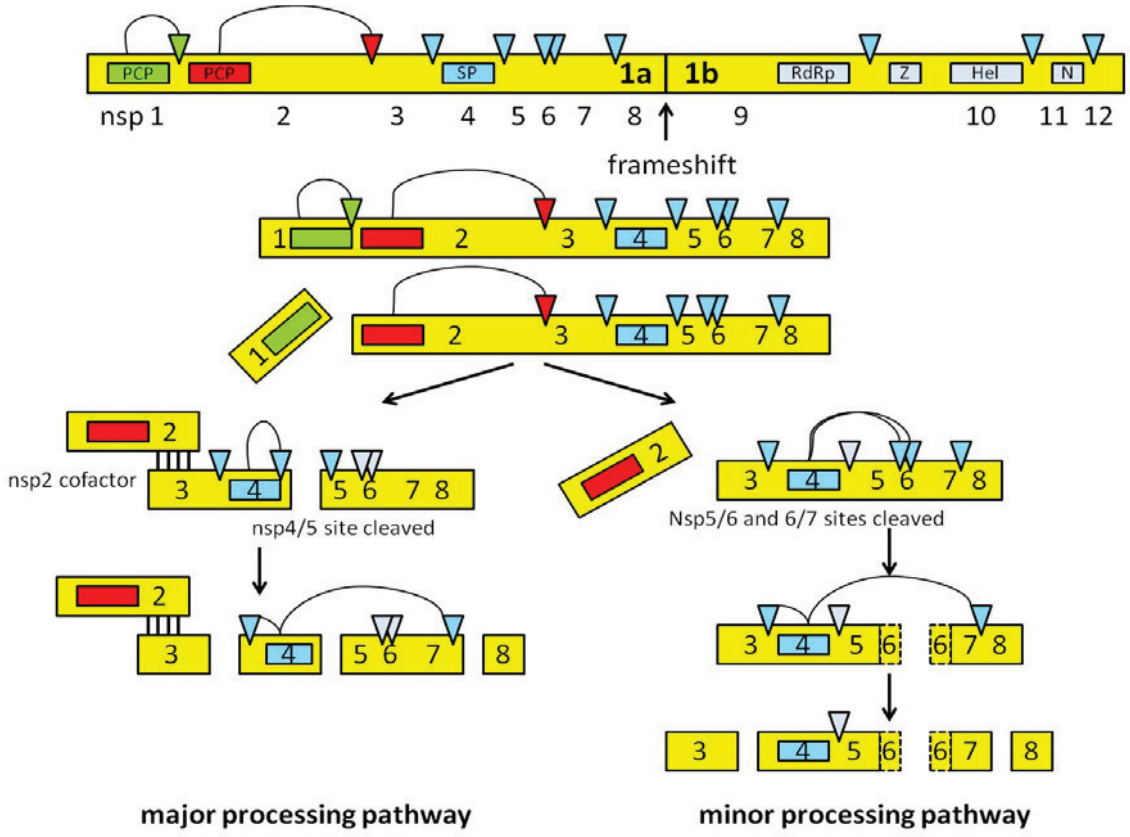

Fig 1.10. Overview of the proteolytic processing of the EAV replicase ORF1a and ORF1ab polyproteins. The three EAV proteinases (located in nsp1, nsp2, and nsp4), their cleavage sites, and the EAV nsp nomenclature are displayed. Abbreviations: PCP, papain-like cysteine proteinase; SP, serine proteinase; RdRP, RNA-dependent RNA polymerase; Z, zinc finger; Hel, helicase; N, Nidovirus-specific conserved domain. The association of cleaved nsp2 with nsp3-8 (and probably also nsp3-12) was shown to direct the cleavage of the nsp4|5 site by the nsp4 proteinase (major pathway). Alternatively, in the absence of nsp2, the nsp5|6 and 6|7 sites are processed, and the nsp4|5 junction remains uncleaved. Figure modified from Wassenar *et al* (1997)[302] with permission.

In the major pathway, the nsp4 first cleaves the nsp 4|5 site, followed by cleavage of the nsp 3|4 and nsp 7|8 junctions, and the nsp 5-7 remained uncleaved. In the minor pathway, the nsp 4|5 is not cleaved. Instead, the nsp 5|6 and nsp 6|7 sites are cleaved, followed by cleavage of the nsp 3|4 and nsp 7|8 sites. These two pathways are mutually exclusive and multiple processing intermediates are generated.[302] The presence of

liberated nsp2 is believed to determine whether the nsp4 serine protease will cleave the nsp 4|5 site of the nsp 3-8 precursor and thus the major pathway takes place.

B. Genome replication

The RNA synthesis (including genome replication and mRNA transcription) depends on the viral-encoded RNA-dependent polymerase. As discussed before, the nsp1, nsp2, and nsp4 are viral proteases. The nsp9 to 11 contain highly conserved domains which are crucial for EAV genome replication and subgenomic transcription. Based on comparative sequence analysis, a putative RNA-dependent RNA polymerase and a NTP-binding RNA/helicase motif were identified in nsp9 and nsp10, respectively.[303-304]

A typical feature of arterivirus replication is the formation of paired membranes and double membrane vesicles (DMV) at 3-6 h post infection.[285] DMV are approximately 80 nm in diameter. The inner and outer membranes of DMV are tightly apposed but clearly separated.[285] These profiles sometimes contain a neck between the paired EM-membrane and a forming DMV which is not pinched off. Biochemical and immunofluorescence assays have revealed that most EAV replicase subunits and viral RNA synthesis co-localize to the perinuclear region of the infected cells.[287] Those replicase subunits are associated with intriguing DMVs which appear to be derived from the endoplasmic reticulum (ER) since the outer membrane of DMV is sometimes continuous with the ER.[285] Very similar membrane alternations can be induced, in the absence of EAV infection, upon expression of the ORF1a-encoded replicase subunits nsp2 and nsp3. However, when nsp2 or nsp3 are individually expressed, DMV are not visible.[286] These data strongly suggest the ORF1a-encoded replicase subunits play important roles in the formation of a membrane-bound scaffold for the EAV replication complex. With the development of a robust *in vitro* RNA synthesis assay, the active EAV replication complex from infected cells was successfully isolated which allowed the initial biochemical characterization of its composition and RNA-synthesizing activity.[305] In that experiment, van Hemert *et al* isolated replication complex from cytoplasmic extracts by differential centrifugation and identified a 59-70 kDa cytosolic host protein factor which is required for the activity of DMV.[305] Replicase subunits directly involved in viral RNA synthesis (nsp9 and nsp10) or DMV formation (nsp2 and nsp3) exclusively co-sedimented with the active replication/transcription complex. Subgenomic mRNAs

appeared to be released from the complex, whereas newly made genomic RNA remained more tightly associated. Taken together, these data strongly support a link between DMVs and the RNA-synthesizing machinery of EAV.[305]

C. Subgenomic RNA synthesis

One of the hallmarks of the nidovirus replication cycle is the generation of a nested set of subgenomic mRNAs from which the the 3′-proximal region of the polycistronic genome is expressed.[256] These sg mRNAs are 3′ coterminal and contain a common 5′ leader sequence which is derived from the 5′ end of the viral genome. The leader sequence is fused to the sg mRNA "bodies" by a discontinuous transcription mechanism. There are two widely considered but conflicting models of arterivirus transcription: leader-primed transcription and discontinuous extension of minus-strand RNA synthesis (Fig 1.11).

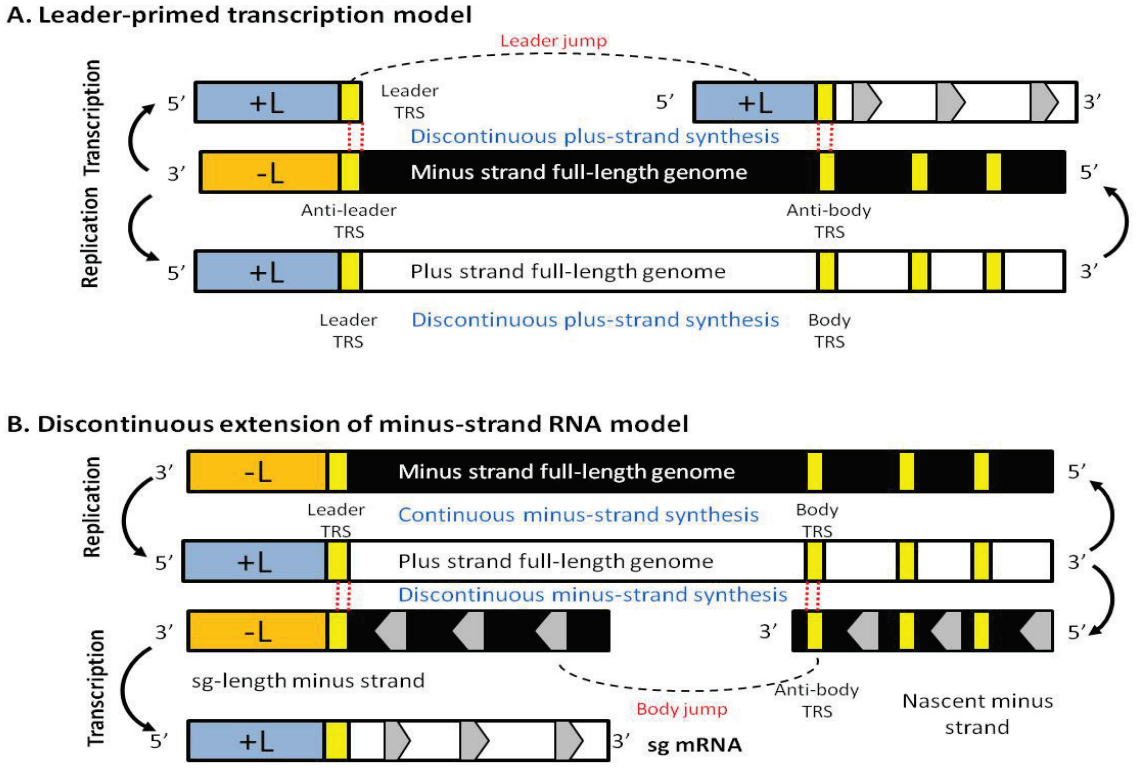

Fig 1.11. Two transcription models in nidoviruses: "leader-primed transcription"[306-308] and "discontinuous extension of minus-strand RNA"[309] models. (A) The "leader-primed transcription" proposes that the discontinuous step of viral sg mRNA synthesis occurs during the plus-strand synthesis. In this model, the production of new

genome RNA is continuous and the discontinuous step occurs during the plus-strand synthesis and the body TRS complementary to the minus-strand genome acts as promoter for transcription. After transcription of a leader primer (+L) from the 3′- end of minus-strand full-length genome, the leader TRS in this primer joins to the anti-body TRS in the minus-strand genome and is extended to generate sg mRNA. (B) The alternative model, "discontinuous extension of minus-strand RNA model" proposes that sg-length negative strand is produced and functions as a template for generation of sg mRNA. The anti-body TRS may serve as a "jump" signal of the nascent minus-strand to leader TRS located at the 5′-end of the plus-strand full-length genome. After the anti-leader (-L) is added to the nascent minus-strand, the sg-length minus-strand functions as template for transcription. The latter model is more widely accepted based on data from biochemical and genetic studies. Modified from Pasternak *et al.* (2006) [310] with permission.

Both models require transcription-regulating sequences (TRS; 5'-UCAAC-3') that determine a base-pairing interaction between positive and nascent minus-strand RNA and are essential for leader-to-body joining. [311-313] In the "leader-primed transcription model", transcription is initiated from the 3′-end of the minus-strand genome to produce a leader primer form with the 3′-terminal leader TRS base paired with the anti-TRS in the minus-strand genome. In this model, the production of new genome RNA is continuous and the discontinuous step occurs during the plus-strand synthesis and the body TRS complementary to the minus-strand genome acts as promoter for transcription.[306-308] Another "discontinuous extension of minus-strand RNA model" was proposed by Sawiki and Sawiki which is also the widely accepted model. [309] In this model, the anti-genome is produced in a continuous fashion while the sg mRNAs are produced by a discontinuous transcription mechanism controlled by the TRS. The EAV sg mRNAs contain a common 5′ sequence of 208 nt "leader", which is identical to the 5′ end of the viral genomic RNA. [258] The leader TRS is located in a hairpin structure at the 3′-end of the leader and the body; the TRS is located upstream of each structural protein gene.[314-316] The EAV genome contains 17 other 5′UCAAC3′ motifs besides the leader TRS, only six of which function as body TRSs participating in a leader-body junction to generate major sg mRNAs 2-7.[260] For instance, the RNA3 uses three alternative leader-body junction sites,

TRSs 3.1, 3.2, and 3.3 among which only TRS 3.2 is functional. There are two UCAAC boxes upstream of ORF4, -5 and -7 whereas three UCAAC sequences are found upstream of ORF2 and -2b.[317] But only a single TRS has been identified as an active site for each sg mRNA. Taken together, the same sequence motif UCAAC can be actively, less actively, or not used for leader-body junction to generate mRNAs. The TRSs are thought to regulate transcription of the genome template and to serve as singles for either attenuation or termination of minus-strand RNA synthesis in all nidoviruses to produce subgenome-sized minus strands that are used for sg mRNA synthesis. [318] Minus-strand RNA synthesis, initiated at the 3′-end of the viral genome, is attenuated at one of the body TRS regions.[310,319] Subsequently, the nascent minus strand carrying the body TRS complement at its 3' end is translocated to the 5′-end of the genomic template. The genomic leader TRS functions as a base-pairing target for the 3′ end of the nascent minus strand. When minus-strand synthesis resumes, nascent strands are extended with the complementation of the genomic leader sequence, producing a nested set of subgenome-length minus-strand templates that are used for the subsequent synthesis of the various sg mRNAs. If attenuation does not occur, minus-strand RNA synthesis proceeds to yield a full-length complement of genome, which then is used as template for genome replication. In this model, the TRS at the 3′-end of the leader transcript base pairs with the complement of body TRS in the negative-stranded template allowing extension of the complement of genomic leader sequence in the nascent negative strand. [309] The resulting sg negative-stranded RNA serves as template for the synthesis of the corresponding sg mRNA. With some exceptions, only the 5′-proximal ORF is translated from each sg mRNA and therefore, the number of sg mRNA produced is proportional to the number of ORFs located downstream of ORF1b.

(III) Virus assembly, budding and release

EAV gains its envelope from the internal membrane of the infected cells rather than from the plasma membrane. The assembly of EAV takes place at the cytoplasmic site of the endoplasmic reticulum (ER), and/or the Golgi complex. The newly synthesized genome is encapsidated into the N proteins forming the nucleocapsid, which becomes enveloped by budding through the ER-Golgi intermediate compartment that contains

membranes with viral envelope proteins. Newly formed virions mature in the Golgi complex via exocytosis and are ultimately released from infected cells.[320]

It has been shown that seven EAV structural proteins (E, $GP2_b$, GP3, GP4, GP5, M, and N proteins) are indispensable for the production of infectious progeny virus.[262,267] However, only the structural proteins GP5, M, and N but not the E, GP2, GP3, or GP4 are essential for the formation of virus-like particles.[268] Interestingly, all attempts to produce virus-like particles by the cotransfection of cells with expression plasmids encoding the EAV GP5, M, and N proteins were not successful indicating there must be additional factors involved in formation of the virus-like particles.[268]

1.2.3 Virus receptors

The life cycle of viruses includes the following stages: attachment, entry, uncoating, replication, virion assembly, and progeny virus release. Virus can only infect cells to which they can bind. Therefore, a successful viral infection starts with the step where viral surface proteins have direct interactions with attachment factors and virus receptors on the surface of the cell. There are several key differences between receptors and attachment factors. The interactions between the virus particles and the attachment factors can be relatively non-specific. These interactions mainly contribute to concentrate virus particles on the cell surface rather than promote entry.[321] In contrast, virus receptors actively promote virus entry into the cell by initiating conformational changes in the virus particle which lead to association with other co-receptors, membrane fusion, and penetration. Furthermore, receptors can activate signaling pathways through the plasma membrane to promote virus endocytic internalization. Therefore, it is the receptors, not the attachment factors, that determine the virus tropism to target cells. Following virus-receptor interaction, viruses are able to enter the host cell to further replicate their genome and produce progeny virus.

Viruses use receptors and attachment factors in very diverse ways. Sometimes, one receptor is not sufficient for productive entry, and a co-receptor is required for virus entry.[322-323] Many viruses use multiple and different attachment factors and receptors to enter into different cell types. Overall, the binding of attachment factors, receptors or co-receptors to viral protein is a well-organized process. For example, human

immunodeficiency virus type 1 (HIV-1) can infect a variety of immune cells such as T lymphocytes and macrophages. The viral envelope glycoprotein gp120 of HIV-1 first attaches to the attachment factor, heparan sulfate, and then binds to its receptor, CD4 molecule, which is mainly expressed on T lymphocytes and to a lesser extent in macrophages.[324-325] After binding to the CD4 receptors, the macrophage tropic and the T lymphocyte tropic HIV strains (M-tropic and T-tropic respectively), require different co-receptors to enter into cells. The β-chemokine receptor CCR5 is the primary co-receptor for the M-tropic strain during the early and chronic phases of infection in macrophage cells. In contrast, the T-tropic isolates use the CXCR4 as the key cofactor in late-stage infection of primary $CD4^+$ T cells.[326] The use of attachment factors and multiple receptors allows conformational changes of gp120 to facilitate successful virus entry into different cell types. [322]

1.2.3.1 Role of carbohydrates as cellular receptors and co-receptors

Carbohydrates covalently linked with other nonsugar moieties are generally classified as glycoconjugates. The glycoconjugates can be divided into different categories such as glycoproteins, glycopeptides, and glycolipids. Glycoconjugates on the cell surface are involved in cell-cell interactions and have an important role during virus attachment and entry into cells.

Sialic acids are a family of acid sugars that are usually found on the terminal capping positions of glycans which are linked to cell-surface glycoproteins and glycolipids. Sialic acids are commonly used as receptors or attachment factors by a number of viruses (e.g. orthomyxo-, paramyxo-, and papovaviruses).[327-329] In the case of influenza A virus, sialic acid which is associated with galactose functions as the receptor.[328] The sialic acid α(2,3)-Gal linkage is recognized by avian and equine influenza viruses and the sialic acid α(2,6)-Gal linkage is recognized by human viruses, whereas porcine viruses are able to recognize both.[328]

This specificity reflects the glycan structure that is expressed in the different species and is critical in preventing cross-species transmission. Since pigs have both types of receptors on respiratory epithelial cells, they were proposed to be the

hypothetical "mixing vessel" for assortment of avian and human influenza viruses. The emergence of influenza pandemics is related to reassortment of different strains of influenza virus resulting in a change of carbohydrate specificity.

In addition to sialic acids, another family of polysaccharides, glycosaminoglycan (GAG), is also a commonly used attachment factor to concentrate viruses on the cell surface and facilitate further entry.[330] GAG is a long branched polysaccharide consisting of a repeating disaccharide unit. It covalently attaches to a core protein to form proteoglycan which is a subclass of glycoprotein. The GAG family includes chondroitin sulfate, dermatan sulfate, heparin, heparan sulfate, keratan sulfate, and hyaluronan. Among all the GAG members, heparan sulfate and heparin are the most commonly used receptors for viruses.

1.2.3.2 Receptors used by Nidoviruses

The order *Nidovirales* consists of three families: the *Coronaviridae*, the *Arteriviridae*, and the *Roniviridae*.[331] Many receptors have been identified for the members of the genus *Coronaviruses* in the family *Coronaviridae*.

Murine hepatitis virus (MHV) strain A59, a member of the *Coronaviridae* family, uses the glycoproteins in the carcinoembryonic antigen-related cell adhesion molecule (CEACAM) family as its receptor.[332-334] It has an extracellular domain with four Ig-like loops which can bind to the viral spike glycoprotein for attachment. Although most strains of coronavirus are species specific, it has also been demonstrated that these viruses can readily mutate during passage *in vitro* or *in vivo* to adapt to environmental changes. Under selective pressure, *in vitro* MHV variants with mutations in the spike glycoprotein can use human CEA as receptors to infect humans to cross the species barrier.[335] Other coronaviruses such as human coronavirus strain 229E (HCoV-229E), transmissible gastroenteritis virus (TGEV), feline infectious peritonitis virus (FIPV), and canine coronavirus all use the cell membrane-bound metalloprotease, aminopeptidase N (APN) of their respective host species as their receptor.[336-337]

Angiotensin-converting enzyme 2 (ACE2) is the receptor for SARS-CoV.[338] It has been shown that liver and lymph node sinusoidal endothelial cells C-type lectin

(LSECtin) functions as the attachment factor for SARS-CoV to concentrate viral particles in liver and lymph nodes.[339] Other lectins such as CD209L can also augment virus entry; however, this molecule is not sufficient to confer susceptibility to a cell without the expression of ACE2.[340] The precise relationship between lectin binding and subsequent specific binding to ACE2 is not clear yet.

Among the four members of the family *Arteriviridae,* only the cellular receptor for PRRSV has been studied extensively. PRRSV has a very restricted host tropism and prefers to infect the cells of porcine monocyte-macrophage lineage. Two putative receptors have been identified on porcine macrophages: heparan sulfate and sialoadhesin.[341-343] It has been shown that both heparan sulfate and sialoadhesin are able to mediate the virus attachment to porcine alveolar macrophages (PAM). Attachment kinetic analysis reveals that the early attachment is mediated mainly via an interaction with heparan sulfate, followed by a gradual increase in interaction with sialoadhesin. By using the CHO cells and CHO mutant cells which are deficient in heparan sulfate expression, it has been shown that heparan sulfate alone is sufficient to mediate PRRSV attachment, but not entry, and sialoadhesin functions as a PRRSV internalization receptor.[344] Recently, Calvet *et al* used a cDNA library derived from PAM cells to identify CD163 as the PRRSV receptor.[345] Transfection of CD163 cDNAs to PRRSV nonsuceptible cells successfully confers susceptibility to the virus and yields a high titer of progeny viruses.[345] Further studies suggest that CD163, rather than being a receptor, functions as entry mediator involved in PRRSV uncoating, based on the observations that cells expressing recombinant sialoadhesin internalize PRRSV without uncoating the virus; whereas cells expressing both recombinant sialoadhesin and CD163 show virus uncoating upon internalization.[346] In the current model for PRRSV infection of porcine macrophages, PRRSV first binds to its attachment factor, heparan sulfate, followed by a more stable interaction involving sialic acids present on the virion and the N-terminal sialic acid-binding domain of sialoadhesin.[347-350] The sialoadhesin mediates the virus internalization process and CD163 is involved in virus uncoating.[346]

It has been reported that the receptor for LDV, another member of the family *Arteriviridae,* on macrophages correlated with the trypsin-sensitive molecule.[351] Inada

and Mims *et al* (1984 and 1985) suggested that the I region-coded antigens (Ia) might be involved in LDV entry because most Ia-positive cells were LDV infected and treatment with trypsin subsequently removed the Ia antigens and simultaneously abolished susceptibility to LDV.[352-353] In contrast, Buxton *et al* (1988) reported that Ia is not the receptor by showing trypsin treatment of macrophages destroyed the LDV receptor with minimal loss of the Ia antigen.[354] Therefore, the receptor for LDV in the mouse macrophage is clearly not yet identified.

1.2.4 Viral proteins responsible for receptor binding

1.2.4.1 Enveloped viruses

Among the enveloped viruses, the spike glycoprotein or projected viral protein is normally responsible for binding to the host cells. Typically, they are oligomeric, type I integral membrane proteins that have the bulk of their mass outside the membrane with the receptor-binding domain exposed.[321]

The hemagglutinin (HA) in the envelope spikes of influenza A virus is the receptor-binding protein of the virus.[328] The HA has two peptide subunits called HA1 and HA2 and the entire HA spike is a trimer formed by three HA1/HA2 molecules. HA1 has a large globule located at the membrane-distal tip. Each of the three large globules from the trimer form a small pocket as the receptor binding domain. As previously discussed, distinct sialic acid linkage expression on host cells decide receptor specificity and generally prevent cross-species transmission; however, there are several other factors that also contribute to the capability of influenza virus to cross the species barrier. Studies have shown that HA can shift binding specificity between sialic acid-α-2,6-galactose and sialic acid-α-2,3-galactose with as few as two amino acid changes (position 182 and 192) and avian H5N1 influenza A viruses with dual specificity have been isolated.[355]

The envelope glycoprotein gp120 of HIV-1 is responsible for binding to the CD4 molecule on T cells. The gp120 binds to the most amino-terminal of the four immunoglobulin-like domains of CD4. The binding induces further conformational changes in gp120 to expose and form the binding sites for subsequent binding of specific chemokine co-receptors, CCR5 and CXCR4.[356] Mutagenesis in conserved gp120 residues reveals several important amino acids for CD4 binding.[357] Amino acid changes in two

hydrophobic regions (Thr-257 and Trp-427) and two hydrophilic regions (Asp-368, Glu-370 and Asp-457) result in significant reductions in CD4 binding.[358] A single amino acid (Trp-432) can abrogate CD4 binding and that mutant virus becomes non-infectious.[359] A recent study has shown that the gp120 contains four heparan sulfate binding regions and three of them are also involved in co-receptor binding.[360]

1.2.4.2 Non-enveloped viruses

In the case of nonenveloped viruses, the attachment depends on whether the virus has spikes or not. Adenoviruses have a triple helix spike which is formed from three identical fiber proteins. The C-terminal amino acids of each fiber form globular shapes that together create a knob with a deep indentation on its exterior surface. The different subgroups of the virus that recognize a given cell surface receptor have a distinctive set of amino acids in the knob indentation, suggesting that is the site for attachment.[361]

All the other nonenveloped viruses that lack spikes use their capsids to directly interact with the host cell receptors. The family *Picornaviridae* is the best studied example to demonstrate this interaction. Poliovirus is a member of the family *Picornaviridae* and the causative agent of poliomyelitis. The icosahedral symmetrical capsid of poliovirus is composed of 60 copies of 4 viral proteins (VP1, VP2, VP3, and VP4).[362] The capsid surface is corrugated. It has a prominent star-shaped peak at the 5-fold axis of symmetry, surrounded by a deep "canyon". The canyon is considered the receptor binding position. [363]

1.2.4.3 Arteriviruses

Among the four members in the family *Arteriviridae,* PRRSV has been studied extensively to identify viral proteins associated with the receptors. The structural M protein and the M-GP5 complex were reported to contribute to PRRSV attachment to a heparin-like receptor on porcine alveolar macrophages.[341] Sialoadhesin was previously shown to be a sialic acid-binding lectin.[364] When sialic acid was removed from the PRRSV virion surface, virus infection was almost completely blocked and virus attachment was reduced up to 50%. These data indicate that sialic acid on viral glycoprotein rather than viral protein itself may mediate virus attachment to sialoadhesin.[347]

In the case of LDV, the cysteine residue in the short N-terminal ectodomain of the envelope protein M forms an intermolecular disulfide bridge with the cysteine residue in the ectodomain of the major envelope protein VP-3 (equivalent to GP5 of PRRSV and EAV). Treatment of LDV virions with 5 to 10 mM dithiothreitol, which is known to reduce disulfide bonds, can reduce the LDV infectivity quickly and irreversibly.[365] These data suggest that the heterodimers of the M protein and the VP-3 glycoprotein are important for receptor binding.

Although it has been speculated that the major glycoprotein in arteriviruses is involved in receptor binding, direct experimental evidence using chimeric viruses containing envelope protein sequences from other arteriviruses have led to the opposite conclusion. In one experimental study, ectodomains of EAV GP5 and M were replaced with sequences from envelope proteins of other arteriviruses and unrelated RNA viruses. The only viable chimeras were those containing the GP5 ectodomains from porcine (PRRSV) or mouse (LDV) arteriviruses. These chimeric viruses can infect RK-13 and BHK-21 cells which are susceptible to EAV but nonsusceptible to PRRSV or LDV.[291] This implies that the ectodomain of GP5 of EAV is not the receptor binding domain in cell culture as expected. Similarly, PRRSV mutants in which the ectodomain of the M protein was replaced by that of other arteriviruses maintained the original cell tropism.[292] The available data of the EAV minor envelope glycoproteins $GP2_b$, GP3, and GP4 suggest that this complex is likely to mediate the initial virus attachment to host cell surface since noninfectious viral particles are produced in the absence of the $GP2_b$, GP3, or GP4 protein, although detailed experiments have not been performed.[262,268,293] A recent study using immunoprecipitation has shown that PRRSV scavenger receptor CD163 interacts with GP2 and GP4.[366]

It has been shown that interaction among all minor (GP2, GP3, and GP4) and major (GP5 and M) enveloped proteins of EAV plays a major role in determining the $CD14^+$ monocyte tropism while the tropism for $CD3^+$ T lymphocytes was determined by GP2, GP4, GP5, and M envelope proteins but not the GP3 protein.[367] Most recently, reverse genetic studies have shown that the minor envelope proteins (GP2, GP3, GP4, and E) play a critical role as viral attachment proteins for EAV.[294]

1.3. Scope and outline of dissertation

Viral respiratory diseases can present a significant threat to both animal and human health. The overlapping clinical presentation of various respiratory infections makes it difficult to predict the pathogens solely based on clinical signs or symptoms. The real-time reverse transcription polymerase chain reaction (rRT-PCR) has become one of the most commonly used methods in molecular diagnostics and research. This molecular technique provides fast, sensitive, and specific detection of viral nucleic acid in clinical specimens and thus becomes an indispensable tool for diagnosing important animal viral pathogens. A number of equine bacterial and viral pathogens cause respiratory infections in horses. Therefore, there is an urgent need for the detection and accurate identification of the viral respiratory pathogens involved in determinating the most appropriate quarantine and control measures to prevent the spread of different viral respiratory diseases.

As an obligatory intracellular infectious agent, viruses can only replicate inside of living cells or organisms. Therefore, successful infection depends on complex interaction between host and virus. At the molecular level, interactions that occur between cellular and viral gene products are the first step of virus infection and determine the host tropism of the infection. Thus, elucidating the functional roles that viral proteins play during productive viral infection as well as identifying the cellular molecules involved in virus interaction is critical in preventing and treating viral diseases.

The objective of this project was to develop highly sensitive and specific real-time PCR assays for the detection of different equine respiratory viruses, and to study the role of major envelope viral protein GP5 and M, as well as minor envelope protein E using infectious cDNA clones, and study the importance of heparin in EAV attachment and entry. Assays using rRT-PCR for the detection of the common equine viral pathogens equine arteritis virus (EAV), equine influenza virus, and equine rhinitis viruses A and B were developed, optimized, and validated. This provides the clinician and diaganostician with their capability to detect these common equine pathogens within a very short period of time. Furthermore, we investigated the functional analysis of viral proteins in relation to cellular tropism using a full-length infectious cDNA clone and reverse genetic systems.

The interactions of viral major and minor structural proteins that determine the host cell tropism are discussed and the role of heparin as an attachment molecule is then addressed. Development of diagnostic methods as well as understanding how cellular proteins interact with viral proteins will allow for a better understanding of viral pathogenesis and disease prevention and control.

Chapter one, literature review, provides a broad prespective on the molecular diagnostic methods and molecular biology of EAV.

Chapter two compares the two published real-time reverse transcription polymerase chain reaction assays for the detection of equine arteritis virus nucleic acid in equine semen and tissue culture fluid. The specificity and sensitivity of these two molecular-based assays were compared to traditional virus isolation (VI) in cell culture. The results revealed that the T1 assay developed by Balasuriya *et al* (2002) has a better sensitivity compared to the T2 assay developed by Westcott *et al* (2003), but was still less sensitive than the gold standard virus isolation test. The results of this study underscore the importance of comparative evaluation and validation of real-time RT-PCR assays prior to their recommended use in a diagnostic setting for the detection and identification of specific infectious agents.

Chapter three describes the development and evaluation of one-step TaqMan® real-time reverse transcription-PCR assays targeting NP, M, and HA genes of equine influenza virus. A total of eight rRT-PCR assays were developed and none of the eight assays cross-reacted with any of the other known equine respiratory viruses. All three rRT-PCR assays targeting the current circulating equine influenza virus H3N8 subtype have greater specificity and sensitivity than virus isolation by egg inoculation (93%, 89%, and 87% sensitivity for EqFlu NP, EqFlu M, and EqFlu HA3 assays, respectively). Comparison of the sensitivities of rRT-PCR assays targeting the NP and M genes of both subtypes with egg inoculation and the Directigen Flu A test clearly shows that molecular assays provide the highest sensitivity.

Chapter four describes the application of three H3N8 specific equine influenza real-time RT-PCR assays targeting the nucleoprotein (NP), matrix (M), and hemagglutinin (HA) genes of equine influenza virus (EIV NP, EIV M, and EIV HA3

assays) for the detection of canine influenza virus (CIV) in clinical specimens. The findings demonstrate that previously described real-time RT-PCR assays targeting NP, M, and H3 HA gene segments of H3N8 EIV are also valuable for the diagnosis of CIV infection in dogs. The assays should expedite the detection and identification of CIV.

Chapter five describes the development of one-step TaqMan® real-time reverse transcription-PCR and conventional reverse transcription PCR assays for the detection of equine rhinitis A and B viruses. The assays targeting the 5′UTR or polymerase regions of rhinitis A and B regions are able to differentiate these two viruses and detect archived viruses. They provide fast and reliable detection methods for equine rhinitis A and B viruses.

Chapter six describes the generation of a panel of chimeric viruses by swapping the N-terminal ectodomains and full-lengths of the two major envelope proteins (GP5 and M) from porcine reproductive and respiratory syndrome virus (PRRSV). The recombinant viruses expressing the N-terminal ectodomain of PRRSV GP5 or M or together (GP5ecto, Mecto, and GP5&Mecto, respectively) in the EAV backbone were viable and genetically stable for more than 10 serial passages in BHK-21 cells. Compared to the parental virus, these three chimeric viruses produced lower titers and smaller plaque sizes indicating that although the viruses are genetically stable, they have a crippled phenotype and are unable to replicate and spread as efficiently as the parental virus. These chimeric viruses were further tested in different EAV or PRRSV susceptible cell lines to evaluate the progeny virus cellular tropism and infectivity. Interestingly, the three chimeric viruses containing the GP5 and/or M ectodomains could only infect EAV susceptible cell lines but not pig alveolar macrophage cells in which PRRSV infects and replicates efficiently. Therefore, the exchange of GP5 and/or M protein N-terminal ectodomains from PRRSV (individual or double) could not alter the cellular tropism of the chimeric viruses.

Chapter seven investigates the role of one of the minor envelope proteins (E) in virus attachment and entry. The data from this study showed that EAV infection of equine endothelial cells is heparin-dependent. Sequence analysis revealed that the C-terminus of E protein contains a putative heparin-binding domain. By using site-directed mutagenesis, we generated a panel of arginine to glycine mutations at the conserved

region in both the full-length EAV cDNA clone and individual E protein expression constructs. The mutant cDNA clones R52G; R57G; R52;60G; R57;63G; and R63,65G have a similar growth pattern and plaque morphology compared to the wild type control. In contrast, the triple mutation R52,60,65G construct grew significantly slower and produced much smaller plaques. When these mutations were introduced in the individual E protein expression construct, double mutant R52,60G completely blocked the interaction between E protein and heparin. Taken together, these data showed that E protein interacts with heparin to facilitate virus attachment and play a major role in EAV infection.

CHAPTER TWO

Comparison of two real-time reverse transcription polymerase chain reaction assays for the detection of equine arteritis virus nucleic acid in equine semen and tissue culture fluid

J Vet Diagn Invest 20:147–155 (2008)
Reprinted with permission

2.1. SUMMARY

Two previously developed TaqMan® fluorogenic probe-based one-tube real-time reverse transcription polymerase chain reaction (real-time RT-PCR) assays (T1 and T2) were compared and validated for the detection of equine arteritis virus (EAV) nucleic acid in equine semen and tissue culture fluid (TCF). The specificity and sensitivity of these two molecular-based assays were compared to traditional virus isolation (VI) in cell culture. The T1 real-time RT-PCR had a higher sensitivity (93.4%) than the T2 real-time RT-PCR (42.6%) for detection of EAV RNA in semen. However, the T1 real-time RT-PCR was less sensitive (93.4%) than the World Organization for Animal Health (OIE)-prescribed VI test (gold standard). The sensitivity of both PCR assays was high (100.0% [T1] and 95.2% [T2]) for detecting EAV RNA in TCF. In light of the discrepancy in sensitivity between either real-time RT-PCR assay and VI, semen that is negative for EAV nucleic acid by real-time RT-PCR should be confirmed free of virus by VI. Similarly, the presence of EAV in TCF samples that are VI-positive but real-time RT-PCR–negative should be confirmed in a one-way neutralization test using anti-EAV equine serum or by immunofluorescence assay using monoclonal antibodies to EAV. If the viral isolate is not identified as EAV, such samples should be tested for other equine viral pathogens. The results of this study underscore the importance of comparative evaluation and validation of real-time RT-PCR assays prior to their recommended use in a diagnostic setting for the detection and identification of specific infectious agents.

2.2. INTRODUCTION

Equine arteritis virus (EAV) is an enveloped, positive-stranded RNA virus in the family *Arteriviridae*, order *Nidovirales*.[255] It is the causative agent of equine viral arteritis (EVA), a contagious disease of horses and other equid species.[212,257] Serologic surveys have confirmed EAV infection in equine populations in North and South America, Europe, Australia, Africa, and Asia.[34,213-216,218,368] However, the seroprevalence of EAV infection of horses varies between countries and different breeds within countries.[34,213] The majority cases of primary EAV infection are asymptomatic.[230] Occasionally infected animals will develop clinical signs of disease. The most common clinical manifestations of EVA include anorexia, depression, fever, and dependent limb edema, and less frequently, ocular and nasal discharge and conjunctivitis. EAV infection may also result in abortion in pregnant mares and interstitial pneumonia or pneumoenteritis in very young foals.[34,369] A variable percentage (up to 10-70%) of acutely infected stallions can become persistently infected and continue to shed virus in their semen.[34,223] Carrier stallions are the natural reservoir of EAV; they ensure the virus is maintained in equine populations between breeding seasons.[34] Furthermore, the long term carrier state in the stallion enables the generation of genetic heterogeneity within the virus that helps to distinguish field strains of EAV.[35,226-227] The two principal modes of transmission of EAV are horizontal, by direct contact with infectious respiratory tract secretions from acutely infected horses, and venereal through natural breeding or artificial insemination with infective semen from persistently infected stallions.[228-231] The continued growth in international trade in horses and semen has served as a significant means of dissemination of EAV strains around the world.[34,216,223,228,231] Identification of the carrier stallion is therefore of critical epidemiological influence in the prevention and control of EAV infection.[34,229-230]

The EAV genome consists of two large replicase genes (open reading frame [ORFs] 1a and 1b) and partially overlapping structural genes (ORFs 2a, 2b, 3-7).[256,320] The EAV RNA is encapsidated by the nucleocapsid protein (N; encoded by ORF7) into an icosahedral core that is surrounded by an envelope containing six structural proteins. Two major envelope proteins of EAV, large glycosylated protein (GP_5; ORF5) and

nonglycosylated membrane protein (M; ORF6), form a covalently linked heterodimer in the virion.[266] In addition to these, small envelope protein E (ORF2a) and three minor glycoproteins named GP_2, GP_3, and GP_4 (ORFs 2b, 3, and 4, respectively) also contribute to the viral particle formation.[256,262] The latter three proteins form a covalently linked heterotrimer in the virion.[320,370]

A definitive diagnosis of EVA is based on isolation of EAV in cell culture, detection of viral nucleic acid by RT-PCR assay, or by serologic means based on testing paired (acute and convalescent) serum samples.[34,229-230,371] Detection of EAV in the semen of carrier stallions is frequently determined by virus isolation (VI) in cell culture or much less frequently, by breeding a stallion to two seronegative mares and testing for development of an antibody response after 28 days.[34,371] Virus isolation is currently the World Organization for Animal Health (OIE)-approved gold standard for the detection of EAV in semen and is the prescribed test for international trade. Isolates of EAV from clinical specimens, including semen, are often confirmed in a one-way neutralization assay using polyclonal equine sera raised against the prototype Bucyrus strain of EAV or by immunofluorescent assay using monoclonal antibodies to EAV.[371-372] These methods, although of proven reliability, are time-consuming, expensive, and cumbersome. The availability of modern nucleic acid-based assays has revolutionized diagnostic testing of clinical specimens for many infectious disease agents.[5,183,188,373-379] Compared to traditional virus isolation, these assays are frequently more sensitive, less expensive, and less time-consuming.[5,183,374-375] Sensitive standard RT-PCR, RT-nested PCR (RT-nPCR), and real-time RT-PCR assays have been developed for the detection of EAV nucleic acid in tissue culture fluid (TCF), nasal secretions, and semen, and these assays are being increasingly used for routine diagnostic purposes.[219,373,376,379-383] However, further validation of most of these assays is needed before they can be fully accepted as providing equivalent reliability to VI in cell culture for the detection of EAV.

The development of two TaqMan® fluorogenic probe-based one-tube real-time PCR assays for the detection of EAV nucleic acid has been previously described.[373,379] The purpose of the present study was to compare the specificity and sensitivity of these specific real-time PCR assays to each other as well as to VI for the detection of EAV in

semen and in TCF. The analytical sensitivity of these 2 assays was also established by using in vitro transcribed (IVT) EAV RNA containing the complete region of ORF7 and flanking portion of ORF6 and 3' nontranslated region (3' NTR) of the virus.

2.3. MATERIALS AND METHODS

Equine semen samples, viruses, and cells

Three hundred raw equine semen samples received between April 2006 and May 2007 by the OIE EAV Reference Laboratory at the Maxwell H. Gluck Equine Research Center, University of Kentucky, were tested for the presence of EAV by VI and EAV nucleic acid by 2 previously referenced real-time TaqMan® RT-PCR assays.[373,379] A total of 155 tissue culture fluid (TCF) samples were included in the study. These comprised one sample containing the modified live virus (MLV) vaccine strain of EAV (ARVAC®),[a] 61 samples containing North American and European strains of EAV, 77 EAV negative samples, and 16 TCF samples containing a variety of other equine viral pathogens. All EAV-positive TCF samples used in the present study were previously confirmed to contain EAV in a one-way serum neutralization assay using polyclonal anti-EAV equine serum or by immunofluorescent assay using monoclonal antibodies to GP_5 of EAV.[371-372] These included TCF samples containing 25 archived EAV field isolates from the OIE Reference Laboratory at the Gluck Center, and TCF samples containing 36 strains of EAV collected at the Animal Health Diagnostic Center, New York College of Veterinary Medicine, Cornell University. The TCF samples included representation of North American and European strains of EAV.[35,226-228,384-385] To determine the specificity of these 2 real-time PCR assays, TCF containing the following equine viral pathogens were included in the study: equine herpesviruses 1-5 (EHV-1 [ATCC VR-700],[b] EHV-2 [ATCC VR-702], EHV-3 [ATCC VR-352],[b] EHV-4 [ATCC VR-2230],[b] and EHV-5[386]); equine rhinitis virus A (NVSL-0600EDV8501)[c] and B (NVSL-0610EDV85010)[c]; equine adenovirus 1 (NVSL-001EDV8401)[c] and 2; equine influenza virus type A1 (equine-1/Prague/1/56 [H7N7]; ATCC VR-297)[b] and A2 (equine/Miami1/63/ [H3N8; NVSL-060IDV0501],[c] equine/Kentucky/81 [H3N8; NVSL-040IDV0001],[c] equine/Alaska/

29759/91 [H3N8; NVSL-020IDV9101])[c]; and Salem virus, a novel paramyxovirus of horses.[387]

The low passage RK-13 cell line (ATCC CCL37; passage level 194-204)[b] and high passage RK-13 cell line (RK-13 KY; passage level 399-409) were maintained in Eagle's minimum essential medium (EMEM)[d] supplemented with 10% ferritin-supplemented bovine calf serum (FSCS),[e] 1% penicillin and streptomycin,[d] and 0.1% amphotericin B (1,000 μg/ml).[d] The overlay medium used for inoculated cultures was of 0.75% carboxymethyl cellulose (CMC)[f] in supplemented EMEM.

Virus isolation

Isolation of EAV from equine semen samples was attempted in both high and low passage RK-13 cell lines according to the standard laboratory protocol used by the OIE Reference Laboratory.[371] Briefly, semen samples were sonicated for 45 sec (3 × 15 sec), and sperm and cellular debris were sedimented by centrifugation (2800 × g, 10 min) at 4 °C. Serial decimal dilutions (10^{-1}-10^{-3}) of the supernatant of each sample were made in supplemented EMEM and 1 ml of each dilution was inoculated into each of 2 × 25-cm^2 flasks containing confluent monolayers of RK-13 cells. Flasks were incubated at 37 °C for 1 hr before being overlaid with supplemented EMEM containing 0.75% CMC. Flasks were incubated at 37 °C and checked for the appearance of cytopathic effect (CPE) on postinoculation days 3 and 4. If there was no detectable CPE, a second blind passage was performed on day 4. The RK-13 cell monolayers were fixed and stained with a 1% crystal violet solution containing 1% formaldehyde on postinoculation day 5 for the first passage and postinoculation day 4 for the second passage in cell culture.

RNA isolation

Viral nucleic acid was directly isolated from semen and TCF samples using a commercial kit.[g,384] Briefly, semen or TCF samples were microcentrifuged at 13,800 × g for 2 min, and 140 μl of supernatant was removed and used for nucleic acid extraction according to the manufacturer's instructions. The viral nucleic acid was eluted in 60 μl of nuclease free water and stored at -80 °C.

Generation of in vitro transcribed RNA

The analytical sensitivity of the 2 real-time TaqMan RT-PCR assays was determined using a decimal dilution series (10^1-10^{10} molecules/reaction) of in vitro transcribed (IVT) EAV RNA containing complete ORF7 and the flanking regions of ORF6 and 3' NTR of EAV genome. Briefly, a 636-bp fragment of EAV (nucleotide [nt] 12069-12704; numbered according to GenBank accession number Y07862[261]) was PCR amplified from the plasmid containing the complete genomic sequence of the virulent Bucyrus strain of EAV (pEAVrVBS)[388] using primers 12069P ([12069-12088] 5'TTTGTTATAGTTGGAAGAGC3') and 12704N ([12681-12704] 5'GGTTCCTGGGTGGCTAATAACTAC3'), and cloned into the pDrive cloning vector according to the manufacturer's instructions.[h] The plasmids were purified using a commercial kit,[i] and the authenticity and orientation of the insert was determined by sequencing both strands of DNA with T7 and SP6 reverse and forward primers. Following sequencing, the recombinant plasmid with ORF7 and flanking ORF6 and 3' NTR sequence downstream of the SP6 promoter was named pORF7.SP6 and used to generate IVT ORF7 RNA. Runoff pORF7.SP6 RNA transcripts were generated from *Bam* HI-linearized pORF7.SP6 plasmid according to a previously described protocol.[384] Briefly, a 50 µl reaction volume containing 2 µg of *Bam* HI-linearized pORF7.SP6 plasmid DNA; 2.5 µl of RNAguard™ RNase inhibitor (37 U/µl)[j]; 5 µl of $m^7G(5')PPP(5')G$ RNA cap structure analogue[k]; 5 µl of ribonucleotides ATP (adenosine 5'-triphosphate), CTP (cytidine 5'-triphosphate), GTP (guanosine 5'-triphosphate), and UTP (uridine 5'-triphosphate; 10 mM each mix)[l]; 2.5 µl of 100 mM dithiothreitol (DTT)[m]; 2.5 µl of SP6 RNA polymerase[m]; and 1 × transcription buffer[m] was incubated at 37 °C for 2 hr. The template plasmid DNA was then digested with RNase-free DNase I.[n] The RNA transcripts were purified using a commercial column,[o] eluted in 50 µl of water, and quantified by spectrophotometrical analysis. The IVT ORF7 RNA was stored at -80 °C until used. The concentration of the IVT ORF7 RNA molecules per microliter was calculated according to the following formula:

No. of IVT ORF7 RNA molecules/µl = $\frac{\text{Avogadro number } (6.022 \times 10^{23}) \times \text{IVT ORF7 RNA concentration (g/µl)}}{\text{IVT ORF7 RNA molecular weight (g)}}$

The dilution of RNA transcripts (10^1-10^{10} molecules) was carried out in RNase- and DNase-free molecular biologic grade water containing 0.1 mg/ml acetylated BSA[m] and 0.74 U/µl RNAguard™ RNase inhibitor.[j]

Real-time TaqMan RT-PCR assays

A one-tube real-time TaqMan RT-PCR assay was performed using the TaqMan® One-Step RT-PCR Master Mix[p] in a 7500 Fast Real-Time PCR System.[q] The primers and probes used in the 2 assays were identical to those previously for each respective assay (Table 2.1).[373,379] Every sample was tested in duplicate in each assay. Briefly, 25 µl of RT-PCR mixture for each reaction contained 12.5 µl of 2 × Master Mix without UNG (uracil-N-glycosylase), 40 × MultiScribe and RNase Inhibitor Mix, 900 nM of forward and reverse primers (0.45 µl), 250 nM probe (0.625 µl), nuclease free water (5.35 µl), and 5 µl of test sample RNA. The following thermocycling conditions were used under standard mode as per manufacturer's recommendation: 30 min at 48 °C, 10 min at 95 °C, followed by 40 cycles at 95 °C for 15 sec and 60 °C for 1 min. Each RT-PCR run included a control without RNA (containing the reaction mix with 5 µl of water [no template control]) and positive controls containing IVT ORF7 RNA. The analytical sensitivity of each real-time PCR assay was determined using IVT ORF7 RNA.

Statistical analysis

Statistical evaluation of the performance of semen and TCF-based real-time PCR assays for the detection of EAV nucleic acids was carried out to estimate and compare the sensitivity, specificity, accuracy, and reproducibility of the T1 and T2 real-time PCR assays in relation to VI. For the purpose of the analysis, T+ denotes a positive real-time PCR test result and I+ denotes a VI-positive specimen, with T- and I- denoting a negative real-time PCR test result and a VI-negative specimen, respectively. Accordingly, the sensitivity (Se) of either diagnostic test is the likelihood that an EAV carrier stallion tests positive, namely Se = Pr(T+|I+), and its specificity (Sp) is Sp = Pr(T-|I-). Accuracy is

defined as the likelihood of a correct test result; this is a composite measure of diagnostic performance based on both sensitivity and specificity. Test repeatability was characterized by the coefficients of variation when duplicates of serial decimal molecule dilutions (10^1-10^{10}) of IVT ORF7 RNA were used in five independent assays.

Sensitivity, specificity, and accuracy were calculated using Clopper-Pearson 95% exact binomial confidence intervals.[389] Exact binomial methods were also used to test the hypothesis of equal sensitivity (i.e., that $Se_1 = Se_2$) versus the two-sided alternative for the semen and tissue culture fluid PCRs. Empirical coefficients of variation (CV) were calculated as the sample standard deviation divided by the sample mean. Statistical significance was set at $\alpha = 0.05$. The analysis was performed using the S-Plus 8.0[r] and Minitab 15[s] software packages.

Table 2.1. Primers and probes used in the T1 and T2 real-time reverse transcription polymerase chain reaction (RT-PCR) assays.

Assay name	Primer or probe	Sequence 5' to 3' (nucleotide location‡)	Length of fragment (bp)	Reference no.
T1 real-time RT-PCR	Forward primer: EAV7.53F	GGCGACAGCCTACAAGCTACA (12,365-12,385; ORF7)	204 (12365-12568)	4
	Reverse primer: EAV7.256R	CGGCATCTGCAGTGAGTGA (12,550-12,568; ORF7)		
	Probe: EAV7.92P	*TTGCGGACCCGCATCTGACCAA† (12,404-12,425; ORF7)		
T2 real-time RT-PCR	Forward primer: EAV10F	GTACACCGCAGTTGGTAACA (12,284-12,303; ORF6)	399 (12284-12682)	50
	Reverse Primer: EAV12R	ACTTCAACATGACGCCACAC (12,663-12,682; 3' NTR)		
	Probe: EAV11P	*TGGTTCACTCACTGCAGATGCCGG† (12,546-12,569; ORF7)		

* Reporter dye (FAM; 6-carboxyfluorescein) labeled nucleotide.

† Quencher dye (TAMRA; 6-carboxy-tetramethyl-rhodamine) labeled nucleotide.

‡ Numbered according to GenBank accession no. Y07862[261].

2.4. RESULTS

Analytical sensitivity of the two real-time RT-PCR assays

In order to determine the analytical sensitivity of the 2 real-time PCR assays in detecting EAV nucleic acid, serial decimal molecule dilutions (10^1-10^{10}) of IVT ORF7 RNA containing EAV ORF7 with flanking regions of ORF6 and 3' UTR were tested in duplicate. The assays were repeated five times, each time with freshly diluted IVT ORF7

RNA. The IVT ORF7 RNA molecule numbers were calculated based on the molecular weight and concentration of the IVT RNA. Regression analysis confirmed linearity in both assays (T1: $R^2 = 0.9984$; T2: $R^2 = 0.9979$; Fig 2.1). The T1 real-time PCR was linear over the full molecule range tested (10^1-10^{10}) with high reproducibility and a mean CV ranging from a low value of 0.32% to a high of 3.18%. While the T2 real-time PCR was also linear, the analytical sensitivity of this test was only 10^2 molecules of IVT RNA. The range of nine orders of magnitude (10^2-10^{10} molecules) detected by the T2 real-time PCR was reproducible with a mean CV from a low value of 1.39% to a high of 9.55%. The T1 real-time PCR always had a lower cycle threshold (Ct) value than the T2 real-time PCR over all the IVT RNA dilutions tested. These data indicate that the T1 real-time PCR has a higher analytical sensitivity than the T2 real-time PCR.

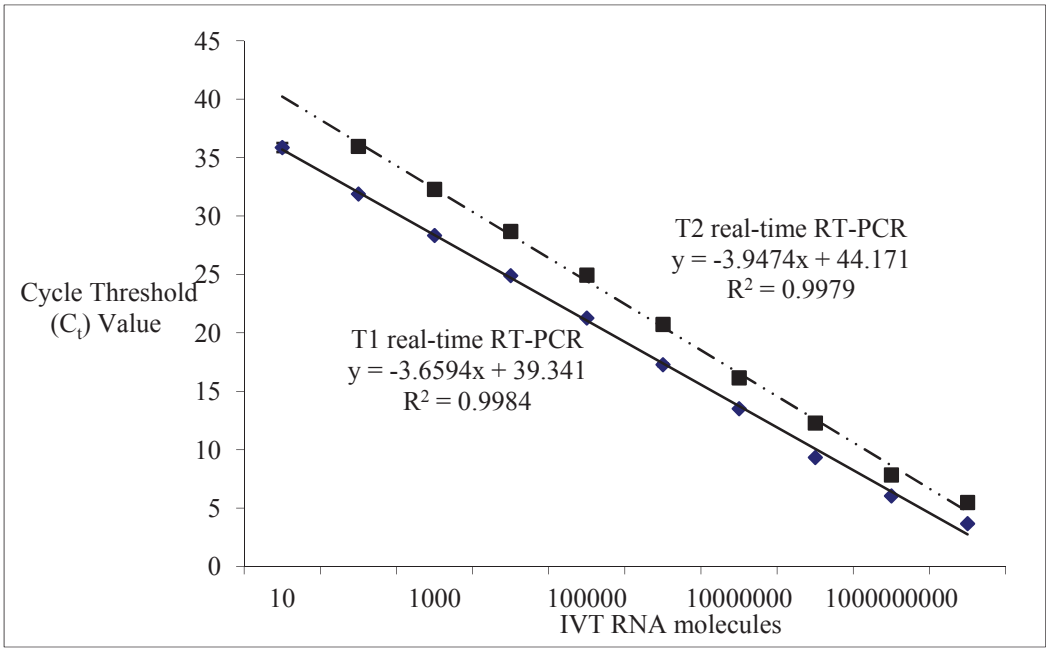

Fig 2.1. Comparison of analytical sensitivity between the two real-time reverse transcription polymerase chain reaction assays, T1 (y = –3.6594x + 39.341, $R^2 = 0.9984$) and T2 (y = –3.9474x + 44.171, $R^2 = 0.9979$), using in vitro transcribed ORF7 RNA.

Evaluation of the two real-time RT-PCR assays for detection of EAV in TCF samples

Nucleic acids extracted from a total of 155 TCF samples were tested by these 2 real-time PCR assays. Of the TCF samples positive for infectious EAV, 62 (62/62) and 59 (59/62) were positive by the T1 real-time PCR and T2 real-time PCR, respectively (Table 2.2). There is no significant difference between the sensitivity of both assays when RNA from TCF containing EAV was evaluated (p = 0.248). Sensitivity of the T1 real-time PCR for detecting EAV nucleic acid in TCF was 100.0% (95% confidence interval [CI]: 95.3-100.0%) whereas the sensitivity of the T2 real-time PCR was 95.2% (95% CI: 86.5-99.0%; Table 2.3). There was no detectable fluorescence signal in the non-template controls containing molecular biologic grade water nor in the tubes that contained nucleic acid from other viral pathogens, confirming that both assays were highly specific (100%) for the detection of EAV nucleic acid. In terms of accuracy, the T1 real-time PCR correctly diagnosed 155 out of 155 samples, providing an accuracy of 100.0% (exact 95% CI: 98.1-100.0%). In the case of the T2 real-time PCR, it correctly diagnosed 152 out of 155 samples, providing an accuracy of 98.1% (exact 95% CI: 94.4-99.6%).

Table 2.2. Detection of equine arteritis virus (EAV) nucleic acid in semen and tissue culture fluid (TCF) using the T1 and T2 real-time reverse transcription polymerase chain reaction (RT-PCR) assays

Sample type (number of samples analyzed)	Virus isolation*		T1 real-time RT-PCR[4]		T2 real-time RT-PCR[379]	
	Positive	Negative	Positive	Negative	Positive	Negative
Semen samples (n = 300)	61	239	57	243	26	274
Tissue culture fluid (n = 155)†	62	93	62	93	59	96

* Virus isolation attempted in 2 rabbit kidney cell lines (RK-13; ATCC CCL37 and RK-13 KY) and confirmed by one-way neutralization assay.

† EAV positive and negative TCF.

Table 2.3. Sensitivity, specificity, and accuracy of two real-time reverse transcription polymerase chain reaction (RT-PCR) assays for detection of equine arteritis virus in tissue culture fluid as compared to virus isolation.

	T1 real-time RT-PCR[4] (%)	T2 real-time RT-PCR[379] (%)
Sensitivity	100.0	95.2
95% CI*	95.3-100.0	86.5-99.0
Specificity	100.0	100.0
95% CI	96.8-100.0	96.8-100.0
Accuracy	100.0	98.1
95% CI	98.1-100.0	94.4-99.6

* Confidence interval.

Evaluation of the two real-time RT-PCR assays for the detection of EAV nucleic acid in semen samples

Of the 300 equine semen samples tested, 61 (61/300) were positive for EAV by VI isolation in the RK-13 cell lines (Table 2.2). When nucleic acid extracted from these semen samples was tested, 57 (57/300) and 26 (26/300) were positive for the presence of EAV RNA using the T1 real-time PCR and the T2 real-time PCR, respectively. The T2 real-time PCR assay had a significantly higher number of false negatives (35) as compared to the T1 real-time PCR assay (4). Of the four false-negative semen samples detected by the T1 real-time PCR, 3 had very low infectivity titers (1×10^1 to 4.5×10^1 pfu/ml). However, 1 semen sample had a moderate infectivity titer (2.9×10^3 pfu/ml).

When these 2 real-time PCR assays were subjected to the exact binomial test of equal sensitivity, the sensitivity of the respective assays was significantly different ($p < 0.001$). The sensitivity of the T1 real-time PCR in detecting EAV nucleic acid in semen was 93.4% (exact 95% CI: 84.1-98.2%), whereas the sensitivity of the T2 real-time PCR was much lower (42.6%; exact 95% CI: 30.0-55.9%; Table 2.4). There was no detectable fluorescence signal in non-template controls containing molecular biologic grade water

nor in the tubes containing RNA from the VI-negative semen samples, confirming that both assays were highly specific (100%) for the detection of EAV nucleic acid. Since the T1 real-time PCR correctly diagnosed 296 out of 300 samples, the accuracy of this assay was 98.7% (exact 95% CI: 96.6-99.6%), compared to the T2 real-time PCR, which correctly diagnosed 265 out of 300 samples for an accuracy of 88.3% (exact 95% CI: 84.1-91.7%).

Table 2.4. Sensitivity, specificity, and accuracy of two real-time reverse transcription polymerase chain reaction (RT-PCR) assays for detection of equine arteritis virus in semen as compared to virus isolation.

	T1 real-time RT-PCR[4] (%)	**T2 real-time RT-PCR[379] (%)**
Sensitivity	93.4	42.6
95% CI*	84.1-98.2	30.0-55.9
Specificity	100.0	100.0
95% CI	98.8-100.0	98.8-100.0
Accuracy	98.7	88.3
95% CI	96.6-99.6	84.1-91.7

* Confidence interval.

2.5. DISCUSSION

The one-tube real-time PCR assay for EAV provides a simple, rapid, and reliable method for the detection and identification of viral nucleic acid in equine TCF and semen. The real-time PCR has the following important advantages over the standard two-step RT-PCR: 1) eliminating the possibility of cross contamination between samples with previously amplified products since the sample tube is never opened; and 2) reducing the chance of false-positive reactions because the real-time PCR product is detected with a sequence specific probe. The original reports describing the respective real-time PCR assays to detect EAV nucleic acid suffered from the limitation that each study was based

on testing only a small number of samples (21 TCF and 20 semen samples in the T1 study;[373] 28 TCF and 33 semen samples in the T2 study[379]). Clearly, before recommending either real-time PCR assay as an alternative to VI for the detection of EAV in TCF and semen, each assay needed to be more comprehensively validated using a significantly larger number of specimens.

In the present study, the analytical sensitivity of the T1 real-time PCR and T2 real-time PCR assays were first evaluated using IVT ORF7 RNA. Both T1 real-time PCR and T2 real-time PCR assays were shown to have a very high analytical sensitivity for IVT ORF7 RNA, detecting 10 and 100 RNA molecules, respectively. The T1 real-time PCR was at least ten times more sensitive than the T2 real-time PCR and consistently had a lower Ct value with different IVT RNA concentrations. The difference in analytical sensitivity between these 2 assays is likely attributable to the size of the amplicons they generated. The T1 real-time PCR amplicon length was much shorter than the T2 real-time PCR amplicon (204 bp vs. 399 bp) which suggested that it was amplified more efficiently than the longer real-time PCR product. Furthermore, it has been reported that shorter PCR products are more responsive to reaction conditions and allow primers and probe to bind to the target molecule more efficiently.[390]

The primary goal of this study was to directly compare the diagnostic sensitivity and specificity of 2 published real-time PCR assays for the detection of EAV nucleic acid based on testing an extensive number of TCF and semen samples. With the exception of the primers and probe, all of the other test conditions were identical for both assays, which were performed in parallel at the same time. Under the conditions of this study, the T1 real-time PCR has a higher diagnostic sensitivity than the T2 real-time PCR in detecting EAV nucleic acid in semen (93.4% vs. 42.6%) and to a lesser degree in TCF (100.0% vs. 95.2%) using the TaqMan One-Step RT-PCR Master Mix Reagents kit.[p]

Several factors could have adversely affected the diagnostic sensitivity of the T2 real-time PCR assay, including the length of the real-time PCR product previously mentioned, nucleotide mismatch in the primer and probe binding regions, and the use of proprietary reagents and cycle parameters that are optimized for use with the ABI 7500 Fast Real-Time PCR system.[q] The authors aligned 54 EAV sequences available in

GenBank (nt # 12069 to 12645 [ORF6-ORF7]; data not shown) to determine the degree of conservation in the regions to which the primers and probe are directed in the 2 assays. The forward primer-binding region (nt # 12365-12385) of the T1 real-time PCR was highly conserved (no mismatches) among the aligned EAV strains. However, both reverse primer- (nt # 12550-12568) and probe- (nt # 12404-12425) binding regions had one nucleotide mismatch. The reverse primer-binding region (nt # 12663-12682) of the T2 real-time PCR was highly conserved (only 17 aligned sequences cover the 3' NTR). In contrast, the forward primer- (nt # 12284-12303) and probe- (nt # 12546-12569) binding regions had three and five nucleotide mismatches, respectively. This clearly suggests that with respect to field strains of EAV, the forward primer- and/or probe-binding regions targeted by the T2 real-time PCR is less conserved than the regions targeted by the T1 real-time PCR. It has been shown that a single nucleotide mismatch in the primer- or probe-binding site may have minimal or zero effect on PCR amplification or detection.[391-392] In contrast, three or four nucleotide mismatches at certain critical locations within the primer- or probe-binding region can have a considerable effect including complete failure of detection.[391-392] In light of this, the mismatches of the forward primer and probe within the T2 real-time PCR assay may have significantly reduced the efficiency of the PCR reaction, especially in the case of specimens containing low quantities of EAV nucleic acid. In order to compare the 2 assays in a standard and normalized manner, a commercial kit and manufacture's recommended real-time RT-PCR cycle parameters were used in this study. Therefore, the reagents and real-time RT-PCR cycle conditions used in this study were not identical to the original T2 assay. These modifications may also have contributed to the reduced sensitivity of the T2 assay.

There was good overall agreement between the T1 real-time PCR and the VI assay, which is the current gold standard for the detection of EAV in semen.[371] However, under the conditions of this study, the T1 real-time PCR was less sensitive (93.4%) than the VI assay for detection of EAV nucleic acid in semen. The sensitivity of the real-time PCR assay versus VI may be adversely affected by various factors including use of the one-step RT-PCR method, reaction conditions (e.g., Mg^{2+} concentration, annealing temperature), amount of virus in the original sample, RT-PCR inhibitory substances in certain samples, mutations in the primer- and probe-binding regions of the template (see

above), inefficient RNA extraction from semen samples, and the potential for RNA degradation before testing. The T1 real-time PCR assay was designed to balance both sensitivity and ease of use so that the procedure could be performed rapidly and on a large scale. A single-step real-time PCR was performed with a commercial kit and RT-PCR conditions pre-optimized by the manufacturer, notwithstanding the fact that the one-step method is reported to be less sensitive than a two-step RT-PCR procedure.[393] The T1 real-time PCR allows detection of EAV in clinical samples or TCF containing at least 50 viral RNA molecules per ml when 140 µl specimen is used for RNA extraction.[373] The titer of EAV in semen from carrier stallions can vary from 1×10^1 pfu/ml to $>10^5$ pfu/ml. Over 97% of the semen samples submitted to the OIE EAV Reference Laboratory contain at least 1.5×10^2 pfu/ml and the remaining samples contain $<1.5 \times 10^2$ pfu/ml. Three of the four false-negative semen samples in the T1 real-time PCR had very low infectivity titers ranging from 1×10^1 pfu/ml to 4.5×10^1 pfu/ml. Interestingly, all these semen samples were from stallions in the process of spontaneously clearing the carrier state. Notwithstanding their very low infectivity content, it was possible to isolate EAV in RK-13 cells from all three semen samples. The fourth false-negative semen sample was of poor quality in that a large amount of smegma-like material was present which may contain some unknown real-time PCR inhibitors. This clearly indicates that the T1 real-time PCR as described is less sensitive than VI attempted in RK-13 cells. In view of this finding, any semen sample negative in the T1 real-time PCR assay that is from an EAV-seropositive stallion should also be screened for virus in RK-13 cells.

It should be noted, however, that genomic variation among field isolates of EAV may reduce the accuracy of the real-time PCR, even when the primers and probe are based on the most conserved region of EAV genome (ORF7). Therefore, the presence of EAV in VI-positive but real-time PCR-negative TCF samples should be confirmed in a one-way neutralization assay using an EAV-positive antiserum or by immunofluorescent assay using monoclonal antibodies to GP_5 of EAV. If negative for EAV, such TCF samples should be tested for other equine viral pathogens.

In summary, 2 previously described real-time PCR assays were compared to each other, as well as to attempted VI in cell culture for the detection of EAV in TCF samples

and semen. The T1 real-time PCR had a higher sensitivity than the T2 real-time PCR in detecting EAV nucleic acid in TCF and semen samples. Neither real-time PCR was superior to the OIE-prescribed VI test (gold standard) for the detection of EAV in semen. In light of these findings, semen from an EAV-seropositive stallion that is negative for viral nucleic acid by real-time PCR should also be tested by VI. The findings of this study illustrate the importance of comparative evaluation and validation of real-time PCR assays prior to their recommended use in a diagnostic laboratory for the detection and identification of infectious agents.

Sources and manufactures

a. EAV modified live vaccine (Arvac®), Fort Dodge Animal Health, Fort Dodge, IA.

b. Equine herpesvirus-1, -2, -3, and -4, equine influenza virus type A1 and low passage RK-13 cell line, American Type Culture Collection, Manassas, VA.

c. Equine rhinitis virus A and B, equine adenovirus 1 and equine influenza virus type A2, National Veterinary Services Laboratory, Ames, Iowa.

d. Eagle's minimum essential medium, penicillin and streptomycin, and amphotericin B, Mediatech Inc., Herndon, VA.

e. Ferritin-supplemented bovine calf serum, Hyclone Laboratories. Inc., Logan, UT.

f. Carboxymethyl cellulose, Sigma-Aldrich, St Louis, MO.

g. QIAamp® Viral RNA isolation kit, Qiagen, Inc., Santa Clara, CA.

h. Qiagen PCR cloning kit, Qiagen, Inc., Santa Clara, CA.

i. QIAamp® Miniprep kit, Qiagen, Inc., Santa Clara, CA.

j. RNA guard, Amersham Bioscience, Pittsburgh, PA.

k. $m^7G(5')PPP(5')G$ RNA cap structure analogue, New England BioLabs, Beverly, MA.

l. 10 mM rATP, rCTP, rGTP, and rUTP, Amersham Bioscience, Pittsburgh, PA.

m. 100mM DTT, SP6 RNA polymerase, 1× transcription buffer and acetylated BSA, Promega Corp., Madison, WI.

n. RNase-free DNase I, Ambion, Austin, TX.

o. QIAamp® RNeasy Mini kit, Qiagen Inc., Santa Clara, CA.

p. TaqMan® One-Step RT-PCR Master Mix, Applied Biosystems, Foster City, CA.

q. 7500 Fast Real-Time PCR System, Applied Biosystems, Foster City, CA.

r. S-Plus 8.0, Insightful Corp., Seattle, WA.

s. Minitab 15, Minitab, Inc., State College, PA.

CHAPTER THREE

Development and evaluation of one-step TaqMan® real-time reverse transcription-PCR assays targeting nucleoprotein, matrix, and hemagglutinin genes of equine influenza virus

J Clin Microbiol. 2009 Dec;47(12):3907-13.

3.1. SUMMARY

The objective of this study was to develop and evaluate new TaqMan real-time reverse transcription-PCR (rRT-PCR) assays by the use of the minor groove binding probe to detect a wide range of equine influenza virus(EIV) strains comprising both subtypes of the virus (H3N8 and H7N7). A total of eight rRT-PCR assays were developed, targeting the nucleoprotein (NP), matrix (M), and hemagglutinin (HA) genes of the two EIV subtypes. None of the eight assays cross-reacted with any of the other known equine respiratory viruses. Three rRT-PCR assays (EqFlu NP, M, and HA3) which can detect strains of the H3N8 subtype were evaluated using nasal swabs received for routine diagnosis and swabs collected from experimentally inoculated horses. All three rRT-PCR assays have greater specificity and sensitivity than virus isolation by egg inoculation (93%, 89%, and 87% sensitivity for EqFlu NP, EqFlu M, and EqFlu HA3 assays, respectively). These assays had analytical sensitivities of >10 EIV RNA molecules. Comparison of the sensitivities of rRT-PCR assays targeting the NP and M genes of both subtypes with egg inoculation and the Directigen Flu A test clearly shows that molecular assays provide the highest sensitivity. The EqFlu HA7 assay targeting the H7 HA gene is highly specific for the H7N7 subtype of EIV. It should enable highly reliable surveillance for the H7N7 subtype, which is thought to be extinct or possibly still circulating at a very low level in nature. The assays that we developed provide a fast and reliable means of EIV diagnosis and subtype identification of EIV subtypes.

3.2. INTRODUCTION

Equine influenza (EI) is an acute, highly contagious viral respiratory disease of equids (horses, donkeys, mules and zebras) caused by infection with type A influenza virus.[394] Equine influenza virus (EIV) possesses a segmented (8 segments), single-stranded RNA genome of negative sense. The eight gene segments encode at least ten polypeptides: two envelope glycoproteins (hemagglutinin [HA] and neuraminidase [NA]), two matrix proteins (M1 and M2), two nonstructural proteins (NS1 and NS2/nuclear export protein), three proteins that make up the viral RNA polymerase (PB1, PB2 and PA) and the nucleoprotein (NP). Some strains of EIV also express a recently discovered PB1-F2 mitochondrial protein.[10,12] The first strain of EIV isolated in 1956 was of H7N7 configuration and designated influenza virus A/equine/Prague/56.[13-14] The last confirmed outbreak caused by an H7N7 subtype in horses was recorded in 1979.[13,16] A second EIV subtype, H3N8 was first isolated in 1963 and designated influenza virus A/equine/Miami/63.[15-16] This subtype has been associated with all confirmed outbreaks of equine influenza since 1980. Extensive antigenic drift has been detected in this virus over the years [17,22,395-399]. This led to categorization of H3N8 EIV isolates from around the world into two lineages: American and Eurasian lineages.[21-22] Currently, equine H3N8 influenza virus continues to be the most important equine respiratory pathogen of horses in many countries around the world. Equine influenza is considered endemic in the USA, UK and many other European countries.[400] New Zealand and Iceland are the only countries that have remained continuously free of equine influenza. In 2005, inter-species transmission of H3N8 EIV from horse to dog was reported for the first time.[24]

Influenza H3N8 virus spreads rapidly in susceptible horses and can result in very high morbidity within 24-48 hours after exposure to the virus. Outbreaks of clinically mild forms of influenza or subclinical infections have been reported among vaccinated horses that are incompletely protected. Furthermore, many of the clinical signs of EI resemble those caused by other equine viral respiratory pathogens such as equine herpesvirus-1 and -4 (EHV-1 and EHV-4), equine arteritis virus (EAV), equine rhinitis virus A and B, and equine adenoviruses.[6-7] In light of its clinical similarity to other equine respiratory diseases, a provisional diagnosis of equine influenza must be

confirmed by laboratory testing. The need to achieve a rapid diagnosis and to implement effective quarantine and movement restrictions are critical in controlling the spread of EI.

Traditionally, the gold standard laboratory test for the diagnosis of EI was attempted virus isolation (VI) from nasal swabs/washings in embryonated hens' eggs.[401] Following isolation, the virus was subtyped by means of the hemagglutination-inhibition test using sera specific for the H3N8 or H7N7 subtypes. These methods are time-consuming and cumbersome. In the past decade, antigen detection immunoassays such as the Directigen Flu A® test kit (Becton-Dickinson, Sparks, MD) and nucleic acid amplification based assays (standard reverse transcription PCR [RT-PCR] or real-time RT-PCR [rRT-PCR]) were developed and evaluated by various groups.[204,402-409] The antigen detection immunoassay kits are designed to detect the NP of both influenza A and B viruses.[16,402] Of the commercially available antigen detection immunoassays, the Directigen Flu A® test has been used for some considerable time to detect EIV in nasal swabs by certain laboratories.[402,407] While this assay has been found to be most useful as an initial screening test to confirm a diagnosis of EI during an outbreak, its limited sensitivity does not make it an ideal method for the diagnosis of EIV infection on an individual animal basis.[408] There have been several reports of the use of RT-PCR assays for the detection of influenza virus in clinical specimens,[403,406,409-410] however, such assays were not widely used for the routine diagnosis of this disease. This changed, however, following the introduction of EI into Australia in 2007, when a rRT-PCR developed to detect the avian influenza virus matrix gene, was used as the molecular diagnostic method of choice for EI.[409,411] That country now requires RT-PCR testing for EIV as part of both the pre-entry and post-entry system of quarantine and testing of horses from countries where EIV is endemic.[412] The objective of the current study was to develop several TaqMan® rRT-PCR assays capable of detecting a wide range of EIV strains comprising both subtypes of EIV without the inherent problems associated with the current laboratory diagnosis of EI. The approach taken was to develop new rRT-PCR assays using a TaqMan® minor groove binding (MGB™) probe targeting the NP, M, H3 and H7 HA genes of the virus. MGB™ rRT-PCR assays targeting the NP and M genes of EIV have not been previously reported. The assays were developed using the subtype prototype strains of EIV and then evaluated using archived strains of EIV and clinical

specimens. The overall goal was to identify which of these assays would be of greatest value for confirmation of a diagnosis of this infection.

3.3. MATERIALS AND METHODS

Viruses

EIV strains A/equine/Prague/56, A/equine/Alaska/91, A/equine/Kentucky/81 and A/equine/Miami/63 were obtained from the National Veterinary Service Laboratories (NVSL), Ames, IA (Table 3.1). Six EIV isolates A/equine/New York/73, A/equine/Kentucky/02, A/equine/Ohio/03, A/equine/Newmarket/2/93, A/equine/Aboyne/05 and A/equine/Richmond/07 were obtained from the OIE (World Organization for Animal Health) Reference Laboratory for EI at the Gluck Equine Research Center, University of Kentucky. In addition, 13 previously confirmed EIV isolates from the Livestock Disease Diagnostic Center, University of Kentucky and the Animal Health Diagnostic Center, New York State College of Veterinary Medicine, Cornell University were also included in the study. In order to determine the specificity of the rRT-PCR assays, other equine viral pathogens were also included in the study: the reference Bucyrus strain of EAV, equine herpesviruses 1 to 5 (EHV-1, EHV-2, EHV-3, EHV-4, EHV-5), equine rhinitis viruses A and B, equine adenovirus 1 and 2, and Salem virus.

Table 3.1. List of Influenza A virus strains and other equine viral pathogens tested by rRT-PCR assays in order to determine the specificity of each assay.

Virus name	Origin	Catalog number
Equine Influenza H3N8 Subtype		
A/equine/Alaska/91	NVSL	020IDV9101
A/equine/Kentucky/81	NVSL	040IDV0001
A/equine/Miami/63	NVSL	060IDV0501
A/equine/New York/73	GERC[b]	N/A[g]
A/equine/Kentucky/02	GERC	N/A
A/equine/Ohio/03	GERC	N/A
A/equine/Newmarket/2/93	GERC	N/A
A/equine/Aboyne/05	GERC	N/A
A/equine/Richmond/07	GERC	N/A
A/equine/Ohio/05	AHDC[c]	N/A
A/equine/Texas/05	AHDC	N/A
A/equine/Montana/07	AHDC	N/A
A/equine/Virginia/05	AHDC	N/A
Equine Influenza H7N7 Subtype		
A/equine/Prague/56	NVSL[a]	021IDV9201
A/equine/New York/07	AHDC	N/A
#110600	AHDC	N/A
#239936-99	AHDC	N/A
#13187-99	LDDC[d]	N/A
#36770-02	LDDC	N/A
#371106-02	LDDC	N/A
#38144-02	LDDC	N/A
#38360-02	LDDC	N/A
#38362-02	LDDC	N/A

Table 3.1-continued

Equine arteritis virus Bucyrus strain	ATCC	VR-796
Equine herpesvirus 1	ATCC	VR-700
Equine herpesvirus 2	GERC	N/A
Equine herpesvirus 3	ATCC	VR-352
Equine herpesvirus 4	ATCC	VR-2230
Equine herpesvirus 5	UCD[f]	N/A
Equine rhinitis virus A	NVSL	0600EDV8501
Equine rhinitis virus B	NVSL	0610EDV85010
Equine adenovirus 1	NVSL	001EDV8401
Equine adenovirus 2	LDDC	N/A
Salem virus	AHDC	N/A

[a] National Veterinary Service Laboratories, Ames, IA

[b] OIE Reference Laboratory, Maxwell Gluck Equine Research Center, University of Kentucky, KY

[c] Animal Health Diagnostic Center, Cornell University , NY

[d] Livestock Disease Diagnostic Center, University of Kentucky, KY

[e] American Type Culture Collection , Manassas, VA

[f] University of California, Davis, CA

[g] Not applicable

Clinical samples

A total of 211 archived nasal swabs from horses experimentally inoculated with the EIV A/equine/Kentucky/02 strain and 149 archived nasal swabs (field samples) submitted to the OIE Reference laboratory for routine EI diagnostic testing were included in the study. The 149 field samples included 48 nasal swab samples collected from horses in pre-export quarantine and the remaining 101 samples were collected from horses with evidence of respiratory disease where EI was suspected. Field samples were submitted as swabs and transported at 4 °C to the OIE Reference Laboratory for EI at the Gluck Equine Research Center. Each nasal swab from the field was resuspended in 2.5 ml of phosphate buffered saline (PBS, pH=7.5) and stored at 4 °C. The 211 archived nasal samples were collected from 25 horses that were experimentally challenged with the A/equine/Kentucky/02 strain of EIV. The samples were collected from day 1 to 8 post exposure. The remaining 11 samples were collected from 11 horses 3 days prior to experimental exposure to the virus. The nasal swabs from experimentally challenged horses were placed in 5 ml of transport medium (PBS containing 10% glycerol, 1mg/ml gentamicin together with 8 IU/ml of penicillin, 8 μg/ml of streptomycin and 0.02 IU/ml of amphotericin B, [Invitrogen, Carlsbad, CA]) and stored at 4 °C.

Virus isolation

All the samples submitted for attempted virus isolation (VI) were processed within 24 hr of collection at the OIE Reference Laboratory for EI at the Gluck Equine Research Center. The 149 nasal swabs collected in the field between 2007 and 2009 and the 211 nasal swabs from an experimental horse challenge study were inoculated into the allantoic cavity of embryonated hens' eggs and harvested as described previously.[401]

Viral nucleic acid isolation

Viral nucleic acid was isolated from archived nasal swabs (stored at -80 °C), allantoic fluid (AF) of EIV isolates or tissue culture fluid (TCF) containing other equine

respiratory viruses using a commercial kit (Macherey-Nagel NucleoSpin 8 Virus Kit, Bethlehem, PA) and automatic nucleic acid extraction machine XTR-1820 (Qiagen Inc., Santa Clara, CA). The rRT-PCR reactions were set up with a CAS-1200 machine (Qiagen Inc., Santa Clara, CA). Briefly, 140 µl of each sample was used for nucleic acid extraction according to the manufacturer's instructions. The viral nucleic acid was eluted in 60 µl of nuclease-free water and stored at -80 °C.

Primers and probes

The primers and probes used in this study were designed using Primer Express® software v3.0 (Applied Biosystems, Forest City, CA). Three primer and TaqMan® MGB™ probe sets (EqFlu NP, EqFlu M and EqFlu HA3) targeting conserved regions of the NP, M and H3 HA genes were designed after aligning 17, 21 and 79 sequences of H3N8 subtype of EIV respectively from GenBank (Table 3.2). The EqFlu HA3-Mia was designed to target the H3 HA gene particularly of the A/equine/Miami/63 strain. Three primer and probe sets (EqFlu NP-Pra, EqFlu M-Pra and EqFlu HA7-Pra) were designed solely based on the NP, M and H7 HA genes of the A/equine/Prague/56 strain, respectively. In addition, the EqFlu HA7 primer and probe set was designed to target a highly conserved region after aligning 12 H7 HA sequences available in GenBank.

Table 3.2. Primers and probes used in the rRT-PCR assays

rRT-PCR assay name	Equine influenza virus subtype	Primer or probe[a]	Sequence 5' to 3' and nucleotide location (nt)	GenBank accession number
EqFlu NP	H3N8	EqFlu NP F	GAAGGGCGGCTGATTCAGA (157-175)	DQ124184
		EqFlu NP R	TTCGTCGAATGCCGAAAGTAC (199-219)	
		EqFlu NP Pr	[b]CAGCATAACAATAGAAAGGA[c] (177-196)	
EqFlu M		EqFlu M F	ACCGAGGTCGAAACGTACGT (38-57)	DQ124188
		EqFlu M R	CGCGATCTCGGCTTTGA (84-100)	
		EqFlu M Pr	[b]CTCTCTATCGTACCATCAGG[c] (59-78)	
EqFlu HA3		EqFlu HA3 F	TCACATGGACAGGTGTCACTCA(448-469)	L39914
		EqFlu HA3 R	GGCTGATCCCCTTTTGCA (485-506)	
		EqFlu HA3 Pr	[b]AACGGAAGAAGTGGAGC[c] (471-487)	
EqFlu HA3-Mia		EqFlu HA3-Mia F	GCAGTGCTTTCAGCAATTGC (346-365)	M29257
		EqFlu HA3-Mia R	AGAGACCGGAGCGATGCA (389-406)	
		EqFlu HA3-Mia Pr	[d]CCATATGACGTCCCTGACT[c] (369-387)	
EqFlu NP-Pra	H7N7	EqFlu NP-Pra F	GGCGTCTCAAGGCACCAA (48-65)	M63748
		EqFlu NP-Pra R	TCTGGCGTTCTCCACCAGTT (87-106)	
		EqFlu NP-Pra Pr	[b]CGACCTTATGAACAAATG[c] (67-84)	
EqFlu M-Pra		EqFlu M-Pra F	CGCGCAGAGACTTGAGAATG (97-116)	CY005801
		EqFlu M-Pra R	CATTCCATGAGAGCCTCAAGATCT(136-159)	
		EqFlu M-Pra Pr	[b]TTTGCAGGGAAAAATA[c] (119-134)	
EqFlu HA7-Pra		EqFlu HA7-Pra F	CAATGGAGAGACTAGCGCATGT (441-462)	X62552
		EqFlu HA7-Pra R	AGAAGCCATTTCATCTCTGCATAA (483-506)	
		EqFlu HA7-Pra Pr	[e]AAGGTCAAGATCTTCC[c] (465-480)	
EqFlu HA7		EqFlu HA7 F	TCCTCTGTGTACGTGCAGATAAAATC (59-84)	X62556
		EqFlu HA7 R	GGGTGTCTACTTTGGTTCCATTAGA (106-130)	
		EqFlu HA7 Pr	[b]CCTAGGACGTCATGCTG[c] (87-103)	

[a]F=Forward primer, R=Reverse primer and Pr=Probe

[b]Reporter dye (FAM; 6-carboxyfluorescein) labeled nucleotide

[c]Nonfluorescent quencher dye (MGB™; minor groove binding) labeled nucleotide

[d]Reporter dye (VIC) labeled nucleotide

[e]Reporter dye (NED) labeled nucleotide

One-step real-time RT-PCR

A one-tube TaqMan® rRT-PCR assay was performed using the TaqMan® one-step RT-PCR Master mix in a 7500 Fast Real-Time PCR system (Applied Biosystems, Foster City, CA) as described previously.[201] Briefly, 25 µl of RT-PCR mixture for each reaction contained 12.5 µl of 2 × Master Mix without UNG (uracil-N-glycosylase), 40 × MultiScribe and RNase Inhibitor Mix (0.625 µl), 50 µM of forward and reverse primers (0.45 µl [900 nM]), 10 µM probe (0.625 µl [250 nM]), nuclease free water (5.35 µl), and 5 µl of test sample RNA. The following thermocycling conditions were used under standard mode as per manufacturer's recommendation: 30 min at 48 °C, 10 min at 95 °C, followed by 40 cycles at 95 °C for 15 sec and 60 °C for 1 min. Each RT-PCR run included a control without RNA (containing the reaction mix with 5 µl of water [no template control]) and positive controls containing *in vitro* transcribed (IVT) RNA.

***In vitro* transcribed RNA synthesis and determination of analytical sensitivity of rRT-PCR assays**

The viral nucleic acid extracted from the H3N8 strains A/equine/Miami/63 and A/equine/Kentucky/02 was used as the template for amplification of the NP, M and H3 HA genes for IVT RNA generation. Briefly, these genes were RT-PCR amplified using forward and reverse primers flanking the target gene sequence in rRT-PCR assays (Table 3.3). The RT-PCR products were gel-purified and cloned into the pDrive cloning vector according to the manufacturer's instructions (Qiagen PCR cloning kit, Qiagen Inc., Santa Clara, CA). The plasmids were purified using a commercial kit (QIAamp® Miniprep kit, Qiagen Inc., Santa Clara, CA). The authenticity of each RT-PCR product was confirmed by sequencing both strands of DNA. Following sequencing, the recombinant plasmids with the NP, M and H3 HA genes from two different EIV H3N8 strains (A/equine/Miami/63 and A/equine/Kentucky/02) were used to generate IVT RNA. Runoff RNA transcripts were generated from *Bam* HI-linearized recombinant plasmids (Sp6 orientation) or Xho I-linearized recombinant plasmids (T7 orientation) according to

a previously described protocol.[384] The concentration of the IVT RNA molecules per microliter was calculated according to the following formula as described before [201]:

$$\text{Number of IVT RNA molecules / µl} = \frac{\text{Avogadro number } (6.022 \times 10^{23}) \times \text{IVT RNA concentration (g/µl)}}{\text{IVT RNA molecular weight (g)}}$$

The analytical sensitivity of the EqFlu NP, EqFlu M, EqFlu HA3 and EqFlu HA3-Mia rRT-PCR assays was determined using the specific IVT RNA generated from the recombinant plasmids.

Table 3.3. Primers used for RT-PCR amplification, cloning and sequencing of NP and M genes

Primers	Target Gene	Virus Strain	Sequence 5' to 3' and nucleotide location	GenBank Accession Number	Length of Fragment (bp)
H3N8 NP 1P[a,b]	NP	A/equine/Miami/63 and A/equine/Kentucky/02	ATGGCGTCTCAAGGCACCAA	DQ124184	507
H3N8 NP 507N[a,b]			GCCTTGCATCAGAGAGCACA		
H3N8 M 1P[a,b]	M		ATGAGTCTTCTAACCGAGGTCG	DQ124188	507
H3N8 M 507N[a,b]			GGTTGTTGTCACCATCTGCC		
H3N8 HA3 1P[a,b]	H3 HA		TCGTCAATCATGAGGACTACCA	D30680	507
H3N8 HA3 507N[a,b]			CAGTCGGCTAAAGAAACTATC		
UNI-12 primer[c]	NP	A/equine/New York/73	AGCAAAAGCAGGGTAGATAATCACTC	AY855342	1565
ENP-1F[b,d]			AGTAGAAACAAGGGTATTTTTCTTTAACTG		
ENP-1565R[b,d]			AGCAAAAGCAGG		NA
ENP-401F[b]			TCTGGCGTCAGGCCAACAATG		NA
ENP-812F[b]			TCATTTTCTTAGCACGATCAGCAC		NA
ENP-1201F[b]			TGGGCAATAAGGACCAGAAGTG		NA
ENP-324R[b]			TCCCGTTTTCTTAGGGTCTTTTCC		NA
ENP-730R[b]			TCCCTTTGAGGATATTGCACATTC		NA
ENP-1131R[b]			TCCTCTGGTTGTTAACTGTCCTC		NA
EM-1F[b,d]	M		AGCAAAAGCAGGTAGATATTTAAAGATGAG	CY005801	1027
EM-1027R[b,d]			AGTAGAAACAAGGTAGTTTTTTACTCCAGC		

[a]Primers were used for PCR cloning

Table 3.3.-continued

[b]Primers were used for sequencing

[c]Primers were used for RT-PCR

[d]Primers were used for PCR

Determination of detection limits of rRT-PCR, Directigen Flu A® test and egg inoculation

Using serial decimal dilutions (10^{-1} to 10^{-10}) of the H7N7 (A/equine/Prague/56 [4.65×10^5 EID_{50}/ml]) and H3N8 (A/equine/Kentucky/02 [10^7 EID_{50}/ml]) subtype strains, the detection limits of the rRT-PCR assays, Directigen Flu A® test (Becton-Dickinson, Sparks, MD) and egg inoculation were evaluated. To avoid inter-assay variation, the same aliquot of each dilution was used in all three assays. Briefly, 5 µl of RNA isolated from 140 µl of each decimal dilution were used in rRT-PCR assays as described above. 125 µl of each specimen was tested in the Directigen Flu A® test according to the manufacturer's recommendations. For egg inoculation, an inoculum of 100 µl of each specimen was used. A total of 4 eggs were inoculated with each sample.[401]

RT-PCR amplification and sequencing of NP, M genes

The full-length NP gene sequence (nucleotide numbers [nt # 1-1565]) and partial M gene sequence (nt # 1-830) of the A/equine/New York/73 strain were RT-PCR amplified using a standard laboratory protocol. Briefly, viral nucleic acid was isolated from AF using a Qiagen viral RNA extraction kit (Qiagen Inc., Santa Clara, CA) according to the manufacturer's instructions. Viral RNA was reverse transcribed with UNI-12 primer (Table 3.3) using the Accuscript™ high fidelity RT-PCR system (Stratagene, La Jolla, CA).[413] Each cDNA was then amplified by PCR using Accuprime Pfx DNA polymerase (Invitrogen, Carlsbad, CA) with NP and M specific forward and reverse primers (Table 3.3). Both PCR products were gel purified and the full-length NP (1565 bp) and partial M (1027 bp) genes of A/equine/New York/73 strain were determined by sequencing both strands of DNA using gene specific primers (Table 3.3). The NP sequence of the A/equine/New York/73 was compared to the published sequences of A/equine/Miami/63 and A/equine/Prague/56 (Genbank accession numbers M22575 and M63748, respectively). Similarly, the partial M sequence of A/equine/New York/73 was compared to the same prototype strains (Genbank accession numbers AF001674 and CY005801, respectively).

Statistical analysis

Statistical evaluation of the performance of the three EIV primer and probe sets (EqFlu NP, EqFlu M and EqFlu HA3) for the detection of EIV nucleic acids was carried out to determine the respective sensitivity and specificity of each assay, and to compare these values with that of VI by egg inoculation. Sensitivities for the three H3N8 subtype specific rRT-PCR assays and VI were estimated by Clopper-Pearson exact binomial methods using experimental samples, with statistical comparisons made employing exact binomial paired tests.[389]

The analysis of data from testing field specimens was conducted using a Bayesian model developed by Branscum *et al*,[414] that enables estimation of the sensitivity and specificity of a test when true infection status is unknown. Separate models were used for comparing VI with each rRT-PCR assay under the assumption of conditional independence of tests. Independent beta prior distributions for the four sensitivities were constructed using information derived from the horse challenge study. Specifically, average sensitivities on days 2 to 8 were used as prior modes for the sensitivity on each of the three rRT-PCR assays, with the smallest values among the lower endpoints of days 2 to 8 used as prior 5th percentiles. The modes and lower percentiles were used to identify an appropriate beta prior distribution. For the VI test, the prior 95th percentile for sensitivity was set at 0.93, with a mode of 0.51. Based on testing for possible cross-reaction with other viruses, the priors for the specificities of each of the 3 rRT-PCRs had a mode of 0.95 and a 5th percentile of 0.80. The specificity of VI was set equal to 1. An empirical Bayes approach was used to place a prior on the prevalence that had a mode of 0.32 and a 99th percentile of 0.45. Gibbs sampling was used to simulate from posterior distributions. Five chains were run with separated starting values (there was no indication of lack of convergence), a burn-in of 10,000 iterates was used, and inferences were based on 100,000 iterates. Data analysis was implemented in R 2.7 and WinBUGS 1.4.3. [415-416]

3.4. RESULTS

Selection of rRT-PCR assays targeting NP, M and HA genes of H3N8 and H7N7 subtypes of equine influenza

A total of eight rRT-PCR assays were developed to target the NP, M, and HA genes of H7N7 and H3N8 EIV subtypes (Table 3.2). The assays were evaluated using prototype strains of each EIV subtype as well as recent virus isolates representing both American and Eurasian lineages (Table 3.4). The EqFlu NP, EqFlu M, EqFlu HA3 and EqFlu HA3-Mia assays were designed to detect EIV H3N8 subtype. The EqFlu NP assay not only detected all tested H3N8 strains but also one H7N7 strain (A/equine/New York/73). The EqFlu M assay successfully distinguished all H3N8 strains and did not cross-react with either of the two H7N7 strains tested. The EqFlu HA3 assay was able to detect all H3N8 subtype strains except for the prototype virus (A/equine/Miami/63). On the other hand, the EqFlu HA3-Mia assay which was designed solely based on the A/equine/Miami/63 sequence could only detect the prototype virus (Table 3.4). Similarly, the other four (EqFlu NP-Pra, EqFlu M-Pra, EqFlu HA7-Pra and EqFlu HA7) assays were designed to detect the EIV H7N7 subtype. Both H7N7 subtype viruses tested gave positive results with EqFlu M-Pra, EqFlu HA7-Pra and EqFlu HA7 assays (Table 3.4). However, the EqFlu NP-Pra assay could only detect the prototype strain (A/equine/Prague/56) but not the A/equine/New York/73 strain. None of these assays specific for the H7N7 subtype cross-reacted with any viruses of the H3N8 subtype. All eight rRT-PCR assays were highly specific in that none of them detected any of the other common equine respiratory viruses tested.

In summary, both EqFlu NP and EqFlu M primers and probe sets were able to detect all eight H3N8 strains representing both American and Eurasian lineages that were included in this study. With the exception of the first A/equine/Miami/63 isolate, the EqFlu HA3 primers and probe set detected most recent H3N8 isolates. Therefore, three out of four rRT-PCR assays specific for H3N8 subtype, EqFlu NP, EqFlu M and EqFlu HA3 were selected for further evaluation with clinical specimens.

Table 3.4. Comparison of the specificity of H3N8 and H7N7 subtype specific rRT-PCR assays

Equine influenza virus subtypes	Equine influenza virus prototype strains and recent isolates	Virus titer (EID_{50}/ml)	Assays to detect H3N8 subtype				Assays to detect H7N7 subtype			
			EqFlu NP	EqFlu M	EqFlu HA3	EqFlu HA3-Mia	EqFlu NP-Pra	EqFlu M-Pra	EqFlu HA7-Pra	EqFlu HA7
H3N8	A/equine/Miami/63	$4.65x10^5$	+[a]	+	-[b]	+	-	-	-	-
	A/equine/Alaska/91[c]	2.14×10^9	+	+	+	-	-	-	-	-
	A/equine/Kentucky/81[c]	3.16×10^8	+	+	+	-	-	-	-	-
	A/equine/Kentucky/02[c]	2.15×10^7	+	+	+	-	-	-	-	-
	A/equine/Ohio/03[c]	$3.16x10^7$	+	+	+	-	-	-	-	-
	A/equine/Newmarket/2/93[d]	1×10^8	+	+	+	-	-	-	-	-
	A/equine/Aboyne/05[d]	6.81×10^3	+	+	+	-	-	-	-	-
	A/equine/Richmond/07[d]	4.65×10^5	+	+	+	-	-	-	-	-
H7N7	A/equine/Prague/56	4.65×10^5	-	-	-	-	+	+	+	+
	A/equine/New York/73	4.7×10^7	+	-	-	-	-	+	+	+

[a] Nucleic acid was detectable by the rRT-PCR (+).

[b] Nucleic acid was undetectable by the rRT-PCR (-).

[c] American lineage

Table 3.4-continued

[d] Eurasian lineage

Analytical sensitivity of the rRT-PCR assays targeting NP, M and H3 HA genes of H3N8 subtype

In order to determine the analytical sensitivity of the rRT-PCR assays targeting the NP, M and H3 HA genes of EIV nucleic acid, serial decimal molecule dilutions (10^0-10^{10}) of IVT RNA containing these genes derived from A/equine/Miami/63 and A/equine/Kentucky/02 strains of EIV were tested with the EqFlu NP, EqFlu M, EqFlu HA3 and EqFlu HA3-Mia rRT-PCR assays. The assays were independently repeated three times. The IVT NP, M or H3 HA RNA from each strain was calculated based on the molecular weight and concentration of the IVT RNA. Regression analysis confirmed linearity in all six assays (EqFlu NP rRT-PCR: R^2=0.9968 for A/equine/Miami/63 and R^2=0.9976 for A/equine/Kentucky/02; EqFlu M rRT-PCR: R^2=0.996 for A/equine/Miami/63 and R^2=0.995 for A/equine/Kentucky/02; EqFlu HA3 rRT-PCR: R^2=0.9987 for A/equine/Kentucky/02; EqFlu HA3-Mia rRT-PCR: R^2=0.9994 for A/equine/Miami/63). The EqFlu NP rRT-PCR detected a minimum of 10 RNA molecules from both A/equine/Kentucky/02 and A/equine/Miami/63 strains, and the cycle threshold (C_t) value for A/equine/Kentucky/02 was at least 4 cycles lower than for A/equine/Miami/63 over all the IVT RNA dilutions tested (Fig 3.1). The ranges of magnitude using the EqFlu M rRT-PCR for the A/equine/Miami/63 and A/equine/Kentucky/02 strains were 1 and 10 molecules, respectively (Fig 3.2). Both EqFlu HA3 and EqFlu HA3-Mia rRT-PCR assays detected a minimum of 10 RNA molecules (Fig 3.3). These data clearly indicate that each of these assays could detect as low as 10 RNA molecules.

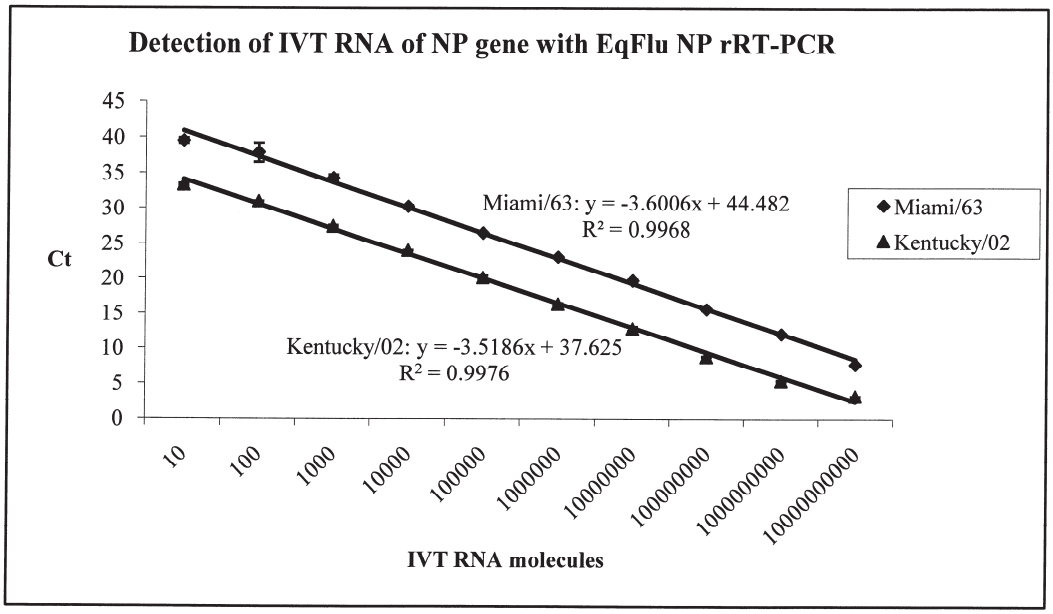

Fig 3.1. Comparison of analytical sensitivity between IVT RNA of different EIA strains using EqFlu NP rRT-PCR ([Miami/63: y=-3.6006x+44.482, R^2=0.9968] and [Kentucky/02: y=-3.5186x + 37.625, R^2=0.9976]). $\pm$2 standard errors were also shown on the figure.

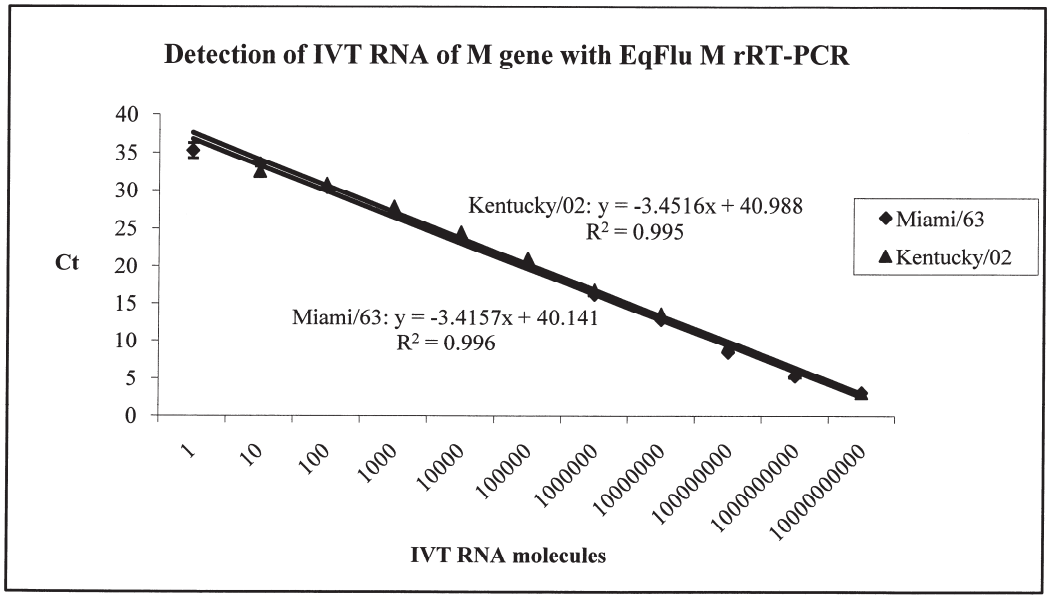

Fig 3.2. Comparison of analytical sensitivity between IVT RNA of different EIA strains using EqFlu M rRT-PCR. ([Miami/63: y=-3.4157x+ 40.141, R^2=0.996] and [Kentucky/02: y=-3.4516x +40.988, R^2=0.995]). $\pm$2 standard errors were also shown on the figure.

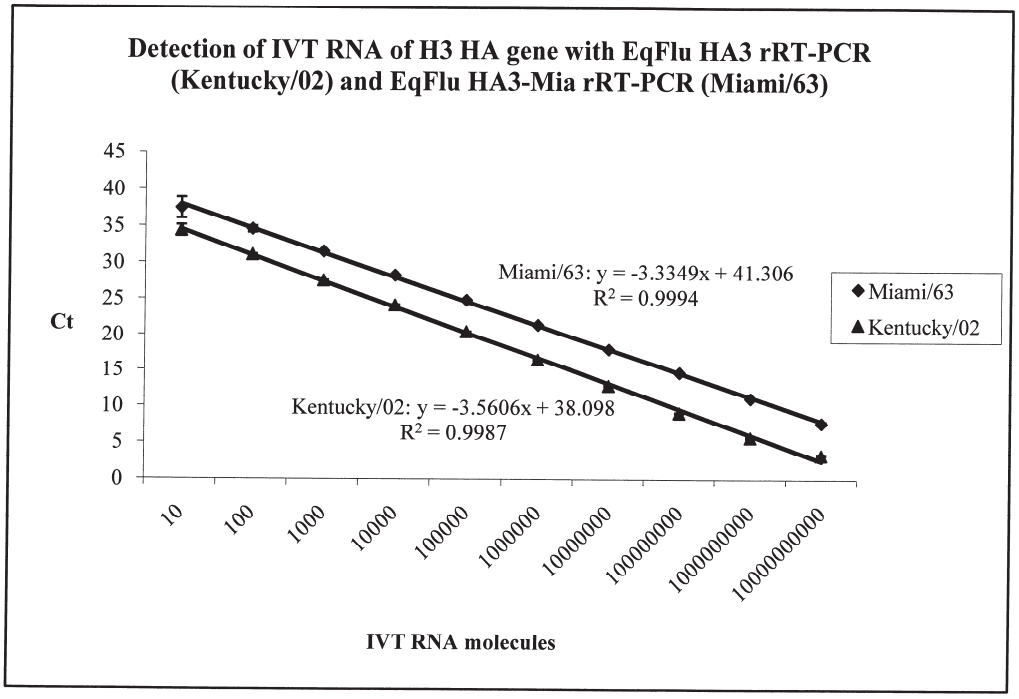

Fig 3.3. Comparison of analytical sensitivity between IVT RNA of different EIV strains using EqFlu HA3 rRT-PCR and EqFlu HA3-Mia rRT-PCR ([Miami/63: y = -3.3349x + 41.306, R^2=0.9994 with EqFlu HA3-Mia rRT-PCR] and [Kentucky/02: y = -3.5606x + 38.098, R^2=0.9987 with EqFlu HA3 rRT-PCR]). $\pm$2 standard errors were also shown on the figure.

Comparison of sensitivity of rRT-PCR assays targeting NP and M genes, Directigen Flu A® test and egg inoculation

Using serial decimal dilutions of A/equine/Kentucky/02 (H3N8 subtype) and A/equine/Prague/56 (H7N7 subtype), the detection limits of the EqFlu NP, EqFlu M, EqFlu NP-Pra and EqFlu M-Pra rRT-PCR assays were compared to the Directigen Flu A® test and egg inoculation (Table 3.5). The highest dilutions that the Directigen Flu A® test and egg inoculation could detect were the 10^{-2} and 10^{-6} virus dilutions, respectively. In contrast, the N and MP specific rRT-PCR assays targeting both subtypes of the virus were at least more than 10^4 times more sensitive than the Directigen Flu A® test. Similarly, the assays had at least one log higher sensitivity than egg inoculation.

Table 3.5. Comparison of subtype specific rRT-PCR assays targeting NP and M genes with egg inoculation and Directigen Flu A® test[a]

EIV prototype strains	Subtype	Virus titer (EID_{50}/ml)	Directigen Flu A® test	Egg inoculation	rRT-PCR assays			
					EqFlu NP	EqFlu M	EqFlu NP-Pra	EqFlu M-Pra
A/equine/Kentucky/02	H3N8	10^{7}	10^{-2}	10^{-6}	10^{-7}	10^{-7}	NA[b]	NA
A/equine/Prague/56	H7N7	4.65×10^{5}	10^{-2}	10^{-5}	NA	NA	10^{-6}	10^{-7}

[a] Serial decimal dilutions of EIV strains were tested in the comparison study by egg inoculation, Directigen Flu A® test and rRT-PCR assays. Numbers shown on the table represent the serial decimal dilution factors.

[b]Not applicable

Evaluation of H3N8 subtype specific rRT-PCR assays for the detection of EIV in clinical specimens

Three rRT-PCR assays (EqFlu NP, EqFlu M and EqFlu HA3 assays) targeting the NP, M and H3 HA genes were further evaluated using a range of clinical specimens. Of the 211 archived nasal swab samples collected from horses that were challenged with the A/equine/Kentucky/02 strain, 164, 166 and 153 tested positive using the rRT-PCR assays targeting NP, M and HA genes, respectively (Table 3.6). Of the 149 archived nasal swabs from field cases of respiratory disease, 41, 25 and 27 tested positive with the NP, M and HA assays, respectively. Of the 149 samples, 48 nasal swabs were from horses that were scheduled for international shipment and all these samples tested negative for EIV nucleic acid using each of these three rRT-PCR assays.

Table 3.6: Virus isolation and rRT-PCR results of archived EIV prototypes and clinical specimens

Clinical specimen tested	Virus isolation		rRT-PCR assays					
			EqFlu NP		EqFlu M		EqFlu HA3	
	Positive	Negative	Positive	Negative	Positive	Negative	Positive	Negative
211 nasal swabs from a horse challenge study	98	113	164	47	166	45	153	58
149 field nasal swabs	7	142	41	108	25	124	27	122

In the case of the experimental horse challenge study, estimated sensitivities of each rRT-PCR assay and p-values for a possible difference in sensitivity with VI by egg inoculation on days 1 to 8 post infection were calculated based on the assumption that every swab tested was truly positive for EIV (Table 3.7). The results indicate that the rRT-PCRs targeting the NP and M genes were significantly more sensitive than VI by egg inoculation on day 1 post-infection; also, these two assays had higher sensitivities between days 3 to 5. At later time points in the horse inoculation experiment (day 6 to 8), all three rRT-PCRs were significantly more sensitive than VI ($P \leq 0.02$). The data demonstrate that the rRT-PCR assays had comparable or greater sensitivity in detecting nucleic acid than VI by egg inoculation at each time point from day 1 to 8 post infection (Table 3.7).

The estimated sensitivity and specificity of each rRT-PCR assay and the difference in sensitivity between rRT-PCR and VI by egg inoculation were calculated using a Bayesian analysis of the 149 field samples (Table 3.8). Seven horses that tested VI + were classified as EIV +. A total of 48 horses that tested negative on all three rRT-PCRs and were VI - were classified as EIV -. The unknown EIV status of the remaining 94 horses was imputed in the Bayesian analysis. All three rRT-PCR assays had higher

sensitivity (with posterior probability of 1) than VI by egg inoculation. The PCR assay targeting the NP gene had the highest sensitivity (93%; 95% credible interval: 77%-99%) and had the largest increase in sensitivity over VI (58%; 95% credible interval: 37%-76%). The other two rRT-PCR assays (EqFlu M and EqFlu HA3) had similar high sensitivities (89% and 87%) with smaller increases in sensitivity over VI (39% and 35%), respectively. All three assays had estimated specificities that were ≥ 96%. The higher sensitivity of the rRT-PCR assay targeting the NP gene of the H3N8 virus compared to the other two assays targeting the M and H3 HA genes is consistent with the sequence conservation seen in the NP gene among various EIV strains.

Table 3.7. Estimated sensitivity of each rRT-PCR assay and *P* values (in parenthesis) for a statistical difference between rRT-PCR and VI by egg inoculation

Days Post Infection	VI	EqFlu NP	EqFlu M	EqFlu HA3
1	8%	32% (0.03)	36% (0.02)	20% (0.25)
2	80%	88% (0.5)	88% (0.5)	84% (1.00)
3	72%	92% (0.06)	92% (0.06)	92% (0.06)
4	72%	92% (0.06)	92% (0.06)	88% (0.22)
5	68%	88% (0.06)	88% (0.06)	88% (0.06)
6	60%	100% (0.002)	96% (0.004)	88% (0.02)
7	28%	88% (<0.001)	88% (<0.001)	84% (<0.001)
8	4%	76% (<0.001)	84% (<0.001)	68% (<0.001)

Table 3.8. Estimates and comparison of test performance parameters of three rRT-PCR assays using field samples

	EqFlu NP	EqFlu M	EqFlu HA3
Estimated sensitivity	93%	89%	87%
95% credible interval	77%-99%	68%-98%	63%-98%
Estimated specificity	96%	97%	96%
95% credible interval	88%-99%	90%-100%	89%-99%
Difference between sensitivity of rRT-PCR and Egg inoculation	58%	39%	35%
95% credible interval	37%-76%	15%-63%	7%-59%
Posterior probability that sensitivity of rRT-PCR is > sensitivity of Egg inoculation	1.00	1.00	0.99

Cross-reaction of EqFlu NP rRT-PCR assay with A/equine/New York/73 (H7N7)

Because the A/equine/New York/73 strain (H7N7 subtype) was detected by the EqFlu NP assay that was originally designed to detect H3N8 strains but not by the EqFlu NP-Pra assay, the NP and partial M gene of this virus were sequenced (Genbank accession numbers FJ499496 and FJ666099, respectively). The M gene of A/equine/New York/73 had 97.7% identity when compared to A/equine/Prague/56 strain as expected. In contrast, the NP gene of that strain had more sequence identity with the H3N8 prototype A/equine/Miami/63 than with the H7N7 prototype A/equine/Prague/56 strain (96.3% and 83.3%, respectively). These data clearly indicate that despite being a H7N7 virus, the NP gene of the A/equine/New York/73 strain is very similar to that of the H3N8 virus. The forward primer of the EqFlu NP assay had a 100% match with the A/equine/New York/73 NP gene, while there was only a single nucleotide mismatch in both reverse primer and probe binding regions. These two changes did not compromise the detection capability of the rRT-PCR assay. In contrast, the reverse primer and the

probe of the EqFlu NP-Pra assay had 2 and 3 nucleotides mismatches, respectively, when compared with the A/equine/New York/73 strain, which compromised the sensitivity of the assay.

3.5. DISCUSSION

Eight new MGB™ probe based rRT-PCR assays targeting the NP, M, H3 and H7 HA genes of two EIV subtypes were developed and evaluated in this study. Four of the primer sets targeted the NP, M and H3 HA genes of H3N8 subtype and the remaining four targeted the respective genes of H7N7 subtype. The assays were based on MGB™ probes which provide several advantages over other real-time PCR chemistries. The MGB™ probes are shorter in length (12-18 bases) compared to conventional TaqMan® probes. Since such probes are less liable to sequence mismatches, this results in increased specificity of the rRT-PCR assays.[417] The 3' end nonfluorescent quencher dye dramatically reduces the background fluorescence of the reaction, hence less chance of false positive results.[150] For the primer and probe design, the conserved regions of these four genes were determined by alignment of sequences of the H3N8 and H7N7 strains available in GenBank. The EqFlu NP and EqFlu M assays were able to detect all the prototype H3N8 strains. The EqFlu HA3 assay did not give a positive reaction with the A/equine/Miami/63 (H3N8) which may be the result of antigenic drift. Sequence comparison with a recent isolate revealed that the H3 HA gene of A/equine/Miami/63 only has 91% sequence homology with that of A/equine/Kentucky/02 (data not shown). There are 1 and 3 nucleotide mismatches in the reverse primer and probe region of the EqFlu HA3 assay, respectively, compared to the H3 HA sequence of A/equine/Miami/63 virus; thus reducing the efficiency of the assay. Sequence analysis of A/equine/New York/73 (H7N7) clearly indicates that its NP gene was derived from the H3N8 subtype, providing confirmation of reassortment between H3N8 and H7N7 strains of EIV in the field since the 1970s as previously reported.[418-420] Since the EqFlu HA7 assay appears to be highly specific for H7N7 EIV, it should enable highly reliable surveillance for the H7N7 subtype which is thought to be extinct or possibly still circulating at a very low level in nature.[10,421-423] Regrettably, the EqFLu HA7 assay could not be adequately

evaluated because of the very limited number of isolates of this EIV subtype available for testing in this study. None of these assays specific for both EIV subtypes gave a positive result with other common equine respiratory viral pathogens such as equine herpes viruses and equine rhinitis viruses, confirming 100% specificity for EIV. In summary, the primer and probe sets designed and evaluated in this study allow identification of both equine influenza subtypes. It would appear they likely can also detect any reassortments of these two EIV subtypes that may currently be in circulation in nature. Furthermore, H3N8 subtype specific assays were able to detect both Eurasian and American lineage strains of EIV.

Three rRT-PCR assays (EqFlu NP, EqFlu M and EqFlu HA3 assays) targeting the NP, M and H3 HA genes of H3N8 EIV subtype were further evaluated by using two sets of clinical samples: nasal swabs from an experimental challenge study and nasal swabs (field samples) submitted to the OIE Reference laboratory for EI for routine diagnostic testing. Using nucleic acid extracted from the samples collected from a group of experimentally inoculated horses, both the EqFlu NP and EqFlu M assays were shown to have significantly higher respective sensitivities than egg inoculation during the time course of the study (day 1 to 8). Furthermore, with few exceptions, all three assays were able to detect EI nucleic acid from day 1 post-challenge before clinical signs of disease were observed. The samples that were positive only by rRT-PCR and not by VI were confirmed truly EIV positive by a previously published standard RT-PCR assay (data not shown).[404] The minimal analytical sensitivity of these assays can reach up to 10 IVT RNA molecules. As such, these assays provide valuable tools for distinguishing EI from clinically similar diseases on an individual animal basis. These newly developed rRT-PCR assays performed exceedingly well not only in virus detection but also in distinguishing the different subtypes of EIV based on the various samples evaluated in this study. Such assays can provide a fast and reliable means of EIV diagnosis and are especially useful in screening samples during a suspected outbreak of EI.

Comparison of the sensitivity of the four rRT-PCR assays targeting the NP and M genes with egg inoculation and the Directigen Flu A® test clearly show that the molecular assays provide the highest sensitivity. Previous studies have compared relative

sensitivities of VI in embryonated eggs, antigen detection (Directigen Flu A® test) and nucleic acid amplification (nested RT-PCR targeting the NP gene and standard RT-PCR targeting the M gene) for detection of EIV.[408] The authors have shown that RT-PCR assays using M primers and VI in embryonated eggs proved to be the most sensitive methods for virus detection. The Directigen Flu A® test was the least sensitive method for detection of EIV. In a similar study, Yamanaka *et al* [407] demonstrated that VI in embryonated eggs is more sensitive than five rapid antigen detection kits evaluated. Furthermore, analysis of nasal swabs from a limited number of experimentally inoculated horses also showed that VI by egg inoculation and the standard RT-PCR had comparable sensitivities in detecting EIV.[408] Data from this study also demonstrated that the Directigen Flu A® test had the least sensitivity followed by VI in embryonated eggs. Furthermore, evaluation of clinical samples and serial dilutions of EIV prototype strains has confirmed that rRT-PCR assays have higher sensitivity than egg inoculation.

In conclusion, newly developed rRT-PCR assays targeting NP, M and HA genes were found to be highly sensitive and specific compared to the Directigen Flu A® test and VI in embryonated eggs. The assays provided a fast and reliable means of virus detection and disease surveillance, with it would appear, the additional advantage of being able to identify antigenic shift between the two subtypes of EIV.

CHAPTER FOUR

Diagnostic application of H3N8-specific equine influenza real-time reverse transcription polymerase chain reaction assays for the detection of Canine influenza virus in clinical specimens

J Vet Diagn Invest 22 (6):942-5 (2010)
Reprinted with permission

4.1. SUMMARY

The objective of the current study was to determine the capability of 3 recently described one-step TaqMan® real-time reverse transcription polymerase chain reaction (RT-PCR) assays targeting the nucleoprotein (NP), matrix (M), and hemagglutinin (HA) genes of H3N8 Equine influenza virus (EIV NP, EIV M, and EIV HA3 assays, respectively) to detect Canine influenza virus (CIV). The assays were initially evaluated with nucleic acid extracted from tissue culture fluid (TCF) containing the A/canine/FL/43/04 strain of Influenza A virus associated with the canine influenza outbreak in Florida in 2004. The EIV NP, EIV M, and EIV HA3 assays could detect CIV nucleic acid at threshold cycle (Ct) values of 16.31, 23.71, and 15.28, respectively. Three assays using TCF or allantoic fluid (AF) samples containing CIV (n = 13) and archived canine nasal swab samples (n = 20) originally submitted for laboratory diagnosis of CIV were further evaluated. All TCF and AF samples, together with 10 nasal swab samples that previously tested positive for virus by attempted isolation in embryonated hens' eggs or Madin-Darby canine kidney cells, were positive in all 3 real-time RT-PCR assays. None of the 3 assays detected the H1N1 Swine influenza virus strain in current circulation. These findings demonstrate that previously described real-time RT-PCR

assays targeting NP, M, and H3 HA gene segments of H3N8 EIV are also valuable for the diagnosis of CIV infection in dogs. The assays could expedite the detection and identification of CIV.

4.2. MAIN TEXT

Influenza A viruses infect a variety of mammalian and avian species, including pigs, horses, birds, certain wildlife species, as well as humans.[11] Interspecies transmission of influenza A virus plays an important role in its ecology and epidemiology.[424] A significant outbreak of canine influenza (CI) was reported in greyhound dogs in Florida in early 2004 which was shown to be due to cross species transmission of H3N8 equine influenza virus (EIV).[24] Furthermore, there are reports of experimental transmission of H5N1 and natural transmission of H3N2 avian influenza viruses to dogs.[425-431] More recently, it has been reported that a novel influenza A/H1N1 virus, a reassortant of human, swine and avian influenza viruses, is capable of infecting dogs.[432-434] Samples from two sick dogs tested positive for A/H1N1 influenza virus and both virus isolates were 99% identical with the strains isolated from humans.[434] However, the significance of transmission of influenza A viruses to dogs from other mammal and avian species including humans has yet to be determined.

Since the initial CI outbreak in Florida, evidence of virus activity has been reported in 30 states in the United States, reportedly affecting tens of thousands of dogs.[24,435] Sequence analysis of the canine influenza virus (CIV) from the original outbreak (A/canine/FL/43/04) revealed that 8 gene segments of this virus shared ≥96% nucleotide sequence homology with that of equine influenza virus (EIV) H3N8 subtype,

suggesting that CIV resulted from direct interspecies transmission of EIV to dogs without genetic reassortment.[24,436] The sequence changes in the hemagglutinin gene (H3 HA) are indicative of adaptive evolution of the virus in its new host. Phylogenetic analysis of 4 greyhound isolates and 2 pet dog isolates revealed that these viruses were closely related to EIV strains recovered from horses since 2000, belonging to the Florida sublineage of the American lineage of equine influenza H3N8 virus.[24,436] The isolation of four closely related EIV H3N8 subtype strains from dogs that died in different locations over a 2-year period of time, together with serological evidence of widespread infection among greyhounds in different states, strongly confirmed sustained circulation of CIV involving dog-to-dog transmission of the virus.[24,436-437]

Most outbreaks of CI occur in rescued, kenneled, or boarded dogs.[435] Clinical signs of the disease include low-grade fever, lethargy, anorexia, nasal discharge and prolonged cough.[435-436] These signs can mimic those caused by other canine respiratory pathogens. Accordingly, it is especially important to be able to distinguish CIV from other agents capable of causing canine respiratory disease.[435] Detection of CIV at the early stage of infection is especially important for facilitating management and control of the disease. Up to the present, there have been few publications describing specific diagnostic assays to detect CIV in clinical specimens. Detection of CIV is frequently attempted by traditional virus isolation (VI) in embryonated hens' eggs or in Madin-Darby canine kidney (MDCK) cells.[435] There have been some conflicting reports over the sensitivity of antigen-capture ELISA tests for the detection of CIV in dogs.[435,438] Presence of CIV nucleic acid in clinical specimens has been confirmed by traditional RT-PCR and real-time RT-PCR (rRT-PCR) assays targeting the matrix (M) gene of avian

influenza virus or by an rRT-PCR assay specific for the H3 HA or the M gene of CIV.[435,436,438] Recently, we developed and evaluated three rRT-PCR assays targeting the nucleoprotein (NP), M and H3 HA genes of H3N8 subtype of EIV (EqFlu NP, EqFlu M and EqFlu HA3 assays, respectively; Table 4.1).[202] EqFlu NP, EqFlu M and EqFlu HA3 primer and probe sets were 100% identical to the published NP, M and H3 HA sequences of CIV, respectively. Therefore, the purpose of this study was to determine whether these three rRT-PCR assays were capable of detecting CIV nucleic acid in nasal swab specimens obtained from infected dogs.

Table 4.1. Primers and probe sets used in this study

rRT-PCR Assay Name	Primer or Probe Name*	Sequence 5' to 3' and Nucleotide Location	GenBank Accession Number
EqFlu NP	EqFlu NP F	GAAGGGCGGCTGATTCAGA (157-175)	DQ124184[11]
	EqFlu NP R	TTCGTCGAATGCCGAAAGTAC (199-219)	
	EqFlu NP Pr	†CAGCATAACAATAGAAAGGA‡ (177-196)	
EqFlu M	EqFlu M F	ACCGAGGTCGAAACGTACGT (38-57)	DQ124188[11]
	EqFlu M R	CGCGATCTCGGCTTTGA (84-100)	
	EqFlu M Pr	†CTCTCTATCGTACCATCAGG‡ (59-78)	
EqFlu HA3	EqFlu HA3 F	TCACATGGACAGGTGTCACTCA (448-469)	L39914[11]
	EqFlu HA3 R	GGCTGATCCCCTTTTGCA (485-506)	
	EqFlu HA3 Pr	†AACGGAAGAAGTGGAGC‡ (471-487)	
H1N1	NH1 forward	TGAGATATTCCCCAAGACAAGTTC (393-416)	FJ966960[3]
	NH1 reverse	TTTGTAGAAGCTTTTTGCTCCAG (489-467)	
	NH1 probe	†TCATGACTCGAACAAAGGTGTAACGG§ (426-451)	

*F=Forward primer. R=Reverse primer. Pr=Probe

†Reporter dye (FAM; 6-carboxyfluorescein) labeled nucleotide

‡Nonfluorescent quencher dye (MGB™; minor groove binding) labeled nucleotide

§BHQ1 (black hole quencher 1) dye labeled nucleotide

In this study we evaluated the capability of EqFlu NP, EqFlu M and EqFlu HA3 assays to detect not only H3N8 CIV but also the novel H1N1 virus that has been in widespread circulation around the world and which has proven capacity to infect dogs.[24,434] Tissue culture fluid (TCF) containing the A/canine/FL/43/04 isolate and 13

other archived CIV isolates from the Animal Health Diagnostic Center, Cornell University, Ithaca, NY and Livestock Disease Diagnostic Center, University of Kentucky, Lexington, KY were tested in the study. Also included were 20 archived nasal swabs from dogs with signs of respiratory illness, 10 of which had previously tested positive for CIV by virus isolation in embryonated hens' eggs or MDCK cells according to standard laboratory protocols. Nasal specimens were collected using cotton or Dacron swabs moistened with a few drops of normal saline or viral transport medium. The presence of CIV in TCF and allantoic fluid (AF) had previously been confirmed by either sequencing the entire genome (n=11) or H3 HA gene (n=3). Of the ten CIV positive nasal swab samples, three were previously diagnosed as positive by rRT-PCR targeting the M gene. These three samples were subsequently tested by an N1 NA specific RT-PCR, thus ruling out H1N1 influenza virus. The remaining seven CIV positive nasal swab samples were part of a study in which H3N8 virus was continuously circulating in a particular animal shelter. The H3 HA gene from three isolates (representative of the total of seven samples) had been sequenced to confirm that they were H3N8 CIV. A total of 38 nasal swabs from pigs that were experimentally infected with the A/CA/04/2009 strain of H1N1 virus, as well as swabs from 12 control pigs were also included in the study.[439] The presence of H1N1 virus in pig samples was previously confirmed by VI in embryonated hens' eggs. All archived nasal swab specimens, TCF and AF samples were stored at -80 °C prior to nucleic acid extraction. Viral nucleic acid was isolated from 50 µl of TCF, AF or nasal swab samples with a commercial viral RNA isolation kit[a] by using a commercial magnetic particle processor.[b] Viral RNA was eluted in 50 µl of nuclease free water and stored at -80 °C until further use. The primers and probes used in this study were

identical to those previously described for the EqFlu NP, EqFlu M and EqFlu HA3 rRT-PCR assays (Table 4.1).[202] The primers and probe set specific for the H1 HA gene of the novel H1N1 strain were previously described (Table 4.1).[440] A 1-tube rRT-PCR assay was performed using a commercial kit and machine[c,d] under the exact same conditions as previously reported.[202] Each sample was tested in duplicate in each assay.

Initially, we determined the ability of all three primer sets to detect CIV using RNA extracted from TCF containing the A/canine/FL/43/04 strain. EqFlu NP, EqFlu M and EqFlu HA3 assays detected CIV RNA with average Ct values of 16.31, 23.71 and 15.28, respectively. In contrast, all three assays failed to detect influenza virus nucleic acid extracted from the A/CA/04/2009 strain of H1N1 virus. Subsequently, we evaluated these assays with RNA extracted from the 13 TCF and AF samples containing other CIV isolates. All samples tested positive, with mean Ct values ranging from 20.12 ± 1.87 (mean ± standard deviation) with EqFlu NP, 26.25 ± 7.61 with EqFlu M and 22.25 ± 4.03 with EqFlu HA3 assays. Comparison of Ct values indicated that the EqFlu NP assay had the lowest Ct value compared to the EqFlu M and EqFlu HA3 assays ($p=0.0095$ and $p=0.0447$, respectively). In addition, 20 canine nasal swab samples were tested in the study. Ten of these canine nasal swabs that were positive by VI were also positive in all three rRT-PCR assays, with mean Ct values ranging from 25.51 ± 3.06 with EqFlu NP, 27.18 ± 2.63 with EqFlu M and 26.98 ± 3.61 with EqFlu HA3 assays. The remaining ten nasal swab samples that were negative by VI were also negative in all three rRT-PCR assays. The EqFlu NP assay had the lowest Ct values with all twenty four samples (TCF, AF and nasal swab samples) compared to the EqFluM and EqFlu HA3 assays ($p=0.0024$ and $p=0.0078$, respectively).

Results of the three rRT-PCR assays using nucleic acid extracted from nasal swabs from dogs highly correlated with the VI results (100% sensitivity and specificity; Table 4.2). These assays provide a rapid and convenient means of detecting CIV nucleic acid in nasal swab samples and for confirming a diagnosis of CI. The sensitivity of the assays has been previously established to be ≥ 10 RNA molecules.[202] The primers and probe specific for the H1 HA gene of the novel H1N1 strain failed to recognize the A/canine/FL/43/04 strain or any other H3N8 positive samples included in this study. In contrast, the assay readily detected the H1N1 viral nucleic acid in the 38 nasal swabs collected from the H1N1 experimentally infected pigs (mean Ct value 24.78; 100% sensitivity).[440] None of the 12 nasal swab samples collected from control pigs reacted with the H1 HA gene specific primers and probe (100% specificity). The data clearly demonstrated that the three EqFlu rRT-PCR assays and the rRT-PCR assay specially designed to detect the novel H1N1 virus are highly specific for each influenza subtype and could be used successfully to diagnose cases of respiratory disease due to either of these viruses in dogs.

Table 4.2. Detection of CIV or swine influenza virus nucleic acid by rRT-PCR assays targeting nucleoprotein (NP), matrix (M) and hemagglutinin (HA) genes of H3N8 equine influenza virus

Specimens Tested	rRT-PCR Assay Names					
	EqFlu NP*		EqFlu M*		EqFlu HA3*	
	Ct value†	Mean±SD	Ct value†	Mean±SD	Ct value†	Mean±SD
TCF or AF Containing CIV Isolates (n=14)						
A/Ca/FL/43/04	16.31		23.71		15.28	
A/Ca/FL/15592/04 MDCK P1	20.21		20.20		19.63	
A/Ca/FL/61156,2/07 MDCK P1	21.80		35.32		23.41	
A/Ca/KY/1198778/06 Egg P1	21.02		21.15		21.88	
A/Ca/CO/17864/06 Egg P2	21.93		22.05		22.96	
A/Ca/NJ/73709/09 Egg P1	19.76		37.31		30.32	
A/Ca/VA/93653/09 Egg P1	19.17		38.87		29.40	
A/Ca/PA/10909/07 egg P2	20.32	20.12±1.87	21.00	26.25±7.61	22.13	22.25±4.03
A/Ca/NY/115809/05 Egg P2	20.09		20.39		20.58	
A/Ca/CO/8880/06 MDCK P1	16.40		16.86		17.24	
A/Ca/PA/10915/06 Egg P2	23.01		23.32		24.75	
A/Ca/NY/49601/06 MDCK P1	20.58		35.39		21.00	
A/Ca/CA/70645/06 Egg P2	20.42		20.55		21.13	
A/Ca/KY/49417-06 MDCK P1	20.59		31.49		21.74	
Canine Nasal Swabs Samples Positive by VI‡ (n=10)						
1623-10-2-1 NY	29.59		30.11		30.34	
3699-10 NY	20.19		23.88		21.35	
133-10 NY	29.00		31.69		30.35	
96978-09 PA	24.57		26.33		32.82	
61621-08 NY	25.78		27.45		26.89	
97293-08 NY	25.24	25.51±3.06	25.91	27.18±2.63	25.29	26.98±3.61
95945-08 NY	24.40		26.50		25.04	
68912-08 NY	24.37		25.99		25.55	
51790-08 NY	29.39		29.96		29.14	
113945-08 NY	22.55		23.94		23.03	
Canine Nasal Swab Samples Negative by VI‡ (n=10)						
1F 09 FL	-		-		-	
2F 09 FL	-		-		-	
3F 09 FL	-		-		-	
4F 09 FL	-		-		-	
5F 09 FL	-		-		-	
6F 09 FL	-	-	-	-	-	-
7F 09 FL	-		-		-	
8F 09 FL	-		-		-	
9F 09 FL	-		-		-	
10F 09 FL	-		-		-	

Table 4.2.-continued

Swine Nasal Swab Sample Positive by VI* for novel H1N1 virus (n=38)			
A/CA/04/2009	-	-	-
Swine Nasal Swab Sample Negative by VI* for novel H1N1 virus (n=12)			
	-	-	-

* The cut-off point for Ct value is 40 cycles
† p value were calculated based on Ct values of all 24 positive samples. p=0.0024 (EqFlu NP compared to EqFlu M) and p=0.0078 (EqFlu NP compared to EqFlu HA3)
‡ Attempted virus isolation in MDCK cells or embryonated hens' eggs

In summary, the three rRT-PCR assays we developed were able to recognize both equine and canine H3N8 viruses in clinical specimens and could be used as a routine laboratory test for the diagnosis of influenza in both animal species. The assays are highly specific and do not detect recently emerged H1N1 strain of influenza virus. Since the EqFlu NP assay has the highest sensitivity, it is recommended for the routine diagnosis of CIV in dogs. Furthermore, the EqFlu HA3 assay has the capability to distinguish canine influenza cases resulting from H3N8 subtype from H1N1 subtype infections which will not be detected by this assay.

Sources and manufacturers

a. MagMAX™-96 viral RNA isolation kit, Applied Biosystems, Foster City, CA.
b. KingFisher® magnetic particle processor, Thermo Fisher Scientific, Waltham, MA.
c. TaqMan® one-step RT-PCR master mix, Applied Biosystems, Foster City, CA.
d. 7500 Fast real-time PCR system, Applied Biosystems, Foster City, CA.

CHAPTER FIVE

Development of one-step TaqMan® real-time reverse transcription-PCR and conventional reverse transcription PCR assays for the detection of equine rhinitis A and B viruses

(submitted to BMC Veterinary Research)

5.1. SUMMARY

Background: Equine rhinitis virus A and B (ERAV and ERBV) are common equine respiratory viruses belonging to the family *Picornaviridae*. There is evidence that these two viral infections are prevalent in countries in which sero-survaillence studies have been undertaken. Currently there is a lack of rapid and reliable diagnostic methods for virus detection and antibody determination. The sensitivity of virus isolation varies between laboratories and is confounded by difficulties in isolating virus from the urine of carrier horses. The objective of this study was to develop molecular diagnostic assays (real-time RT-PCR [rRT-PCR] and conventional RT-PCR [cRT-PCR] assays) capable of detecting and distinguishing ERAV from ERBV without the inherent problems associated with the current laboratory diagnosis of these infections.

Results: Three rRT-PCR assays targeting the 5'-UTR of ERAV and ERBV were developed. One assay was specific for ERAV, whereas the remaining two assays were specific for ERBV. In addition, six cRT-PCR assays targeting the 5'-UTR and 3D polymerase regions of ERAV and ERBV were also developed. Both rRT-PCR and cRT-PCR assays were evaluated using RNA extracted from 21 archived tissue culture fluid samples which were previously determined to be positive for ERAV or ERBV with virus specific rabbit antiserum. All rRT-PCR and cRT-PCR assays targeting ERAV could only detect ERAV isolates (n=11) and did not cross-react with any ERBV isolates (n=10). Similarly, the rRT-PCR and cRT-PCR assays targeting ERBV could only detect ERBV isolates and did not cross-react with ERAV isolates. None of the rRT-PCR or cRT-PCR assays cross-reacted with any of the other common equine respiratory viruses. With the

exception of one cRT-PCR assay, the detection limit among all these assays was 1 plaque forming unit per ml (pfu/ml).

Conclusion: These new rRT-PCR and cRT-PCR assays provide useful diagnostic tools for the detection and differentiation of ERAV and ERBV. While the results of this study are very promising, a much greater number of clinical specimens needs to be tested before each assay is fully validated for the detection of ERAV and/or ERBV in suspect cases of either viral infection.

5.2. INTRODUCTION

The family *Picornaviridae* is a large family of viruses classified into several genera with extensive diversity in physical properties, antigenicity and mechanisms of pathogenesis.[441] Although there are many different picornaviruses with various degrees of relatedness, all share several features in common. All picornaviruses have a single-stranded positive-sense RNA genome whose 5'-end is covalently linked to a VPg (virion protein genome-linked) protein. The RNA genome contains a 5′ untranslated region (UTR) with an internal ribosome entry site (IRES), a single open reading frame (ORF) encoding the viral capsid proteins and the viral replicase proteins, a 3′ UTR and a 3′ poly(A) tail.[442] The ORF is divided into three regions: P2 encodes four structural proteins (VP1-VP4), P2 (2A-2C) and P3 (3A-3D) encode seven non-structural proteins.[443] A key component of the replication machinery is the RNA-dependent RNA polymerase (RdRp), also referred to as 3D polymerase ($3D^{pol}$) in picornaviruses. This protein is responsible for the synthesis of both plus- and minus- strand viral RNA.[444] Equine piconaviruses, formerly known as the equine rhinoviruses 1, 2 and 3 have been reclassified as equine rhinitis A virus (ERAV) and equine rhinitis B 1 and 2 viruses (ERBV1 and ERBV2, respectively). ERAV (formerly equine rhinovirus 1 [prototype ERAV.P393/76]) is a member of the genus *Aphthovirus,* in the family *Picornaviridae*, and was first isolated in the United Kingdom in 1962.[32,445-446] The genome organization and structure of ERAV is very similar to other Picornaviruses (e.g. foot-and-mouth disease virus). The second equine rhinitis virus, ERBV1 (formerly equine rhinovirus 2

[prototype P1436/71]) was first isolated in Switzerland and subsequent sequence determination resulted in it being classified in a new genus *Erbovirus*, also in the family *Picornaviridae*.[446-447] The ERBV1 serotype comprises two distinct phylogenetic groups, one of which is phenotypically acid stable and the other is acid labile.[448] Subsequently, a third equine rhinovirus virus (equine rhinovirus 3) was also isolated in Switzerland and following sequence analysis of its viral capsid proteins, it was shown to be a second serotype in the genus *Erbovirus*, and was designated as ERBV2 (prototype P313/75).[448-450]

Strains of ERAV, ERBV1 and ERBV2 have been identified with both subclinical and clinical upper respiratory tract infections in horses worldwide.[28,33,451-452] Little is known about the pathogenesis of ERAV and ERBV, which could be attributable in part to the lack of suitable laboratory methods for the diagnosis of these infectious agents. Seroprevalence data reported by different investigators indicate that neutralizing antibodies to ERAV and ERBV can be found in 50% to 80% of horses worldwide and the seropositive percentage seems to be correlated with the age of the animals.[9,28-31] Most ERAV, ERBV1 and ERBV2 isolates were recovered from horses with acute febrile respiratory disease with clinical signs of high fever for 1-3 days, serous to mucopurulent nasal discharge, anorexia, leg edema and enlarged lymph nodes of the head and neck that were sensitive on palpation. A significant number of horses may carry and shed virus in their urine for a long time. Subclinical infection and subsequent seroconversion have also been reported.[32-33,453-454]

The clinical signs of equine influenza virus, equine herpesvirus-1 and -4, equine rhinitis A and B (ERAV, ERBV1, ERBV2), equine adenovirus 1 (EAdV1) and equine arteritis virus (EAV) infections are very similar and resemble a number of other infectious and non-infectious equine respiratory diseases.[6-7] Accordingly, a provisional clinical diagnosis based solely on the respiratory signs must be confirmed by laboratory testing. Furthermore, rapid and accurate identification of these viruses is critical to the control of the diseases they cause, particularly in light of the fact that each of them can cause very similar clinical signs in affected horses. Therefore, the development of rapid, highly sensitive and specific diagnostic assays is essential to the identification and

differentiation of ERAV and ERBV in infected horses during outbreaks of disease. In addition, such assays would facilitate epidemiological investigations.

Traditionally, ERAV and ERBV have been detected by virus isolation in susceptible cells lines such as African green monkey kidney (Vero) or rabbit kidney-13 (RK-13) cells. The source of these viruses can include nasal swabs, blood, feces and urine.[33,455-456] Virus isolation can be challenging because strains of these viruses may grow poorly in cell culture and may not give rise to visible cytopathic effect.[27,457] A modified culture medium supplemented with $MgCl_2$ can enhance the growth of some ERBV strains, but it is unsuitable for diagnostic purposes due to lack of sensitivity.[457] Furthermore, successful virus isolation frequently requires multiple blind passages and subsequent confirmation by electron microscopy or immunofluorescence for testing in the case of non-cytopathic strains. ERAV and ERBV can also be detected serologically by demonstration of a four-fold or greater rise in antibody titer between paired sera by serum neutralization[33,447,458] or complement fixation.[451,459] These traditional serologic techniques, although sensitive and specific, are time consuming and tedious. Several rapid molecular tests such as conventional RT-PCR (cRT-PCR) and real-time RT-PCR (rRT-PCR) have been developed for ERAV and ERBV.[106,205-206,457] The primers used in these assays were located in the $3D^{pol}$, 3'-UTR, 5'-UTR or VP1-2A regions of the viral genome. In the present study, we developed a panel of three new rRT-PCR assays for ERAV and ERBV targeting the 5'-UTR region of each viral genome, respectively. In addition, a panel of six cRT-PCR assays targeting the 5'-UTR and $3D^{pol}$ regions of ERAV or ERBV were also developed.

5.3. MATERIALS AND METHODS

Viruses and cells

Twenty-one TCF samples containing ERAV, ERBV1 and ERBV2 were included in this study. These samples were previously isolated from nasal swabs and urine samples from horses and characterized by the late Dr. William H. McCollum at the Maxwell H. Gluck Equine Research Center, University of Kentucky.[460] The prototype

strains of ERAV (NVSL-0600EDV8501) and ERBV (NVSL-0610EDV85010) from NVSL, Ames, IA were also included in the study. Virus working stocks were produced by propagating the viruses in RK-13 cells (ATCC CCL37).

To determine the specificity of the rRT-PCR and cCR-PCR assays, viral nucleic acid from each of the following equine viral pathogens was included in the study: equine arteritis virus (ATCC VR-796), equine herpesviruses 1-5 (EHV-1 [ATCC VR-700], EHV-2 [ATCC VR-701], EHV-3 [ATCC VR-352], EHV-4 [ATCC VR-2230], and EHV-5[386]); equine adenovirus 1 (NVSL-001EDV8401) and 2; equine influenza virus (EIV) type A1 (equine/Prague/1/56 [H7N7]; NVSL-021IDV9201) and A2 (equine/Miami/63/ [H3N8]; NVSL-060IDV0501], equine/Kentucky/81 [H3N8; NVSL-040IDV0001], equine/Alaska//91 [H3N8; NVSL-020IDV9101]); and Salem virus, a novel paramyxovirus of horses.[387] The EHV-5 and Salem virus were kindly provided by Dr. Stephen Bell at University of California, Davis, CA and Dr. Edward Dubovi, Cornell University, Ithaca, NY, respectively.

The high passage RK-13 cell line (RK-13 KY; passage level 399–409) was maintained in Eagle minimum essential medium (EMEM) supplemented with 10% ferritin-supplemented bovine calf serum (Hyclone Laboratories, Inc., Logan, UT), 1% penicillin and streptomycin, and 0.1% amphotericin B (1,000 µg/ml). The overlay medium used for inoculated cultures was 0.75% carboxymethylcellulose (CMC) (Sigma-Aldrich, St. Louis, MO) in supplemented EMEM. All of the other reagents were obtained from Mediatech, Inc., Herndon, VA.

RNA extraction

Viral RNA was prepared from virus-infected tissue culture fluid (TCF) using the MagMAX™-96 Viral RNA Isolation Kit (Life Technologies, Forest City, CA) according to the manufacturer's instructions. Briefly, TCF samples were microcentrifuged at 13,800 ×g for 2 min, and 50 µl of supernatant was removed and used for nucleic acid extraction. The viral nucleic acid was eluted in 50 µl nuclease free and stored at -80 °C.

Primers and probes

The conserved and variable regions of each equine rhinitis virus serotype (ERAV and ERBV) have been determined by alignment of 12 sequences (8 ERAV [GenBank accession numbers: L43052, DQ272127, NC_003982, X96870, DQ272578, DQ272577, DQ268580 and DQ272128], 2 ERBV1 [GenBank accession numbers: NC_003983 and X96871] and 2 ERBV2 [GenBank accession numbers: AF361253 and NC_003077]) available in GenBank. The rRT-PCR fluorescent TaqMan® MGB™ (minor groove binding) probes and forward and reverse primers for ERAV, ERBV1 and ERBV2 were designed to the conserved regions in 5'-UTR of each strain using Primer Express™ software (Life Technologies, Foster City, CA). Similarly, the cRT-PCR forward and reverse primers from both serotypes were designed to target the 5'-UTR and $3D^{pol}$ regions of the genome using Vector NTI (Life Technologies, Foster City, CA). The four primers from a nested RT-PCR assay developed by Black *et al* (2007) were included in the study as four one-step RT-PCR assays according to the primers location.[457] The primers and probe from a rRT-PCR assay developed by Quinlivan *et al* (2010) was also included in this study using our rRT-PCR reagents.[206]

One-step rRT-PCR assay

The one-step TaqMan® rRT-PCR assay was performed using the TaqMan One-Step RT-PCR Master Mix in a 7500 Fast Real-Time PCR System as previously described.[201] Every sample was tested in duplicate in each assay. Briefly, 25 µl of RT-PCR mixture for each reaction contained 12.5 µl of 2 × Master Mix without UNG (uracil-N-glycosylase), 0.625 µl of 40 × MultiScribe and RNase Inhibitor Mix, 0.45 µl of 50 µM of forward and reverse primers (final concentration 900 nM), 0.625 µl of 10 µM probe (final concentration 250 nM), 5.35 µl of nuclease free water, and 5 µl of test sample RNA. The following thermocycling conditions were used under standard mode as per manufacturer's recommendation: 30 min at 48 °C, 10 min at 95 °C, followed by 40 cycles at 95 °C for 15 sec and 60 °C for 1 min. Each RT-PCR run included a control

without RNA (containing the reaction mix with 5 µl of water [no template control]) and positive controls containing ERAV or ERBV RNA.

cRT-PCR assay and sequencing analysis

The cRT-PCR was performed using a Qiagen OneStep RT-PCR kit (Qiagen, Santa Clara, CA) and 5 µl of test sample RNA in a mastercycler gradient thermal cycler (Eppendorf, Westbury, NY) according to the manufacturer's recommendation. Briefly, 50 µl of RT-PCR reaction contains 10 µl of 5 × Qiagen OneStep RT-PCR buffer, 2 µl of Qiagen OneStep RT-PCR enzyme mix, 2 µl of 10 mM dNTP mix, 1 µl of RNase Inhibitor, 1 µl of each of the forward and reverse primers, 28 µl of nuclease free water and 5 µl of RNA template. The following thermal cycler conditions were used: 50 °C for 30 min, 95 °C for 15 min, followed by 40 cycles of 30 sec 94 °C denaturation, 30 sec 50 °C annealing, 1 min 72°C extension with a 10 min 72 °C final extension.

The authenticity of the cRT-PCR products amplified from ERAV or ERBV NVSL prototype strains were sent out for further sequencing using the primers which were used to amplify the products. The sequence data were analyzed using Aligner version 1.5.2 (CodonCode, Dedham, MA) software program.

Determination of detection limits of rRT-PCR and cRT-PCR assays

Using serial decimal dilutions (10^{-1} to 10^{-10}) of ERAV and ERBV prototype strains (NVSL-0600EDV8501 and NVSL-0610EDV85010, respectively), the detection limits of the rRT-PCR and cRT-PCR assays were evaluated. To avoid inter-assay variability, equal aliquots of each dilution were used in all three assays. Briefly, 5 µl of RNA extracted from 50 µl of each decimal dilution were used in rRT-PCR and cRT-PCR assays as described above. RNA was run in duplicate in rRT-PCR assays, and both cRT-PCR and rRT-PCR assays were repeated three times independently.

5.4. RESULTS AND DISCUSSION

Development of rRT-PCR assays for the detection of ERAV and ERBV

Three ERAV and ERBV specific primer and probe sets were developed targeting the conserved 5'-UTR region of the viral genomes (Table 5.1). One primer and probe set was specific for ERAV (named ERAV rRT-PCR assay) and the primers were degenerated to accommodate nucleotide variations found in the sequences that are available in GenBank. The other primer and probe set named ERBV1 rRT-PCR assay was specific for ERBV1 strain. The third assay named ERBV2 rRT-PCR assay consists of the same reverse primer and probe sequences as in the ERBV1 assay with the exception of the forward primer is specific for ERBV2. The 4-nucleotide difference in the forward primer between ERBV1 and ERBV2 assays was designed to increase the likelihood of detection of ERBV2 strains. Three rRT-PCR assays were initially tested with two prototype strains of ERAV and ERBV obtained from the National Veterinary Services Laboratories (NVSL), Ames, IA. All the assays were optimized using RNA xtracted from the prototype strains of ERAV and ERBV with different primers and probe concentrations using TaqMan® one-step RT-PCR master mix in a checkerboard assay. The optimal primer and probe concentrations producing the highest sensitivity and specificity for detection of ERAV and ERBV were selected for the final assay as developed in the material and methods section. The ERAV assay could only detect the ERAV prototype strain with a mean cycle threshold (Ct) of 21.79 $\pm$ 0.30 (mean $\pm$ standard deviation [STD]) ranging from 21.58 to 22.00 and there was no cross-reaction with ERBV prototype strain. Both ERBV rRT-PCR assays only the detected ERBV prototype strain but not the ERAV strain with the mean Ct of 12.99 $\pm$ 0.01 (ranging from 12.98 to 13) for ERBV1 and 29.01 $\pm$ 0.02 (ranging from 29.00 to 29.03) for ERBV2 assays, respectively. Subsequently, the specificity of these assays was tested using a range of other equine respiratory viruses including equine arteritis virus, equine influenza virus type A1 and A2, equine adenovirus 1 and 2, equine herpesvirus 1-5, and Salem virus. The assays were shown to be 100% specific with no cross-reactivity with nucleic acid extracted from the above mentioned equine respiratory pathogens.

Table 5.1. Primers and probes used in the rRT-PCR assays

rRT-PCR Assay Name	Primer or Probe[a]	Sequence 5' to 3' and Nucleotide Location (nt)	GenBank Accession Number	Length of Fragment (bp)	Target Genes
ERAV	ERAV F	AGCGGC**K**[d]TGCTGGATTTTC (397-415)	L43052	60	5'-UTR of ERAV
	ERAV R	CAT**Y**[e]TG**Y**CAGCTTGGTGACA (438-457)			
	ERAV Pr	FAM[b]-CGGTGCCATTGCT-MGB[c] (417-429)			
ERBV1	ERBV1 F	CCCC**TT**[f]CCCT**GA**AGATTGCT (148-167)	NC_003983	61	5'-UTR of ERBV1
	ERBV2 R	GGCAAACGACCAACACATCA (190-209)			
	ERBV2 Pr	FAM-TTCTTCCAACTAAACCC-MGB (169-185)			
ERBV2	ERBV2 F	CCCC**AA**CCCT**TG**AGATTGCT (148-167)			

[a]F=Forward primer. R=Reverse primer. Pr=Probe

[b]Reporter dye (FAM; 6-carboxyfluorescein) labeled nucleotide

Table 5.1-continued

[c]Nonfluorescent quencher dye (MGB™; minor groove binding) labeled nucleotide

[d]K represents G or T

[e]Y represents C or T

[f] Nucleotide difference between the forward primers of ERBV1 and ERBV2 were bold.

The three assays were further evaluated for detection capability using 21 archived ERAV (n=11) or ERBV (n=10) isolates whose identity was previously confirmed in a one-way neutralization test using virus specific rabbit antisera.[33] All three assays identified the ERV subtype accurately and no cross-reactions between subtypes were observed. The mean Ct values of ERAV, ERBV1 and ERBV2 rRT-PCR assays are 24.53 $\pm$ 3.45 (ranging from 22 to 29), 29.50 $\pm$ 3.58 (ranging from 24 to 34) and 29.14 $\pm$ 5.22 (ranging from 18 to 35), respectively. Both ERBV1 and ERBV2 rRT-PCR assays could detect two previously well characterized ERBV1 isolates (NS Count Wayne and 58-13 NVS) [448]. Therefore, none of the ERBV1 or ERBV2 rRT-PCR assays were able to distinguish viral RNA between ERBV1 and ERBV2 subtypes tested in the study. Overall, the two assays designed to distinguish ERBV1 and ERBV2 were able to detect the NVSL prototype strain of ERBV, indicating that the nucleotide mismatches in the forward primer were not sufficient to provide serotype specificity. This was further confirmed by their inability to distinguish the archived isolates as ERBV1 or ERBV2.

Previously Quinlivan *et al* (2010) developed two TaqMan® rRT-PCR assays targeting the conserved region of the 5'-UTR of the ERV genomes (Table 5.2).[206] These two assays were also tested with our prototype strains of ERV and 21 field isolates. The assay targeting ERAV could detect the ERAV prototype strain and the 11 ERAV positive isolates without cross-reacting with any ERBV samples. The mean Ct values were 15.31 $\pm$ 1.29 (ranging between 14 and 19), which were lower than the ERAV assay developed in this study (24.53 $\pm$ 3.45), indicating the published ERAV assay is more sensitive in detecting the field isolates as compared to the ERAV rRT-PCR assay developed in our study. In contrast, the assay targeting ERBV could not detect any of the ERBV isolates nor the prototype strain of ERBV. However, the reagents used in this study were not identical to the original publication by Quinlivan *et al* (2010) which may also have contributed to the reduced sensitivity of the ERBV assay.

Table 5.2. Primers and probes used in the rRT-PCR assay developed by Quinlivan *et al* (2010)

rRT-PCR Assay Name	Primer or Probe[a]	Sequence 5' to 3' and Nucleotide Location (nt)	GenBank Accession Number	Length of Fragment (bp)	Target Genes
ERAV	ERAV 468F	CCAGGTAACCGGACAGCG (468-485)	NC_003982	118	5'-UTR of ERAV
	ERAV 569R	GGCAGCGCTACCACAGG (569-585)			
	ERAV 508b	FAM[b]-CATTGCTCTGGATGGTGT-MGB[c] (508-525)			
ERBV	ERBV 77F	TGATGCTTGGCTCTCAGAAA (77-96)	NC_003983	132	5'-UTR of ERBV
	ERBV 189R	GCAAACGACCAACACATCAA (189-208)			
	ERBV 171b	FAM[b]-CTTCCAACTAAACCC-MGB[c] (171-185)			

[a]F=Forward primer. R=Reverse primer. Pr=Probe

[b]Reporter dye (FAM; 6-carboxyfluorescein) labeled nucleotide

[c]Nonfluorescent quencher dye (MGB™; minor groove binding) labeled nucleotide

Development of cRT-PCR assays for the detection of ERAV and ERBV

To provide more diagnostic options, we developed an additional panel of six cRT-PCR assays to target the 5'-UTR and $3D^{pol}$ regions of ERAV and ERBV (Table 5.3). All primers were designed to distinguish ERAV and ERBV subtype and were initially tested with the prototype strains of ERAV and ERBV from NVSL. All primer pairs could detect the prototype strains for which they were designed and the cRT-PCR products matched the predicted size (Fig 5.1). The authenticity of the cRT-PCR products were confirmed by sequencing. Subsequently, the primers were tested with the archived ERV TCF specimens. Similar to the rRT-PCR results, the ERAV 5'-UTR, ERAV Poly 1 and ERAV Poly 2 cRT-PCR assays could detect all the ERAV field isolates and did not cross-react with the ERBV isolates. The ERBV Poly 1 and ERBV Poly 2 cRT-PCR assays were also highly specific for ERBV strains without any cross-reacting with ERAV isolates. Sequence comparison analysis between the ERBV1 prototype P1436/71 (GenBank accession number X96871) and ERBV2 prototype P313/75 (GenBank accession number AF361253) revealed that these two strains shared 92.5% sequence identity in the $3D^{pol}$ region which is consistent with the previous findings that the $3D^{pol}$ region of ERBV is highly conserved and therefore commonly used for primer design [205,450]. The high sequence similarity between ERBV1 and ERBV2 in $3D^{pol}$ region is good for primer design to differentiate ERBV from ERAV but may also prevent the successful differentiation between ERBV1 and ERBV2 serotypes. In contrast to the high sensitivity of ERBV cRT-PCR assays targeting $3D^{pol}$ regions, the ERBV 5'-UTR cRT-PCR assay that was developed could only detect 2 out of the 10 ERBV positive isolates (Table 5.4). All six assays were specific for ERV and did not react with other common equine respiratory viruses. Therefore, we concluded that the assays developed in our laboratory could be used to distinguish ERAV from ERBV but not between ERBV serotypes.

Previously Black *et al* (2007) developed four primers for a RT nested-PCR for ERBV.[457] We took these four primers and mix and matched them depending on their positions to generate four standard RT-PCR assays (Table 5.3). These four assays (ERBV OUTER 1, ERBV OUTER 2, ERBV INNER 1 and ERBV INNER 2) could distinguish all ERBV positive isolates from ERAV isolates in a single reaction. The

application of one-step RT-PCR has a greater advantage over the nested RT-PCR because it eliminates the possibility of cross-contamination between samples and reduces the turnaround time.

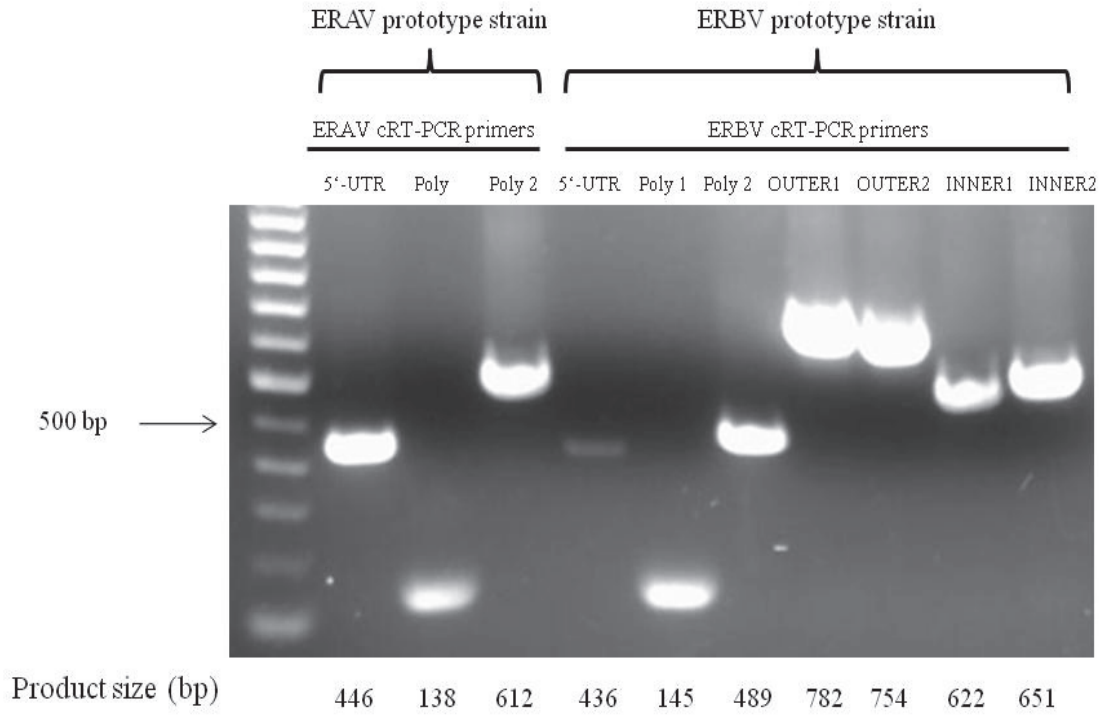

Fig 5.1. Agarose gel electrophoresis of ERAV or ERBV prototype strains from NVSL amplified with ERAV or ERBV specific cRT-PCR primers. The anticipated product sizes were shown.

Table 5.3. Primers and probes used in the cRT-PCR assays

cRT-PCR Assay Name	Primer	Sequence 5' to 3' and Nucleotide Location (nt)	Genbank Accession Number	Length of Fragment (bp)	Reference
ERAV 5'UTR	ERAV 5'UTR F	TCAGCCCCCTGTCATTGACT (341-360)	NC_003982	446	This study
	ERAV 5'UTR R	TG**R**[a]TCAGGGCTGTAACCA (769-786)			
ERAV Poly	ERAV Poly F	TGGATGAAGTGGTTTTTGC (6384-6402)	NC_003982	138	This study
	ERAV Poly R	CAGTCAAAGCCTGGTTGTCA (6502-6521)			
ERAV Poly2	ERAV Poly F	TGGATGAAGTGGTTTTTGC (6384-6402)	NC_003982	612	This study
	ERAV Poly R2	ACTCTCATTGCATCAGCTGC (6977-6996)			
ERBV 5' UTR	ERBV 5'UTR F	TTTCGTTCC**W**[b]CTTTAGC**R**[a]GG (349-368)	NC_003983	436	This study
	ERBV 5'UTR R	TCAGATCCGCACTCTATGAAG (764-784)			

Table 5.3.-continued

ERBV OUTER1	ERBV OUTER F	TTTTGATGCTTCACATTCTCC (7986-8006)	NC_003983	782	Black *et al,* 2007
	ERBV OUTER R	CGCTGTACCCTCGGTCCTACTC (8746-8767)			
ERBV OUTER2	ERBV OUTER F	TTTTGATGCTTCACATTCTCC (7986-8006)	NC_003983	754	Black *et al,* 2007
	ERBV INNER R	GCCTCGGCGAGTGAAGAG (8721-8739)			
ERBV INNER1	ERBV INNER F	CTTACTA**Y**^{c}GAATGTGARGGGGC (8117-8138)	NC_003983	622	Black *et al,* 2007
	ERBV INNER R	GCCTCGGCGAGTGAAGAG (8721-8739)			
ERBV INNER2	ERBV INNER F	CTTACTAYGAATGTGARGGGGC (8117-8138)	NC_003983	651	Black *et al,* 2007
	ERBV OUTER R	CGCTGTACCCTCGGTCCTACTC (8746-8767)			

Table 5.3.-continued

ERBV Poly1	ERBV Poly F	TTGAGTTGACCCTTCTGCA (7409-7427)	NC_003983	145	This study
	ERBV Poly R	TCATACTCTGAAATG**R**[a]**K**[d]TCCATTG (7530-7553)			
ERBV Poly2	ERBV Poly F	TTGAGTTGACCCTTCTGCA (7409-7427)	NC_003983	489	This study
	ERBV Poly R2	GCTGAACCAATGCCTAATCC (7879-7898)			

[a]R represents A or G

[b]W represents A or T

[c]Y represents C or T

[d]K represents G or T

Table 5.4: Archived ERAV and ERBV isolates tested with rRT-PCR assays and cRT-PCR assays

Sample	Serotype	Origin and/or Reference	rRT-PCR assays						cRT-PCR assays						
			ERAV	ERBV		ERAV			ERBV						
			ERAV	ERBV 1	ERBV 2	ERAV 5'-UTR	ERAV Poly	ERAV Poly 2	ERBV 5'-UTR	ERBV Poly 1	ERBV Poly 2	ERBV OUTER 1[c]	ERBV OUTER 2[c]	ERBV INNER 1[c]	ERBV INNER 2[c]
ERAV	ERAV	NVSL[a]	+	-	-	+	+	+	-	-	-	-	-	-	-
PERV, P4 (KY)/TCF 2004 A		GERC[b]	+	-	-	+	+	+	-	-	-	-	-	-	-
Plowright ,P4(KY)/ TCF 2004 A		GERC	+	-	-	+	+	+	-	-	-	-	-	-	-
T3 Isolate P10/2004 A		GERC	+	-	-	+	+	+	-	-	-	-	-	-	-
T10 isolate P9/ 2004 A		GERC	+	-	-	+	+	+	-	-	-	-	-	-	-
945 isolate P4/ 2004 A		GERC	+	-	-	+	+	+	-	-	-	-	-	-	-
ERV-1 (A) Plowright P4 KY		GERC	+	-	-	+	+	+	-	-	-	-	-	-	-
ERV-1 (A) PERV P4KY		GERC	+	-	-	+	+	+	-	-	-	-	-	-	-

Table 5.4-continued

Amp 87-73-69-945	ERAV	GERC	+	-	-	+	+	+	-	-	-	-	-	-	-
NS-T3		GERC	+	-	-	+	+	+	-	-	-	-	-	-	-
NS-T10		GERC	+	-	-	+	+	+	-	-	-	-	-	-	-
U-187		GERC	+	-	-	+	+	+	-	-	-	-	-	-	-
ERBV	ERBV	NVSL	-	+	+	-	-	-	+	+	+	+	+	+	+
Swiss isolate P6(KY)/ 2004 B		GERC	-	+	+	-	-	-	-	+	+	+	+	+	+
NS CW		GERC/ Black *et al,* 2005	-	+	+	-	-	-	+	+	+	+	+	+	+
U-198V		GERC	-	+	+	-	-	-	-	+	+	+	+	+	+
NS-SD		GERC	-	+	+	-	-	-	-	+	+	+	+	+	+
Mare 189		GERC	-	+	+	-	-	-	-	+	+	+	+	+	+
51-12NVS		GERC	-	+	+	-	-	-	-	+	+	+	+	+	+
57-10NVS		GERC	-	+	+	-	-	-	-	+	+	+	+	+	+
57-11NVS		GERC	-	+	+	-	-	-	-	+	+	+	+	+	+
57-13NVS		GERC	-	+	+	-	-	-	-	+	+	+	+	+	+
58-13 NVS		GERC/ Black *et al,* 2005	-	+	+	-	-	-	-	+	+	+	+	+	+

[a] National Veterinary Services Laboratories.

[b] Maxwell H. Gluck Equine Research Center. All archived samples from GERC were obtained from the late Dr. William H. McCollum.

[c] These assays were developed by Black *et al* (2007).

Comparison of sensitivities of the rRT-PCR and cRT-PCR

Using serial decimal dilutions (10^{-1} to 10^{-10}) of the TCF containing ERAV and ERBV prototype strains, the detection limits of all rRT-PCR and cRT-PCR assays were compared (Table 5.5, Fig 5.2). Viral RNA from each of the serial dilutions was eluted in 50 µl of nuclease free water and 5 µl tested in duplicate in the rRT-PCR and cRT-PCR assays. The plaque number in the highest dilution was used to calculate the number of infectious particles that can be detected by each assay. The amplification efficiency of the three ERAV, ERBV1 and ERBV2 rRT-PCR assays was 97.0%, 94.8% and 94.2%, respectively, calculated according to a previously described method (Fig 5.2.).[373] The ERAV rRT-PCR assay and ERAV 5'-UTR cRT-PCR assay could detect viral RNA up to 10^{-6} dilution of the ERAV in TCF which is approximately 1 pfu/ml of infectious virus particles. The other two ERAV cRT-PCR assays (ERAV Poly1 and ERAV Poly 2) were 10-fold less sensitive (10^{-5} virus dilution, approximately 10 pfu/ml) as compared to the rRT-PCR and cRT-PCR assays targeting the 5'-UTR regions (Fig. 5.2). The ERBV1 rRT-PCR assay could detect ERBV viral RNA up to 10^{-7} dilution which equals 1.2 pfu/ml infectious virus particles. The third rRT-PCR assay targeting ERBV2 was 3 logs less sensitive compared to the ERBV1 rRT-PCR assay and could detect more than 550 pfu/ml infectious virus particles. This suggests that the ERBV1 rRT-PCR assay is more suitable for the detection of ERBV in clinical samples. All the ERBV cRT-PCR assays except ERBV 5'-UTR cRT-PCR assay could detect 10 to 30 pfu/ml infectious virus particles (10^{-5} to 10^{-6} dilutions). The ERBV 5'-UTR cRT-PCR assay was the least sensitive and could only detect virus in the 10^{-1} dilution of TCF (2.75×10^5 pfu/ml infectious virus particles).

Table 5.5: Detection limit of virus particles with rRT-PCR assays and cRT-PCR assays[a]

ERV strains[b]	Assay Name													
	Cell culture	rRT-PCR assays			cRT-PCR assays									
		ERAV	ERBV		ERAV			ERBV						
		ERAV	ERBV 1	ERBV 2	ERAV 5'-UTR	ERAV POLY1	ERAV POLY2	ERBV 5'-UTR	ERBV OUTER 1[d]	ERBV OUTER 2[d]	ERBV INNER 1[d]	ERBV INNER 2[d]	ERBV Poly 1	ERBV Poly 2
ERAV	10^{-7}	10^{-6}	NA[c]	NA	10^{-6}	10^{-5}	10^{-5}	NA	NA	NA	NA	NA	NA	NA
ERBV	10^{-7}	NA	10^{-7}	10^{-4}	NA	NA	NA	10^{-1}	10^{-5}	10^{-4}	10^{-4}	10^{-4}	10^{-4}	10^{-5}

[a] Serial decimal dilutions of ERAV and ERBV were tested in a comparison study by virus isolation in cell culture, rRT-PCR and standard RT-PCR assays. Numbers shown on the table represent the serial virus dilution.

[b] ERAV and ERBV prototype strains were obtained from NVSL.

[c] Not applicable.

[d] The primers used in these four assays were obtained from a nested RT-PCR developed by Black *et al* (2007).

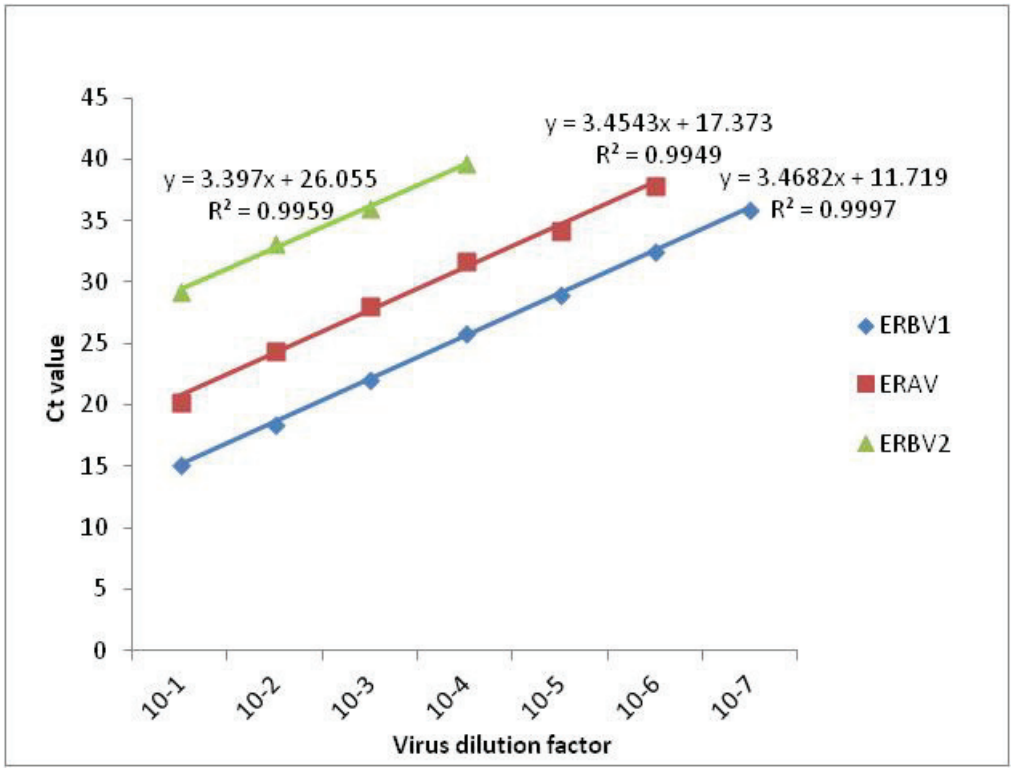

Fig 5.2. Comparison of detection sensitivity of the three rRT-PCR assays using ERAV or ERBV prototype strains from NVSL (ERAV rRT-PCR assay [y = 3.4543x + 17.373, R^2=0.9949], ERBV1 rRT-PCR assay [y = 3.4682x + 11.719, R^2=0.9997] and ERBV2 rRT-PCR assay [y = 3.397x + 26.055, R^2=0.9959]).

Overall, the rRT-PCR assays were more sensitive than the cRT-PCR assays. There is approximately a 10-fold difference in the limit between the rRT-PCR and cRT-PCR assays in detecting ERAV strains. There was significant difference in the sensitivity of the rRT-PCR and cRT-PCR assays targeting the ERBV strains. The ERBV 5'-UTR cRT-PCR assay is the least sensitive among all the developed assays. This might be explained by the fact that the reverse primer of the ERBV 5'-UTR cRT-PCR assay was located in the higher order internal ribosome entry site.[446] This complex sequence region may prevent efficient binding of the reverse primer to target sequences. However, no plausible explanation can be provided for the high sensitivity of the ERAV 5'-UTR cRT-PCR assay which was targeting the similar region as compared to ERBV.

Although ERAV and ERBV infections are considered a common disease in horses, limited data are available about the pathogenesis and disease prevalence, likely attributable at least in part to the absence of suitable diagnostic methods for these infections.[27-31,33,451-452,461-462] Currently there are few rapid molecular tests for the detection of these viruses including a duplex rRT-PCR developed by Mori *et al* (2009) [205] and single rRT-PCR assays for ERAV or ERBV developed by Quinlivan *et al* (2010).[206] The duplex rRT-PCR by Mori *et al* (2009) was developed to differentiate ERAV from ERBV, but in reality, none of the tested samples were ERAV positive.[205] Therefore the detection capability for ERAV in this duplex rRT-PCR assay is questionable. The single rRT-PCR assays developed by Quinlivan *et al* (2010) detected 30 ERAV and 5 ERBV positives in 300 nasal swab samples collected over a 7 year period.[206] As we discussed above, the ERBV rRT-PCR assay developed in that study was unable to detect any ERBV isolates tested in this study under the current rRT-PCR conditions. The assays developed in our study were tested with a limited number and well-characterized ERAV and ERBV samples.[448,457] The authors admitted that prior to the application of the assays on a routine diagnostic basis, both would need to be more fully evaluated using a greater number of clinical specimens positive for both ERAV and ERBV.

5.5. CONCLUSION

In the current study, we developed 1 rRT-PCR assay and 3 cRT-PCR assays for the detection of ERAV and 3 rRT-PCR assays and 3 cRT-PCR assays for ERBV. Twenty-one archived ERAV or ERBV field isolates were used to evaluate the detection capability of the assays. Both the rRT-PCR and cRT-PCR assays designed for ERAV or ERBV could detect the serotype specific isolates without cross-reacting with other equine viral pathogens. Comparison of the respective sensitivities of rRT-PCR assays and cRT-PCR assays confirmed that the molecular rRT-PCR assays have the same or greater sensitivity in detecting ERV in decimal serial dilutions of tissue culture fluids. Overall, the newly developed assays provide valuable tools for the detection of ERAV and ERBV.

CHAPTER SIX

Chimeric viruses containing the N-terminal ectodomains of GP5 and M proteins of porcine reproductive and respiratory syndrome virus do not change the cellular tropism of equine qrteritis virus

(submitted to Virology)

6.1. SUMMARY

Equine arteritis virus (EAV) and porcine reproductive and respiratory syndrome virus (PRRSV) are members of family *Arteriviridae*; they share many biological properties but differ significantly in cellular tropism. Using an infectious cDNA clone of EAV, we engineered a panel of six chimeric viruses by exchanging the N-terminal ectodomains and/or full-lengths of the two major envelope proteins (GP5 and M) from PRRSV. The recombinant viruses expressing the N-terminal ectodomain of PRRSV GP5 alone or M alone or together (GP5ecto, Mecto and GP5&Mecto, respectively) in the EAV backbone were viable and genetically stable. Compared to the parental virus, these three chimeric viruses produced lower titers and smaller plaque sizes indicating that they have a compromised phenotype. The three chimeric viruses could only infect EAV susceptible cell lines but not PRRSV susceptible cells. Therefore, the two major envelope proteins may not be determining factors in the cellular tropism of EAV and other arteriviruses.

6.2. INTRODUCTION

Members of the family *Arteriviridae* include equine arteritis virus (EAV), porcine reproductive and respiratory syndrome virus (PRRSV), lactate dehydrogenase-elevating virus (LDV) of mice and simian hemorrhagic fever virus (SHFV).[255,463] Arteriviruses are small, enveloped animal viruses with an isometric core containing a positive sense RNA genome.[320,464] EAV and PRRSV are the causative agents of equine viral arteritis (EVA) in horses and porcine reproductive and respiratory syndrome (PRRS) in pigs, respectively.[212,465-466] The EAV and PRRSV genomes are polycistronic and contain at least 10 open reading frames [ORFs].[260,263,467] The 5'-proximal three-quarters are occupied by two large ORFs (1a and 1b) that together encode all viral enzyme functions (collectively referred to as "replicase") required for genome replication and subgenomic mRNA (sgmRNA) production.[284,468] The ORFs 1a and 1b are translated to produce polyproteins 1a and 1ab (pp1a and pp1ab), with the latter being a C-terminally extended version of the former.[256,264-265] Following autoproteolytic processing of the replicase pp1a and pp1ab, at least 12 (EAV) or 14 (PRRSV) cleavage products or 'nonstructural proteins' (nsps) are produced.[265,284,320] The ORFs 2a, 2b, 3, 4, 5a, 5, 6, and 7 of EAV and PRRSV are partially overlapping and are located in the 3'-one-quarter of the genome, encoding seven envelope proteins (E, GP2, GP3, GP4, ORF5a protein, GP5 and membrane [M]) and a nucleocapsid protein (N).[263,265,320,464,467] The glycosylated GP5 and the unglycosylated M protein (encoded by ORF5 and ORF6, respectively) are the major envelope proteins of EAV and PRRSV; they form a disulfide-linked heterodimer in the mature virus particles.[266,469] The formation of GP5/M heterodimer is critical for the expression of neutralization epitopes of both viruses.[272,470-472] The M protein is the most conserved envelope protein of arteriviruses.[473] It consists of a short 19-amino acid N-terminal domain exposed at the surface of the virion followed by three successive membrane-spanning domains and a C-terminal endodomain of 81-87 amino acids.[474-476] The GP5 protein has a similar membrane topology as compared to M protein except that it contains a cleavable N-terminal signal peptide and the ectodomain of EAV is approximately 68 amino acids (a.a.) longer than that of PRRSV.[476-477] The GP5/M heterodimer is presumed to play important roles in attachment to the host cell receptor and in cell entry.[464] In addition, the arterivirus envelope contains a heterotrimer of three

minor membrane glycoproteins (GP2 [encoded by ORF2b in EAV and ORF2a in PRRSV], GP3 [encoded by ORF3] and GP4 [encoded by ORF4]) and two unglycosylated envelope proteins (E [ORF2a in EAV and ORF2b in PRRSV][478-479] and ORF5a protein [ORF5a]).[263,467] It has been shown that all three major structural proteins (N, GP5 and M) and four of the minor envelope proteins (E, GP2, GP3 and GP4) are essential for the production of infectious progeny virus.[268,480] It has also been shown by reverse genetics that the elimination of ORF5a protein expression by knocking down the start and stop codon will cripple the EAV virus and lead to progeny virus with a small plaque phenotype and a significantly reduced virus titer in transfected cells.[263]

Arteriviruses are highly species specific and macrophages are the primary target cells of virus replication.[235,481-485] However, EAV can replicate in a variety of primary cells including equine pulmonary artery endothelial,[486] horse kidney, rabbit kidney and hamster kidney cells and a number of continuous cell lines including baby hamster kidney (BHK-21),[281,487] rabbit kidney-13 (RK-13), African green monkey kidney (VERO),[241,488] rhesus monkey kidney (LLC-MK2), MARC-145 and hamster lung (HmLu)[488] cells. In contrast, PRRSV can only replicate in a limited number of cell types. North American PRRSV (Type 2) strains replicate in primary porcine alveolar macrophages (PAM), and the African green monkey cell line, MA-104, or its derivative, MARC-145.[489] Most, if not all, European PRRSV (Type 1) strains replicate best or exclusively in PAMs, but can be adapted to grow in MA-104 derived cell lines, including CL2621 and MARC-145. Until recently, the viral envelope protein(s) involved in virus attachment and entry of EAV and PRRSV have not been fully characterized.[294,490] In a previous study, Dobbe et al (2001) demonstrated that EAV expressing the ectodomain of GP5 of PRRSV IAF-Klop strain[491] did not change the cellular tropism of the virus. Recently, in our laboratory, we have developed an infectious cDNA clone of the modified live virus (MLV) vaccine (ARVAC®) of EAV (prMLVB).[492] This infectious cDNA clone was originally developed to design a marker vaccine for EAV and to increase the safety and efficacy of the current MLV vaccine, as well as a vector platform to express heterologous genes from other viruses. In this study, we describe the use of this infectious cDNA clone to characterize the role of the major envelope proteins (GP5 and M) for investigating the cellular tropism of EAV.

6.3. MATERIALS AND METHODS

Cells and viruses

The cell lines used in the study included equine pulmonary artery endothelial cells (EECs, P12 to P22) [486], high passage rabbit kidney-13 cells (RK-13 KY, P399 to P409), baby hamster kidney cells (BHK-21 [ATCC CRL-12072], Manassas, VA), MARC-145 cells and porcine macrophage cells 3D4/21 (ATCC CRL-2843, Manassas, VA). The EECs were maintained in DMEM with high glucose supplemented with 10% fetal bovine serum (Hyclone, Logan, UT), penicillin, streptomycin, L-glutamine and non-essential amino acids (Life Technologies, Grand Island, NY). RK-13 KY, BHK-21 and MARC-145 were maintained at 37 °C in Eagle's minimum essential medium with 10% ferritin-supplemented bovine calf serum (Hyclone, Logan, UT) penicillin, streptomycin, amphotericin B, and sodium bicarbonate (Life Technologies, Grand Island, NY). In addition, porcine alveolar macrophages (PAM) were isolated and stored at -80 ºC until used (kindly provided by Dr. Kay Faarberg, USDA-ARS, Ames, IA). The PAM cells were maintained in Dulbecco's MEM supplemented with 5% fetal bovine serum and 5% antibiotic/antimycotic (Life Technologies, Grand Island, NY). The PRRSV IA1107 strain was kindly provided by Fort Dodge Animal Health Laboratories (now Pfizer Animal Health Inc, Kalamazoo, MI). This strain was isolated from the lung of a pig that died of PRRS and working virus stock was made by passaging once in MARC-145 cells.

Construction of EAV/PRRSV chimeric infectious cDNA clones by swapping ORF5 and 6 from PRRSV

The development and characterization of an infectious cDNA clone (prMLVB) of the modified live vaccine strain of EAV (ARVAC®) that was used as the backbone to develop the chimeric viruses has been previously described (GenBank accession number FJ798196).[492] The generation of chimeric infectious cDNA clones was performed by a previously described method with some modifications.[493] Briefly, three plasmid constructs were generated by separating the overlapping regions between ORFs 4/5 and 5/6 of the prMLVB infectious cDNA clone of EAV (Fig 6.1). The unique XbaI site at nt

position 14530-14535 was knocked out in the prMLVB clone to generate the shuttle vector prMLVB-XbaIko to facilitate the cloning strategy. The ORFs 4/5 overlapping region ($_{11144}$CAATGCTATCTATGATT$_{11160}$) was first removed from the prMLVB-XbaIko clone by site-directed mutagenesis and then the 5'CAGTGCTATCTGTGAacttaagcaacatgctgtccatgaTT3′ sequence was inserted into the corresponding region to obtain the prMLVB4/5 (GenBank accession number JQ844153) in which the ORF4 and ORF5 overlapping regions were separated. A unique restriction site AflII (5′CTTAAG3′) was introduced into the region separating ORF4 and ORF5. Similarly, the ORFs 5/6 overlapping region $_{11899}$GTATGGGAGCCATAGAT$_{11915}$ was removed from the prMLVB-XbaIko clone by insertion of the nucleotides 5′GTGTGGGAGCCATAGagcggccgccaatgggagccatagAT3′ into the corresponding region to obtain the clone prMLVB5/6 (GenBank accession number JQ844154). A unique restriction site NotI (5′GCGGCCGC3′) was introduced into the region separating ORF5 and ORF6 to facilitate the next cloning step. Subsequently, using a similar approach, a third construct was developed in which both 4/5 and 5/6 ORFs were separated (prMLVB4/5/6, GenBank accession number JQ844155). These three clones were used to generate various EAV/PRRSV chimeric viruses by swapping ORF5 and ORF6 (N-terminal ectodomains and as well as full-length) from PRRSV IA1107 strain.

The GP5 N-terminal ectodomain of PRRSV IA1107 strain (nt 11788-11979; numbered according to GenBank accession number U87392) was reverse transcribed with primer PVGP5ectoN followed by PCR amplification using primers PVGP5ectoP and PVGP5ectoN (Table 6.1) using a commercial one-step RT-PCR kit (Qiagen, Valencia, CA). The PRRSV GP5 ectodomain was then cloned into the plasmid prMLVB4/5 using unique restriction sites AflII and EcoRI to obtain the recombinant plasmid prMLVB4/5GP5ecto (GenBank accession number JQ844156). The GP5 full-length domain of PRRSV IA1107 (nt 13788-14390) was RT-PCR amplified with primer PV15364N followed by PCR amplification using primers PVGP5ectoP and PVGP5fullN and cloned into prMLVB4/5 with restriction sites NotI and XbaI to obtain the recombinant plasmid prMLVB4/5GP5full. Similarly, the M full-length domain of PRRSV IA1107 (nt 14375-14899) was reverse transcribed with primer PV15364N and PCR amplified using primers PVMfullP and PVMfullN and cloned into prMLVB5/6 with

restriction sites NotI and XbaI to generate the chimera construct prMLVB5/6Mfull. Because of the short length of the M protein N-terminal ectodomain sequence, the N-terminal ectodomain of PRRSV IA1107 M protein (nt 14375-14425) was directly inserted into the shuttle vector prMLVB-XbaIko4/5/6RemMecto, in which the M protein N-terminal ectodomain of EAV was removed via site-directed mutagenesis, using primer EAVinsPVMectoP and EAVinsIA1107MectoN to generate prMLVB4/5/6 Mecto (GenBank accession number JQ844157). The specific nucleotide locations were identified according to the North American VR2332 strain of PRRSV sequence (GenBank accession number U87392). The prMLVB4/5/6 Mecto and prMLVB4/5/6 Mfull were further used as vectors to introduce the PRRSV GP5 N-terminal ectodomain and GP5 full-length sequences using the above described cloning strategies to generate prMLVB4/5/6 GP5&Mecto (GenBank accession number JQ844158) and prMLVB4/5/6 GP5&Mfull plasmids. The nucleotide sequences of the primers used in this study are listed in the Table 6.1. The panel of chimeric constructs between the EAV and PRRSV major envelope protein coding genes is shown in Figure 6.1.

Sequencing of the plasmid constructs

The region spanning from ORFs 4-7 of prMLVB4/5, prMLVB5/6, and prMLVB4/5/6 plasmids, as well as all five chimeric plasmids were PCR amplified and sequenced to confirm their authenticity. Briefly, each of the plasmids was amplified using primers that were specific for the 5' end of the ORFs 4 and the 3' end of ORF7 (10763P and 12568N primers [Table 6.1]; numbered according to the published sequence of the VB strain of EAV, GenBank accession number DQ846750) using the high-fidelity proofreading *Pfu* Turbo DNA polymerase (Agilent Technology, Santa Clara, CA) according to a previously described protocol.[494] Both sense and antisense strands of the chimeric plasmids were sequenced using EAV specific primers 10763P, 11691N, 11557P and 12568N (Table 6.1) at MWG Operon, Huntsville, AL. The sequence data were analyzed using Aligner version 1.5.2 (CodonCode, Dedham, MA) software program. Comparative nucleotide and amino acid sequence analysis of the 3'-end of all the plasmid were performed with Vector NTI (Life Technologies, Carlsbad, CA) software.

Table 6.1. EAV specific primers used to sequence EAV-PRRSV chimeric GP5 and M protein genes

Primer	Sequence (5'→3')	Nucleotide position	Purpose
10763P[a]	ACTTTCTACCCATGCCACGC	10763-10782	Amplify and sequence chimeric ORF 4-6 regions
11691N[a]	CAGGCATAACCACAGTAATTGG	11691-11712	
11557P[a]	CTACCCTATGCTACGCTTATTC	11557-11578	
12568N[a]	CGGCATCTGCAGTGAGTGA	12550-12568	
PVGP5ectoP[b]	ATCTGTGAACTTAAGCAACATGTTG GGGAAATGCTTGAC	11151-11189	Clone N-terminal ectodomain of PRRSV ORF5 region
PVGP5ectoN[b]	AACTATGCCGAATTCCACTGCCCAG TCGAAATTTC	11342-11376	
PV15364N[c]	TCGCCCTAATTGAATAGGTGAC	15343-15364	Clone full-length ORF5 of PRRSV
PVGP5fullN[c]	AACTATGCCGAATTCCTAAGGACGA CCCCATTGTTC	11752-11787	
PVMfullP[d]	AGCCATAGAGCGGCCGCCAATGGGG TCGTCCTTAGATG	11906-11943	Clone full length ORF6 of PRRSV
PVMfullN[d]	CAGAATAAAGTAATCTAGATATTAT TTGGCATATTTAACAAGG	12428-12470	
EAVinsIA1107MectoP	GCCATAGAGCGGCCGCCAATGGGGT CGTCCTTAGATGACTTTTGCAATGAC AGCACGGCTCCACAAAAGTATCTAG ATTACTTTATTC	NA	Site-directed mutagenesis to clone N-terminal ectodomain of PRRSV M protein
EAVinsIA1107MectoN	GAATAAAGTAATCTAGATACTTTTG TGGAGCCGTGCTGTCATTGCAAAAG TCATCTAAGGACGACCCCATTGGCG GCCGCTCTATGGC		

[a] Primers numbered according to the complete genome of EAV Bucyrus strain (GenBank accession number: DQ846750)

[b] Primers numbered according to the position at plasmid prMLVB4/5GP5ecto (GenBank accession number: JQ844156)

[c] Primers numbered according to the position at plasmid prMLVB4/5GP5full

[d] Primers numbered according to the position at plasmid prMLVB5/6Mfull

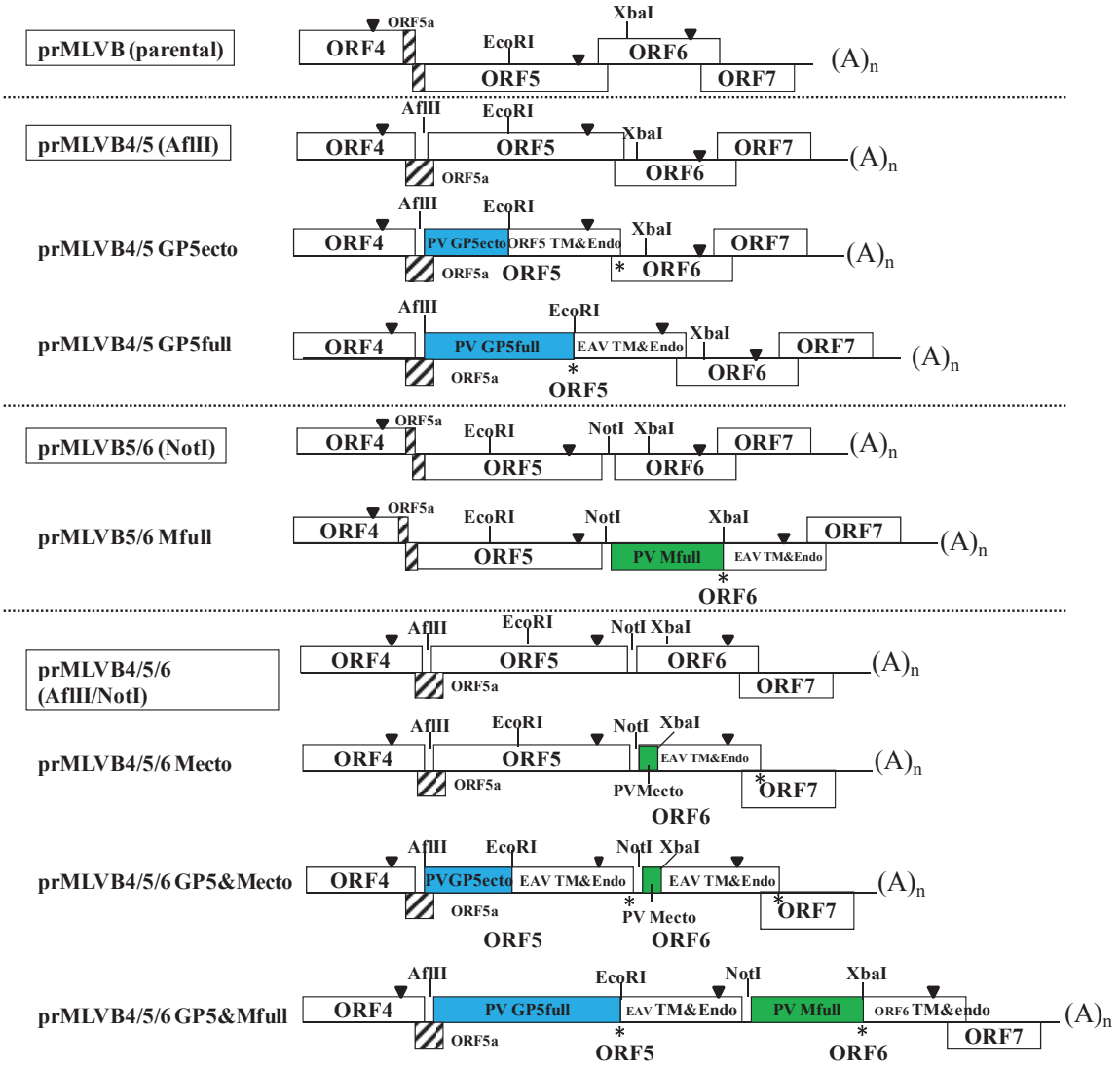

Fig 6.1. Schematic presentation of parental, recombinant and chimeric cDNA clones. Only the ORFs 4 to 7 and 3' nontranslated region is depicted. The restriction sites introduced to separate ORF4 and 5 (AflII), and ORF 5 and 6 (NotI), and ORF 4, 5, and 6 (AflII and NotI) are depicted. The transcriptional regulatory sequences (TRS) that regulate leader-body junction during viral subgenomic RNA synthesis are indicated by triangles. The stop codon for each chimeric construct is identified with an asterisk (*). The N-terminal ectodomain or full-length of PRRSV GP5 protein is labeled in blue. The N-terminal ectodomain or full-length of PRRSV M protein is labeled in green.

In vitro transcription (IVT) and generation of recombinant chimeric viruses

Run-off viral RNA transcripts were generated as previously described from each recombinant/chimeric infectious clone after linearization with restriction enzyme *XhoI*.[261] Eighty micrograms of full-length IVT RNA generated from each recombinant and chimeric plasmid construct were transfected into BHK-21 cells by electroporation as previously described.[261,388] Cells were incubated at room temperature for 10 min after electroporation and mixed with 12 ml of complete BHK-21 medium warmed to room temperature. The cells were seeded into 10-cm-diameter tissue culture plates (Falcon) and incubated at 37 ºC for 48-72 hr until cytopathic effect (CPE) was evident. The tissue culture fluid (TCF) supernatant collected after IVT RNA transfection was designated P0 virus and used for further characterization. The stability of each recombinant/chimeric virus was determined by 10 sequential passages in BHK-21 cells and sequencing the RNA extracted from passages 0, 5 and 10 (See below).

RT-PCR amplification and sequencing of ORF5 of recombinant viruses

The authenticity of each recombinant/chimeric virus stock was determined by RT-PCR amplification and sequencing of the ORFs 5-6 region from RNA that was isolated from TCF from P0, P5 and P10 of each virus as previously described.[384] Briefly, RNA was directly isolated from the TCF using QIAmp viral RNA isolation kit (Qiagen, Valencia, CA). The purified RNA was treated with DNase I (Life Technologies, Grand Island, NY) for 30 min at 37 ºC to remove any contaminating plasmid DNA before RT-PCR amplification. The ORFs 5-6 region was RT-PCR amplified using EAV specific primers 10763P and 11691N (Table 6.1). The PCR was also performed with a non-RT step to eliminate the possibility of amplifying any remaining plasmid DNA. Sequence data were analyzed as described previously.

Antibodies

The monoclonal antibodies (MAbs) 3E2 and SDOW-17 (Rural Technology Inc., Brookings, SD) against N proteins of EAV and PRRSV, respectively, have been previously described.[251,495] Swine polyclonal anti-PRRSV serum (PHGB 2008 ID#1467) was obtained from a PRRSV infected pig showing high PRRSV neutralizing activity. Commercial fluorescent labeled anti-swine (FITC conjugated anti-swine IgG [Santa Cruz Biotechnology, Santa Cruz, CA]) and anti-mouse (Texas red-conjugated goat anti-mouse IgG [Thermo Scientific, Rockford, IL]) were used in indirect immunofluorescence assays.

Indirect immunofluorescence assay (IFA)

Various cell types (EEC, BHK-21, RK-13, PAM, 3D4/21, MARC-145) grown in Lab-Tek™ eight-well chamber slides (Nalge-Nunc, Rochester, NY) were either mock infected or infected with various recombinant chimeric viruses (P0) and incubated at 37 °C for 36-48 hrs. The slides were fixed with 3% paraformaldehyde in PBS (pH=7.4) and stained with EAV N protein specific MAb 3E2 followed by secondary Texas red-conjugated goat anti-mouse IgG staining. The MARC-145, PAM and 3D4/21 cells infected with PRRSV were stained with FITC conjugated MAb against PRRSV N protein (SDOW-17).[251,495] Since PRRSV GP5 and M protein specific antibodies were not available, swine polyclonal anti-PRRSV serum was used detect the chimeric PRRSV proteins in infected cells. EAV antibodies were incubated for 1 hr at room temperature prior to secondary antibody staining. PRRSV MAb against N protein (SDOW-17) or swine polyclonal anti-PRRSV serum was incubated for 1 hr at 37 ºC followed by 4 ºC overnight incubation to enhance the antibody signal.

***In vitro* growth characteristics of EAV-PRRSV chimeric viruses**

BHK-21 cells grown in six-well plates were inoculated with EAV-PRRSV chimeric viruses (P0) as well as parental rMLVB virus and its derivatives (rMLVB4/5, rMLVB5/6 and rMLVB4/5/6) at an MOI of 1 and incubated at 37 ºC for 1 hr. The inocula were removed and cells were washed with PBS (pH=7.4) three times to remove

unbound virus before being overlaid with 4 ml of EMEM. At 0, 6, 12, 24, 48, 72 hr post-infection, TCFs were collected and virus titers were determined by plaque assays in RK-13 cells as previously described.[279]

Plaque morphology

The plaque morphology of the recombinant viruses was determined by plaque assays in EECs. Briefly, confluent monolayers of EECs in 6-well culture plates were infected with 10-fold serial dilutions of each recombinant/chimeric virus (rMLVB, rMLVB4/5 and rMLVB4/5/6, rMLVB4/5GP5ecto, rMLVB4/5/6Mecto and rMLVB4/5/6GP5&Mecto) virus in duplicate. Following 1 hr incubation, 0.75% CMC (caboxymethylcellulose)-DMEM was added to each well and cells were incubated at 37°C for 96 hr.[276] Plaques were stained with 1% formalin-crystal violet solution containing 1% formaldehyde at 96 hr post-infection and titers were expressed as pfu/ml.

6.4. RESULTS AND DISCUSSION

Generation of EAV/PRRSV chimeric viruses

The infectious cDNA clone (prMLVB) of the MLV vaccine strain of EAV (ARVAC®) was used as the backbone to generate a panel of 6 recombinant chimeric viruses by replacing either the full-length or the N-terminal ectodomains of GP5 and M proteins of EAV with the IA-1107 strain of North American PRRSV (Fig 6.1, Table 6.1). Because of the overlapping gene arrangement in the 3' end of the EAV genome, it was necessary to separate ORF 5 from flanking ORFs 4 and 6 without disrupting the coding sequences of each of the three ORFs. The ORFs 4 and 5, ORFs 5 and 6, and ORFs 4, 5 and 6 were separated in the prMLVB plasmid to generate the plasmids prMLVB4/5, prMLVB5/6 and prMLVB4/5/6 (GenBank accession numbers JQ844153, JQ844154 and

JQ844155), respectively. The authenticities of these plasmid constructs were first confirmed by sequencing ORFs 4-7 (data not shown). The same amount of full-length *in vitro* transcribed (IVT) RNA generated from linearized prMLVB, as well as mutant prMLVB4/5, prMLVB5/6 and prMLVB4/5/6 cDNA clones were electroporated into BHK-21 cells for generation of recombinant viruses as previously described.[261,384] The viability of each recombinant clone was determined by indirect immunofluorescence assay (IFA) using EAV N protein specific monoclonal antibody (MAb 3E2) to stain BHK-21 cells 24 hours post transfection with IVT RNA generated from each linearized plasmid construct (data not shown). The cells transfected with each of the three recombinant transcripts produced 90-100% cytopathic effect (CPE) in transfected cells after 72-96 hours post transfection, and virus stocks were made from these tissue culture fluids (TCF; P0). The authenticity of all three recombinant viruses was confirmed by sequencing ORFs 4-7 from RNA extracted from each TCF (P0). All virus sequences were identical to the plasmid sequence from which they were derived. The TCFs (P0) containing each recombinant virus were then used to infect BHK-21 cells at a multiplicity of infection (MOI) of 1 and progeny viruses were collected at different time points for titration. The growth characteristics and plaque morphology were compared in RK-13 and EEC, respectively. All of the recombinant rMLVB4/5, rMLVB5/6 and rMLVB4/5/6 viruses had the highest progeny virus titer at 48 hours post infection. They had approximately 2 $\log_{10}$ lower titer as compared to the parental rMLVB virus at this time point (Fig 6.2). When compared to the parental virus, the recombinant viruses showed a 48-60% reduction in plaque size in EECs. The parental rMLVB produced 5 mm diameter large sized plaques while the recombinant rMLVB4/5, rMLVB5/6 and rMLVB4/5/6

produced 2.4, 3 and 2.8 mm diameter medium sized plaques in EECs, respectively. However, there was no significant difference in growth characteristics among these three recombinant viruses. All three recombinant viruses were stable for more than 10 serial passages in BHK-21 cells. The separation of these ORFs did not alter the amino acid sequence of GP4, GP5 and M proteins of EAV but the ORFs 4/5 separation changed the N-terminal amino acid sequence of ORF5a protein (Fig 6.3). In a recent study, we demonstrated that complete elimination of ORF5a protein experimentally could lead to 2-3 log lower virus titer and tiny plaques.[263] Interestingly, the addition of extra nucleotides to the ORF5a coding sequence did not cripple the recombinant viruses to the same extent as the ORF5a knockout virus[263] indicating that this region of the EAV genome was tolerant for insertion of a small stretch of nucleotides (see below). Collectively, these data demonstrated that separation of these ORFs did not seriously compromise the viruses. Furthermore, the constructs were stable and could be used for further studies.

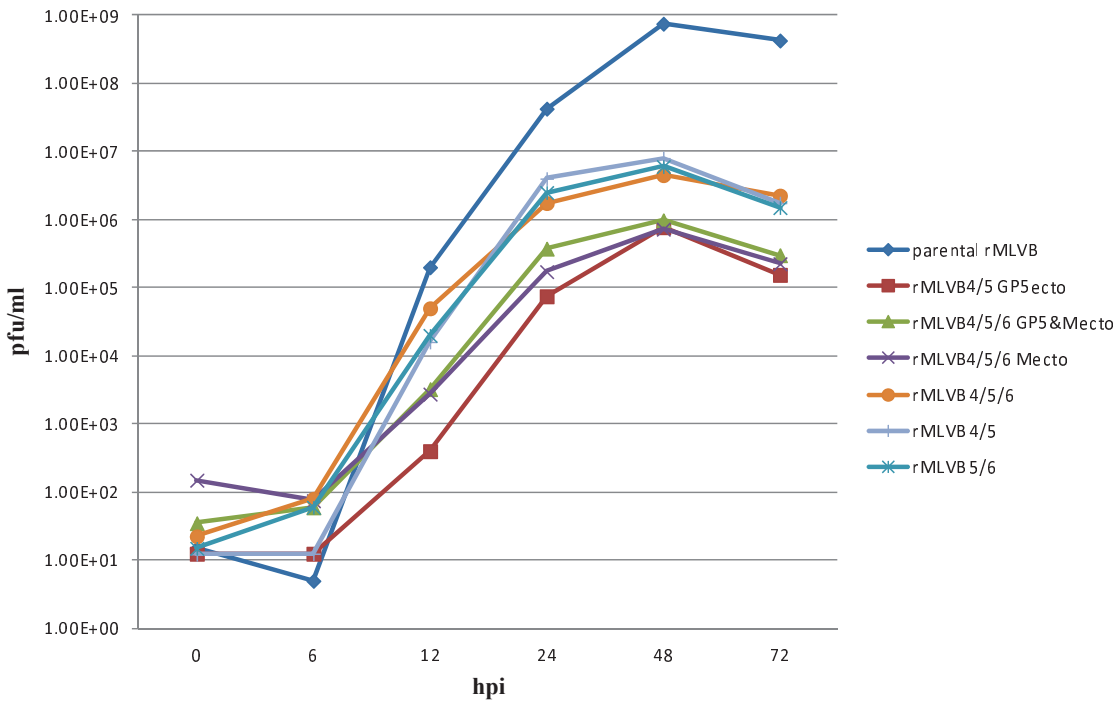

Fig 6.2. Replication characteristics of parental rMLVB, recombinant rMLVB4/5, rMLVB5/6 and rMLVB4/5/6 and chimeric rMLVB4/5 GP5ecto, rMLBV4/5/6 Mecto and rMLVB4/5/6 GP5&Mecto viruses in BHK-21 cells. Subconfluent monolayers of BHK-21 cells were grown in 6-well plates, inoculated with each P0 virus (MOI of 1) and incubated at 37 ºC for 1 hr. After removal of the inoculum, the cells were rinsed three times with PBS and overlaid with 4 ml of EMEM. At indicated time points, supernatants were harvested and titrated by plaque assay in RK-13 cells.

Fig 6.3. Sequence alignments of amino acids of the ORF5a and GP5 proteins of parental EAV and chimeric viruses. The amino acid sequence changes due to ORF4 and 5 separations are highlighted in blue. The remaining ORF5 from EAVrMLVB backbone in the GP5ecto chimera construct is marked in green. The ectodomains of PRRSV are labeled in red. The common region of ORF5a between PRRSV and GP5ecto chimera is labeled in purple.

The next step was to generate a panel of EAV-PRRSV chimeric plasmids by replacing the nucleotide (nt) sequence encoding the N-terminal ectodomain or full-length of GP5 and/or the M protein on an EAV backbone with corresponding sequences from North American PRRSV IA1107 strain using prMLVB4/5, prMLVB5/6 and prMLVB4/5/6 plasmids (Fig 6.1, Table 6.2). We have exchanged the N-terminal ectodomain (a.a. 1-64) and full-length (a.a. 1-200) of PRRSV GP5 with ectodomain (a.a. 1-114) of EAV GP5 to generate prMLVB4/5 GP5ecto and prMLVB4/5 GP5full constructs on a prMLVB4/5 backbone. Similarly, the N-terminal ectodomain (a.a. 1-17) and full-length (a.a. 1-175) of PRRSV M were exchanged with the N-terminal

ectodomain (a.a. 1-16) of EAV M protein, respectively, to generate prMLVB4/5/6 Mecto and prMLVB5/6 Mfull constructs on the prMLVB4/5/6 and prMLVB5/6 backbones, respectively (Fig 6.1, Table 6.2). The ORF5 and ORF6 regions of all chimeric plasmid constructs were RT-PCR amplified with two EAV specific primers (10763P and 12568N) and visualized by agarose gel electrophoresis (Fig 6.4). Subsequently, the RT-PCR products were sequenced to confirm the authenticity of the chimeric plasmid constructs. All chimeric constructs maintained in-frame coding sequences in ORF5a, ORF5 and ORF6. Full-length IVT RNA from linearized chimeric plasmids were transfected into BHK-21 cells as previously described [261,384]. A portion of transfected cells were seeded into chamber slides for IFA staining to check for the expression of EAV N protein 24 hours post transfection. With the exception of BHK-21 transfected with prMLVB4/5 GP5full, prMLVB5/6 Mfull and prMLVB4/5/6 GP5&Mfull, cells transfected with prMLVB4/5 GP5ecto, prMLVB4/5/6 Mecto and prMVLB4/5/6 GP5&Mecto stained positive for EAV N protein (data not shown). This observation was further confirmed by the development of 90-100% CPE 72-120 hours post transfection in BHK-21 cells that were transfected with IVT RNA from prMLVB4/5 GP5ecto, prMLVB4/5/6 Mecto and prMLVB4/5/6 GP5&Mecto. The experiments have been repeated two times independently. Collectively, these data suggested that only 3 of the 6 chimeric constructs could produce infectious progeny viruses. Each of the three progeny viruses was harvested (P0) and subjected to further *in vitro* characterization. Of the 6 chimeric constructs, only rMLVB4/5 GP5ecto, rMLVB4/5/6 Mecto and rMLVB4/5/6 GP5&Mecto could generate infectious progeny viruses following transfection of IVT RNA into BHK-21 cells (GenBank accession numbers JQ844156, JQ844157 and JQ844158, respectively).

The IVT RNA generated from plasmids containing full-length GP5 or M replacement of PRRSV IA-1107 strain (prMLVB4/5 GP5full, prMLVB5/6 Mfull and prMLVB4/5/6 GP5&Mfull) failed to generate infectious progeny viruses. The genetic stabilities of each of the three replicating chimeric viruses were determined by 10 serial passages in BHK-21 cells and subsequent RT-PCR amplification and sequencing of ORF5-6 from RNA extracted from P0, P5 and P10 TCF. The sequence data revealed no substitutions, insertions or deletions in this region of all three chimeric viruses following serial cell culture passage. These results unequivocally demonstrated that these three chimeric viruses are highly stable following serial passage in cell culture. The failure to generate chimeric viruses containing full-length PRRSV GP5, M or GP5/M proteins on the EAV backbone may due to the fact that being the smallest arterivirus in the family *Arteriviridae*, EAV has evolved to the point that it does not tolerate any large nucleotide inserts into the genome. However, it has been reported that EAV can tolerate small segments of nucleotides in the structural proteins genes.[291,496]

Table 6.2. Composition of the GP5 and M proteins of EAV-PRRSV chimeric constructs

Construct	Chimeric protein	GP5	Fused to	M	Fused to	Production of progeny virus[a]	Plaque size[b] (mm)	GenBank number
prMLVB	n.a.[c]	Parental (pt) EAV GP5	n.a.	pt EAV M	n.a.	+	5	FJ798196
prMLVB4/5	n.a.	pt EAV GP5		pt EAV M	n.a.	+	2.4	JQ844153
prMLVB4/5 GP5ecto	GP5ecto	PRRSV GP5 ectodomain a.a. 1-64	EAV GP5 a.a. 115-255	pt EAV M	n.a.	+	1	JQ844156
prMLVB4/5 GP5full	GP5full	PRRSV GP5 full-length a.a. 1-200	EAV GP5 a.a. 115-255	pt EAV M	n.a.	-	n.a.	n.a.
prMLVB5/6	n.a.	pt EAV GP5	n.a.	pt EAV M	n.a.	+	3	JQ844154
prMLVB5/6 Mfull	Mfull	pt EAV GP5	n.a.	PRRSV M full-length a.a. 1-175	EAV M a.a. 17-162	-	n.a.	n.a.
prMLVB4/5/6	n.a.	pt EAV GP5	n.a.	pt EAV M	n.a.	+	2.8	JQ844155
prMLVB4/5/6 Mecto	Mecto	pt EAV GP5	n.a.	PRRSV M ectodomain a.a. 1-17	EAV M a.a. 17-162	+	0.5	JQ844157
prMLVB4/5/6 GP5&Mecto	GP5&Mecto	PRRSV GP5 ectodomain a.a. 1-64	EAV GP5 a.a. 115-255	PRRSV M ectodomain a.a. 1-17	EAV M a.a. 17-162	+	0.5	JQ844158
prMLVB4/5/6 GP5&Mfull	GP5&Mfull	PRRSV GP5 full-length a.a. 1-200	n.a.	PRRSV M full-length a.a. 1-175	n.a.	-	n.a.	n.a.

[a]The production of progeny virus was evaluated with IFA staining with EAV N antibody and development of cytopathic effect.

[b]Plaque morphology study was done in EEC.

Table 6.2-continued

[c]Not applicable.

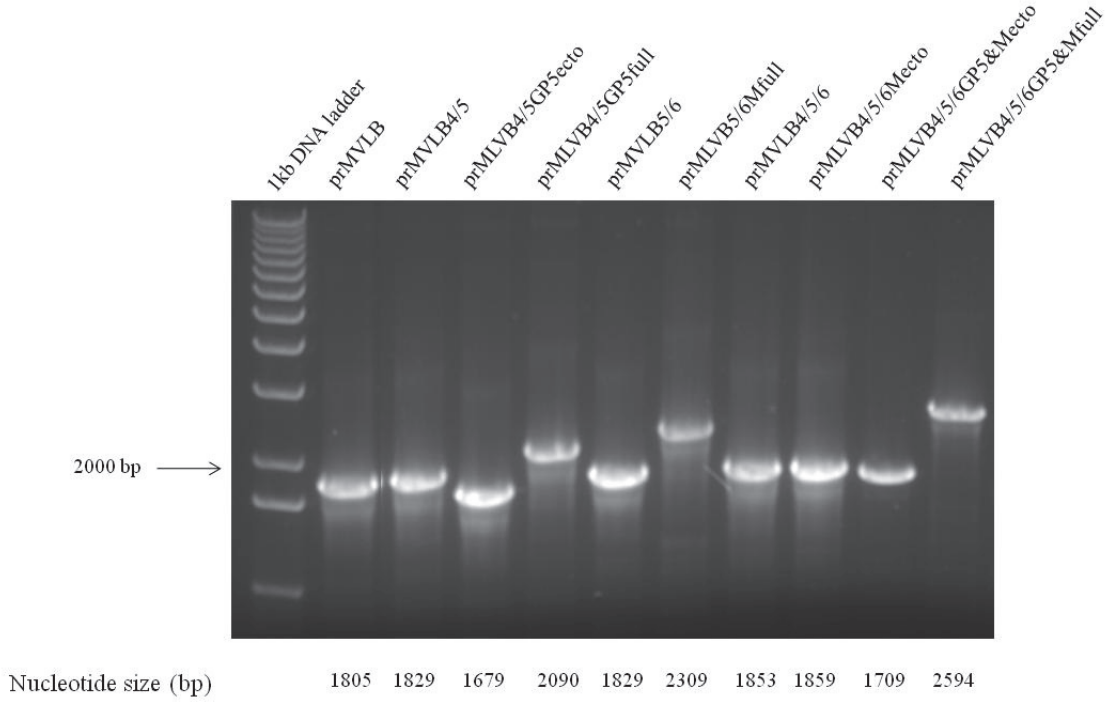

Fig 6.4. Agarose gel electrophoresis of RT-PCR amplified ORF5 and ORF6 products of EAV-PRRSV chimeric plasmids using EAV specific primers.

Growth characteristic and plaque morphology of EAV/PRRSV chimeric viruses

The growth characteristics and plaque morphologies of rMLVB4/5 GP5ecto, rMLVB4/5/6 Mecto and rMLVB4/5/6 GP5&Mecto chimeric viruses were compared in RK-13 cells and EEC, respectively, as described before. All three EAV-PRRSV chimeric viruses rMLVB4/5 GP5ecto, rMLVB4/5/6 Mecto and rMLVB4/5/6 GP5&Mecto gave similar growth curves. Replication titers were 3 $\log_{10}$ lower as compared to parental rMLVB virus and 1 log lower as compared to the recombinant cloned viruses (rMLVB 4/5 and rMLVB4/5/6); these were derived 48 hours post infection (Fig 6.2). Furthermore, P5 and P10 TCF of all three chimeric viruses gave

similar growth curves as compared to P0 TCF (Table 6.3). Plaque assays were performed in EECs for all three chimeric viruses and their plaque morphology was compared to parental rMLVB, recombinant rMLVB4/5, rMLVB5/6 and rMLVB4/5/6 viruses. The three chimeric viruses (rMLVB4/5 GP5ecto, rMLVB4/5/6 Mecto and rMLVB4/5/6 GP5&Mecto) produced small sized plaques (0.5 mm to 1 mm) as compared to the parental rMLVB virus (5 mm) and the three recombinant viruses from which the chimeric viruses were derived from (2.4 to 3 mm). The lower titers and smaller plaque sizes of the chimeric viruses clearly indicated that although the viruses are genetically stable (Fig. 6.5), they have significantly compromised phenotypes and were disabled in replication and spreading when compared to parental rMLVB or the three recombinant viruses from which they are derived (ORF4/5, ORF5/6 and ORFs4/5/6). Interestingly, when progeny viruses (P0) produced in BHK-21 cells were titrated in RK-13 cells for growth curve analysis, the reduction of titer of the chimeric viruses was not as significant as that observed in EECs, in which there was a reduction in plaque size (medium to pinpoint). This observation suggested that infection and spreading depended on the cell in which the viruses are propagated. Specifically, EAV field strains were found to produce different plaque sizes in EEC but not in RK-13.[278] Taken together, the data clearly showed that the presence of PRRSV N-terminal ectodomains of GP5 and M altered the growth characteristics and cell to cell spread of the chimeric viruses. Furthermore, it has long been proposed that the GP5 and M proteins of arteriviruses play a major role in virus attachment.[252,291,497] However, nonspecific interactions have been shown between PRRSV M protein and a heparin-like receptor on PAM cells.[341]

Table 6.3: Stability of EAV- PRRSV chimeric viruses following 10 serial passages in BHK-21 cells

Virus passage	Virus titer (pfu/ml)		
	rMLVB4/5 GP5ecto	rMLVB4/5/6 Mecto	rMLVB4/5/6 GP5&Mecto
P0*	3.5×10^6	8.2×10^5	2.6×10^6
P1	1.1×10^6	3.8×10^5	3.6×10^6
P2	1.2×10^6	3.4×10^5	1.5×10^6
P3	1.3×10^6	5.1×10^5	2.1×10^6
P4	8.3×10^5	2.6×10^5	2.4×10^6
P5*	1.0×10^6	2.5×10^5	2.5×10^6
P6	5.5×10^6	8.9×10^5	3.0×10^6
P7	1.3×10^6	1.6×10^5	1.3×10^6
P8	5.9×10^6	2.6×10^5	5.4×10^6
P9	2.0×10^6	1.8×10^5	1.7×10^6
P10*	9.7×10^6	7.3×10^5	2.3×10^6

*P0, P5 and P10 viruses were sequenced and found genetically stable.

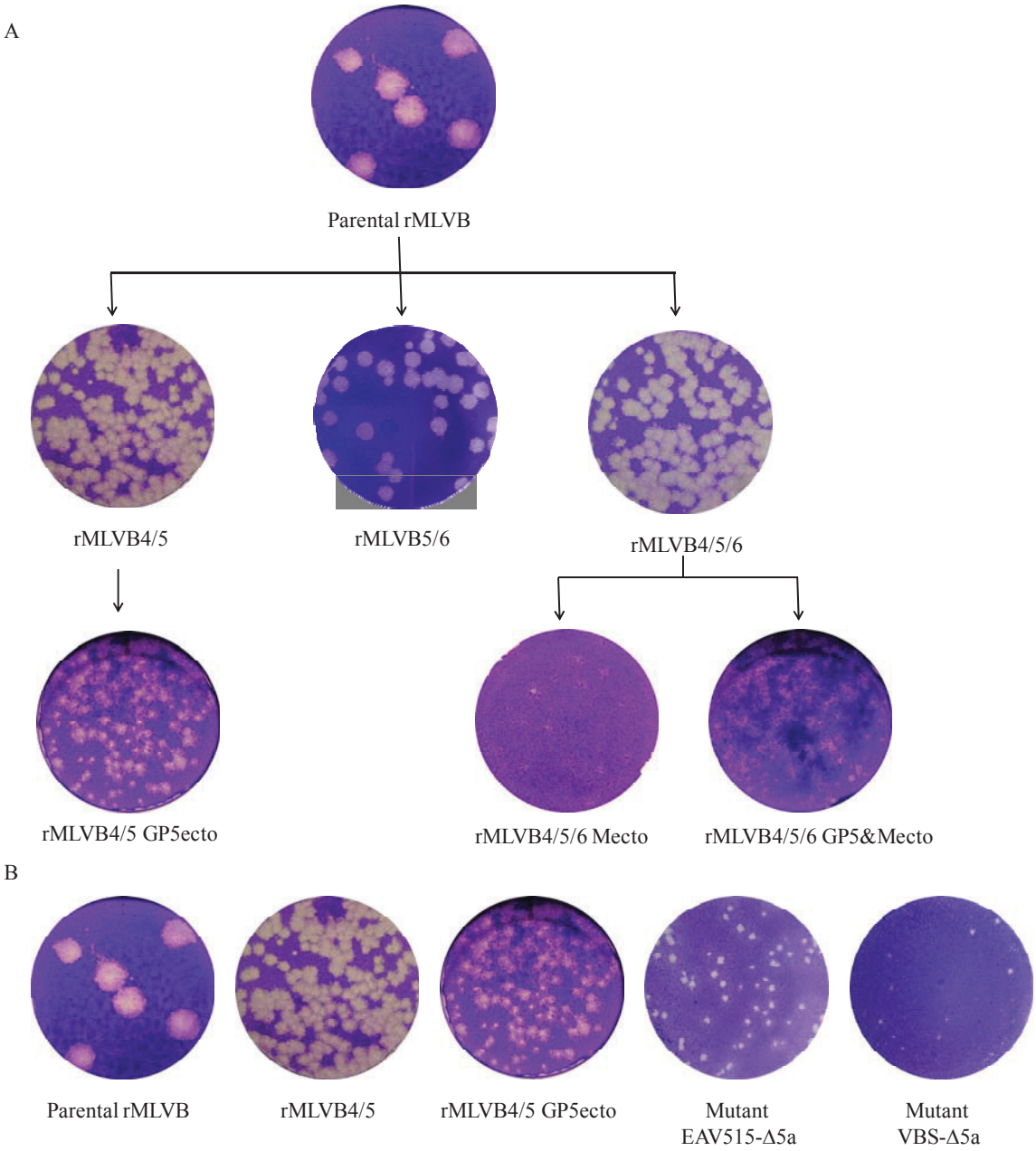

Fig 6.5. (A). Comparison of plaque morphology on equine endothelial cells (EEC) of parental rMLVB, recombinant rMLVB4/5, rMLVB5/6 and rMLVB4/5/6 and chimeric rMLVB4/5 GP5ecto, rMLVB4/5/6 Mecto and rMLVB4/5/6 GP5&Mecto viruses. (B). Illustration of plaque morphology of ORF5a knockout mutants (EAV515-Δ5a, VBS-Δ5a) as compared to the parental rMLVB, recombinant rMLVB4/5 and chimeric rMLVB4/5/ GP5ecto viruses. The insertion of 8-10 amino acids into the ORF5a protein of EAV did not cripple the virus to the same extent as the knockout mutants.

Cellular tropism of EAV/PRRSV chimeric viruses

Although EAV and PRRSV infect cells from the monocyte/macrophage lineage in their natural host, they present different cellular tropisms in cell culture.[256,482,485] EAV can infect a wide variety of cell lines while PRRSV can only infect PAM and African green monkey kidney (MA-104) cells and their derivative (MARC-145).[256,481] The chimeric viruses derived by swapping the ectodomains of PRRSV GP5 and M proteins into an EAV backbone provide valuable tools to study cellular tropisms. Therefore, the three viable chimeric viruses were tested in different EAV-susceptible cell lines (EEC, RK-13, BHK-21, MARC-145), PRRSV-susceptible cell lines (PAM and MARC-145) and porcine alveolar macrophage cell line (3D4/21) to confirm the progeny virus cellular tropism and infectivity. Virus replication in various cell lines was determined by IFA staining with MAb 3E2 (α-N of EAV) and polyclonal pig anti-PRRSV sera (Fig 6.6 and Table 3). Interestingly, the three chimeric viruses (rMLVB4/5 GP5ecto, rMLVB4/5/6 Mecto and rMLVB4/5/6 GP5&Mecto), along with the rMLVB parental virus, were able to infect EEC, MARC-145, BHK-21, and RK-13 cells as determined by IFA staining for the N protein of EAV (Fig 6.6). Similarly, MARC-145 cells were infected with the wild type PRRSV, parental rMLVB and the three chimeric viruses (rMLVB4/5 GP5ecto, rMLVB4/5/6 Mecto and rMLVB4/5/6 GP5&Mecto) as determined by positive staining in IFA with pig anti-PRRSV polyclonal serum. None of the viruses were able to infect 3D4/21 cells. This finding was consistent with previous observations that 3D4/21, a continuous porcine alveolar macrophage cell line, does not support replication of PRRSV.[498] The exchange of GP5 and/or M protein N-terminal ectodomains from PRRSV (individual or double) could not alter the tropism of the chimeric viruses.

Similarly, a previous study has shown that exchanging the GP5 ectodomains from another PRRSV IAF-Klop strain did not change the EAV or PRRSV cell tropism.[291] In that study, it was shown that chimeric viruses containing the N-terminal ectodomains of M envelope proteins of PRRSV and LDV on an EAV backbone are replication- and transcription-competent (as determined by the synthesis of both non-structural and structural proteins), but unable to produce infectious progeny virus. Dobbe et al (2001) indicated that this was due to the failure of formation of the GP5/M heterodimer in the chimeric proteins. In contrast, we demonstrated that the N-terminal ectodomain of the M protein of EAV can be replaced by the N-terminal ectodomain of PRRSV M protein without compromising the production of viable progeny virus using a different infectious cDNA clone of EAV and a more recent North American strain of PRRSV IA1107. Our findings indicate that neither the GP5 nor M protein is involved in determining the cellular tropism of EAV. This supports the hypothesis that EAV and perhaps PRRSV major envelope proteins are not determinants of the cellular tropism of these two viruses. Interestingly, in a very recent study, PRRSV infectious cDNA clone was used as a vector to construct a chimera in which PRRSV ORFs 2a, 2b, 3 and 4 were replaced by the corresponding ORFs from EAV [294]. This PRRSV/EAV chimeric virus gained the broad cell tropism that is typical of EAV, and clearly indicated that the minor envelope protein (GP2, GP3 and GP4) and E protein play a key role in determining the cellular tropism of arteriviruses and play a major role in virus attachment and entry.[294] However, the major neutralization determinants of EAV and PRRSV are both localized in the N-terminal ectodomain of GP5 [252,471,499-501] and we have shown previously that recombinant EAV (A45.C2) containing the GP5 ectodomain of PRRSV (IAF-Klop) is not neutralized by

any EAV specific MAbs or by the polyclonal equine antisera.[253] Therefore, it will be interesting to determine the replication and immunogenic kinetics of these viable EAV/PRRSV chimeras in pigs.

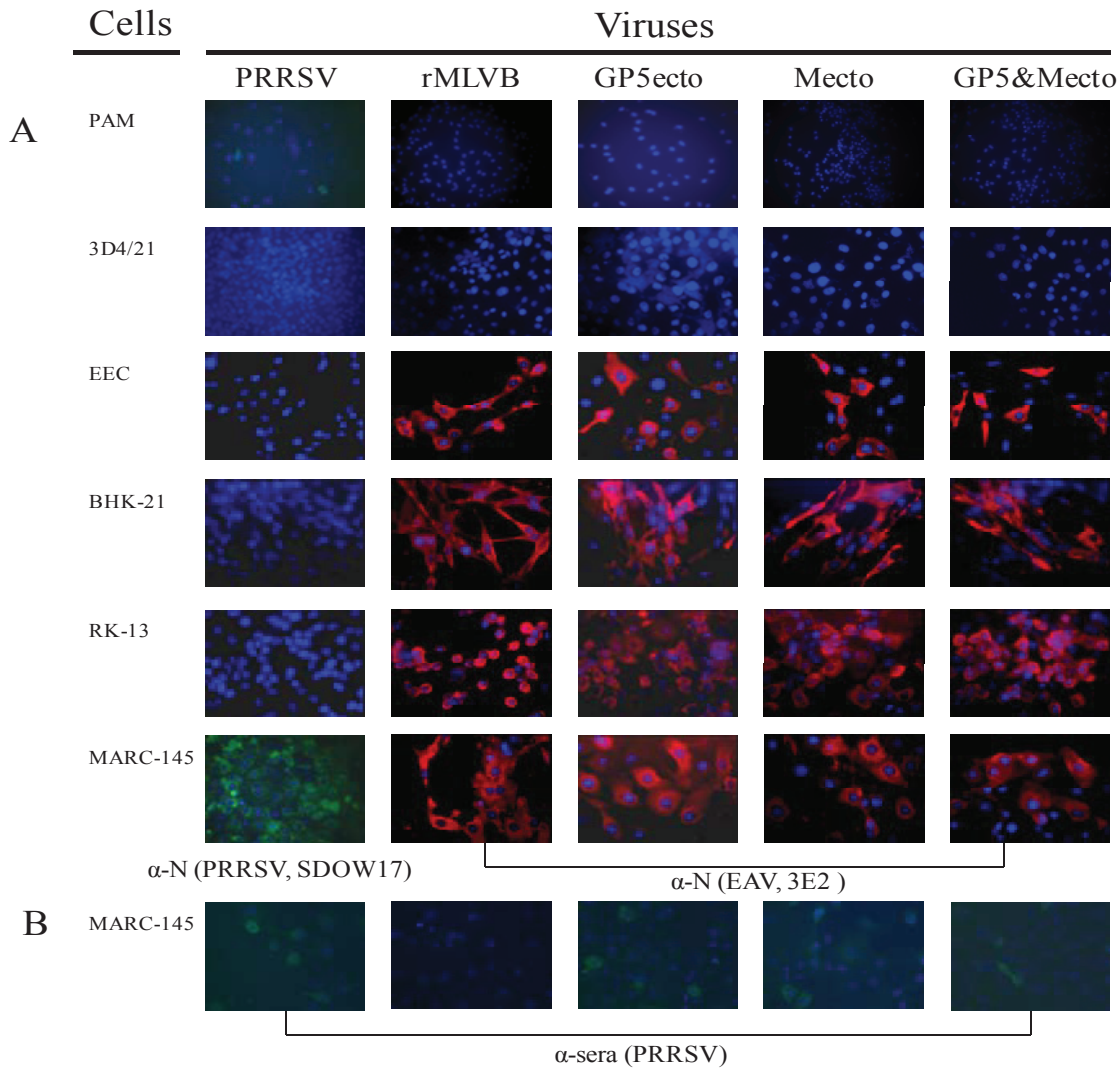

Fig 6.6. Determination of cellular tropism of EAV-PRRSV chimeric viruses using indirect immunofluorescence assay (IFA). Various cell lines used in this study are listed on the left side of the figure. The names of the P0 viruses used to infect cells are identified at the top center. The primary antibodies or anti-sera used in IFA are shown at the bottom of the figure. In Fig. 6A, PRRSV infected cells (first column) were stained with FITC-conjugated SDOW17 MAb which was used to stain PRRSV N protein (green). The remaining columns show the chimeric virus-infected cell lines stained with EAV

MAb (3E2) against N protein followed by Texas-red conjugated secondary antibody staining (red). In Fig. 6B, MARC-145 cells infected with PRRSV or rMLVB or chimeric viruses were stained with pig polyclonal anti-PRRSV sera followed by FITC-conjugated secondary antibody staining.

Effect of ORFs4/5 and ORFs5/6 separations on ORF5a protein, GP5 and M proteins

Recently, a novel small ORF5a protein (encoded by ORF5a) which overlaps with the 5' end of ORF5 has been identified.[263,467] The effect of ORF4/5 separation on ORF5a protein and GP5 were determined by comparative amino acid sequence analysis (Fig. 6.3). The insertion of the 24 nucleotide sequence to separate ORFs4/5 in the prMLVB vector resulted in replacement of 4 amino acids (NAIY [a.a. 12-15]) with 12 amino acids (SAICELKOHAVH [a.a. 12-23]) which expanded the length of the EAV ORF5a protein by 8 amino acids. The insertion of 24 nucleotides did not affect the transcriptional regulatory sequence (TRS) upstream of ORF5 of rMLVB4/5. It also did not alter the coding sequences of GP5 and M proteins nor the TRS upstream of ORF6. The growth curve and plaque morphology of rMLVB4/5 indicated that separation of ORF4/5/6 had some negative impact on the recombinant viruses. However, these changes did not have a significant crippling effect on the recombinant virus. Previously it was reported that a complete knock out of the ORF5a protein in two infectious cDNA clones pEAV515, a derivative of pEAV030[261] and pEAVrVBS[388], had a significant crippling effect on the progeny viruses, which produced lower titered virus and pinpoint plaques.[263] In this current study, insertion of 8 random amino acids to the ORF5a protein of EAV ORF4/5 recombinant virus did not cripple the virus to the same extent compared to the ORF5a knockout mutants (Fig 6.5B). Following the replacement of EAV GP5 N-terminal ectodomain (a.a. 1-114) with PRRSV IA1107 GP5 N-terminal ectodomain (a.a 1-64), the

new EAV/PRRSV fusion ORF5a protein consists of 11 amino acids (MFFYDWYVGLN) from EAV ORF5a protein followed by 10 random amino acids (SAICELKQHV) encoded by the nucleotide sequence that was inserted for the separation of ORFs4/5 and the PRRSV ORF5a amino acid sequence (a.a. 22-62) corresponding to amino acids 6 to 46 of the PRRSV ORF5a protein. The recombinant EAV/PRRSV ORF5a fusion protein containing the PRRSV GP5 ectodomain was 16 amino acids longer (46 versus 62 a.a.) than the authentic protein and its first 11 amino acids were identical to EAV ORF5a protein. Interestingly, the chimeric viruses with this ORF5a protein (rMLVB4/5 GP5ecto and rMLVB GP5&Mecto) were stable and replicated to titers of 9.5×10^5 pfu/ml. Taken together, these data further confirmed the importance of the ORF5a protein in virus infection as well as the plasticity of this region to accommodate small stretches of additional nucleotides. This observation is further supported by previous attempts to engineer an EAV vectored vaccine by fortuitously introducing a 24 nt insertion to disrupt the ORF4/5 overlap.[493] Furthermore, the difference in length of the ORF5a protein among arteriviruses (EAV 59 codons, PRRSV-NA 46 or 56 codons, PRRSV-EU 43 codons, LDV 47 codons and SHFV 64 codons) and spontaneous insertion of 12 nt into ORF5a during 70 serial passages of PRRSV-NA strain[502] indicate the plasticity of this region of EAV and other arteriviruses.

In summary, in this study, we have generated three viable EAV/PRRSV chimeric viruses (rMLVB4/5GP5ecto, rMLVB4/5/6Mecto and rMLVB4/5/6GP5&Mecto). The chimeric viruses containing PRRSV M ectodomain are novel. We have used these three viruses to demonstrate unequivocally that the ectodomains of GP5 and M are not the major determinants of cellular tropism, further supporting the recent findings that the

minor envelope proteins GP2, GP3, GP4 and E are the critical proteins in mediating cellular tropism.[294]

CHAPTER SEVEN

Conserved arginine residues in the E protein of equine arteritis virus may play a role in heparin binding

7.1. SUMMARY

Equine arteritis virus (EAV) is the causal agent of equine viral arteritis, a disease of members of the family Equidae. EAV has a relatively broad cell tropism and can infect a range of mammalian cells *in vitro*. In horses, EAV primarily replicates in macrophages and endothelial cells of small blood vessels. As yet, neither the cellular receptor(s) nor the mechanism(s) of virus attachment and entry have been determined for this virus. Previous studies have shown that heparin can inhibit EAV infection of RK13 cells. In this study, we investigated EAV attachment to equine endothelial cells (EECs). When heparin was mixed with EAV, it reduced virus infectivity in EEC up to 93%. Other glycosaminoglycans, similar to heparin, had no significant effect on EAV infectivity. Heparinase treatment of EECs resulted in a significant reduction in infection of EEC. When solubilized EAV virion proteins were subjected to heparin-affinity chromatography and SDS-PAGE analysis, it was found that the structural proteins E, GP2, GP5, M and N of EAV could bind heparin. We subsequently cloned and expressed each individual structural protein in mammalian cells and confirmed that all these proteins can interact with heparin. Comprehensive sequence analysis of 90 field strains of EAV revealed a conserved XBBXBX (X is a basic and B is a nonbasic amino acid) domain at the carboxyl terminus of the E protein which was previously predicted to be the heparin binding domain. Five basic arginine (R) residues are highly conserved within the region. To further characterize the role of this heparin binding domain, we used site-directed mutatagenesis to generate a panel of arginine (R) → glycine(G) mutations at the conserved C-terminal region in both the full-length EAV cDNA clone and in individual E protein expression vectors. The mutant viruses rVBS R52G, rVBS R57G, rVBS R52,60G, rVBS R57,63G and rVBS R63,65G have similar growth patterns and plaque morphology compared to the parental control. In contrast, triple mutant rVBS

R52,60,65G virus grew significantly slower and produced tiny sized plaques. When these mutations were introduced in the E protein expression plasmid, mutant E R52G and E R57G did not affect the heparin binding capability while double mutant E R52,60G completely blocked the interaction between E protein and heparin. Other mutants could not be tested because the mutations involved the target locations of the E antibody. The results for double mutant R52,60G in which heparin interaction is blocked but virus infectivity was intact suggest that other attachment molecules may also exist. Collectively, our data suggest that while the conserved arginine residues at the C-terminus of the E protein are important for heparin binding of EAV, other as yet unknown attachment molecules might also be involved.

7.2. INTRODUCTION

Equine arteritis virus (EAV) is a single-stranded, positive sense RNA virus in the family *Arteriviridae*, genus *Arterivirus*, order *Nidovirales*. It is the causative agent of equine viral arteritis (EVA) in horses and other equids species.[212,255,257] Besides EAV, the family *Arteriviridae* contains three other viruses: porcine reproductive and respiratory syndrome virus (PRRSV), simian hemorrhagic fever virus (SHFV), and lactate dehydrogenase-elevating virus (LDV) of mice.[256] The genome of EAV is approximately 12.7 kilobases (kb) and includes 5' and 3' untranslated regions as well as ten known open reading frames (ORFs).[256,263] The first two ORFs (1a and 1b) are approximately 9.5 kb and all located at the 5' portion of the genome. They encode for the replicase polyproteins (pp 1a and pp 1ab), with the latter requiring a -1 ribosomal frame-shift just before termination of the pp 1a translation.[256,260,320] The pp 1a and pp 1ab are post-translationally processed by three ORF 1a-encoded proteinases, (non-structural protein [nsp] 1, nsp 2 and nsp 4), yielding a number of processing intermediates and thirteen end-products: nsp 1-12, including nsp 7α and nsp 7β.[256,264,503-504] The remaining eight ORFs (ORFs 2a, 2b, 3, 4, 5a, 5-7) located at the 3' end of the genome are approximately 2.7 kb and encode E, GP_2, GP_3, GP_4, ORF5a, GP_5, M envelope proteins, and the nucleocapsid protein (N), respectively.[256,262-263] The EAV genomic RNA is encapsidated by the N protein into an isometric core which is surrounded by an envelope containing seven structural proteins.[256] The glycosylated protein GP_5 and nonglycosylated protein M are

the most abundant structural proteins in the envelope and occur in the virion as covalently linked heterodimers.[266] The GP_2, GP_3 and GP_4 are all minor glycoproteins and form a covalently linked heterotrimer in the virion.[320,370] It has been suggested that the small envelope protein E interacts with GP_2, GP_3 and GP_4 heterotrimer complex and draws the minor envelope glycoproteins into nascent particles.[268] All seven structural proteins (excluding ORF5a) are essential for virus infectivity while inactivation of ORF5a expression by reverse genetics yielded a severely crippled EAV mutant which replicated to lower titer and produced tiny plaques.[263,268]

EAV has a relatively broad cell tropism and infects a range of animal and human cells *in vitro*.[230,320] However, *in vivo*, it primarily infects equine macrophages and endothelial cells, but the virus can also replicate in other cell types such as epithelial cells, mesothelium, and smooth muscle cells of small blood vessels and myometrium.[36,234-235] It has been shown that EAV enters baby hamster kidney (BHK) cells via clathrin-dependent endocytosis.[283] However, details of the mechanism of virus attachment and entry *in vivo* are still not clear. Asagoe *et al* (1997) have shown that heparin can inhibit EAV infection on BHK cells but the mechanism of the inhibitory activity by heparin was not elucidated.[289]

The small envelope E protein is a 67-amino-acid protein which consists of three domains: an N-terminal domain containing a potential myristoylation signal, a hydrophobic domain and a hydrophilic C-terminus containing a cluster of basic amino acids.[262] The topology of the E protein within the viral membrane is not known. It is speculated that the hydrophobic domain might span the membrane once, leaving either the N or C terminus on the virion surface. Alternatively, the E protein may span the lipid bilayer twice with both termini exposed on the same side of the membrane. It is also possible that the E protein adopts a more complex multiple transmembrane configuration.[262] The role of the E protein in EAV infection has not been well studied. Reverse genetics studies have shown that cells transfected with mutants lack the expression of E, GP2, GP3 or GP4 release virus-like particles (VLPs) consisting of viral RNA and the GP5, M and N proteins.[268,505] Absence of the E protein completely blocked the incorporation of GP2, GP3 and GP4 proteins into viral particles.[268] These finding

suggests that the E protein is essential for the production of infectious progeny but dispensable for virus assembly and release. The E protein may have an intermediate receptor binding and/or virus entry function with the $GP_2/GP_3/GP_4$ complex. A detailed amino acid function study revealed that although the N-terminal glycine site of the E protein is myristoylated, but myristoylation is not required for membrane association and particle budding.

Diverse cellular surface carbohydrates are major mediators of cell-to-cell interactions.[506] The glycan synthesis of glycoproteins is associated with two main processes: N-glycosylation, which adds N-acetylglucosamine (GlcNAc) to the nitrogen atom of an asparagine residue, or O-glycosyaltion, which adds N-acetylgalactosamine (GalNAc) or xylose to the oxygen atom of a serine or a threonine residue. The xylose addition leads to the synthesis of glycosaminoglycans (GAGs). There are six different groups within GAGs depending on their structures: chondroitin sulphate, heparin sulphate (HS), dermatan sulphate, keratin sulphate, hyaluran, and heparin.[507-509] HS is a copolymer of sulphated glucosamine and sulphated glucuronic or iduronic acid.[510-511] The structural diversity of HS is derived from the modification of individual disaccharide units within the oligosaccharide, which enables them to interact with a great variety of extracellular proteins, such as growth factors, cytokines, chemokines, matrix proteins and antimicrobial peptides and to get involved in many biological processes, such as morphogenesis, tissue repair, energy balance and host defence.[510] HSs are commonly used as binding molecules for numerous viruses and other pathogens as they are ubiquitously present on the surface of animal cells and in the extracellular matrix, where the initial interactions of viruses and target cells occur. Herpes simplex virus, influenza A virus, Sendai virus, Japanese encephalitis virus, human cytomegalovirus, respiratory syncytial virus, dengue virus, adeno-associated virus, and many others, bind to HSs.[327-329,512-518] HSs contain a considerable number of negative charges under physiologic conditions and these may contribute to virus-cell interaction. However, this binding could be far more complex than just nonspecific ionic interactions.[519] While heparin is the structural analog of HS, it undergoes more extensive sulfation and uronic acid eprimization.[509] In addition to its anticoagulant function, heparin has also been used as a research reagent, in particular for affinity-purification of heparin-binding proteins.[520] The

heparin-binding properties of many of these proteins represent their physiological interactions with HS, as the surface of most animal cells and extracellular matrices of a wide variety of tissues. Heparin-binding domains of heparin-binding proteins have been shown to contain consensus sequence motifs, such as XBBXB and XBBBXXBX, where B is a basic amino acid and X is a neutral or hydrophobic amino acid.[521] Besides the consensus sequence motifs, the spatial orientation of basic residues rather than sequence proximity is critical in determining heparin-binding affinity.[522]

The purpose of this study is to investigate the role of heparin in EAV infection of its natural target cell, the equine endothelial cell (EEC). We aligned the sequences available for E protein and identified the putative heparin-binding protein domain in this protein. A panel of conserved arginine to glycine mutations at the C-terminus of the E protein was generated using site-directed mutagenesis and reverse genetics. The effect of mutations on EAV infection and heparin binding was investigated.

7.3. MATERIALS AND METHODS

Cells and viruses

Equine pulmonary artery endothelial cells (EECs) were maintained and propagated in Dulbecco's modified essential medium (DMEM, Mediatech, Herndon, VA) supplemented with sodium pyruvate, 10% fetal bovine serum (Hyclone Laboratories, Inc., Logan, UT), 100U/ml of penicillin/streptomycin and 200mM L-glutamine (Life Technologies, Grand Island, NY).[486,523] RK-13 (ATCC, CCL-37) and mouse connective tissue (LM; ATCC CCL-1.2) cells used in the virus attachment study were cells were cultured and maintained in Eagle's minimum essential medium (EMEM; [Mediatech, Herndon, VA]) supplemented with 10% fetal calf serum (FCS; Hyclone, Logan, UT), 100U/ml penicillin, 100µg/ml streptomycin, 1µg/ml amphotericin B and 0.06% sodium bicarbonate at 37°C. The experimentally derived highly virulent Bucyrus strain (VBS) of EAV (ATCC VR-796)[524] was propagated in EEC to prepare high tittered working stock as previously described.[486,523] Briefly, EECs infected with the VBS strain of EAV (thereafter named as EAV for simplicity) were frozen at -80ºC when 90-100% cytopathic

effect (CPE) was observed. Cell lysates were clarified by centrifugation (500 ×*g*) at 4°C for 15 min, followed by ultracentrifugation (Beckman Coulter, Miami, FL) at 121,600 ×*g* through a 20% sucrose cushion in NET buffer (150 mM NaCl, 5 mM EDTA, and 50 mM Tris-HCl, pH 7.5) at 4 °C for 4 h to pellet the virus. The partially purified VBS strain of EAV was resuspended in phosphate buffered saline (PBS; pH 7.4) and frozen at -80 °C. Virus stock was titrated by standard plaque assay in RK-13 cells (ATCC CCL-37; American Type Culture Collection, Manassas, VA) and infectivity titers were expressed as pfu/ml.[525] The virus was used to characterize the effect of heparin on EAV infectivity on EECs.

Antibodies

To detect the viral proteins that interacted with heparin in western blotting test, Previously described monoclonal antibodies (MAbs) against EAV nucleocapsid protein (N; MAb 3E2)[234,254] and GP5 protein (MAb 6D10)[475,526] were used in the study. Similarly, polyclonal rabbit antisera recognizing EAV GP2 (rabbit 4033),[475] M (rabbit 8887)[251] and E (rabbit 2855 and 2586)[262] were also included. The MAbs and antisera were used individually in the western blotting test.

Treatment of viruses with heparin, other GAGs or heparinase I

To study the role of heparin and other GAGs on EAV infectivity, EAV was incubated with different concentrations (0, 0.01. 0.1, 0.5, 1, 1.5, 2, 2.5 3 and 6 mg/ml) of GAGs (heparin, heparan sulfate, chondroitin sulfate A and dermatan sulfate; Sigma-Aldrich, St Louis, MO) at 37 °C for 1 hr to saturate putative heparin-binding viral proteins and thus prevent successful virus infection. The VBS-GAG mixture was subsequently inoculated onto the confluent monolayers of EECs at a multiplicity of infection (MOI) of 2 and the inoculated cultures incubated at 37 °C for 1 hr. The EEC culture were washed three times with Eagle's minimal essential medium (MEM, Life Technology, Grand Island, NY) to remove any unbound virus and monolayer fixed at 12 hpi with 4% paraformaldehyde for subsequent flow cytometric analysis. In a separate

experiment, confluent EECs were treated with heparinase I for 1 hr at 37 ºC to remove the putative heparin-like molecules expressed on the surface of EECs. EECs were then extensively washed with plain MEM to remove residual heparinase I followed by inoculation with EAV at a MOI of 2 for a further hour at 37 ºC. Following incubation, EECs were again washed with MEM three times to remove unbound virus and fixed at 12 hpi for flow cytometric analysis.

Virus binding assay

The binding of EAV to EEC suspension was determined using a previously published protocol.[341] Briefly, subconfluent monolayers of EEC were trypsinzed, washed and resuspended in ice-cold PBS supplemented with 2% FBS (PBS-F). Cell suspensions were held on ice during the whole experiment. An MOI of 15 of biotinylated VBS and different concentrations of heparin (0, 0.01, 0.1, 0.5, 1, 1.5, 2, 3, and 6 mg/ml) were mixed and added to the suspensions and inoculated for 1 hr at 4 ºC. Subsequently, the cells were incubated with 200 µl of a 1:100 dilution of streptavidin-FITC conjugate (GE healthcare, Pittsburgh, PA) in PBS-F buffer for an additional hr on a shaker at 4 ºC. Cells were then washed with ice-cold PBS-F and resuspended in PBS-F for immediate flow cytometric analysis.

Flow cytometric analysis

The intracellular immunofluorescence staining of EAV nsp1 was used to determine the infectivity of the VBS strain of EAV for EECs after GAG or heparinse I treatment. After the GAG and heaprinase I treatment, EECs were fixed with 4% paraformaldehyde for 30 min followed by incubation for 5 min in membrane permeabilization buffer (PBS containing 1% heat-inactivated normal goat serum, 0.1% sodium azide and 0.1% saponin, Sigma-Aldrich, St Louis, Mo). The permeablized EECs were incubated with EAV α-nsp1 IgG (MAb 12E4) conjugated with Alexa Fluor® 488 (Invitrogen, Carlsbad, CA) for 30 min. 10^6 EECs were obtained and analyzed with

FACScalibur and Cellquest software (Becton-Dickinson, San Jose, CA) to determine the percentage of EAV positively infected cells.

The detection of biotinylated EAV surface proteins was used to determine whether there had been interaction between heparin and those proteins. A 10^6 EECs were mixed with the biotinylated VBS strain of EAV were obtained and analyzed using FACScalibur and Cellquest software. The median fluorescence intensity (MFI) was calculated according to the following formula: 100 × (MFI when heparin was added/MFI when no heparin was added).

Cloning and expression of E, GP2 and N proteins of EAV

To individually express EAV viral proteins, the genes encoding E (ORF2a), GP2 (ORF2b) and N (ORF7) proteins were cloned into the pVR21 plasmid vector downstream of a 26S promoter following a previously described protocol.[272] The recombinant plasmids containing the E, GP2 and N genes of EAV were designated pVR21-E, pVR21-GP2 and pVR21-N, respectively. The authenticity of the cloned genes was confirmed by sequencing. Two plasmids expressing major envelope proteins GP5 and M (pVR21-GP5 and pVR21-M) was also included in this study.[272]

Runoff RNA transcripts were generated from Not I-linearized recombinant plasmids including pVR21-GP2, pVR21-GP5, pVR21-M, pVR21-E and pVR21-N to generate *in vitro* transcript RNA (IVT RNA) according to a previously described protocol.[384] Individual IVT RNA was transfected into EEC using a BTX electroporator (Harvard Apparatus, Holliston, MA) according to the manufacturer's instructions. The transfected EECs were solublized at 24 hpt to collect the expressed proteins and confirmed by western blot testing. Individual expressed structural protein was used to determine its binding capability to heparin sepharose beads.

Binding of viral proteins to heparin sepharose

The approach was modified from the protocol described by Delputte *et al* (2002).[341] Firstly, partially purified EAV or individually expressed recombinant proteins of EAV (E, GP2, GP5, M and N) were solublized in solubilization buffer (20 mM

Tris.HCl [pH 7.6], 150 mM NaCl, 1% NP-40, 1mM EDTA) containing Halt protease inhibitor cocktail (Pierce, Rockford, IL) for 30 min at room temperature. Then the solublized EAV viral proteins or recombinant proteins were incubated with heparin sepharose CL-6B (GE Healthcare, Piscataway, NJ) at room temperature for 1 hr with agitation and then washed with PBS containing 0.1% NP-40 (PBS-N) as recommended by the manufacturer. Bound viral proteins or recombinant proteins were eluted under different conditions including PBS-N containing 4 mg of heparin per ml (PBS-N-H) and a final concentration of 2 M NaCl as described previously.[341] In a parallel experiment, the plain sepharose beads without heparin (Sigma-Aldrich, St Louis, MO) were used as a negative control. The eluted proteins were mixed with lamella sample buffer containing 100 nM DTT (Pierce, Rockford, IL) prior to running them on a 12% SDS-PAGE gel.[499,526] The solublized VBS proteins were then transferred on to PVDF membranes and immunoblotted with EAV protein specific antibodies.

SDS-PAGE and western blotting

The solubilized VBS proteins or recombinant EAV viral proteins were mixed with 5X sample reducing buffer containing 100mM dithiothreitol (DTT; Pierce, Rockford, IL) and incubated for 10 min at room temperature. Samples were resolved in a SDS-12% polyacrylamide gel (PAGE). The gel was transferred to PVDF membranes (Bio-Rad, Hercules, CA) and blocked with TBS-T (10mM Tris-HCl [pH 7.6], 150mM NaCl, 0.05% Tween 20) with 5% skim milk powder. Blots were incubated with primary antibody for 1 h at room temperature followed by exposure to a 1:5000 dilution of biotinylated goat anti-mouse or anti-rabbit antibodies (Invitrogen, Carlsbad, CA) for 1 hr. Subsequently, the blots were incubated with a 1:2000 dilution of streptavidin-horseradish peroxidase tertiary antibody (Invitrogen, Carlsbad, CA) and detected by means of an enhanced chemiluminescence reaction (ECL, Amersham, Piscataway, NJ).

Comparative amino acid sequence analysis and membrane topology prediction of E protein

The EAV ORF2a nucleotide sequences which are available in the GenBank (n=90) were downloaded and translated into amino acid sequences using the Vector NTI Advance™ 11 software (Invitrogen, Carlsbad, CA). Multiple amino acid sequence alignments were performed using CLUSTAL_X v1.83 to identify the conserved regions of E proteins.[527] Prediction of membrane topology for E protein was performed using five most commonly used topology prediction methods available on the Internet: PSIPRED (http://www.psipred.net/psiform.html),[528-529] TMHMM (http://www.cbs.dtu.dk/services/TMHMM/),[530] TMPred (http://www.ch.embnet.org/software/TMPRED_form.html), TOPPRED (http://mobyle.pasteur.fr/cgi-bin/portal.py?#forms::toppred)[531] SOSUI (http://bp.nuap.nagoya-u.ac.jp/sosui/sosui_submit.html) . All user-adjustable parameters were left at their default values.

Site-directed mutagenesis to generate recombinant E protein mutants

The full-length infectious cDNA clone pEAVrVBS[388] was used to generate a panel of arginine to glycine mutations at the heparin-binding domain in the C-terminus of EAV ORF2a region using QuikChange Multi Site-directed Mutagenesis Kit (Stratagene, Santa Clara, CA) described previously.[532] The mutations engineered are listed in Table 1. Arginine residues at position 52, 57, 60, 63, 65 were mutated to glysine to make single (R52G and R57G), double (R52,60G, R57,63G and R63,65G) or triple (R52,60,65G) mutations. BHK-21 cells were transfected with IVT RNAs by following previously described protocols[384] to generate the recombinant viruses rVBS R52G, rVBS R57G, rVBS R52,60G, rVBS R57,63G, rVBS R63,65G and rVBS R52,60,65G. A small portion of tranfected cells were seeded onto coverslips and incubated for 18 hr post transfection before being stained with EAV specific MAb (3E2) against N protein to confirm the replication of recombinant virus by IFA. The tissue culture fluid (TCF) supernatant collected after IVT RNA transfection was designated P0 virus and used for further characterization. Similarly, the pVR21-E plasmid was used to generate the same panel of arginine to lysine mutations as described above. The expressed mutant proteins (R52G, R57G, R52,60G, R57,63G, R63,65G and R52,60,65G) were named E R52G, E R57G, E

R52,60G, E R57,63G, E R63,65G and E R52,60,65G, respectively. These mutant E proteins were used to determine the interaction with heparin in a heparin binding assay.

Immunofluorescence assays

For the indirect immunoflurorescence assay (IFA), EECs transfected from IVT RNA generated from the full-length infectious pEAVrVBS clone or various E mutants were seeded on coverslips and fixed at 18 hpt in 4% paraformaldehyde in phosphate-buffered saline (PBS; pH7.4) for 30 min at RT followed by washing three times in PBS (pH 7.4) containing 10mM glycine (glycine/PBS). After permeabilization with 0.2% Triton X-100 in PBS (pH 7.4) for 10 min, coverslips were incubated with EAV MAb 3E2 specific for the N protein in PBS containing 5% fetal bovine serum (FBS). After three 10mM glycine/PBS washes, coverslips were incubated with FITC-conjugated goat anti-mouse (Southern Biotech, Birmingham, AL) for 1 h at RT. Cover-slips were washed and mounted in 4', 6'-diamidino-2-phenylindole (DAPI) containing aqueous mounting medium (Vector Laboratories, Burlingame, CA) and examined under an inverted fluorescence microscope.

Growth characteristics and plaque morphology of mutant E viruses

Subconfluent monolayers of BHK-21 grown in six-well plates were inoculated with parental EAV rVBS or mutant E viruses at MOI of 1 and held at 37 ºC for 1 hr. The inocula were removed and the cells were washed three times with PBS to remove unbound virus before being overlaid with 4 ml of EMEM. At 6, 12, 18, 24 hpi, supernatants were collected and virus titers were determined by plaque assay in RK-13 cells.[279] For the plaque morphology study, EECs were used for virus infection and overlaid with DMEM containing 0.75% carboxymethyl cellulose and incubated for 4 days.[263]

7.4. RESULTS

Effect of heparin and heparinase I on EAV infectivity

EAV was firstly incubated with various concentrations of heparin prior infection of EEC to see whether heparin could reduce the infectivity of EAV. Cells were fixed at 12 hpi which only allows one cycle of viral replication. The number of EAV infected cells was determined by intracellular immunofluorescent staining of EAV nsp1 protein and flow cytometric analysis. A dose-dependent reduction of EAV infection was observed, with a maximal 93% and 91% reduction in a heparin concentration of 3 and 6 mg/ml, respectively (Fig 7.1.). To confirm that the inhibition effect was due to the interaction between heparin and virus and not between heparin and the cells, in a separate experiment, EEC was incubated with heparin prior EAV infection. As shown in Figure 1, pretreatment of EEC with heparin had no significant effect on EAV infection. To investigate if heparan sulfate proteoglycans, present on the cell surface, are involved in EAV infection, EEC was treated with different concentrations of heparinase I prior to EAV infection. There was a significant reduction after heparinase I treatment of the EEC, with a maximum of 65% at 80 U/ml (Fig 7.2.)

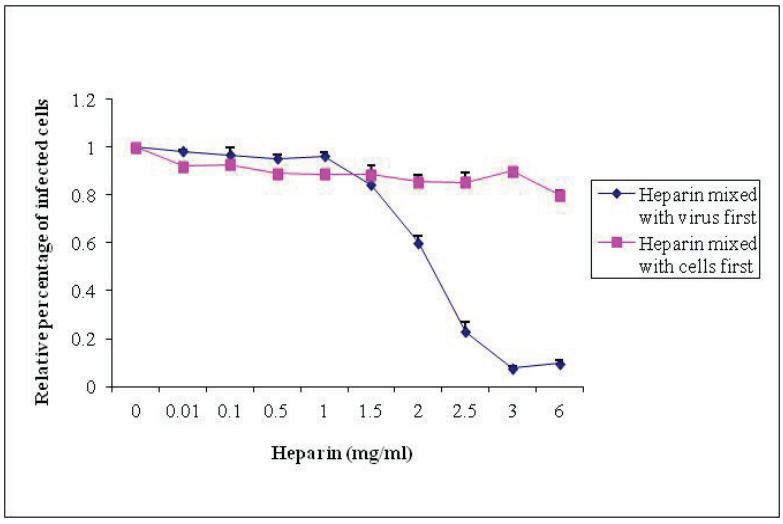

Fig 7.1. Effect of heparin on EAV infection of EEC. EAV (♦) was incubated with various concentrations of heparin and the heparin and EAV mixture was inoculated into EECs and incubated at 37 °C for 1 hr. Subsequently, the cell monolayer was washed to remove unbound virus and finally stained with MAb 12A4 specific for nsp1 protein with flow cytometry at 12 hpi. In another experiment, EEC monolayer (■) was incubated with

heparin for 1 hr followed by extensive washing steps. Subsequently, EAV was inoculated into EEC monolayer for 1 hr followed by extensive washing. EECs were stained with MAb 12A4 for nsp1 with flow cytometry. The data represents the means± standard errors (error bars) of triplicate experiments.

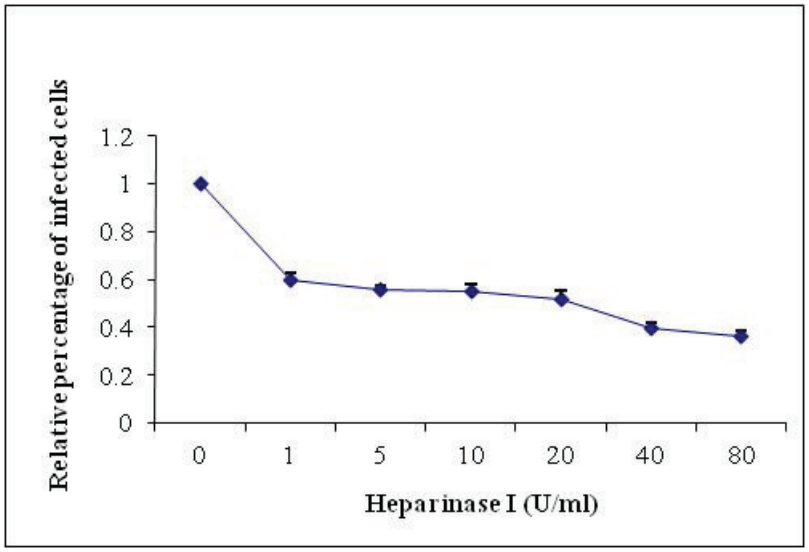

Fig 7.2. Effect of heparinase I treatment of EEC on EAV infection. EEC was pretreated with heparinase I for 1 hr, extensively washed and infected with EAV for another hour at 37 ºC. EEC were fixed at 12 hpi and stained with MAb12A4 for nsp1 for flow cytometric analysis. The data represents the means± standard errors (error bars) of triplicate experiments.

Effect of other glycosaminoglycans on EAV infection to EEC

To investigate if the reduction of EAV infection was due to a specific interaction of the virus with heparin or due to a general interaction with negatively charged molecules, EAV was incubated with other GAG molecules including heparan sulfate, chondroitin sulfate A and dermatan sulfate before inoculation. At the highest concentration of 6 mg/ml, all three GAGs reached their maximal reduction of 91% ± 1%, 55% ± 1% and 35% ± 12% (means ± standard error), respectively, as compared to untreated control. Chondroitin sulfate A at 0.1, 0.5, 1 or 3 mg/ml could reduce the EAV

infection to 30% as of the control. Other concentrations of GAGs did not have significant reduction effect on EAV infectivity (Fig 7.3.).

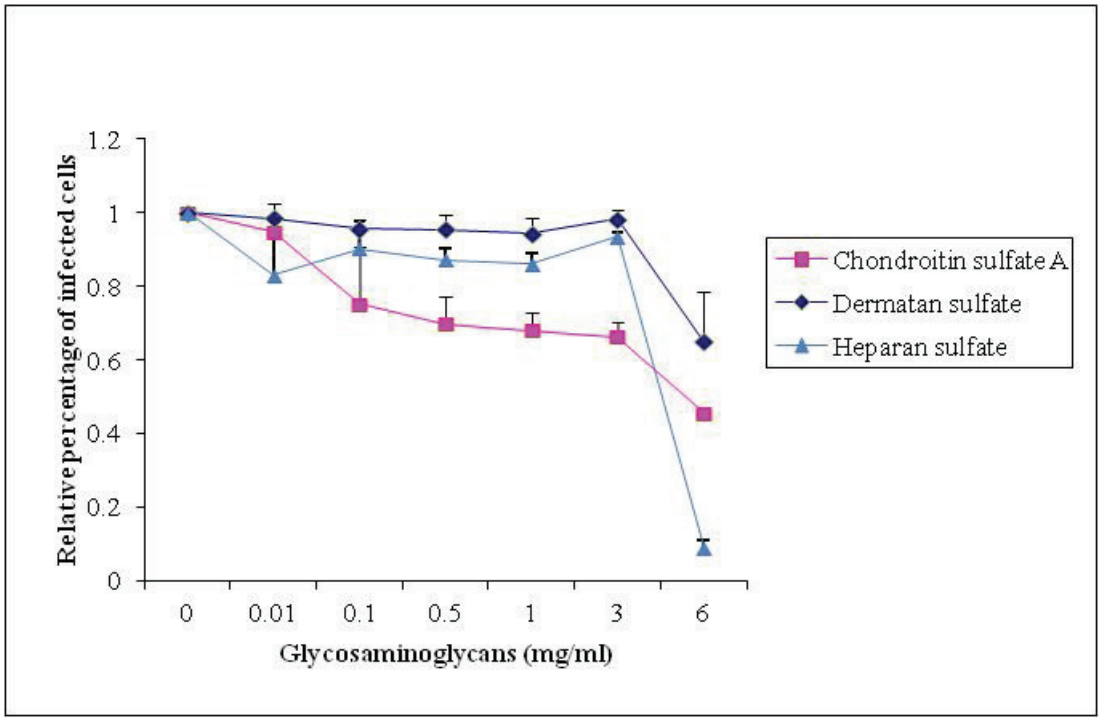

Fig 7.3. Effect of other glycoaminoglycans on EAV infection to EEC. Different concentration of heparan sulfate (▲), chondroitin sulfate A (■), dermatan sulfate (♦) were mixed with EAV for 1 hr at 37 ºC. Subsequently, the EAV-GAG mixture was inoculated to the EEC monolayer for 1 hr at 37 ºC. The EAV-GAG mixture was removed and EEC monolayer was stained with MAb12A4 against EAV N protein for flow cytometric analysis at 12 hpi. The data represents the means± standard errors (error bars) of triplicate experiments.

Binding of EAV to heparin sepharose and identification of EAV heparin binding proteins

To identify the viral proteins which can bind to heparin, solublized EAV viral proteins were incubated with heparin sepharose beads for 1 hr at 37 ºC. After extensive washing, the bound proteins were eluted with heparin in combination with high salt concentration. The proteins bound to heparin were identified by western blotting using MAb or polyclonal sera specific for the major envelope proteins (GP5 and M), minor

envelope proteins (E and GP2) and nucleocaspid protein N. The results showed that all these tested structural proteins were able to bind to heparin sepharose beads (Fig. 7.4b). The representative gel for GP2 (Fig. 7.4a) clearly showed that GP2 can be detected in the original EAV solublized protein prior to heparin binding and the first two washing steps. No residual GP2 protein was found in the 5^{th} and 8^{th} washings. In the subsequent elution step, GP2 protein was able to be eluted in all three elution steps suggesting the bound GP2 were successfully washed off from the beads. When control sepharose beads were used, none of the proteins were eluted either from solublized EAV proteins or expressed proteins.

To further confirm the viral protein interaction with heparin, in another experiment, individually expressed EAV viral proteins E, GP2, GP5, M and N were mixed with heparin sepharose beads. Proteins were eluted and subsequently identified in a western blotting assay using protein specific antibodies. Each individually expressed protein was able to bind with heparin sepharose beads same as solublized EAV proteins (Fig. 7.4c). One of the most interesting finding was the binding of minor envelope E protein to heparin sepharose. The E protein occurs in virion particles in small amounts and its function is not fully understood. Therefore, we tried to investigate the mechanism of heparin and E protein interaction in detail.

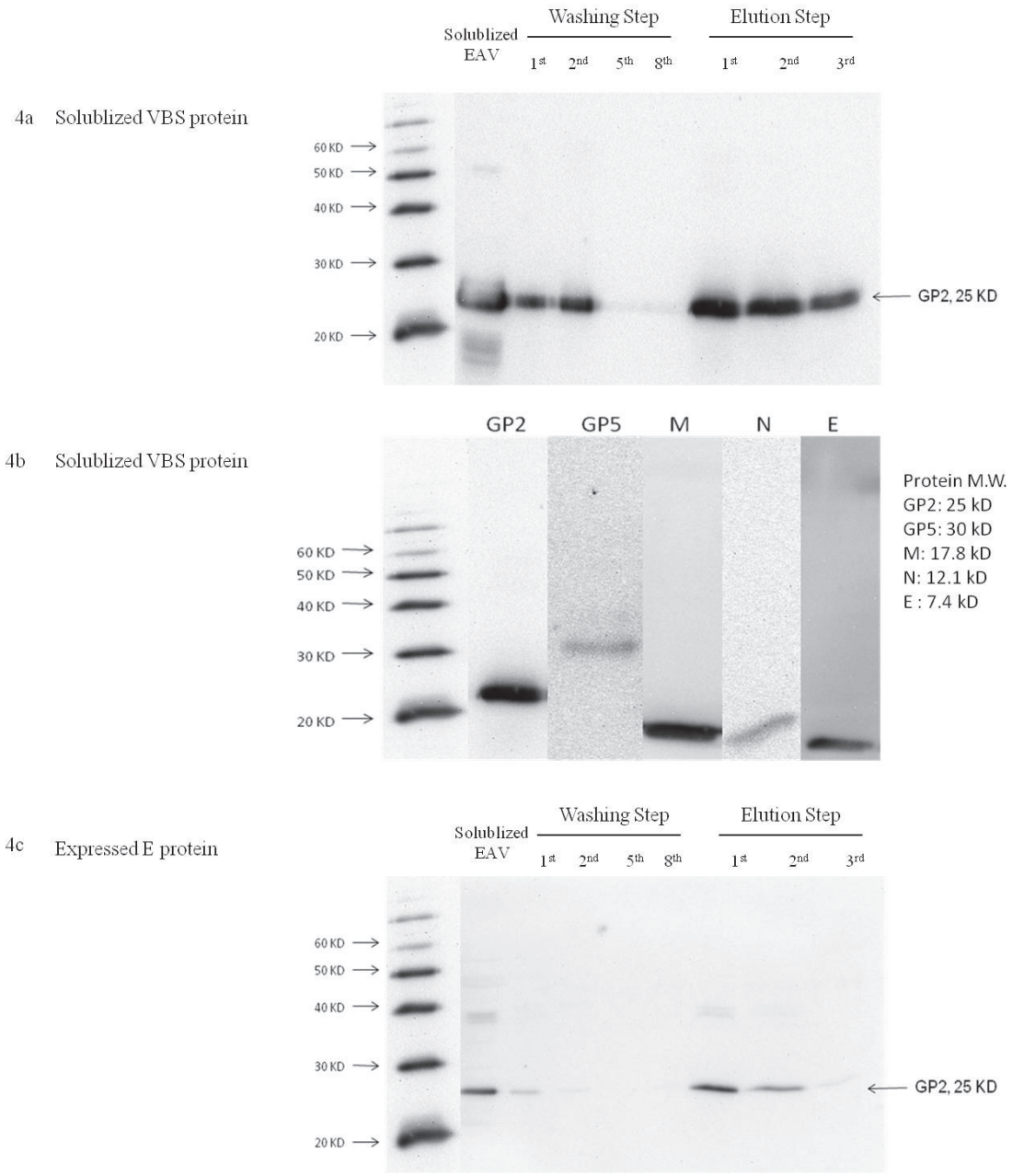

Fig 7.4. Western blotting analysis of the binding of EAV proteins to heparin sepharose. EAV particles were solublized and run through heparin sepharose column. The column was washed with PBS containing 0.1% NP40 (PBS-N) for eight times. The heparin bound proteins were eluted using PBS-N containing 4 mg of heparin per ml (PBS-N-H) and a final concentration of 2 M NaCl. 4a: Representative gel of GP2 from solublized purified VBS viral proteins binding to heparin sepharose. 4b: All the EAV viral proteins that were tested in this study could bind to heparin sepharose beads. 4c: Representative gel of expressed GP2 protein could bind to heparin sepharose beads.

Identification of a conservative heparin-binding motif in E protein

The search for a heparin-binding motif in the EAV proteins was guided by the heparin binding motif XBBBXXBX, where B stands for a basic amino acid (arginine in this sequence) and X is a neutral or hydrophobic amino acid. Sequence analysis showed that with the exception of E protein, GP2, GP5, M and N proteins did not have an obvious heparin binding pattern. The amino acids RSLVARCSRGARYR at C-terminus of E protein contain a cluster of basic R (arginine) residues which is consistent with the heparin binding motif. Comparative amino acid sequence analysis of E protein from ninety EAV strains showed that five arginine residues at amino acid positions 52, 57, 60, 63 and 65 were highly conserved among all aligned EAV sequences. Other arteriviruses such as PRRSV, LDV and SHFV have at least two arginine residues and a lysine residue, which is also a basic amino acid (Fig 7.5.).

The membrane topology of E protein was predicted and results were quite variable. SOSUI predicted that the E protein has two transmembrane helices with C-terminus toward the exterior side of the virion. All the other programs predicted that the C-terminus is located in the cytoplasm. Despite the variable prediction, we continued to investigate the role of conserved the arginines using site-directed mutagenesis.

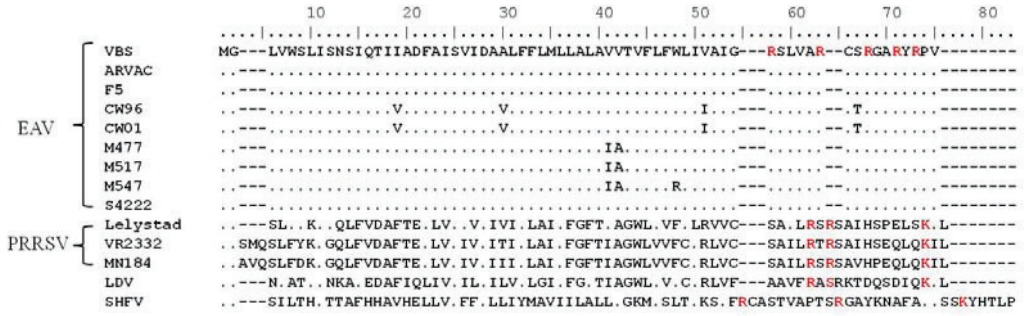

Fig 7.5. Alignment of the sequences of E protein of all arteriviruses. Representative field strains of EAV and PRRSV were shown in the alignment. The conserved basic arginines (R) are highlighted in red.

Growth characteristic and plaque morphology of E mutant viruses

A panel of mutant constructs both in full-length infectious cDNA pEAVrVBS clone and expression pVR21 vector was generated substituting the conserved basic arginines with the neutral, nonpolar glycine. The selection of glycine for mutagenesis was solely to maintain the in-frame coding of other overlapping ORFs. Single mutant (R52G and R57G), double mutant (R52,60G; R57,63G and R63,65G) and triple mutant (R52,60,65G) were introduced to both pEAVrVBS (Table 7.1) and pVR21 constructs (Table 7.2).

Table 7.1. Overview of the genotype and phenotype of EAV E protein mutants virus used in this study[a]

Construct Name	pEAVrVBS Parental Codon	pEAVrVBS Mutant Codon	Mutation	IFA[b]	Infectious Progeny (pfu/ml)[c]	Summary of Phenotype[d]
pEAVrVBS	NA[e]	NA	None (parental)	+	+ (1×10^5)	Wild type
R52G	CGC	GGC	Arg-52→Gly	+	+ (7.5×10^4)	Wild type
R57G	CGG	GGG	Arg-57→Gly	+	+ (8.5×10^4)	Wild type
R52,60G	CGC CGA	GGC GGA	Arg-52→Gly Arg-60→Gly	+	+ (5.25×10^4)	Wild type
R57,63G	CGG CGT	GGG GGT	Arg-57→Gly Arg-63→Gly	+	+ (7.5×10^4)	Wild type
R63,65G	CGT AGA	GGT GGA	Arg-63→Gly Arg-65→Gly	+	+ (3.0×10^4)	Wild type
R52,60,65G	CGC CGA CGT	GGC GGA GGT	Arg-52→Gly Arg-60→Gly Arg-63→Gly	+	+ (8.0×10^2)	Severely Crippled (pinpoint sized plaques)

[a] Data from two independent transfection experiments are summarized. +, positive

[b] Transfected cells were stained with EAV MAb (3E2) against N protein after one cycle of replication at 18 hr posttransfection. IFA, immunofluorescence assay.

[c]Results indicate the detection of infectious progeny using plaque assays in the medium from transfected cells harvested at 72-96 hr posttransfection when 90-100% CPE were developed, approximate virus titers are shown between brackets.

[d] Phenotypes are based on growth characterization and plaque morphology.

[e] Not applicable.

Table 7.2. Overveiw of the genotype and heparin binding capacity of EAV E mutant proteins used in this study

pVR21					
Construct Name	Parental Codon	Mutant Codon	Mutation	IFA[a]	Heparin binding capability
pVR21-E	NA[b]	NA	None (parental)	+	+
R52G	CGC	GGC	Arg-52→Gly	+	+
R57G	CGG	GGG	Arg-57→Gly	+	+
R52,60G	CGC CGA	GGC GGA	Arg-52→Gly Arg-60→Gly	+	-
R57,63G	CGG CGT	GGG GGT	Arg-57→Gly Arg-63→Gly	NA	NA
R63,65G	CGT AGA	GGT GGA	Arg-63→Gly Arg-65→Gly	NA	NA
R52,60,65G	CGC CGA CGT	GGC GGA GGT	Arg-52→Gly Arg-60→Gly Arg-63→Gly	NA	NA

[a] Transfected cells were stained with antisera against E protein at 18 hr post transfection. The IFA and heparin binding assay were unavailable to the R57,63G; R63,65G; R52,60,65G mutants because the mutation overlap with the antibody reconition site. IFA, immunofluorescence assay. + positive

[b] Not applicable

The same amount of full-length IVT RNA generated from linearized pEAVrVBS, as well as clones containing E mutants were electroporated into EEC for generation of recombinant mutant viruses. The viability of each mutant clone was determined by indirect immunofluorescence assay (IFA) using EAV monoclonal antibody (MAb 3E2) specific for N protein at 18 hr post transfection (Fig 7.6.). The cells transfected with each of the parental and mutant transcripts produced 90-100% cytopathic effect (CPE) in

transfected cells after 72-96 hours post transfection, and virus stocks were made from these tissue culture fluids (TCF; P0).

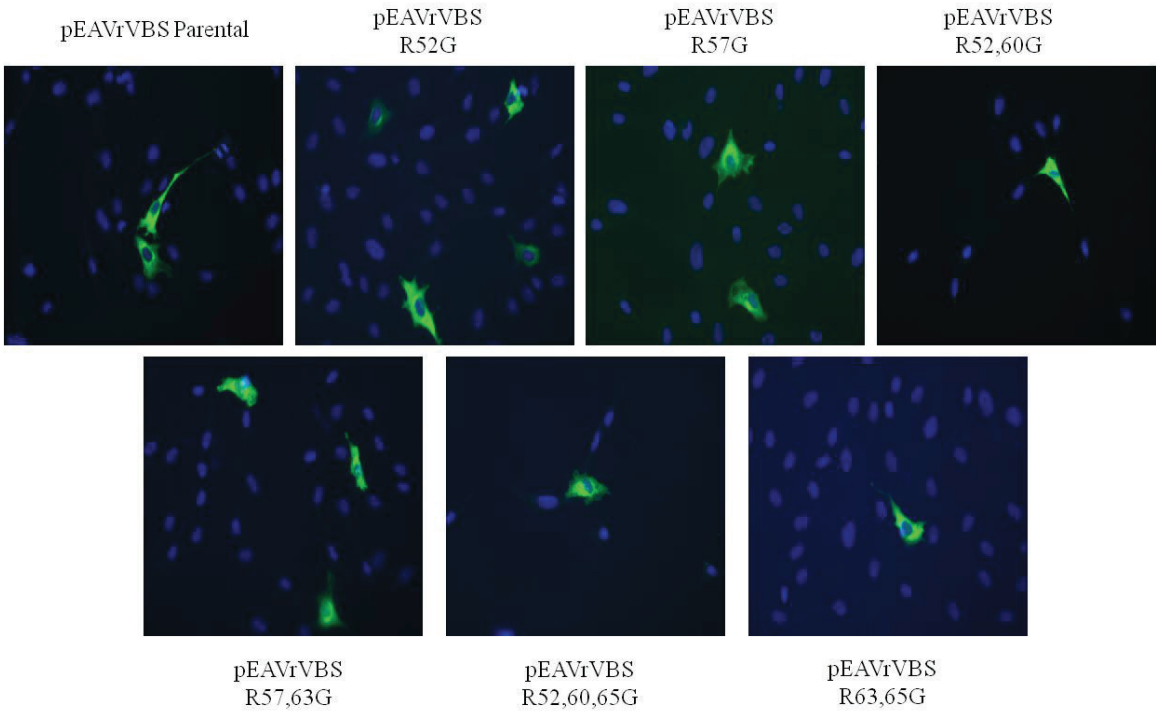

Fig 7.6. Immunofluorecence staining of nucleocapsid (N) protein of EECs transfected with parental EAV (pEAVrVBS) and E mutants IVT RNA at 24 hr posttransfection.

The authenticity of all mutant viruses was confirmed by sequencing ORF2a from RNA extracted from each P0 TCF. All virus sequences were identical to the plasmid sequence from which they were derived. The titers of the single or double arginine mutant P0 viruses were similar to the parental rVBS virus (10^4-10^5 pfu/ml) but the titer for the triple mutant virus (rVBS R52, 60, 65G) was significantly reduced (10^2 pfu/ml) (Table 7.1). The TCFs (P0) containing each mutant virus were then used to infect BHK-21 cells at a multiplicity of infection (MOI) of 1 and progeny viruses were collected at different time points for titration. The growth characteristics and plaque morphology were compared in RK-13 and EEC, respectively. All the mutant viruses had the highest virus titer at 24 hr post infection. With the exception of rVBS R52,60,65G virus which had approximately 2 $\log_{10}$ lower titer at this time point, all the other mutant viruses had similar titer as

compared to the parental rVBS virus (Fig 7.7.). When compared to the parental virus, all the mutant viruses except rVBS R52,60,65G virus showed similar medium sized plaques in EEC (2.5 mm to 3 mm) (Fig 7.8.). The triple mutant rVBS R52,60,65G produced a pinpoint sized plaques (0.5 mm).

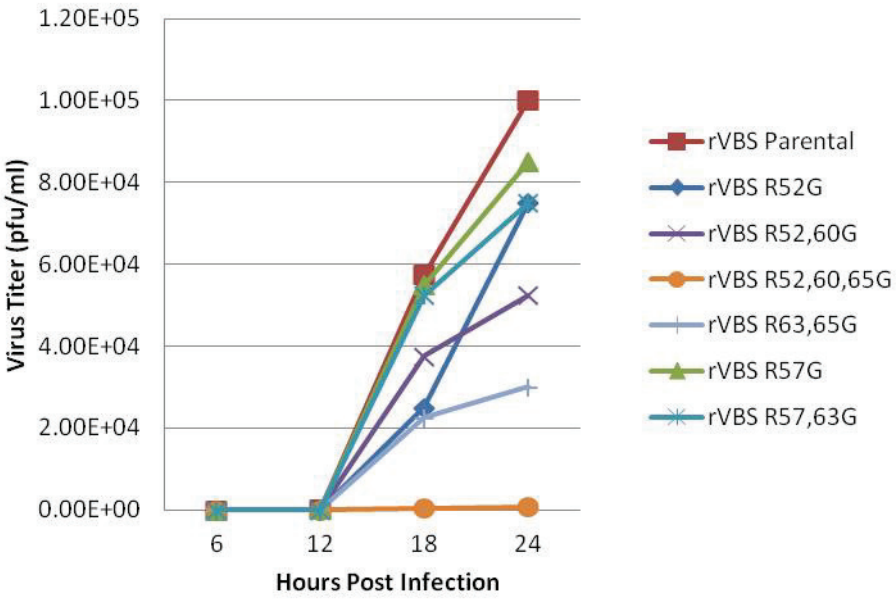

Fig 7.7. Growth curve of E mutant viruses and parental rVBS virus. BHK21 cells were infected with an MOI of 1 of P0 transfected virus and tissue culture fluid containing progeny viruses were harvested at indicated time points. Virus titers were determined by plaque assays in RK-13 cells.

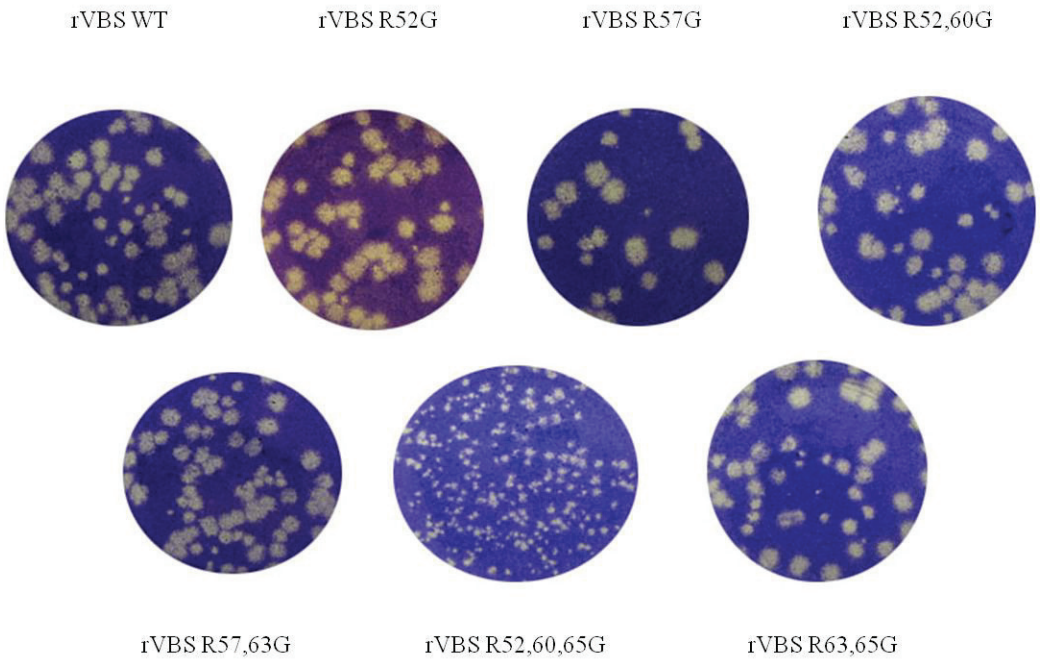

Fig 7.8. Comparison of plaque morphology on EECs of parental rVBS and E mutant viruses. All the mutants except triple mutation rVBS R52,60,65G produce similar plaque size as compared to the parental virus. The rVBS R52,60,65G triple mutant virus is severely crippled with pinpoint sized plaques.

Arginine mutations abolish interaction with heparin

The effect of arginine residues on heparin binding were investigated using the expressed E mutant proteins. Each mutant pVR21-E construct was transfected into EEC and expressed proteins were collected for heparin binding assay. Wild type E protein was included as positive control. Heparin sepharose beads were mixed with expressed E protein prior to extensive washing and final elution. Washing fractions and eluted proteins were collected and tested in western blot using rabbit sera against E protein. Both wild type E protein and single mutant R52G protein and R57G protein were able to bind heparin (Table 7.2 and Fig 7.9.). Double mutant R52, 60G protein lost its heparin binding capability as no E protein was detected in the elution fractions. We were unable to detect the interaction between the double R63, 65G protein and triple R52,60,65G protein with heparin because these mutants disrupt the antisera recognition sites and failed to detect these two mutants in western blot.

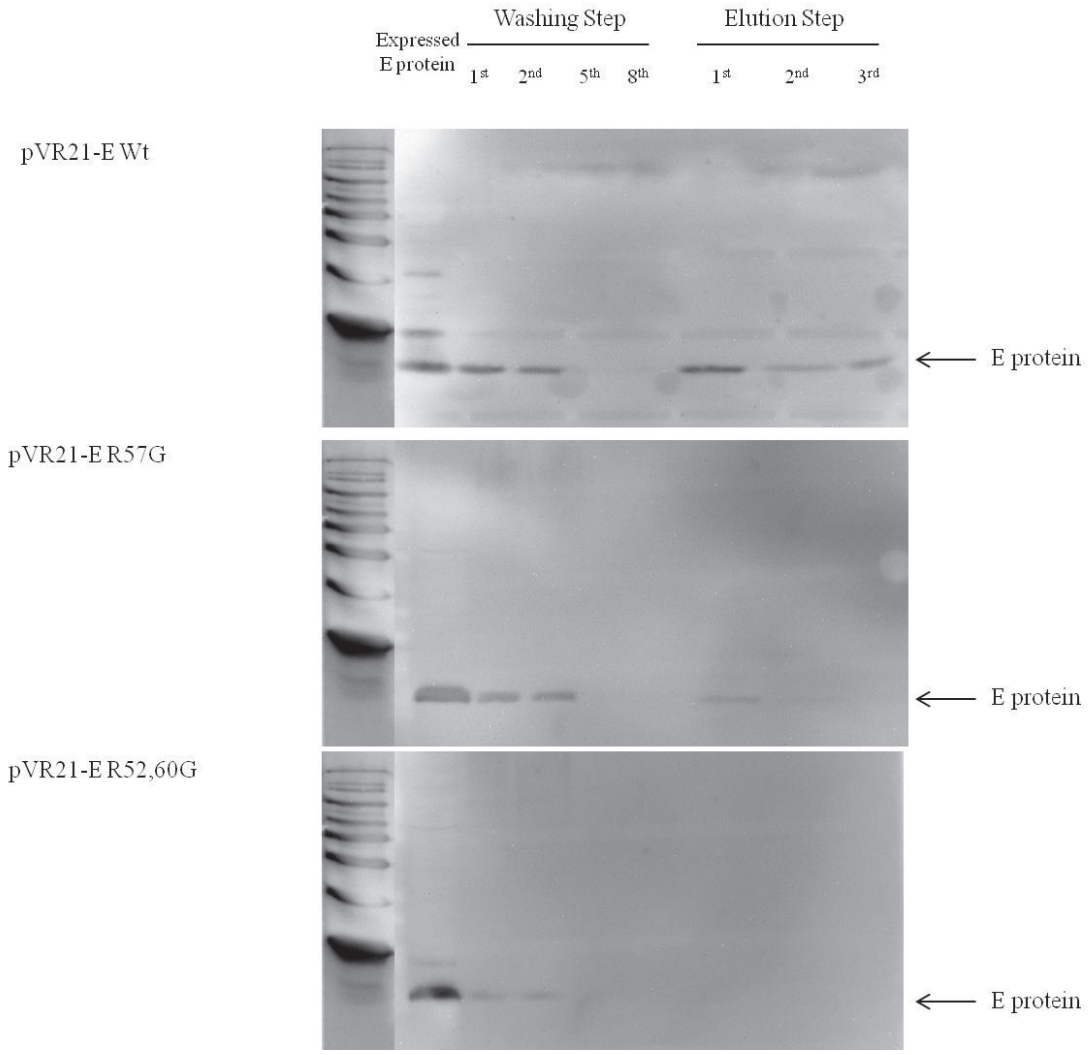

Fig 7.9. Western blotting analysis of the binding of EAV E protein to heparin sepharose. Wild type or mutant (R57G and R52,60G) E protein expressed from pVR21-E vector was solublized with Tris buffer containing 1% NP-40. Solublized proteins were mixed with heparin sepharose beads, and washed 8 times with washing buffer (PBS containing NP-40). Bound fractions were eluted with PBS containing 4 mg/ml heparin and 2M NaCl (PBS-H-NaCl). The original expressed E protein prior to heparin sepharose bead binding, various wash fractions and three elution fractions were detected with rabbit sera against E protein under reducing condition.

7.5. DISCUSSION

In this study, we characterized the role of heparin on EAV infection of EEC in detail. Heparin could significantly reduce the infectivity of EAV in a dose-dependent manner by interacting with the virus. The results are consistent with the previous finding that heparin can inhibit EAV infection in RK-13 cells.[289] The viral proteins interacting with heparin are major envelope proteins GP5 and M, minor envelope proteins E and GP2 and nucleocapsid N protein. The conserved arginines on the linear heparin-binding motif found in the C-terminus of E protein play important roles on the interaction between heparin and E protein. The double mutant R52,60G of E protein completely blocked the virus-heparin interaction however this mutant could still produce infectious progeny virus with a similar titer and plaque morphology as compared to parental rVBS virus. There are several possible explanations: 1) Although sequence analysis did not reveal an obvious heparin-binding motif in major envelope proteins GP5 and M, it could not exclude the possibility that these major proteins could still interact with heparin in some way. In fact, through an analysis of the available experimentally determined heparin-protein complexes, it became obvious that the spatial orientation of basic residues rather than sequence proximity is an important factor in determining heparin-binding affinity.[522] In such case, even the interaction between E and heparin is blocked, the major envelope proteins GP5 and M are still able to interact with heparin to facilitate virus infection. 2) There might be other attachment molecules besides heparin involved in EAV infection. We have shown that the EAV infection on EEC could be reduced by heparin, however, no complete block of infection was observed. Collectively, our data showed that heparin-like molecule on the EEC surface may function as an attachment factor to concentrate virions on the cell surface, hence allowing a more efficient infection but the presence of additional attachment factors may also be possible. A very recent publication by Tian *et al* described the use of a PRRSV infectious cDNA clone as a vector to construct a chimera in which PRRSV ORFs 2a, 2b, 3 and 4 were replaced by the corresponding ORFs from EAV.[294] This PRRSV/EAV chimeric virus gained a broad cell tropism that is typical of EAV, and clearly indicated that the minor envelope protein (GP2, GP3 and GP4) and E protein play a key role in determining the cellular tropism of arteriviruses and play a major role in virus attachment and entry. [294]

PRRSV is a close family member of EAV with its attachment and entry steps well-studied. It is speculated that the PRRSV virion initially attaches to heparan sulfate GAGs present on the macrophage surface followed by a more stable binding between the sialoadhesin receptor and M/GP5 glycoprotein complexes in the viral envelope. Upon attachment of sialoadhesin, the virus receptor complex is internalized via clathrin-mediated endocytosis.[489] Scavenger receptor CD163 is essential for genome release and may exert its function through interaction with GP2 and GP4.[345-346,533-534] Our results are consistent with the findings in PRRSV that the M and N protein could bind to the heparin-like receptor on porcine alveolar macrophage cells.[341] It is possible that EAV use a similar attachment and entry pathway as compared to PRRSV. However, it is important to keep in mind that compared to PRRSV, EAV has a much broader cellular tropism. EAV might also use different cellular proteins and entry pathways depending on the cell type. A well-studied example is herpes simplex virus (HSV), which can infect a variety of host cells, including lymphocytes, epithelial cells, fibroblast and neurons.[535] The pathways of HSV entry vary and depend on the host cell being targeted.[535]

There are several topology predictions of E protein according to its hydropathy profile although the exact membrane interaction feature is unknown yet. If the protein spans the membrane only once, it is predicted that the E protein is compatible with a type III protein orientation with the N terminus protruding outside of the cell and C terminus inside the cytoplasm ($N_{exo}C_{cyt}$).[262] It is also possible that the E protein spans the lipid bilayer twice, with both termini located at the cytoplasmic face of the membrane.[262] A more complicated viral membrane topology has been identified in Sindbis virus and hepatitis B virus where the E2 glycoprotein of Sindbis virus can have transient translocation of the cytoplasmic domain into cellular membranes and the large envelope protein of HBV can have dual topology.[536-538] Results in our study clearly showed that the double arginine mutant (R52,60G) blocked the interaction of heparin binding indicating that the C-terminus of E protein is likely exposed at the exterior site of the virus.

CHAPTER EIGHT

SUMMARY OF DISSERTATION

Accurate and rapid identification of viral infectious pathogens is not only of interest to equine practitioners but also to research scientists. The ready availability of a confirmed diagnosis of a specific pathogen enables the veterinarian to take an early decision on patient care and management, address appropriate treatment strategies, and allow timely notification and discussion of management issues relevaent to prevention of disease spread. This is particularly important after the discovery in 2004 that a strain of equine H3N8 influenza virus had crossed the species barrier and caused an extensive epidemic of respiratory disease in dogs. In 2007, a second canine influenza that was confirmed in Korea and on that occasion, the causative agent was H3N2 avian influenza virus of avian origin. Although there is no evidence that equine respiratory viruses are zoonotic, the close association between humans and dogs, and to a lesser extent horses, emphasize the need for better surveillance and control strategies for emerged diseases in companion animals. The first part of this dissertation focused on development and evaluation of rRT-PCR assays for the detection of common equine respiratory viruses including equine arteritis virus, equine influenza virus, equine rhinitis virus A and B. The application of equine influenza virus rRT-PCR to the diagnosis of canine influenza virus was also discussed. These molecular diagnostic assays were compared with conventional diagnostic tests and the advantage and disadvantage of each molecular method were discussed. Each assay was evaluated using a large amount of clinical specimens. Taken overall the assays that were developed were found to be highly sensitive and specific for the respective target viruses. Each had a very short turnaround time. They provide fast and realible techniques for diagnosticians to use as diagnostic as well as confirmation tests. Based on currently available rRT-PCR assays, we could develop a multi-plex rRT-PCR for all these common equine respiratory viruses in the future. This should provide a much simipler and rapid means of diagnosing multiple viral pathogens in a single reaction. However, optimization of a multi-plex rRT-PCR is critical to establish the sensitivity and specificity of the assay before it can be used in a diagnostic setting.

The second part of this dissertation is focused on the role of viral envelope proteins of EAV that might be involved in cellular tropism determination and host cell interaction. At this proint, neither a virus attachment molecule nor a specific cell receptor has yet been identified for EAV. It has been assumed that the major envelope proteins GP5 and M may determine the cellular tropism of EAV based on the fact that these two proteins carry neutralization antibody epitopes. Using an infectious cDNA clone of the modified live virus (MLV) vaccine (ARVAC®) of EAV (prMLVB), we generated a panel of 6 recombinant chimeric viruses by replacing either the full-length or the N-terminal ectodomains of GP5 and M proteins of EAV with the IA-1107 North American strain of PRRSV, a member of the genus Arterivirius which has very narrow cellular tropism. The recombinant viruses expressing the N-terminal ectodomain of PRRSV GP5 alone or M alone or both (GP5ecto, Mecto, and GP5&Mecto, respectively) in the EAV backbone were viable and genetically stable. Compared to the parental virus, these three chimeric viruses produced lower titers and smaller plaque sizes indicating that they have a compromised phenotype. The three chimeric viruses could only infect EAV susceptible cell lines but not PRRSV susceptible cells. Therefore, the two major envelope proteins may not be determining factors in the cellular tropism of EAV. However, in light of the lack of an effective PRRSV vaccine, these chimeric viruese might be good candidates to inoculate pigs and check their immunogenic kinetics. The marker prMLVB vaccine could be easily differentiated serologically between naturally infected animals and vaccinated animals. Although GP5 and M were not involved in cellular tropism determination, they were important in interaction with a heparin-like molecule on the surface of EECs, playing a siginificant role in EAV infection of equine endothelial cells. Using heparin-affinity chromatography and SDS-PAGE analysis, five structural proteins of EAV, E, GP2, GP5, M and N were identified as heparin-binding proteins. A specific heparin-binding domain on E protein was found on the C-terminus of the protein. Using site-directed mutagenesis, five basic arginine residues were mutated to glycine and the growth characteristic of the mutant viruses and heparin binding capacity were investigated. A double mutant R52,60G completely blocked the interaction with heparin but still replicated similar to the wild type virus control, indicating that another attachment molecule may exsit. The triple mutant R52,60, 65G had very tiny plaque morphology on

EECs suggesting that the spread of the mutant virus had been affected. These studies are valuable data in providing a better understanding the initial attachment step of EAV to its natural host cell, which is critical in appreciating the pathogenesis of the virus.

Collectively, the development of diagnostic methods for specific equine viral respiratory pathognes and investigation of the role of selected proteins of EAV on viral attachment to the cell are important in disease control and prevention. This dissertation will benefit both equine practitioner and research scientist involving in the field of equine infectious disease.

APPENDIX 1

List of Abreviations

aa	Amino acid
ACE2	Angiotensin-converting enzyme 2
APN	Aminopeptidase N
Arg	Arginine
Asp	Aspartate
BHK-21	Baby hamster kidney-21
bp	base pair
cDNA	Complementary deoxyribonucleic acid
CEACAM	carcinoembryonic antigen-related cell adhesion molecule
CI	Canine influenza
CIV	Canine influenza virus
CMC	Caboxylmethyl cellulose
CoV	Coronavirus
CPE	Cytopathic effect
Ct	Cycle threshold
Cys	Cysteine
DMV	Double membrane vesicle
DNA	Deoxyribonucleic acid
Dpi	Days post infection
Ds	Double stranded
E	Envelope protein
EAV	Equine arteritis virus
EAdV	Equine adenovirus
EDTA	Ethylenediaminetetraacetic acid
EEC	Equine endothelial cells
EHV	Equine herpes virus
eGFP	Enhanced green fluorescence protein
EI	Equine influenza
EIV	Equine influenza virus
ELISA	Enzyme-linked immunosorbent assay
EM	Electron microscope
EMPF	Equine multinodular pulmonary fibrosis
EPAEC	Equine pulmonary artery endothelial cells

ERAV	Equine rhinitis virus A
ERBV	Equine rhinitis virus B
ER	Endoplasmic reticulum
ERGIC	ER-Golgi intermediate complex
ERV	Equine rhitnis virus
EtBr	Ethidium bromide
EToV	Equine Torovirus
EU	European
EVA	Equine viral arteritis
FIPV	Feline infectious peritonitis virus
FRET	Fluorescence resonance energy transfer
GAD	Glutamate decarboxylase
GAG	Glycosaminoglycan
GFP	Green fluorescent protein
Gly	Glycine
GP	Glycoprotein
HA	Hemagglutinin
HEL	Helicase
Hela	human cervix cells
HEK	Human embryonic kidney
His	Histadine
HIV	Human immunodeficiency virus
HK	Horse kidney
HMPV	Human metapneumovirus
IEM	Immune electron microscope
IF	Immunoflourescence
IVT	*In vitro* transcription
kDa	kilodalton
LDV	Lactase dehydrogenase-elevating virus
L-M	Mouse connective tissue
LNA	Locked nucleic acid
LSECtin	Lymph node sinusoidal endothelial cell C-type lectin
M	Membrane protein
MAb	Monoclonal antibody
MDBK	Madin-Darby bovine kidney
MGB	Minor-groove binding
MHV	Murine hepatitis virus

MLV	Modified live virus
MOI	Multiplicity of infection
mRNA	Messenger RNA
MW	Molecular weight
N	Nucleocapsid protein
NA	Neurominidase
NC	Nucleocapsid
NP	Nucleoprotein
Nsp	Nonstructural protein
NTR	Nontranslated region
OIE	World Organisation for Animal Health
ORF	Open reading frame
PAM	Porcine alveolar macrophage
PCP	Papain-like cysteine protease
PCR	Polymerase chain reaction
PFU	Plaque forming unit
pp	Polyprotein
PRRS	Porcine reproductive respiratory syndrome
PRRSV	Porcine reproductive respiratory syndrome virus
qrRT-PCR	quantitative real-time reverse-transcription PCR
PSCID	Primary severe combined immunodeficiency disease
RdRp	RNA-dependent RNA polymerase
RFS	Ribosomal frameshift
RK	Rabbit kidney
RK-13	Rabbit kidney-13
rMLV	recombinant MLV
RNA	Ribonucleic acid
RT-PCR	Reverse transcription-polymerase chain reaction
rRT-PCR	Real time reverse transcription-polymerase chain reaction
rVBS	recombinant VB strain
SARS	Severe acute respiratory syndrome
SARS-CoV	Severe acute respiratory syndrome coronavirus
SDS-PAGE	Sodium dodecyl sulfate polyacrylamide gel electrophoresis
Ser	Serine
sg mRNA	Subgenomic mRNA
SHFV	Simian hemorrhagic fever virus
SNP	Single nucleotide polymorphism

SP	Serine protease
ss	Single stranded
TCF	Tissue culture fluid
TCID50	50% tissue culture infective dose
TGEV	Transmissible gastroenteritis virus
Thr	Threonine
Tm	Melting temperature
TRS	Transcription regulation sequence
UTR	Untranslated region
VB	Virulent Bucyrus
VBS	Virulent Bucyrus strain
Vero	African green monkey kidney
VI	Virus isolation
VN	Virus neutralization
VNT	Virus neutralization test
VP	Viral protein
VRP	Venezuelan equine encephalitis virus replicon particle
ZBD	Zinc-binding domain
ZF	Zinc finger

APPENDIX 2

Experimental Methods

REAL TIME RT-PCR TECHNIQUES

PRIMER AND PROBE DILUTION

Orders from Applied Biosystems (Now Lifetechnologies)

Primers:

1. Quickly spin down the primer tube to make sure that powder is on the botttom.
2. In PCR work station, add sterile nuclease-free water (store at -4C fridge in Room 440) to dissolve the powder.
3. Put the tube into the shaker for half an hour to completely dissolve primer. Aliquote primer into 40µl/epp and freeze at -20C

Primer ID	Taqman Primer mass (pmols)	µmol	Working stock solution 50 µmolar (µM) in liters (L)	Working stock solution 50 µM in ml	Resuspend the primer in nuclease-free water (µl) to get 50µM working stock
Example	*119000*	*0.119*	*0.00238*	*2.38*	*2380*
EAV 10F	10000	0.01	0.0002	0.2	200
EqFlu NP F	80000	0.08	0.0016	1.6	1600

Probes:

1. After thawing, quickly spin down the probe tube to remove drops from the inside of the lid.
2. Add stock probe into 1X TE buffer (store at -4C fridge in Room 440) in PCR hood room 446 Vortex completely.
3. Spin down. Aliquote 60µl/epp and freeze -20C Rm 440
4. Try to limit the time exposure to the light.
5. NOTE: 1× TE buffer: 1mM Tris, 0.1mM EDTA, pH 8.0)

probe ID	Original Stock Pmol	Original stock volumn (uL)	Concentration	Working stock of 10 µM	Add µl of stock solution into 1X TE (1mM Tris, 0.1mM EDTA, pH8.0) to get 10µM working stock
Example	6000	60	100 µM	1:10	540 µl
EAV 7.92P	20000	200	100 µM	1:10	1800 µl
ERAV	6000	60	100 µM	1:10	540 µl

Orders from Bioresearch Technologies

Primers and probes for swine influenza virus H1N1 subtype were obtained from Bioreseaerch Technologies.

Primers

1. See the lable on the tube, for example, if the tube has 15 nmol, 15*10=150. So add 150 ul of H2O to get 100 uM.
2. To be consistent with ABI 50 uM working stock, in such case (15 nmol primer), we need to disolve in 300 ul of H2O.

Primer ID	nmol (from lables)	Add ul of H2O to get 100 µM	To be consistent with ABI condition, add ul of H2O to get 50 µM
NH1 forward	39.23	392.3	784.6
NH1 reverse	39.83	398.3	796.6
Aliquote 400 ul each for primers			

Probes

1. Probes will be provided as 10 nmol pure powder. (This number is fixed for all the probes received, unlike primers)
2. Dissolve in 100 µl H2O or TE (preferred) to get 100 µM probe. To be consistent with ABI 10 µM working stock, the probes are actually dissolve in 1000 µl TE buffer.
3. NOTE: The TE buffer in Bioresearch Technolgies is 10 mM Tris.HCl/1mM EDTA, pH 8.0, which is different from the TE buffer used in ABI probe dilution

10 mM Tris/1mM EDTA buffer dilution				
Stock	need	dilution factors	solution	
1 M Tris pH 8.0	10 mM Tris	x100	10 ul	
0.5 M EDTA pH 8.0	1 mM EDTA	x 500	2 ul	in 988 ul H2O

Probe ID	nmol (fixed amount, powder)	Add ul of TE buffer (10 mM Tris.HCl/1mM EDTA, pH 8.0, from company flyer came with the order) to get 10 uM working stock
NH1 probe	10	1000
Aliquote 100 ul each for probes		

Orders from Operon

1. Primers and probes diluted in water as indicated in the product sheets. Here is one example.
2. To further make 50 µM working stock primers and 10 µM working stock probes, the primes and probes were further diluted 1:2 or 1:10 for primer and probes, respectively. The 50 µM primer and 10 µM probe concentrations are the same of ABI concentration.

Tube #		Seq 5' to 3'	OD	Vol.ul	nmol	ug	MW	Tm	Scale	Add x µl H2O for 100 µm
1	AHSNS1FW08	GTTGACCTCGCTC TGCTTGAC	16.8	dry	93.2	592.9	6364.2	64.5	50nmol	932
2	AHSNS1REV08	AATCGCTTCCTTC GTTGTATGAC	18.8	dry	90.8	634.1	6980.6	61	50nmol	908
3	AHSNS1Prb08	[6~FAM]TCCCAGT GGTTGATTCAAA AGTTGC[BHQ1a~6 FAM]	3.1	dry	11.5	100.8	8764.1	62.9	50nmol	115

EMD REAL-TIME PCR REAGENT KIT ASSEMBLY

1. Equine influenza virus, equine rhinitis virus and swine influenza virus H1N1 use the Taqman One-step RT-PCR reagents (Life Techonologies, 4309169). This kit contains two components: 2 × master mix (5 ml) and 40 × multiscribe reverse transcriptase and RNase inhibitor mix (250 µl).
2. Equine arteritis virus use the QuantiFast™ Probe RT-PCR kit (Qiagen, 204554). This kit contains RT-PCR master mix, ROX dye.

For equine influenza kit:

Kit Name	EMD FluDetectNP®
Catalogue Number	EMD-001
Quantity	60 reactions
Kit information	TaqMan® One-Step RT-PCR Master Mix Reagents Kit (ABI 4309169) (store at -20C freezer in RM 440) The kit contains: 2X master mix: 5 ml 40X Multiscibe reverse transcriptase and Rnase Inhibitor mix: 250 ul

Product Information	
Components	#1 EqFlu RT-PCR Master Mix (1 vial)--Need to aliquot from the ABI kit (the tube containing 2x master mix) #2 EqFlu Inhibitor Mix (1 vial)-- Need to aliquot from the ABI kit (the tube containing 40 X multriscribe reverse transcriptase and RNase Inhibitor mix) #3 EqFlu Primers and Probe Mix (1 vial)-- Need to mix primer and probes (-20ºC freezer Rack 1 boxes "Eq influenza real-time PCR probe general" and "Eq influenza real-time PCR primer general")

	#4 Nuclease Free water (1 vial) #5 EqFlu Positive Control RNA (1 vial))—in Room 423 (centrifuge room) -80C freezer, Box "EIV positive control RNA"
Recommended Use	Detection of equine influenza virus nucleic acid in nasal secretions
Features and Benefits	
Declaration	Kit components are assembled in the Molecular Virology Laboratory at the Gluck Equine Research Center

Components	**Volume per reaction (µl)**	**Volume for 70 reactions (µl)**
#1 RT-PCR Master Mix	12.5	875
#2 Inhibitor Mix	0.625	43.75
#3 Primers and Probe Mix (total 1.525 ul/rxn)	NP F Primer 0.45	31.5
	NP R Primer 0.45	31.5
	NP Probe 0.625	43.75
#4 Sterile Water	5.35	500 ul
Mix	**20**	
RNA	5	
Total Volume per reaction	**25**	

Probe setting:

Reporter Dye: FAM

Quencher Dye: None

Thermal Cycler Conditions: (Applied Biosystems 7500 Fast Real-time PCR machine, use Standard Mode)

Reverse Transcription	48°C for 30 minutes
Predenaturation	95°C for 10 minutes
40 Cycles	
Denaturation	95°C for 15 seconds
	60°C for 1 minute

For swine influenza H1N1 kit:

Kit Name	EMD SwineFlu H1N1
Catalogue Number	EMD-003
Quantity	60 reactions

Product Information	
Components	#1 RT-PCR Master Mix (1 vial, 750 µl) #2 Inhibitor Mix (1 vial, 37.5 µl) #3 Primers and Probe Mix (1 vial, 91.5 µl) #4 Nuclease Free water (1 vial, 500 µl) #5 Control RNA (1 vial, 20 µl, Ct ≈20)
Recommended Use	Detection of swine influenza virus H1N1 (2009) virus
Features and Benefits	Rapid detection of swine influenza virus nucleic acid in clinical specimens
Declaration	Kit components are assembled in the Molecular Virology Laboratory at the Gluck Equine Research Center

Shipping and Storage Information	
Storage	With the exception of control RNA (component #5), save all other components at -20°C (do not use a frost free freezer). Component # 5 should be stored at -80°C.
Expiration Date	One year from the date of shipment
Shipping	Shipped on dry ice

Components	**Volume per reaction (µl)**	**Volume for 60 reactions (µl)**
#1 RT-PCR Master Mix	12.5	750
#2 Inhibitor Mix	0.625	37.5
#3 Primers and Probe Mix (total 1.525 µl/reaction)	NH1 Forward 0.45	27
	NH1 Reverse 0.45	27
	NH1 Probe 0.625	37.5
#4 Sterile Water	5.35	321
Mix	**20**	**1200**
RNA	5	
Total Volume per Reaction	**25**	

Probe setting:

Reporter Dye: FAM

Quencher Dye: None

Thermal Cycler Conditions: (Applied Biosystems 7500 Fast Real-time PCR machine, use Standard Mode)

Reverse Transcription	48°C for 30 minutes
Predenaturation	95°C for 10 minutes
40 Cycles	
Denaturation	95°C for 15 seconds
	60°C for 1 minute

For equine arteritis virus kit:

Kit Name	EMD EAVDetectN®
Catalogue Number	EMD-002
Quantity	60 reactions
Kit information	QuantiFast™ Probe RT-PCR Kit (QIAGEN,204554) (store at -20C freezer in RM 440)

Product Information	
Components	#1 EAV RT-PCR Master Mix (1 vial)—Need to aliquot from the QIAGEN kit #2 Primers Probes and ROX Mix (1 vial)—Need to mix primer probes (-20C freezer at RM 440, Rack 1 boxes named as "EAV primer 50 uM real-time PCR" and "Real-time probe stock 10 uM" and ROX dye (from the QIAGEN kit) #3 Nuclease Free water (1 vial) #4 Control RNA (1 vial)—in Room 423 (centrifuge room) -80C freezer, Box "EAV positive control RNA"
Recommended Use	Detection of equine arteritis virus nucleic acid in semen and tissue culture fluid
Declaration	Kit components are assembled in the Molecular Virology Laboratory at the Gluck Equine Research Center

Components	**Volume per reaction (µl)**	**Volume for 62 reactions (µl)**
#1 RT-PCR Master Mix	12.75	790.5
#2 Primers Probe and ROX Mix (total 1.8 ul/rxn)	7.53 F Primer 0.4 x60 = 24	24.8
	7.256 R Primer 0.4*60=24	24.8
	7.92 Probe 0. 5*60=30	31
	50x ROX Dye 0.5*60=30	31
#3 Sterile Water	5.45	500 ul
Mix	**20**	
RNA	5	
Total Volume per Reaction	**25**	

Probe setting:

Reporter Dye: FAM

Quencher Dye: TAMRA

Thermal Cycler Conditions: (Applied Biosystems 7500 Fast Real-time PCR machine, use Standard Mode)

Reverse Transcription 48°C for 30 minutes

Predenaturation 95°C for 10 minutes

40 Cycles

Denaturation 95°C for 15 seconds

60°C for 1 minute

For canine influenza virus mix:

Reagent	Working Stock Concen	Volume per Reaction(µl)	Final Concentration	# n reactions
2X Master Mix without UNG	2X	12.5	1X	**12.5 x n**
40X MultiScribe and RNase Inhibitor Mix	40X	0.625	0.25U/µl 0.4U/µl	**0.625 x n**
EqFlu NP F	50 µM	0.45	900nM	**0.45 x n**
EqFlu NP R	50 µM	0.45	900nM	**0.45 x n**
EqFlu NP MGB Probe	10 µM	0.625	250 nM	**0.625 x n**
Sterile Water		5.35		**5.35 x n**
MASTER PREMIX		**20**		**20 x n**
RNA		5		
Total		**25**		

Probe setting:

Reporter Dye: FAM

Quencher Dye: None

Thermal Cycler Conditions: (Applied Biosystems 7500 Fast Real-time PCR machine, use Standard Mode)

Reverse Transcription 48°C for 30 minutes

Predenaturation 95°C for 10 minutes

40 Cycles

Denaturation	95°C for 15 seconds
	60°C for 1 minute

HOTSTART PCR TO AMPLIFY GENE FROM PLASMID FOR PCR CLONING

Components	**Volume (ul)**	**# of Reactions**		
10x PCR Buffer (with 15 mM MgCl2)	5.0	5	25	
25 mM MgCl2 (to get final conc. 2.5 mM)	2.0	5	10	
dNTP Mix (10 mM of each dNTP)	1.0	5	5	
QIAGEN HotStart DNA Polymerase	0.3	5	1.25	
RNase free water	38.3	5	191.25	
Master Mix Volume (ul) ***Aliquot 46.5 ul into reaction tubes***	**46.5**		**232.5**	
Master Mix Per Reaction (ul)	46.5			
Primer 1	0.5	EAV 12069P (12069-12088)		upstream of ORF7
Primer 2	0.5	EAV 12750N (12729-12750)		downstream ORF7
Template DNA (ul)	2.5			
Total Volume (ul)	**50.0**			

Tube #	**EHV**	**Primer pair**	**Volumn (ul)**	**Size (bp)**
EAV 1	DNA plasmid pEAV2421/211 (from JQ, store in -20C freezer Rm416)	1	1	681
2		2	1	681
3	"Zhengchun cDNA box"	3	1	681
4		4	1	681

Thermal Cycler Conditions:		
Initial activation step	95C/15 min.	
3-step cycling (35 cycles)		
Denaturation	94C/30 sec.	
Annealing	gradient T/30 sec.	#1 43.1C #2 45C #3 48.4C #4 49.9C
Extension	72C/1 min.	
Final extension	72C/ 10 min.	

The PCR product will be used for ligation in pDrive cloning vector to calculate IVT RNA molecule numbers.

pDRIVE VECTOR CLONING FOR IVT RNA MOLECULE CALCULATION (Qiagen PCR cloning kit, 231122)

Important notes before starting

• Use of PCR products generated with proofreading DNA polymerases (i.e., DNA polymerases with 3'-5' exonuclease activity) will dramatically lower ligation efficiency as these PCR products do not have an A overhang.

• We recommend using a molar ratio of 5–10 times more PCR product DNA than pDrive Cloning Vector DNA for ligation (Table 2). However, less PCR product may also be sufficient. PCR products can be concentrated using MinElute™ Kits.

• Purification of PCR products prior to ligation (e.g., using QIAquick® or MinElute PCR

Purification or Gel Extraction Kits) is optional but recommended, as this will generally result in higher transformation efficiency. See "Purification of PCR products" (Appendix, page 23).

• The 5'-terminal base of the PCR primers can affect addition of an A overhang to PCR products by non-proofreading DNA polymerases. See "Effect of the 5'-terminal base of PCR products on cloning efficiency" (Appendix, page 21).

• Background colonies may appear following transformation if the PCR template was plasmid DNA containing a resistance gene for the antibiotic used for colony selection (i.e., an ampicillin- or kanamycin-resistance gene). In these cases the PCR product should be gel-purified prior to ligation to remove template plasmid DNA. Gel-purification can be avoided by using kanamycin for selection if the template plasmid contains the ampicillin-resistance gene, and vice versa.

• If **electrocompetent** cells will be used instead of QIAGEN EZ Competent Cells for transformation, we strongly recommend inactivating the ligase prior to electroporation by incubating the ligation-reaction mixture for 10 min at 70°C (see protocol step 4).

Table 2. Guide for the amount of PCR product to use in the ligation reaction

	Amount of PCR product to use in the ligation reaction	
PCR product size	**5-times molar excess***	**10-times molar excess***
100 bp	6.5 ng	13 ng
200 bp	13 ng	26 ng
500 bp	32.5 ng	65 ng
1000 bp	65 ng	130 ng
1500 bp	97.5 ng	195 ng
2000 bp	130 ng	260 ng
3000 bp	195 ng	390 ng

** Calculated for 50 ng pDrive Cloning Vector using the following equation:*

ng PCR product required = 50 ng x PCR product size (bp) x molar ratio

3851 bp

Procedure

1. Thaw 2x Ligation Master Mix, pDrive Cloning Vector DNA, and distilled water (provided). Place on ice after thawing.

It is important to mix the solutions completely before use to avoid localized concentrations of salts. Keep 2x Ligation Master Mix on ice and immediately store at –20°C or –70°C after use.

2. Prepare a ligation-reaction mixture according to the following scheme:

Component	**Volume/reaction**
pDrive Cloning Vector (50 ng/µl)	1 µl
PCR product	1–4 µl*
Distilled water	variable
Ligation Master Mix, 2x†	5 µl
Total volume	**10 µl**

** Purified PCR product. If using non-purified PCR product, do not add more than 2 µl PCR product.*

† We recommend adding the Ligation Master Mix last.

3. Briefly mix the ligation-reaction mixture then incubate for 30 min at 4–16°C (e.g., in a refrigerator, water bath, or thermal cycling block).

Mix gently, for example by pipetting the ligation-reaction mixture up and down a few times.

Note: Increasing the ligation time to 2 h can result in a 2–3 fold increase of recombinants.

This might be especially useful for PCR fragments longer than 2 kb. If the total number of recombinants is not essential, however, the ligation time can be as short as 15 min.

4. Proceed with the transformation protocol (page 14) or store ligation-reaction mixture at –20°C until use.

IMPORTANT: The transformation protocol on page 14 is for use with QIAGEN EZ Competent Cells. If **electrocompetent** cells will be used, we **strongly recommend** inactivating the ligase in the ligation-reaction mixture prior to electroporation.

Incubate the ligation-reaction mixture for 10 min at 70°C, then proceed with electroporation. Alternatively, the MinElute Reaction Cleanup Kit can be used to remove ligase from the ligation-reaction mixture. The ligase does not need to be inactivated when using QIAGEN EZ Competent Cells.

QIAGEN PCR Cloning*plus* Kit Transformation Protocol

Important notes before starting

• This protocol is for use with QIAGEN EZ Competent Cells. It is not for use with

electrocompetent cells. If electrocompetent cells will be used, we **strongly recommend** inactivating the ligase in the ligation-reaction mixture prior to electroporation. See step 4 of the ligation protocol (page 13) for details.

• Competent cells are extremely sensitive to temperature and mechanical stress. **Do not allow QIAGEN EZ Competent Cells to thaw at any point prior to transformation.** Keep thawed cells on ice. Avoid excessive and/or rough handling, especially pipetting. Mix cells by **gentle** flicking.

• Thaw SOC medium and warm to room temperature. Store at –20°C or –70°C after use.

• Prepare fresh LB agar plates containing either ampicillin (100 µg/ml LB agar) or kanamycin (30 µg/ml LB agar) as a selection marker. Include IPTG (50 µM) and X-gal (80 µg/ml) for blue/white screening of recombinant colonies. See Appendix (page 27) for recipes.

Procedure

1. Thaw the appropriate number of tubes of QIAGEN EZ Competent Cells on ice. Thaw SOC medium and warm to room temperature.

IMPORTANT: Competent cells should only be thawed on ice. Do not allow unused

QIAGEN EZ Competent Cells to thaw. Test whether cells are thawed by gently flicking the tube. Proceed immediately to the transformation step once the cells have thawed.

2. Add 1–2 µl ligation-reaction mixture per tube of QIAGEN EZ Competent Cells, mix gently, and incubate on ice for 5 min.

Mix gently, for example by flicking the transformation mixture a few times.

3. Heat the tube(s) in a 42°C water bath or heating block for 30 s without shaking.

4. Incubate the tube(s) on ice for 2 min.

5. Add 250 µl room temperature SOC medium per tube and directly plate 100 µl each transformation mixture onto LB agar plates containing ampicillin.

Note: For **kanamycin** selection, incubate the cells at 37°C for 30 min with shaking prior to plating to allow recombinant outgrowth.

The transformation mixture can be plated using a sterile bent glass rod or a specialized spreader. It is generally recommended to plate different amounts of each transformation mixture onto separate plates (e.g. 100 µl and 20 µl) to ensure good separation of colonies for subsequent single-colony isolation. For more efficient plating of small volumes of transformation mixture (<50 µl) we recommend pipetting 100 µl LB medium onto the plate, and then pipetting the transformation mixture into the liquid LB.

6. Incubate the plate at room temperature until the transformation mixture has absorbed into the agar. Invert the plate and incubate at 37°C overnight (e.g., 15–18 h).

Note: For blue/white screening, we recommend a second incubation at 4°C (e.g. in a refrigerator) for a few hours. This "cold" incubation step enhances blue color development and thereby facilitates differentiation between blue colonies and white colonies.

GENERATION RECOMBINANT VIRUS FROM *IN VITRO* TRANSCRIBED RNA

A. PURIFICATION OF LINEARIZED PLASMID

1. Linearization of plasmid EAV infectious cDNA clone. Digestion of each plasmid DNA with *Xho I* to linearize the plasmid DNA.

Plasmid DNA	35.0 µl
Xho I (40U/µl, Roche)	1.0 µl

Buffer H (10x) (Roche)	4.0 µl
Total:	40.0 µl

Prepare 1 digestion reaction for each plasmid DNA. Incubate at 37°C for 2 hours.

2. Run 1 µl digested plasmid DNA on 1% agarose gel to make sure that the plasmid DNA is linearized.

Digested plasmid DNA	1.0 µl
6x loading buffer	2.0 µl
nuclease free water	9.0 µl
Total:	12.0 µl---------loading amount per well

Run 12 µl 1 kb DNA ladder (Invitrogen)

3. Add 2 µl of 20 mg/ml Proteinase K (Ambion) and bring the volume to 200 µl with nuclease free water and incubate at 37°C for 30 min.

4. 2× phenol chloroform extract and precipitate the DNA with 100% ethanol.
   - add 200 µl of phenol : chloroform : isoamyl alcohol (25:24:1) (Cat # P3803, Sigma) and mix until an emulsion is formed
   - centrifuge at 13,000 rpm for 4 min at room temperature
   - remove 180 µl of the upper aqueous phase into a new tube
   - add 180 µl of phenol : chloroform : isoamyl alcohol (25:24:1) and repeat the extraction
   - remove 160 µl of the upper aqueous phase into a new tube
   - add 500 µl of 100% ethanol and 16 µl of 3M sodium acetate to the DNA sample
   - mix and centrifuge at 13,000 rpm for 10 min

5. Wash with 140 µl of 70% ethanol. Spin at 13,000 rpm for 4 min. Aspirate the 70% ethanol and dry on the bench for 4-5 min.

6. Resuspend the pellet in 32 µl of nuclease free water and run 1 µl on gel.

Phenol chloroform extracted linearized plasmid DNA	1.0 µl
6x loading buffer	2.0 µl
nuclease free water	9.0 µl
Total	12.0 µl---------loading amount per well

B. *IN VITRO* TRANSCRIPTION

1. Prepare *in vitro* transcription reactions as follows. For linear DNA, rNTPs, BSA, DTT, 5 x transcription buffers, and cap analog, thaw them out at room temperature. Mix well before use. Always leave RNA guard RNase inhibitor and T7 RNA polymerase on ice. Use XhoI-linearized and phenol-chloroform purified plasmid DNA

***Master mix for in vitro* transcription**

Linear DNA	15.0 µl
rNTPs mix (10mM each)	5.0 µl
BSA (1mg/ml)	5.0 µl
100 mM DTT	2.5 µl
5X T7 Transcription buffer	10.0 µl
Cap analog (10mM)	5.0 µl
RNA guard RNase Inhibitor	2.5 µl
T7 RNA polymerase	2.5 µl
Nuclease free water	2.5 µl
	50.0 µl

Incubate at 37ºC for 2 hours.

2. Wash electrophoresis unit (electrophoresis tank, gel cast and running trays, comb) thoroughly with detergent. Then rinse thoroughly with dH_2O. Spray electrophoresis unit with RNaseZap, then rinse thoroughly with dH_2O. Let it air dry.
3. Prepare 1x TAE buffer. Cast 0.8% agarose gel.
4. After 1 h of *in vitro* transcription at 37ºC, run 2 µl of *in vitro* transcribed RNA on a 0.8% agarose gel.

TE Buffer (pH=7.2)	8.0 µl
10%SDS	1.0 µl
0.5M EDTA (pH=8.0)	0.25 µl
RNA	2.0 µl

- place mix at 70ºC for 2 minutes and then place on ice for 2 minutes
- add 2.25 µl of 6X gel loading buffer
- load 13.5 µl mixtures to each well of the gel. Run the gel at 90V.

5. Check the gel under UV light.
6. Measure RNA concentration with spectrophotometry.
7. Dilute 2 µl *in vitro* transcribed RNA into 198 µl nuclease-free water and measure A260. Use nuclease-free water as blank control.

IVT RNA MOLECULE CALCULATIONS

- Template: IVT RNA pDriveClone/NY/73/NVSL M product (5.1; 12-28-7, aliquot 1)
  438.4 ug/ml ≈ 430 ng/ul (12-28-7)

  Size: 4359 bp

  Eq pDrive-Flu/NY/73/NVSL M RNA molecular weight = 1402612.8g = 1.4026×10^6g

  (1161A*329.2 + 1017C*305.2+ 1078G*345.2+ 1103U*306.2+159 (for 5' triphosphate))

- Avogadro-number is 6.022×10^{23}
- Y (No of molecules per ul) = (Avogadro x concentration g/ul)/ molecular weight
  $= (6.022 \times 10^{23} \times 430 \times 10^{-9}$ g/ul)/ 1.4026×10^6g

  $= \underline{\mathbf{1.846 \times 10^{11}\ molecules/ul}} \approx \underline{\mathbf{1.0 \times 10^{11}\ molecules/ul}}$

Copy # (within the 5ul to RT-PCR)		Stock concentration of IVT RNA (molecules/µl)
10^{10}		5×10^{10}
10^9		5×10^9
10^8		5×10^8
10^7	*** 5 µL**	5×10^7
10^6		5×10^6
10^5		5×10^5
10^4		5×10^4
10^3		5×10^3
10^2		5×10^2
10^1		5×10^1

- Serial dilution:
- **Prepare dilution buffer [44ul H2O+5ul 1mg/ml acetylated BSA (promega) +1ul RNase guard (pharmacia)] to stabilize RNA:**
- **880ul H2O + 100ul 1mg/ml BSA + 20 ul RNase guard=1000 ul stabilization buffer**
  (calculation based on IVT RNA and EAV one-step RT-PCR protocol)

10^{10} copies: 2 ul of IVT RNA pDriveClone/NY/73/NVSL M product stock 1**.0 x 10^{11} molecules/ul** into 98 ul RNA STABILIZATIONBUFFER

final concentration is 1.0*100*2/100= 2x 10^{9} molecules/ul

take 5ul out of 2x 10^{9} molecules/ul into real time PCR well to get 10^{10} copies

10^{9} copies: 10ul of 10^{10} copies stock+ 90 ul RNA STABILIZATIONBUFFER

final concentration is 10*2x 10^{9}/100= 2x 10^{8} molecules/ul

take 5ul out of 2x 10^{8} molecules/ul into real time PCR well to get 10^{9} copies

10^{8} copies: 10ul of 10^{9} copies stock+ 90 ul RNA STABILIZATIONBUFFER

final concentration is 10*2x 10^{8}/100= 2x 10^{7} molecules/ul

take 5ul out of 2x 10^{7} molecules/ul into real time PCR well to get 10^{8} copies

10^{7} copies: 10ul of 10^{8} copies stock+ 90 ul RNA STABILIZATIONBUFFER

final concentration is 10*2x 10^{7}/100= 2x 10^{6} molecules/ul

take 5ul out of 2x 10^{6} molecules/ul into real time PCR well to get 10^{7} copies

10^{6} copies: 10ul of 10^{7} copies stock+ 90 ul RNA STABILIZATIONBUFFER

final concentration is 10*2x 10^{6}/100= 2x 10^{5} molecules/ul

take 5ul out of 2x 10^{5} molecules/ul into real time PCR well to get 10^{6} copies

10^{5} copies: 10ul of 10^{6} copies stock+ 90 ul RNA STABILIZATIONBUFFER

final concentration is 10*2x 10^{5}/100= 2x 10^{4} molecules/ul

take 5ul out of 2x 10^{4} molecules/ul into real time PCR well to get 10^{5} copies

10^{4} copies: 10ul of 10^{5} copies stock+ 90 ul RNA STABILIZATIONBUFFER

final concentration is 10*2x 10^{4}/100= 2x 10^{3} molecules/ul

take 5ul out of 2x 10^{3} molecules/ul into real time PCR well to get 10^{4} copies

10^{3} copies: 10ul of 10^{4} copies stock+ 90 ul RNA STABILIZATIONBUFFER

final concentration is 10*2x 10^{3}/100= 2x 10^{2} molecules/ul

take 5ul out of 2x 10^{2} molecules/ul into real time PCR well to get 10^{3} copies

10^{2} copies: 10ul of 10^{3} copies stock+ 90 ul RNA STABILIZATIONBUFFER

final concentration is 10*2x 10^{2}/100= 2x 10^{1} molecules/ul

take 5ul out of 2x 10^{1} molecules/ul into real time PCR well to get 10^{2} copies

10^{1} copies: 10ul of 10^{2} copies stock+ 90 ul RNA STABILIZATIONBUFFER

final concentration is 10*2x 10^{1}/100= 2x 10^{0} molecules/ul

take 5ul out of 2x 10^{0} molecules/ul into real time PCR well to get 10^{1} copies

TRANSFECTION OF BHK21 CELLS WITH ELECTROPORATION

Preparation of cells

1. Make sure to use cells that are not confluent. Typically a flask of BHK21 cells were split 1:4 two days before planning to do the electroporation. One T-150 cm^2 flask of BHK21 cells will be used for 2 electroporations.

2. Aspirate the medium from T-150 flasks of subconfluent BHK21 (P67) cells. Wash cells twice with PBS. Add 4 ml ATV to each T-150 flask. Shake for 30 sec. Let it sit at room temperature for 1 min. Then remove the ATV and put the flasks at 37ºC for a few minutes.
3. After cells slough off, add 10 ml EMEM to each T-150 flask.
4. Use a pipet with a wide bore to transfer cells to 50 ml conical centrifuge tube. **Place immediately on ice.**
5. Spin cells at 4ºC, 600 rpm for 5min. Place cells back on ice.
6. Remove medium and add 25 ml sterile ice cold PBS. Resuspend cell pellet by gentle shaking of tube. If you need to use a pipet to resuspend cells, use a wide bore pipet and pipet gently.
7. Spin cells at 4ºC, 600 rpm for 5min. Place cells back on ice.
8. Remove media and wash cells by the addition of 25 ml sterile ice cold PBS. At this time take a small sample of cells for counting with a hemocytometer.
9. Spin cells at 4ºC, 600 rpm for 5min. Place cells back on ice.
10. Remove PBS with a pipet and resuspend cell pellet in ice cold PBS to a final concentration of 1 x 10^7 cells/ml.

Electroporation of cells

1. Place 25 µl of freshly thawed *in vitro* transcribed into each microcentrifuge tube. Set up one tube without RNA as negative control.
2. Add 500 µl of BHK21 cells (5×10^6 cells) into microcentrifuge tube containing *in vitro* transcribed RNA and mix gently.
3. Transfer RNA-cells mixture into each electroporation cuvette (0.4 cm electrode gap). Place the cuvette into the cuvette holder and pulse cells twice. The following settings are used: 850 volts, capacitance set at 25 µF, and the pulse controller set at infinite ohms. When doing pulses, push the two buttons together until you hear the beep, then immediately push them again until you hear the second beep.
4. After electroporation is complete, set cells aside (room temperature) for a 10 min 'recovery period'.
5. Do the next sample.
6. After the recovery period is complete, transfer the cells from the cuvette into 15 ml of room temperature growth medium (EMEM) in a T-75 flask. Aliquot 0.15 ml of cells to each well of 8-well chamber slides for immunofluorescence assay (2 wells-mock transfected and 2 wells transfected).
7. Place cells at 37ºC CO_2 incubator. Check the development of CPE. When CPE is complete (usually 72-96 h post transfection), tissue culture fluids were harvested and centrifuged at 1900 rpm for 10 min at 4ºC. The tissue culture fluids were titrated in RK13 cells.

ELECTROPORATION USING BTXPRESS ELECTROPORATOR AND ELECTROPORATION SOLUTION

Method

A. PREPARE THE CELLS

Divide the cells 18-24 hours prior to electroporation as needed and culture overnight.

B. PREPARE FOR ELECTROPORATION

1. Warm all solutions to RT before use.
2. Harvest cells for electroporation, and count cells to determine cells/ml.

3. Determine the total volume needed for all the electroporations. Multiply the number of electroporations needed by 0.1 ml (for 0.2 cm cuvettes) OR by 0.25 ml (for 0.4 cm cuvettes) and add 10% more for pipetting errors. Total volume needed= _____ ml.
4. Determine the volume of cells required for each electroporation according to the formula:

5. Volume needed (ml) = (#cells needed/ml [5 x 10^6 cells/ml]/# counted cells/ml) × Total volume of BTXpress Solution from step C

6. Enter the calculated volume needed = _____ml
7. Pipette the volume of cells determined in step d into a new tube and centrifuge at 1000 ×g for 5 minutes. Aspirate the supernatant.
8. Prepare a culture vessel with pre-warmed complete medium.
9. Immediately transfer to 60mm petri dish (21 cm^2 surface area) containing growth medium. (Each well of 6 well-plate is 10 cm^2)→ I decide to put everything in 6 well plate with 4 ml growth medium. Then take 500 ul into chamber slides for IFA.
10. Resuspend the centrifuged cells from step e in ____ ml BTXpress Solution according to the volume determined in step c.

C. Add _____ µl IVT RNA (use 20 µg/ml of cells= 5 µg) to the cells. Mix gently.
   i) pEAV-GFP IVT RNA (total 49 µl RNA)
   ii) mock infection

   b) Aliquot 100 µl (0.25 cm cuvette) or 250 ul (0.4 cm cuvette) DNA/cell mix to each cuvette.
   c) Eletroporate at RT. Using a square wave system set the voltage and pulse length given for your cells as described in Table1. If using an exponential decay set the capacitance to 950 µF and resistance to "None". Use the voltage given for your cells from Table 1&2 for complete protocol. Voltage=____260 V____

D. Electroporation settings:

Choose Mode:	**T**	500 V/Capacitance & Resistance (LV)
Capacitance:	**C**	950□F
Set Resistance:	**R**	R1 (13ohm)
Chamber Gap: BTX Disposable Cuvette P/N 640 (4mm gap)		
Set Charging Voltage:	**S**	260V
Desired Field Strength:	**E**	650 V/cm
Desired Pulse Length:	**t**	Approximately 9 msec (Reality: 10 msec)

   a) Immediately mix the cells gently and transfer to the dish prepared in step B-f.
   b) Incubate in complete medium for 12-72 hours or as required.
   c) Harvest cells and perform assay as required.

MAMMALIAN CELL TRANSFECTION USING LIPID-BASED TRANSFECTION REAGENT

Materials

1. Lipofectamine™ 2000 (Invitrogen, Cat# 11668-027)
2. Fugene HD (Roche, Cat# E2311)

Method

1. Place sterile glass cover slips onto wells to be used for IFA staining.
2. Trypsinize T-75 flask of Vero 76 (ATCC #CRL-1587) cells and count the cells (One confluent T-75 contains approx. 1×10^7 Vero cells).
3. One day before transfection, plate 2×10^5 cells/well in 500 µl of growth medium so that cells will be 90-95% confluent at the time of transfection.

4. For each transfection sample, prepare complexes as follows:
   a. Dilute 0.8 µg of plasmid DNA in 50 µl of Opti-MEM I. Mix gently.
   b. Mix Lipofectamine™ 2000 gently before use, then dilute 2.0 µl of Lipofectamine in 50 µl of Opti-MEM I medium. Incubate for 5 min at RT.
   c. After the 5 min incubation, combine the diluted DNA with diluted Lipofectamine™ 2000 (total volume = 100 µl). Mix gently and incubate for 20 min at RT.
5. Add the 100 µl of transfection mix to each well containing cells and medium. Mix gently by rocking the plate back and forth.
6. Incubate cells at 37°C in a CO2 incubator for 4 hr.

   After incubation for 4 hr with the transfection mix, replace the mix with 500 µl of growth media (containing FBS). Incubate at 37°C for 18-48 hours prior to testing for transgene expression.

SITE-DIRECTED MUTAGENESIS

PRIMER DILUTION

Primers are diluted in water to get 1 µg/µl working stock.

1. Prepare sample reactions as indicated below:

Vector: make 150 ng/ul stock. In Tube 1, use 150 ng in the reaction. In tube 2, JQ said just use 1ul (220 ng) should be fine.

Primer: 100 ng/ul (more strict)

		Tube 1	Tube 2
Components	pEAVrMLVB-NotI (TEMPLATE)	pVR21-2A R52G	pEAV2421 (full length VBS strain) R52G
10× reaction buffer	5 µl	5 µl	5 µl
Plasmid template	pEAVrMLVB-1 14553 bp (150 ng/µl) 1.0 µl	pVR21-2A 10130 bp (97 ng/µl) 1.5 µl	pEAV2421 (12-25-05 from JQ) 12704 bp (220 ng/ul) 1.0 µl
Primer 1	Primer EAVinsNotI11431P 1.25 µl (125 ng)	Primer C7715g 1.25 µl (125 ng)	Primer C7715g 1.25 µl (125 ng)
Primer 2	Primer EAVinsNotI11431N 1.25 µl (125 ng)	Primer C7715g_antisense 1.25 µl (125 ng)	Primer C7715g_antisense 1.25 µl (125 ng)
dNTP mix	1 µl	1 µl	1 µl
QuikSolution	3 µl	3 µl	3 µl
dH_2O	36.5 µl	36 µl	36.5 µl
PfuUltra HF DNA polymerase (2.5 U/µl)	1 µl	1 µl	1 µl

2. Perform cycling.

Segment	Cycles	Temperature	Time (Tube 1)	Time (Tube 2)
1	1	95°C	1 minute	1 minute
2	18	95°C	50 seconds	50 seconds
		60°C	50 seconds	50 seconds
		68°C	11 minute (1min/kb of plasmid length)	13 minute (1min/kb of plasmid length)
3	1	68°C	7 minute	7 minute

3. Following temperature cycling, place the reaction on ice for 2 minutes to cool the reaction to ≤37 °C.
4. Add 1 µl of the Dpn I restriction enzyme (10 U/µl) directly to each amplification reaction.
5. Gently and thoroughly mix each reaction mixture by pipetting the solution up and down several times. Spin down the reaction mixtures in a microcentrifuge for 1 minute and immediately incubate each reaction at 37C for 1.5 hours to digest the parental (i.e. the nonmutated supercoiled dsDNA).
6. Gently thaw the XL10-Gold ultracompetent cells on ice. For each control and sample reaction to be transformed, aliquot 45 µl of the ultracompetent cells to a prechilled 14-ml BD Falcon polypropylene round-bottom tube. (In my case, not necessary to use control reaction)
7. Add 2 µl of the β-ME mix provided with the kit to the 45 µl of cells.
8. Swirl the contents of the tube gently. Incubate the cells on ice for 10 minutes, swirling gently every 2 minutes.
9. Transfer 2 µl of the Dpn I-treated pVR21-2A R52G reaction mixture to separate aliquots of the supercompetent cells. Swirl the transformation reactions gently to mix and incubate the reaction on ice for 30 minutes.
10. Heat pulse the transformation reactions for **30 seconds at 42C** water bath and then place the reactions on ice for 2 minutes. (The duration of the heat pulse is critical for obtaining the highest efficiencies. Do not exceed 42C).
11. Add 0.5 ml of SOC medium preheated to 42C and incubate the transformation reactions at 37C for 1 hour with shaking at 225-250 rpm.
12. Plate 250 µl of sample reaction on each of two agar plates containing ampicillin.
13. Incubate the transformation plates at 37C for > 16 hours.

CONVENTIONAL ONE-STEP RT-PCR ASSAYS

This assay can be used to detect EIV, EAV, ERAV and ERBV.

Eq Influenza virus QIAGEN OneStep RT-PCR

Components	**Volume (ul)**	**# of Reactions**	
RNase free water	14.0	34	476
5x QIAGEN OneStep RT-PCR Buffer	5.0	34	170
dNTP Mix (10 mM of each dNTP)	1.0	34	34
QIAGEN OneStep RT-PCR Ezyme Mix	1.0	34	34
RNase Inhibitor (RNA Guard; Pharmacia)	0.5	34	17
Master Mix Volume (ul)	**21.5**		**731**

Aliquot 43.0 ul into reaction tubes

Master Mix Per Reaction (ul)	21.5
Primer pair MIX (1 ul of each)	1.0
Template RNA (ul)	2.5
Total Volume (ul)	**25.0**

Thermal Cycler Conditions:

Reverse transcription	50C/30 min.
Initial PCR activation	95C/15 min.
3-step cycling (40 cycles)	
Denaturation	94C/30 sec.
Annealing	50C/30 sec.
Extension	72C/1 min.
Final extension	72C/ 10 min.

CONVENTIONAL PCR ASSAYS

Herpes Virus DNA QIAGEN HotStar Taq PCR (Adenovirus primers)

Components	Volume (ul)	# of Reactions	
10x PCR Buffer (with 15 mM MgCl2)	5.0	5	25
25 mM MgCl2 (to get final conc. 2.5 mM)	2.0	5	10
dNTP Mix (10 mM of each dNTP)	1.0	5	5
QIAGEN HotStart DNA Polymerase	0.3	5	1.25
RNase free water	38.3	5	191.25
Master Mix Volume (ul)	**46.5**		**232.5**

Aliquot 46.5 ul into reaction tubes

Master Mix Per Reaction (ul)	46.5
Primer 1	0.5
Primer 2	0.5
Template DNA (ul)	2.5
Total Volume (ul)	**50.0**

Tube #	Template	Primer pair
1	Equine Adenovirus 1 NVSL	EAdV1 990P+1286N
2	(extract on 8-22-6 ZC) 001 EDV 9401 EAD EEK EEC P1	EAdV2 3948P+4516N

Thermal Cycler Conditions:

Initial activation step	95C/15 min.
3-step cycling (35 cycles)	
Denaturation	94C/30 sec.

Annealing	60C/30 sec.
Extension	72C/1 min.
Final extension	72C/ 10 min.

TISSUE CULTURE MEDIA RECIPES

EPAEC (EQUINE PULMONARY ARTERY ENDOTHELIAL CELLS):

DMEM (with high glucose [4.5 g/L], without L-glutamine; Cellgro 15-013-CM)	1L
Fetal bovine serum (FBS, 10%; Hyclone SH30396.03)	110mL
Penicillin and streptomycin (10,000 U/ml and µg/ml; Gibco 15140-122)	11mL
0.1 mM Non-essential amino acids (10 mM [100X] Gibco 11140-050)	11mL
2 mM L-glutamine (200 mM [100X] Gibco 25030)	10 mL

HEK293T (HUMAN EMBRYONIC KIDNEY 293T CELLS):

DMEM (with high glucose [4.5 g/L], without L-glutamine; Cellgro 15-013-CM)	500 mL
Fetal bovine serum (FBS, 10%; Hyclone SH30396.03)	50 mL
Penicillin and streptomycin (10,000 U/ml and µg/ml; Gibco 15140-122)	5 mL
200 mM L-glutamine (200 mM [100X] Gibco 25030)	5 mL

A594 (HUMAN ALVEOLAR BASAL EPITHELIAL CELLS: ATCC CAT. # CCL-185):

F-12 Kaighn's modification (Hyclone SH30526.01)	500 mL
Fetal bovine serum (FBS, 10%; Hyclone SH30396.03)	50 mL
Penicillin and streptomycin (10,000 U/ml and µg/ml; Gibco 15140-122)	5 mL

PBMC (PERIPHERAL BLOOD MONONUCLEAR CELLS):

RPMI 1640 (without L-glutamine; Gibco 21870)	500 ml
Fetal bovine serum (FBS, 10%; Hyclone SH30396.03)	50 mL
Penicillin and streptomycin (10,000 U/ml and µg/ml; Gibco 15140-122)	5 mL
200 mM L-glutamine (200 mM [100X] Gibco 25030)	5 mL
55 µM 2-mercaptoethanol (55 mM [1000X]; Gibco 21985-023)	0.5 ml

RABBIT KIDNEY 13 HIGH PASSAGE AND LOW PASSAGE (P207) FROM BILL MCCOLLUM, UKY:

Laboratory Designated Name: RK-13 HP# (High passage), RK-13 LP# (Low passage)

EMEM (With Earle's salts and L-glutamine; GIBCO 11095-080	500 ml
Cosmic calf serum 10% (Hyclone SH30087.03)	50 ml
Penicillin and Streptomycin (GIBCO 15140-122)	5 ml

RABBIT KIDNEY 13 (ATCC CATALOG NO. CCL-37):

Laboratory Designated Name: CCL-37-RK13

Minimum Essential Medium (EMEM;	
With Earle's salts and L-glutamine; GIBCO 11095-080	500 ml
Fetal Bovine Serum 10% (Hyclone SH30396.03)	50 ml
Penicillin and Streptomycin (GIBCO 15140-122)	5 ml
1.0 mM Sodium pyruvate (100 mM [100x] GIBCO 11360-070)	5 ml
0.1 mM Nonessential amino acids (10 mM [100x] GIBCO 11140-050)	5 ml

RABBIT KIDNEY 1 (ATCC CATALOG NO. CCL-106):

Laboratory Designated Name: LLC-RK1

Medium 199 (GIBCO 11150-059)	500 ml
Horse serum 10% (Hyclone SH30074.03)	50 ml
Penicillin and Streptomycin (GIBCO 15140-122)	5 ml

VERO 76 (ATCC CATALOG NO. CRL-1587):
Laboratory Designated Name: VERO 76

DMEM (With high glucose [4.5g/L] and L-glutamine; GIBCO 11965-092)	500 ml
Fetal Bovine Serum 10% (Hyclone SH30396.03)	50 ml
Penicillin and Streptomycin (GIBCO 15140-122)	5 ml

VERO C1008 (ATCC CATALOG NO. CRL-1586):
Laboratory Designated Name: VERO C1008

EMEM (With Earle's salts and L-glutamine; GIBCO 11095-080	500 ml
Fetal Bovine Serum 10% (Hyclone SH30396.03)	50 ml
Penicillin and Streptomycin (GIBCO 15140-122)	5 ml
1.0 mM Sodium pyruvate (100 mM [100x] GIBCO 11360-070)	5 ml
0.1 mM Nonessential amino acids (10 mM [100x] GIBCO 11140-050)	5 ml

BHK-21 (C-13; ATCC CATALOG NO. CCL-10):
Laboratory Designated Name: BHK-21

EMEM (With Earle's salts and L-glutamine; GIBCO 11095-080	500 ml
Fetal Bovine Serum 10% (Hyclone SH30396.03)	50 ml
TPB (Tryptose phosphate broth)	50 ml
Penicillin and Streptomycin (GIBCO 15140-122)	5 ml

EQUINE DERM CELLS (NBL-6; ATCC CATALOG NO. CCL-57):
Laboratory Designated Name: ED (Equine derm)

Minimum Essential Medium (EMEM;	
With Earle's salts and L-glutamine; GIBCO 11095-080	500 ml
Fetal Bovine Serum 10% (Hyclone SH30396.03)	50 ml
Penicillin and Streptomycin (GIBCO 15140-122)	5 ml
1.0 mM Sodium pyruvate (100 mM [100x] GIBCO 11360-070)	5 ml
0.1 mM Nonessential amino acids (10 mM [100x] GIBCO 11140-050)	5 ml

MDBK (BOVINE KIDNEY CELLS; ATCC CATALOG NO. CCL-22)
Laboratory Designated Name: MDBK

EMEM (With Earle's salts and L-glutamine; GIBCO 11095-080)	500 ml
Horse Serum 10% (Hyclone SH30396.03)	50 ml
Penicillin and Streptomycin (GIBCO 15140-122)	5 ml
1.0 mM Sodium pyruvate (100 mM [100x] GIBCO 11360-070)	5 ml
0.1 mM Nonessential amino acids (10 mM [100x] GIBCO 11140-050)	5 ml

FETAL EQUINE KIDNEY PRIMARY CELLS (FEK-XX1) FROM BILL MCCOLLUM, UKY
Laboratory Designated Name: FEK

EMEM (With Earle's salts and L-glutamine; GIBCO 11095-080)	500 ml
Fetal Bovine Serum 10% (Hyclone SH30396.03)	50 ml
Penicillin and Streptomycin (GIBCO 15140-122)	5 ml

EQUINE PULMONARY ARTERY ENDOTHELIAL CELL MEDIUM (ECMM)

Laboratory Designated Name: EPAEC

DMEM (With high glucose [4.5g/L], *without* L-glutamine; Cellgro 15-013-CM)	1 L
Fetal Bovine Serum 10% (Hyclone SH30396.03)	110 ml
Penicillin and Streptomycin (GIBCO 15140-122)	11 ml
L-glutamine (200 mM; GIBCO	10 ml
0.1 mM Nonessential amino acids (10 mM [100x] GIBCO 11140-050)	11 ml

CELL LINES GROWN WITH EMEM 10% FSCS IN INCUBATOR WITHOUT CO_2

BHK-21 (Baby Hamster Kidney 21: C-13; ATCC Cat. # CCL-10); RK-13 (Rabbit Kidney 13 Low passage [P194-P204] from Bill McCollum, KY); RK-13 (Rabbit Kidney 13 High passage [P399-P409] from Bill McCollum, KY); Vero 76 (African Green Monkey Kidney: ATCC Cat. # CRL-1587); MDBK (Bovine Kidney cells: ATCC Cat. # CCL-22); ED (Equine Dermal cells: NBL-6; ATCC Cat. # CCL-57)

LARGE SCALE (10 L) CELL CULTURE MEDIA, EMEM 10% FSCS:

Materials

1. EMEM (NEAA, L-glutamine; Mediatech #50-011-PB; 10L/bt) — 10L/bottle
2. Ferritin supplemented calf serum (FSCS; Hyclone SH30072.03) — 1000 mL
3. Penicillin and streptomycin (10,000 U/ml and µg/ml; Gibco 15140-122) — 100 mL
4. Fungizone (Sigma A-9528, one vial) — 10 mL

Fungizone	50 mg
Sterile distilled water	50 ml

   Dissolve fungizone in dH_2O and dispense in 10 ml aliquots. Store at -20 °C. Unreconstituted vial should be stored at 4 °C.

5. Sodium bicarbonate ($NaHCO_3$; Sigma Cat. # S5761-500g) — 6 g
6. Glass fiber prefilter (Millipore Cat. # AP2012450)
7. Durapore® membrane filters (045 µm; Millipore Cat. # HVLP14250)
8. 12 L bottle and stir bar

Method

EMEM	96.1g
$NaHCO_3$	6.0 g
Penicillin/Streptomycin	100 ml
Fungizone (Amphotericin 1,000µg/ml)	10 ml
Serum –ferritin supplemented calf serum (FSCS)	1000 ml
dH2O (tissue culture grade water)	q.s. to 10,000 ml

1. Add 8 L dH2O to 12 L bottle with stir bar.
2. Place on stirrer/hotplate and turn stirrer to setting #3.
3. Add EMEM bottle (rinse twice with water) and mix until dissolved, about 15 min.
4. Add sodium bicarbonate (color should change from yellow to red), penicillin/streptomycin (p/s), fungizone (f), and serum (rinse each container twice with water).
5. Final concentration of penicillin/streptomycin 100 U/ml and 100µg/ml and fungizone 1 µg/ml.
6. Add water to 10 L and mix 5 min.
7. In cell culture room, filter through sterile Millipore filter unit using a prefilter. Dispense 1 L/sterile 1 L bottle.
8. Perform sterility check. Store at 4 °C.

CARBOXYMETHYLCELLULOSE (CMC) OVERLAY MEDIA (1.3X EMEM 10% FSCS):

Materials

1. Carboxymethylcellulose, medium viscosity (Sigma C-4888) 6.0 g
2. Distilled water 140 ml

Method

1. Add water to a 1 L bottle, swirl while adding 0.75% carboxymethylcellulose (CMC) and then shake if necessary.
2. Let stand overnight at room temperature (shake occasionally).
3. Autoclave for 20 min at 121 °C (liquid setting).
4. When cooled to approx. 40 °C, add 1.3X EMEM 10% FSCS to the 800 ml mark.

1.3X EMEM 10% FSCS:

EMEM	96.1g
$NaHCO_3$	6.0 g
Penicillin/Streptomycin	100 ml
Fungizone (Amphotericin 1,000µg/ml)	10 ml
Serum –ferritin supplemented calf serum (FSCS)	1000 ml
dH2O (tissue culture grade water)	q.s. to 7,800 ml

Prepare same as for EMEM 10% FSCS except start with 6 L dH2O and q.s. to 7.8 L.

5. Perform sterility check. Store at 4 °C.
6. Before using, add 0.8 ml gentamicin/bottle (working concentration – 50 µg/ml).

VIRUS TRANSPORT MEDIUM:

Hanks's Balanced Salt Solution w/ Phenol Red 1X (Invitrogen; 14170112)	500 ml
HEPES Buffer (final concentration 25 mM; Invitrogen; 15630080)	20 ml
Bovine Serum Albumin V (final concetration 0.5%; Sigma: A9647)	2.5 g
Antibitic-Antimycotic (100X, Peniillin, Steptomycin & Amphotericin B; Invitrogen; 15240112)	5 ml
Gentamicin Sulfate (final concentration 250 mg/L) Cellgro; 30-005-CR	2.5 ml

NET BUFFER (PH 7.5) FOR RESUSPENSION OF VIRUS PELLET:

Materials

50 mM Tris hydrochloride (500 ml dH_2O)	3.938 g
50 mM Tris base (500 ml dH_2O)	3.029 g
5 mM EDTA	0.95 g
150 mM NaCl	4.383 g

Method

1. Add Tris base to Tris-hydrochloride until the mixture reaches pH 7.5. (Add about 100ml of 50mM Tris-Base to 500ml of 50mM Tris-HCl to get pH 7.5)
2. Add 5 mM EDTA and 150 mM NaCl to above 50 mM Tris-HCl pH 7.5
3. Filter and store at 4 °C.

DULBECCO'S PHOSPHATE-BUFFERED SALINE (PBS):

PBS (Gibco 21600-069)	95.5 g (1 bottle)
Sterile distilled water	q.s. to 10,000 ml

1. Add 9 L dH_2O to 12 L bottle with stir bar. Place on stirrer/hotplate and turn stirrer to setting #3.
2. Add PBS bottle (rinse twice with water) and mix for 10 min.
3. Add 800 ml to each 1 L bottles. Autoclave for 20 min at 121 °C (liquid setting).
4. Cool to room temperature before tightening caps and labeling. Perform sterility check. Store at room temperature.

TRYPSIN EDTA SOLUTION:

PBS (sterile 1X)	180 ml
Trypsin EDTA (no phenol red [10X]; Gibco 15400-054)	20 ml

FREEZING MEDIA:

Dimethylsulfoxide (DMSO; Sigma D-2650)	10%
EMEM 10% FSCS	90%

or

Recovery™ Cell Culture freezing medium (Gibco; 12648-010)

GUINEA PIG COMPLEMENT:
100 ml/bottle, (Rockland Cat # C300-0100). Thaw and dispense (on ice) into 1 or 2 ml volumes and store at -70 °C.

MISCELLANEOUS:

0.5% Trypsin EDTA (no phenol red [10X]; Gibco 15400-054)
Phosphate buffered saline (PBS, pH 7.4, without calcium chloride/magnesium chloride; Gibco 10010)
Dulbecco's Phosphate buffered saline (PBS 10L/bottle, Gibco 10010)
HEPES buffer solution (1M; Gibco 15630)

ANTIBIOTICS FOR CELL CULTURE

Gentamicin:
Gentamicin sulfate, 50 mg/ml, 10 ml/vial **(**Mediatech 30-005-CR). Store at 4 °C.

Pen-Strep:
Penicillin and streptomycin (10,000 U/ml and μg/ml; Gibco 15140-122)

Antibiotic-Antimycotic:
Anti-Anti (100X; Gibco 15240)

Fungizone:
Amphotericin B Solubilized (Sigma A-9528)

BACTERIAL MEDIA RECIPES

LIQUID MEDIA

LB Medium (Luria-Bertani Medium; 500 ml):

Deionized water	500 ml
Bacto-tryptone	5 g
Bacto-yeast extract	2.5 g
NaCl	5 g

1. Stir until the solutes have dissolved. Adjust the pH to 7.0 with 5N NaOH.
2. Sterilize by autoclaving for 20 minutes on liquid cycle.

Psi Broth (500 ml):

Bacto-tryptone	5.0 g
Bacto-yeast extract	2.5 g
NaCl	2.5 g
4 mM MgSO4	
10 mM KCl	
dH2O	to 500 ml

1. Autoclave liquid cycle 30 min.

MEDIA CONTAINING AGAR

LB Agar Plates:

Deionized water	500 ml
Bacto-tryptone	5 g
Bacto-yeast extract	2.5 g
NaCl	5 g

1. Prepare LB medium according to the above recipe. Just before autoclaving, add 7.5 g of Bacto agar. Sterilized by autoclaving for 20 minutes on liquid cycle.
2. When the medium is removed from the autoclave, swirl it gently to distribute the melted agar throughout the solution (need to be very careful, the media may boil over when swirled). Allow the medium to cool to 45-50^{0}C before adding antibiotics*.
3. To avoid air bubbles, mix the medium by swirling. Pour 20-25 ml of medium in a petri dish (use the tissue culture hood and fluorescent light should be off).
4. When medium has hardened completely, invert the plates and wrap in aluminum foil and store them at 4 °C until needed. The plates should be removed from storage 1-2 hours before they are used and allow them to dry.

*Antibiotics solutions

Antibiotic	**Working concentration**
Ampicillin	50 μg / ml
Streptomycin	50 μg / ml
Tetracycline	50 μg / ml
Kanamycin	50 μg / ml
Carbenicillin	60 μg / ml
Chloramphenicol	170 μg / ml

Stock solutions should be stored at -20^{0}C. Avoid repeated freeze thawing and exposure to light. Magnesium ions are antagonists of tetracycline. Use media without magnesium salts for selection of bacteria resistant to tetracycline.

STORAGE MEDIA FOR BACTERIA

Cultures Containing Glycerol:

1. Aliquot 0.85 ml of bacterial culture in to a freezing vial and add 0.15 ml of sterile glycerol (sterilized by autoclaving for 20 minutes on liquid cycle). Vortex the culture to disperse glycerol evenly. Freeze the culture in ethanol-dry ice or liquid nitrogen, and then transfer the tube to -70 °C.
2. To recover the bacteria, scrape the frozen surface of the culture with a sterile inoculating needle, and then immediately streak the bacteria that adhere to the needle onto the surface of an LB agar plate containing the appropriate antibiotics. Incubate the plate at 37 °C. Return the frozen culture to storage at -70 °C.

COMMONLY USED SOLUTIONS AND BUFFERS FOR MOLECULAR BIOLOGY

0.5 M EDTA (pH 8.0)

Deionized water	115 ml
EDTA (di-sodium)	27.918 g
5N NaOH	15,825 µl

Bring the volume to 150 mls with deionized water

5.0 M Sodium chloride

29.22 g of NaCl in 100 mls of distilled water

10% SDS

10 g in of SDS in 100 mls of deionized water

3.0 M Sodium acetate (pH 5.2)

Dissolve 24.609 g of sodium acetate in 60 mls of deionized water. Adjust the pH to 5.2 with glacial acetic acid (approximately 25.6 mls). Bring the volume to 100 mls with deionized water.

10 M Ammonium Acetate (50 ml)

Ammonium acetate	38.5 g
Deionized water to	50 ml

1 M $MgCl_2$ (100 ml):

$MgCl_2$ $6H_20$	20.3 g
Deionized water to	100 ml

1 M Dithiothreitol (DTT; 10 ml)

DTT	1.55 g
10 mM Sodium acetate (pH 5.2) to	10 ml

Store at -20^{0}C

1M Tris HCl (pH 8.0)

Tris HCl	Tris base	Molarity
4.44 g / l	2.65 g / l	0.05 M
88.8 g / l	53.0 g / l	1.0 M
8.88 g / 100 mls	5.30 g / 100 mls	1.0 M
17.76 g / 200 mls	10.6 g / 200 mls	1.0 M

1M Tris HCl (per liter)

Tris Base 121.1g

Add deionized water to 800 ml

Desired pH	Volume of HCl
pH 7.4	70 ml
pH 7.6	60 ml
pH 8.0	42 ml

Add deionized water to 1 liter

TE BUFFER

pH 8.0
10 mM Tris HCl (pH 8.0)
1 mM EDTA (pH 8.0)

pH 7.6
10 mM Tris HCl (pH 7.6)
1 mM EDTA (pH 8.0)

pH 7.4
10 mM Tris HCl (pH 7.4)
1 mM EDTA (pH 8.0)

TAE (Tris-acetate; 50X concentrated stock solution [per liter])

Tris base	242 g
Glacial acetic acid	57.1 ml 0.5
0.5 M EDTA (pH 8.0)	100 ml
Deionized water	q.s.

Working concentration 1X (dilute 10 ml in 490 ml of deionized water)

Proteinase K 2X Buffer

Reagent	**Final concentration**	**To make 100 mls of buffer**
Tris HCl (pH 8.0)	0.2 M	20 ml of 1.0 M Tris HCl (pH 8.0)
NaCl	0.3 M	6.0 ml of 5.0 M NaCl
EDTA (pH 8.0)	25 mM	5.0 ml of 0.5 M EDTA (pH 8.0)
SDS	2.0%	20 ml of 10% SDS
Deionized water		49 ml

Ethidium Bromide (EtBr; 10 mg/ml)

1. Add 1 g of EtBr to 100 ml of deionized water.
2. Stir on a magnetic stir for several hours to ensure that the dye has dissolved.
3. Wrap the container in aluminum foil or transfer the solution to a dark bottle and store at room temperature.
4. Final concentration to be used: 0.5 µg/ml

Method

1. EtBr in agarose: 5.0 µl of EtBr (10 µg/µl) solution per 100 ml of agarose
2. EtBr staining solution (1× TAE with 0.5 µg/ml EtBr): 25 µl of EtBr stock solution in 500 ml of 1× TAE buffer

Gel Loading Buffer (6X)
0.25% bromophenol blue (MW 691.9)
30% glycerol
Dissolved in 1X TAE solution

To make 40 ml 6X loading buffer:

0.25% bromophenol blue (MW 691.9)	0.1 g
30% glycerol	12 ml
1X TAE solution	to 40 ml

Preparation of 25 bp DNA ladder (Invitrogen Cat. # 10597-011)

100 bp DNA ladder (1 µg/µl)	50µl
6× loading buffer	100 µl
Nuclease free water	450 µl

Preparation of 100 bp DNA ladder (Invitrogen Cat. #)

100 bp DNA ladder (1 µg/µl)	50µl
6× loading buffer	100 µl
Nuclease free water	450 µl

Preparation of 1 kb plus DNA ladder (Invitrogen Cat. # 15615-024)

1 kb plus DNA ladder (1 µg/µl)	50 µl
6× loading buffer	100 µl
Nuclease free water	450 µl

Preparation of low DNA mass ladder (Invitrogen Cat. # 10068-013)

Low DNA mass ladder	100 µl
6× loading buffer	100 µl
Nuclease free water	400 µl

Preparation of PCR products

PCR products	10 µl
6× loading buffer	2 µl

Preparation of PCR products to estimate concentration

PCR products	2 µl
6× loading buffer	2 µl
Nuclease free water	8 µl

BUFFERS AND REAGENTS FOR WESTERN IMMUNOBLOTTING

10X SDS-PAGE RUNNING BUFFER (4 LITERS)

Glycine	580 g
Tris base	120 g
SDS	40 g
Distilled water to	4 liters

TRANSFER BUFFER FOR WESTERN IIMMUNOBLOTTING (FOR PROTEINS <80,000 M.W)

	1 Liter	4 Liters
Tris base 25 mM	2.9 g	11.6 g
Glycine 190 mM	14.5 g	58.0 g
Methanol 20%	200 ml	800 ml

Make up to 1 liter or 4 liters with distilled water (800 or 3200 mls)

WASHING BUFFER FOR WESTERN IMMUNOBLOTTING (TBS-T/ TRIS BUFFERED SALINE WITH 0.05% TWEEN 20; pH 7.6)

	1 Liter	4 Liters
Tris base	2.42 g (20 mM)	9.68 g
NaCl	8.0 g (137 mM)	32.0 g
6N HCl	3.8 ml	10.4 ml
Tween 20 (0.05%)	500 µl	2 ml
Deionized water to	1 liter	4 liters

ANTIBODY DILUTION BUFFER (ADB) FOR WESTERN IMMUNOBLOTTING

Nonfat dry milk	10 g
Sodium azide (NaN_3)	0.1 g
NaCl	9.0 g
Na_2HPO_4	4.5 g
NaH_2PO_4	0.5 g
PBS (1X)	1 L

AVIDIN-HRP CONJUGATE DILUTION BUFFER IN PBS FOR WESTERN IMMUNOBLOTTING

PBS (1X)	500 ml
1% Nonfat dry milk	5g
0.05% Tween 20	250 µl

BLOCKING AGENT FOR WESTERN IMMUNOBLOTTING

5% Nonfat dry milk in TBS-T (25 g for 500 ml)
(Use nonfat dry milk for horse serum to reduce the high background. Generally BSA can be used as a blocking agent for western immunoblotting).

MOLECULAR WEIGHT MARKERS AND SAMPLE BUFFER

BenchMark™ Pre-stained protein ladder (Invitrogen; Cat. #10748-010)

MagicMark™ XP Western protein standard (20-220kDa; Invitrogen; Cat. #LC5602)

Lane Marker Reducing sample buffer (5X) (Thermo Scientific Pierce; Cat. # 39000)

Laemmli sample buffer (2X) (BioRad; Cat. # 161-0737)

SOLUTIONS AND REAGENTS

1.5 M Tris HCl, pH 8.8 (BioRad; Cat. # 161-0798)

0.5 M Tris HCl, pH 6.8 (BioRad; Cat. # 161-0799)

SDS solution 10% w/v (BioRad; Cat. # 161-0416)

TEMED (N, N, N', N'-Tetra-methylethylenediamine) (BioRad; Cat. # 161-0801)

Blocking grade blocker non-fat dry milk (BioRad; Cat. # 170-6404)

COMMONLY USED STAINS

Crystal violet stain (stock solution):

Crystal violet (Mallinckrodt 8839)	12g
Methanol (Fisher A412-20)	600 ml

Crystal violet stain (working solution):

1 part of above stock solution
9 parts 10% buffered formalin (Fisher 23-245-685)

Coomassie Blue R protein stain

Brilliant blue R	0.41 g
Glacial acetic acid	50 ml
95% Ethanol	225 ml
Distilled water	225 ml

0.2% Trypan Blue for cell counting

Trypan blue	0.2 g
PBS	100 ml
Sterile filter.	

ANTIBODIES

EAV SPECIFIC ANTIBODIES

Specificity	Clone	Species Origin	Specifity
EAV GP5	6D10	Mouse (MAb)	EAV GP5
EAV GP5	FP55	Rabbit	EAV GP5
EAV M	8887	Rabbit	EAV M
EAV N	3E2	Mouse (MAb)	EAV N
GP2	4033	Rabbit	EAV GP2
GP3	3509	Rabbit	EAV GP3
GP4	7466	Rabbit	EAV GP4
EAV nsp1	12A4	Mouse (MAb)	EAV nsp1
EAV nsp2	L3	Rabbit	EAV nsp2
EAV nsp3	98E	Rabbit	EAV nsp3
EAV nsp4	T1	Rabbit	EAV nsp4
Nsp7 and 8	D (M1)	Rabbit	EAV nsp7 and nsp8
α-EAV antibody[†]	11412	Rabbit	EAV

CONJUGATED-EAV SPECIFIC ANTIBODIES

Specificity	Clone	Species Origin	Conjugated Form	Specifity
Rabbit 8887 PB IgG	Rabbit polyclonal	Rabbit	Alexa Fluor 488	Prebleed
EHV-1	Monoclonal	Mouse (MAb)	Alexa Fluor 488	EHV-1
EAV anti-nsp1	12A4	Mouse (MAb)	Alexa Fluor 488	EAV nsp1
EAV anti-N	3E2	Mouse (MAb)	Alexa Fluor 488	EAV N

SECONDARY CONJUGATED ANTIBODIES

Specificity	Conjugate Form	Company	Catalog #
Goat F(ab')$_2$ Anti-mouse IgG1	FITC	SouthernBiotech	1072-02
Goat F(ab')$_2$ Anti-mouse IgG1	R-PE	SouthernBiotech	1072-09
Goat Anti-mouse IgG (H+L chain specific)	Texas Red® (TXRD)	SouthernBiotech	1031-07
Goat F(ab')$_2$ Anti-rat IgG (H+L chain specific)	FITC	SouthernBiotech	3052-02
Goat Anti-horse IgG (H+L chain specific)	FITC	Jackson ImmunoResearch	108-096-003
Goat Anit-guinea Pig IgG (H+L)	FITC	Vector Laboratories	FI-7000
Goat Anti-rabbit IgG (H+L)	Texas Red®	Vector Laboratories	TI-1000
Goat Anti-horse IgG (H+L)	Biotin	Vector Laboratories	BA-8000
Goat Anti-horse IgG (H+L)	Peroxidase	Jackson ImmunoResearch	108-035-003
Donkey F(ab')$_2$ Anti-goat IgG (H+L chain specific)	Allophycocyanin	Jackson ImmunoResearch	705-136-147
Goat Anti-mouse IgG	Alexa Fluor 488	Invitrogen	A31561
Goat Anti-rabbit IgG (H+L)	DyLight 549	KPL	072-04-15-16
Goat F(ab')$_2$ Anti-mouse IgG (H+L chain specific)	PE-Cy5.5	Caltag (Invitrogen)	M35018
Goat F(ab')$_2$ Anti-mouse IgG (H+L chain specific)	R-PE	Caltag (Invitrogen)	M35004-1
Goat F(ab')$_2$ Anti-rabbit IgG (H+L chain	R-PE	Caltag	L43001

specific)		(Invitrogen)	
Goat F(ab')$_2$ IgG	Unlabeled (UNLB)	Southern Biotech	0110-01
Goat F(ab')$_2$ Anti-mouse IgG (H+L chain specific)	Alexa Fluor 488	Invitrogen	A11017
Goat F(ab')$_2$ Anti-mouse IgG (H+L chain specific)	R-PE	Invitrogen	A10543
Goat α-rabbit IgG (H+L)	Biotin-XX	Invitrogen	B2770
Goat α-mouse IgG (H+L)	Biotin-XX	Invitrogen	B2763
Goat α-rabbit IgG (H+L)	HRP	Southern Biotech	4050-05
Goat α-mouse IgG (H+L)	HRP	Southern Biotech	1031-05

TISSUE CULTURE TECHNIQUES

PROPAGATION OF CONTINUOUS CELL LINES (RK-13, BHK-21 AND VERO CELLS)

Materials

1. Trypsin EDTA (keep in the water bath for few minutes, at 37^0C)
2. Confluent T-75 flask of cells
3. Appropriate cell culture medium

Method

1. Cells must be confluent (3-7 days old).
2. Pour off media.
3. Rinse cells 2-3 times with PBS (pH 7.4)
4. Add 1 ml (25 cm^2 flask), 2 ml (75 cm^2 flask), 4 ml (150 cm^2 flask) trypsin-EDTA, and rock gently for 30 seconds, then let the flask(s) sit at RT for 1 min
5. Pour off trypsin-EDTA (optional) and incubate the flask(s) another 7-8 minutes at 37 °C.
6. Add appropriate amount of media EMEM + 10% FSCS + p/s/f for 1:5 split.

Once a week split cells: 1-150 cm^2 flask with confluent RK-13 cells is made up to approx. 300-335 ml EMEM 10% FSCS.

10 ml is added to 25 cm^2 flask,
30 ml to 75 cm^2 flask,
60 ml to 150 cm^2 flask

Note

To get a confluent monolayer within 24-36 hours transfer 2 ml of cell suspension into a T-75 flask and add 20 ml of complete medium to the flask (1:5 split).
Generally one T-75 flask is sufficient to seed five 96 well plates for neutralization or microtitration assays. For specific cell lines:

One T-75 flask of BHK-21 cells (confluent) is sufficient for 5-10, 96 well plates.
One T-75 flask of Vero cells (confluent) is sufficient for 3-4, 96 well plates.
One T-75 flask of RK-13 cells (confluent) is sufficient for 3-4, 96 well plates.

COUNTING OF CELLS

Manual method

1. Trypsinize the cells and add 10 ml of complete medium.
2. Centrifuge and resuspend the cells in 10 ml of complete medium.
3. Make a 1:10 dilution of cell suspension (100 µl in 900 µl of complete medium). Take 0.5 ml of diluted cell suspension into a snap cap tube and add 0.5 ml of 0.2% Trypan blue (1:2 dilution). Load the hemocytometer and count the cells in each of the four large squares. Some cells will be touching the outside borders. Count only those cells touching two of the outside borders (e.g., the upper and left).

Determine the average number of cells per 10^{-4} ml (cells / ml = average number of cells per large square × 10^4 / ml × dilution factor).

Automated method using cell viability analyzer, ViCell XR (Beckman Coulter)

Materials

ViCell XR Quad reagent pak (Beckman Coulter Cat. # 383722)
4 ml sample cup 120/bag (Beckman Coulter Cat. # 383721)

1. Make 1 ml of 1:10 dilution of cell suspension (100 µl in 900 µl of complete medium)
2. Place 1 ml in a 4 ml sample cup (Beckman Coulter Cat. # 723908)
3. Place the sample cup in the machine (position 1-10)
4. Log in sample: position, sample ID, cell type, dilution factor. OK or next sample when done.
5. Start queue
6. "Camera image" provides cell image while counting and "Autosample queue" provides average of number of counted cells and viability

FREEZING CELLS

Materials

1. Freezing medium
2. Cells in log phase of growth
3. Trypsin EDTA (keep in the water bath for few minutes, at 37^0C)
4. Nalgene™ Cryo 1 °C freezing container (Nalgene Cat. # 5100-0001)

Method

1. Pour off the media.
2. Add 3-4 ml of trypsin EDTA solution and rinse the cells (this is to remove the fetal bovine serum).
3. Add 3-4 ml of fresh trypsin EDTA solution and leave it for 3-4 min. (preferably at 37^0C) and bang on the flask to detach the cells from the surface.
4. Add 10-12 mls of complete medium (the medium contain 10% fetal bovine serum and this will inhibit trypsin) and pour into a 50 ml conical tube.
5. Centrifuge at 1100 or 1300 rpm (200 ×g) in a table top centrifuge for 5 minutes at 25^0C.
6. Aspirate the supernatant and resuspend the cell pellet in freezing medium at approx. 10^7 cells / ml. Freeze in 2 ml vials (1 ml per vial).
7. Freeze cells first in Nalgene™ Cryo 1 °C freezing container with isopropanol at -80 °C for 1 day
8. Transfer frozen cell vials to liquid nitrogen container

RECOVERY OF FROZEN CELLS

Material

1. Frozen cells (-70 °C) in aliquots.
2. Growth medium

Method:

1. Rapid thawing of the cells is necessary. Thaw the cells in the water bath at 37 °C, by swirling the tube (do not submerge the lid to avoid contamination of the cells).
2. Resuspend in 15 ml of growth medium and centrifuge at 1200 or 1300 rpm (200 ×*g*) in a table top centrifuge for 5 minutes at 25 °C.
3. Aspirate the supernatant and resuspend the cells in 10 ml of growth medium. Transfer the cell suspension into a T-75 flask and add 10 ml of medium. Incubate at 37 °C for 2-3 days.

CLASSICAL VIROLOGY TECHNIQUES

PROCESSING OF NASAL SWABS FOR VIRUS ISOLATION

Materials

10 ml syringes
Autoclaved plastic forceps
0.45 µm syringe filter (Corning Cat. # 431220 or Millipore, Millex™ Cat. # SLHA033SB)
1.7 ml screw cap tubes (Sardstedt Cat. # 72.694.996 [color cap], #72.694.006 [clear cap])
15 ml conical tubes

Methods

1. Thoroughly swab the nasopharyngeal area with a sterile rayon swabs (1/2" x 1") with plastic shafts (16").
2. After collection, the rayon tip of each swab is cut off into 7 ml of virus transport medium (Hank's balanced salt solution with penicillin, streptomycin, gentamicin sulfate and amphotericin B; all from Life Technologies, Carlsbad, CA).
3. Squeeze the swab to recover maximum amount of media and centrifuge at 300 ×g for 10 min to remove debris.
4. Transfer individual nasal swabs in transport medium to the barrel of a 12 ml disposable syringe and express through 0.45 µm syringe filter (Millipore).
5. Collect the filtrate into a 15 ml conical tube. Bring up the sample volume to 7 ml with plain MEM to normalize samples (e.g. after filtration usually approx. 6 ml is recovered). Leave approximately 2.0 ml for virus isolation and aliquot the remaining filtrate (approximately 1 ml × 2) into tubes. Freeze at -70 °C until tested.
6. Aspirate off media from confluent RK-13 cells in 6-well plates and inoculate 500 µl specimen/well in duplicate.
7. Incubate plates at 37 °C in presence of 5% CO_2 for 1-2 hours.
8. Add 10ml CMC overlay to each flask and incubate at 37 °C in the presence of 5% CO_2 for 5 days.
9. Do second passage on day 4 using the same cells. Stain cells on day 5 with crystal violet. Archive the TCF at -80 °C.

SERUM PROCESSING

Materials

Vacutainer needles
Vacutainer adapters (Termuno, Venoject II Cat. # P-1316R)
15 ml BD Vacutainer tubes (Kendall Monoject [no additive] Cat. # 8881 301819)
1.7 ml screw cap tubes (Sardstedt Cat. # 72.694.006)
Transfer disposable pipets for serology (Samco scientific Cat. # 202-1S)

Methods

1. Collect blood into vacutainer tubes via jugular venipuncture (about 15 ml blood).
2. Transport blood tubes to the lab. Spray tubes with diluted Roccal-D (1:200). Rinse tubes and dry with paper towel. Let stand at room temperature for 4-5 hours or for 1 hour at 37 °C (water bath works faster).
3. Sediment blood cells at 2000 rpm (300 ×g) for 10 min.
4. Collect serum and aliquot into tubes (1.4 ml × 4). Freeze at -20 °C until tested for virus or antibody.
5. Proceed as in steps 5-8 above for virus isolation.

BUFFY COAT PROCESSING FOR VIRUS ISOLATION (WITHOUT GRADIENT PURIFICATION)

Methods

1. Draw blood by venipuncture into vacutainer tubes containing sodium citrate or EDTA and mix thoroughly.
2. Allow blood to stand for 1-2 hours or sediment at 600-700 rpm (100 ×g) for 10 min. Remove plasma layer and sediment at 2000 rpm for 10 min. The few red blood cells in pellet cause no apparent concern.
3. Aspirate off supernatant; resuspend pellet in 5 ml EMEM 10% FSCS and vortex thoroughly. (If desired, pellet can be washed with PBS before resuspending in EMEM media). Freeze or inoculate.
4. Proceed as in steps 5-8 above.

PERIPHERAL BLOOD MONONUCLEAR CELLS (PBMCS) PROCESSING FOR VIRUS ISOLATION

Materials

15 ml BD vacutainer tubes w/ACD (Citrate-dextrose solution; Sigma C3821- 50ML)
Ficoll-Paque Plus (GE Healthcare Cat#17-1440-03)
15 ml conical tubes
50 ml conical tubes
1.7 ml screw cap tubes (Sardstedt Cat. # 72.694.006)

Preparation of Vacutainer tubes with Acid Citrate Dextrose (ACD)

Using a small gauge needle and a 10 ml syringe, add 1.5 ml ACD to each 15 ml vacutainer tube. Mark tubes to identify that they contain ACD. Store at 4 °C.

Preparation of Ficoll-Paque Plus gradients in 15 ml conical bottom polypropylene tubes

Place 4.0 ml Ficoll-Paque Plus in each tube (will need 15 ml tube per 20 ml vacutainer of collected blood). Centrifuge briefly to pull all of Ficoll-Paque Plus to bottom of the tube. Store at 4 °C but warm to room temperature before use.

Methods

1. Collect blood via venipuncture into tubes with ACD (about 13.5 ml blood and the final volume is about 15 ml per tube). Invert several times to mix. Keep on ice at farm.
2. Transport blood tubes to the lab. Spray tubes with dilute Roccal. Rinse tubes and dry with paper towel. Invert tubes several times to re-mix blood (prevents PBMC from settling on top of RBC too much). Keep at room temperature.
3. Wait approximately 20-30 min until RBC has settled again, leaving cloudy, yellow plasma layer on top of RBC layer.
4. Layering plasma onto Ficoll-Paque Plus using transfer disposable pipet.
5. Using serological pipet, carefully aspirate plasma of one Vacutainer tube, stopping aspiration as reach the RBC layer (a few RBCs are OK but try not to pull lost of RBCs into pipet). Layer plasma onto Ficoll-Paque Plus in conical tube. Plasma from one 20 ml vacutainer of blood should approximately fill the Ficoll-Paque Plus tube to 14-15 ml height in tube. Cap tube when finished. Keep at room temperature. Continue, using the same pipet, and harvest all plasma layers from the vacutainers collected from one horse.
6. Centrifuge at 500 ×g (2800 rpm), 30 min, 25 °C.
7. Harvesting PBMC from gradient:
    - Aspirate plasma layer above gradient down to cloudy band of PBMC. Discard into sterile beaker. With same pipet, aspirate PBMC at interface (approx. 2-3 ml/15 ml tube) and place into 50 ml polypropylene centrifuge tube. Continue removing plasma, harvesting interfaces. Combine PBMC from 4 gradient (15 ml conical) tubes into a 50 ml tube for washing.

8. Cell washing steps:
    - Add sterile PBS (pH 7.4) to bring the volume to 40 ml. Cap tube and mix cells by inverting tube 5 times (or tapping tube with the index finger).
    - Centrifuge for 15 min at 500 ×g (2800 rpm), 4 °C.
    - Aspirate the supernatant without disturbing the cell pellet.
    - Add sterile PBS to bring the volume to 40 ml and cap tube. Mix cells by tapping the tube with the index finger or by vortexing.
    - Centrifuge for 10 min at 500 ×g (2800 rpm), 4 °C.
    - Aspirate the supernatant without disturbing the cell pellet.
    - Resuspend the pellet in 8.0 ml of 10% EMEM (this gives about $1.5 \times 10^7 – 3.0 \times 10^7$ cells per ml). Leave 2.0 ml of buffy coat cells in the conical tube for virus isolation and aliquot the remaining cells (approximately 1.2 ml × 5) into tubes.
    - Freeze the remaining cells at -80 °C.

ISOLATION OF EAV FROM SEMEN

1. Thaw 15 ml tube containing semen sample in warm tap water, then place on ice.
2. Label 8 flasks ($25cm^2$) [4 RK-14 (KY) "high pass" and 4 RK-13 (ATCC-CCL37) "low pass"]/semen, 2×10^{-1}, 1×10^{-2}, 1×10^{-3} for high pass, 2×10^{-1}, 1×10^{-2}, 1×10^{-3} for low pass.
3. Sonicate (output 20, #4.5 on dial) samples on ice 3 × 15 sec.; let set on ice for 15 sec. 1 min between sonications (dilute small volumes to 5 ml). Clean sonicator probe with 95% EtOH 2X between each sample. Spin 300 × g (1900 rpm) for 10 min to remove sperm and debris, save and use supernatant (SSP).
4. Set up 3 tubes (10^{-1} to 10^{-3}) for each sample, 4.5 ml EMEM 10% FSCS per tube.
5. Aspirate off media from 25 cm^2 (3-6 day old RK-13 monolayers). Do not rinse! Make 10^{-1} (0.5 ml sample in 4.5 ml diluent), vortex; with new pipet add 0.5 ml of 10-1 to tube #2 (10^{-2}) and 1 ml to each of 4 flasks marked 10^{-1}. Continue the same way with dilutions 10^{-2} and 10^{-3} (2 flasks each).
6. Incubate all flasks at 37 °C in air incubator (incubator without CO_2) with caps closed for 1 hour (2 hours maximum).
7. Add 10 ml of CMC overlay to each flask and incubate at 37 °C in air incubator (incubator without CO_2) with caps closed.
8. Check for CPE on day 4.
   If bacterial contamination occurs, redo after bacteriological examination and sensitivity testing to find out which antibiotics to used in the TC media. Repeat test as above and also note contamination. Specimen may be filtered through a 0.45 μm filter using a 5 or 10 cc syringe, if necessary.
9. If negative, a second passage is performed on day 4. (See 2nd passage)
10. If sample is toxic this material is passages as is (2nd passage).
11. If positive, supernatant is usually harvested from a 10-2 flask showing viral activity (store at -20 °C) and a reverse SN-test is performed against known positive and negative sera (See reverse SN-test).
12. After 5 days harvest supernatant from flasks and stain flasks with crystal violet using 2 ml crystal violet in buffered formalin. Stain 1-24 hours, remove stain, rinse flasks with tap water and read.
13. All semen samples are placed in freezer zip lock storage bags and stored at -70 °C.
14. Permanently store negative SSP at -20 °C and positive SSP at -70 °C.

Second passage

1. Aspirate media from 2 "high pass" and 2 "low pass" confluent 3-5 day old RK-13 cells in 25 cm^2 flasks for each negative semen sample.
2. From 2 flasks of 10^{-1} passage #1 take up 0.5 ml from each with same pipet (1ml) and add 1 ml to 1 new flask for each high and low pass. Do the same for 10^{-2} passage #1, taking up 1 ml from each. Do 10^{-1} and 10^{-2} only. Close caps and incubate at 37 °C for 1-2 hours (minimum 1 hour) in air incubator.

3. Add 10 ml of CMC overlay to all flasks, close caps, and incubate at 37 °C in air incubator (without CO_2).
4. Read after 3-4 days.
5. After 4 days, harvest media and stain flasks (See passage #1).

MAKING WORKING VIRUS STOCKS

Materials

1. EAV
2. Five confluent monolayers of RK-13 cells in T-150 flasks
3. EMEM
4. RK-13 medium
5. 50 ml conical centrifuge tubes
6. Freezing vials

Method

1. Inoculate monolayers with EAV at an m.o.i. of 1. Resuspend the virus in approximately 50 ml of serum free MEM and add 10 ml per T-150 flask.
2. At the same time mock infect one T-75 flask of RK-13 cells.
3. Adsorb for 1 hour at 37 °C. .
4. Add 40 ml of complete RK -13 medium / T-150 flask. Incubate at 37 °C for 48 hours or until 95% - 100% CPE.
5. Centrifuge at 5000 g (or 3000 rpm in the table top centrifuge) at 4 °C for 15 minutes.
6. Make 1.8 ml and 0.5 ml aliquots of supernatant and store at -70 °C.
7. Use one 0.5 ml frozen vial to titrate the virus.

PREPARATION OF HIGH TITER VIRUS STOCKS

Methods

1. Seed cells into 3, triple-deck flasks and grow until confluency.
2. Remove the medium and leave approx. 50 ml of complete medium containing 10% fetal bovine serum. Add 500 µl-1 ml of virus per flask. If the titer of the virus is known use an m.o.i of 1 (higher m.o.i will may produce deletion mutant).
3. Adsorb for 1 hour at room temperature on the orbital shaker.
4. Add 20-40 ml of complete medium containing 10% fetal bovine serum and incubate at 37 °C for 3-4 days. Check for signs of infection 2 days after the start of infection.
5. Pellet down the cellular debris (3000 rpm / 4 °C / 15 minutes) and aliquot into freezing vials and store at 4 °C (stable for up to 6 months) and / or -70 °C (for long term storage). Virus should be stored away from the fluorescent lights since the virus titer appears to decrease when exposed to fluorescent light for prolonged period of time.
6. Determine the virus titer using the plaque assay procedure.

CONCENTRATION OF EQUINE ARTERITIS VIRUS USING A 20% SUCROSE CUSHION

Materials

1. 20% sucrose in NET buffer
2. SF-MEM
3. RK-13 Medium
4. NET buffer

Method

1. Five T-150 flasks with 3 days old confluent monolayers of RK-13 cells.
2. Inoculate EAV PP^3 P^3 at an m.o.i. of 5. Use approximately 2 vials (1 ml / vial) / T-150 flask. 10 vials of virus for five T-150 flasks.
3. Dissolve the virus in SF-MEM.

1. 10 mls / T-150 × 5 = 50 mls
2. Take 40 mls of SF-MEM and add 10 ml of virus
3. Add 10 mls / T-150 flask
4. At the same time mock infect one T-75 flask of RK-13 cells.
5. Adsorb for 1 hour at 37^0C. .
6. Add 20 ml of complete RK -13 medium / T-150 flask. Incubate at 37^0C for 48 hours or until 95% - 100% CPE.
7. Collect the supernatant and centrifuge at 5000 g (or 3000 rpm) / 4 °C / 15 minutes to remove cellular debris.
8. Filter the supernatant through 4.5µm bottle-top filter (optional) and overlay on to approx. 3-5 ml of 20% sucrose cushion placed in ultracentrifuge clear tubes. Place each tube into ultracentrifuge bucket and balance to equal weight.
9. Pellet the virus by ultra-centrifugation [36,000 rpm (155,300 g) / 4 °C / 4 hours in AH 650 rotor]. Remove brake.
10. Aspirate the supernatant and resuspend the virus pellet in 300-500 µl PBS (pH 7.4). Sonicate for 15/15 sec on and off for three times
11. Store at -80 °C.
12. It is better to collect following samples for micro-titration assay to determine the efficiency of purification.

MICROTITRATION ASSAY TO ESTIMATE EQUINE ARTERITIS VIRUS TITERS

Materials:

1. 96 Wells microtitration plates (Falcon® 3072)
2. Sterile snap cap tubes (Fisher or Falcon® 2054)
3. Multi channel pipette (8 or 12 channels)
4. Antiserum or ascitic fluid (Monoclonal antibodies)
5. Negative control serum or control ascitic fluid
6. EMEM (BioWhittaker®)
7. Complete RK-13 medium
8. Confluent RK-13 cells (one T-75 flask is sufficient for 5 ninety six well plates)
9. Equine arteritis virus stock to be titrated
10. Crystal violet staining / fix solution

Method:

1. Each test virus is done in triplicate. Label the 96 well plates with cell controls.
2. Dilute the test virus from 10^{-1} to 10^{-8} in EMEM (ten fold serial dilution). Use 200 µl of virus + 1800 µl of EMEM.
3. Add 50 µl of EMEM to all the wells except to control wells (column 10, 11 and 12) where 100 µl of EMEM should be added.
4. Trypsinize a confluent T -75 flask of RK-13 cells and resuspend the pellet in 10 ml of RK-13 medium. Take 2 ml of the cell suspension and resuspend in 10 ml (1:5) of RK-13 medium (or 4 ml in 20 ml would be better. This gives enough volume to work).
5. Add 50 µl of diluted virus to test wells in triplicate. Start with the highest dilution (10^{-8}) and go to the lowest dilution (10^{-1}; therefore, can use the same pipet tip)
6. Add 100µl of resuspended RK-13 cells to each well. Incubate at 37 °C for four days.
7. Feed the plates with 50 µl of growth media on day 2 and day 3 (if necessary) to maintain monolayers.
8. When CPE occurs (usually 4 days), dump out the media in sink and stain with 1% crystal violet solution/fix for 20-30 minutes (it is easy to leave the plate(s) in a bucket containing 1% crystal violet/fix solution because the 1% crystal violet/fix solution can be reused.) and then wash gently with tap water to remove excess Crystal violet (three times). Air dry plates and determine EAV titer by Reed and Munch method.

9. 50% end point values, by Read and Munch Method: Under lined numbers indicate logarithmic characteristic of end point dilution. Triplicates;

3 - 2 - 0 - 0 = 0.25	3 - 1 - 2 - 0 = 0.5
3 - 2 - 1 - 0 = 0.5	3 - 1 - 3 - 0 = 0.2
3 - 2 - 2 - 0 = 0.0	3 - 0 - 0 - 0 = 0.5
3 - 2 - 3 - 0 = 0.3	3 - 0 - 1 - 0 = 0.7
3 - 1 - 0 - 0 = 0.75	3 - 0 - 2 - 0 = 0.8
3 - 1 - 1 - 0 = 0.0	3 - 0 - 3 - 0 = 0.0

10. Report virus titers as $TCID_{50}$ per 50 µl.

PLAQUE ASSAY

Materials:

6 well plates
RK-13 cells
Carboxymethylcellulose (CMC) overlay media (1.3X EMEM 10% FSCS)
Virus for titration

METHOD:

1. Prepare RK-13 in 6-well plates.
2. Make virus dilution (10^{-1} to 10^{-8}) in complete 10% EMEM growth media.
3. Aspirate the medium and add 200 µl of diluted virus to each well in duplicate(Start from 10^{-8} and go to 10^{-1}). Mix gently by rocking the plate.
4. Incubate the plate at 37 °C for 1 hour to allow virus particles to adsorb into cells.
5. Following 1 hour incubation period, overlay cells with 4 ml (per well) of CMC overlay media adding to the side of the plate.
6. Allow plates to sit undisturbed on a leveled surface for 4 days until visible plaques develop.
7. After 4 days, discard supernatant and stain with crystal violet staining solution.
8. Count >10 to <100 plaques per well.
9. PFU/ml = (# of plaques in each well [duplicate]/2) × (highest dilution that gives # of plaques) × (dilution factor)
10. e.g. $[(25 + 30)/2] \times 10^{-5} \times 5$ (200 µl) = $137.5 \times 10^{-5} = 1.37 \times 10^{-7}$ pfu/ml

SEROLOGY

VIRUS NEUTRALIZATION TEST (VNT)

Methods

1. Inactivate sera at 56 °C for 30 minutes
2. Put 25µl of serum diluent (10% GP complement in EMEM 10% FSCS [keep on ice until used]) in all wells.
3. Put 25µl of test serum to the first well of two rows (No row for checking toxicity*). Dilute with 25 µl multichannel pipettor.
4. Add 25 µl of virus (200 $TCID_{50}$) diluted in EMEM 10% FSCS to all wells except controls ("See controls").
5. Incubate plates at 37 °C (5% CO_2 incubator) for one hour.
6. Add 125 µl of trypsinized cells (prepared as directed below) to every well.
7. Seal plates and incubate at 37 °C (5% CO_2 incubator). Read after 48, read and final at 72 hours.

Controls: cell controls, known positive and negative sera, and virus titration controls.
Cell controls: add 50 µl serum diluent to 2 wells.
Serum controls: add 25 µl serum diluent to 1 well/each test serum, add 25 µl test serum.
Known positive serum and known negative serum are set up the same way as test sera.

Virus titration: Add 25 µl serum diluent into each of 4 wells for cell controls (Row #1).
Add 25 µl of working virus dilution to each of 4 wells (Row #2).
Add 25 µl of 1:10 dilution of working virus in EMEM 10% FSCS to each of 4 wells (Row #3).
Add 25 µl of 1:100 dilution of working virus in EMEM 10% FSCS to each of 4 wells (Row #4).
Add 25 µl of 1:100 dilution of working virus in EMEM 10% FSCS to each of 4 wells (Row #5).
Add 125 µl of trypsinized cells to all 20 wells.

*If serum is toxic in serum control well (1:4 dilution), then repeat test with a row to check for toxicity.

REVERSE SN-TEST FOR EAV VERIFICATION – confirmation test

Materials

1. Known positive serum, inactivated and diluted 1:4 in PBS (should come from field sample(s), not from vaccinated horses).
2. Known negative serum inactivated and diluted 1:4 in PBS.
3. Stock virus (Bucyrus)
4. Unknown virus isolate

Methods

1. Add 0.3 ml of known negative serum to 4 tubes for each virus sample to be tested (including stock virus).
2. Add 0.3 ml of known positive serum to 3 tubes for each virus sample to be tested (including stock virus).
3. Make up 1:10 dilution of guinea pig complement in EMEM + 10% FSCS + antibiotics (10 ml for each sample).
4. Make up 10^{-1} to 10^{-5} dilutions of all virus samples to be tested using 1.8 ml of media in #3 and 0.2 ml of virus (It may be necessary to dilute stock virus to 10^{-3} before starting these dilutions).
5. To positive serum (3 tubes) add 0.3 ml of 10^{-1}, 10^{-2} and 10^{-3} virus dilutions.
6. To negative serum (4 tubes) add 0.3 ml of 10^{-2}, 10^{-3}, 10^{-4} and 10^{-5} virus dilutions.

7. Incubate serum-virus mixture for 1 hour at 37 °C.
8. 14 flasks 25 cm^2 [7 RK-13 (KY) "high pass", 7 RK-13 (ATCC-CCL37) "low pass"] are used for each virus to be tested. Aspirate off media from 3-5 day RK-13 flasks and add 0.25 ml of above serum-virus mixture to 2 flasks/dilution.
9. Incubate for 2 hours at 37 °C (closed caps, no CO2), rock flasks after 1hour.
10. Add 10 ml of CMC overlay/flask. Incubate for 4-5 days according to development of CPE, remove media, and stain with crystal violet plaque stain.

TREATMENT OF SERUM WITH TOXICITY DUE TO (DUVAXYN) ANTIBODIES TO RK-13 CELLS

This procedure has been used successfully to eliminate (or reduce to readable at 1:4) toxicity from serum samples demonstrating the vaccine-induced "European" toxicity at 1:4 and greater in the EAV SNT. These horses have been vaccinated with Duvaxyn EHV 1,4 (the EHV-1 component is made in RK-13 cells). Always treat a known negative and a known positive serum whenever this treatment is performed on toxic serum specimens. Preferably, use serum that has not been previously inactivated. Use sterile technique for the following steps:

Methods

1. Decant growth media from as flask of 7-10 day old RK-13 (KY) cells (P399-409). Wash flask 3X with 10 ml Dulbecco's PBS. Add 1 ml trypsin EDTA/flask, rotate to spread over cell monolayer, then incubate approximately 6-8 min at 37 °C.
2. When cells have detached, add 2 ml EMEM with 10% FSCS/flask. Mix well with 5 ml pipet, then divide between three 1.5 ml microcentrifuge tubes.
3. Spin tubes at 2,0000 rpm for 15 sec in microcentrifuge. Use a Pasteur pipet to remove and discard all supernatant.
4. Add 0.5 ml of toxic serum or control serum per tube; mix with pipet until cells are resuspended; label tube appropriately. Incubate for 1 hour at 37 °C. Flick tubes after 30 min to resuspend.
5. Spin 2,500 rpm for 15 sec. Use a Pasteur pipet to transfer each serum to a new, labeled 1.5 ml microcentrifuge tube.
6. Inactivate at 56 °C for 30 min if serum has not been inactivated previously. Proceed with EAV SNT test, running sera (toxic, negative, positive) as usual and in pre-seeded (planted 18-24 hours prior) plates.

MOLECULAR BIOLOGY/ RECOMBINANT DNA TECHNIQUES

DESIGNING OF PRIMERS

The approach for designing of specific and efficient primers remains somewhat empirical; there are no hard and fast rules. With experience and by using a good primer designing program (e.g., MacDNASIS v3.5; Hitachi) the majority of the primers can be made to work. Following are some guidelines to design specific and efficient primers.

1. Where possible, select primers with an average G+C content of around 50%.
2. Where possible, select primers with a random base distribution. Try to avoid primers with stretches of polypurines, polypyrimidines, or other unusual sequences.
3. Melting temperature (T_m) should be between 55-75 °C.
4. Increasing the T_m, therefore, the annealing temperature enhances discrimination against incorrectly annealed primers and reduces misextension of incorrect nucleotides at the 3' end of the primers. Therefore, increasing the annealing temperature will help to increase the specificity. An applicable annealing temperature is 5 °C below the true T_m of the amplification primer. The best annealing temperatures is in the range of 55-72 °C. Quick way to calculate annealing temperature is:
5. Annealing temp. (°C) = (# of A and T [A+T] $\times$ 2 + # of G and C [G+C] $\times$ 4) – 5 °C.
6. Try to design both positive and negative primers with same T_m (1-2^{0}C difference will not matter).
7. Make sure the primer ends (3') with a G or C.
8. Primer length should be between 19 and 30 bases (19 to 22 bases are preferred).
9. If possible select a unique area of the genome to design the primer.
10. Avoid sequences with significant secondary structure (computer programs are very useful for this).
11. Check the primers against each other for complementarily. Avoiding primers with 3' overlaps will reduce the incidence of "primer-dimer" artifacts.
12. If possible do a simple homology matching (compare the primers with the whole genome using a computer program) and see whether primer(s) have <50% homology in the area closer to be amplified (or to the desired area). This will reduce the number of nonspecific products of same size.

AGAROSE GEL ELECTROPHORESIS

Materials

1. Agarose (SEAKEM® LE agarose; FMC Bio Products).
2. 50X TAE buffer (Tris Acetate EDTA, pH 8.0).
3. Gel casting plate.
4. Gel sealing tape
5. Buffer tank.

Method

1. Make 1000 ml of 1X TAE, by measuring 20 ml of 50X stock into a 1000 ml graduated cylinder and q.s. to 1000 ml mark with deionized distilled water.
2. Weigh 1.0 g of agarose (for 1% gel) and dissolve it in 100 ml of 1X TAE. Melt agarose solution in microwave until completely dissolved. Let stand at room temperature (or at 45 °C in a water bath) to remove air bubbles but not enough to solidify.
3. Prepare gel-casting plate by taping the ends with gel sealing tape. Place the sample comb in the proper position on the plate.
4. Pour 100 ml of 1% agarose on to the gel casting plate slowly and allow it to solidify (volume of agarose needed depends on the size of the gel casting plate). The gel should be between 0.3 and 0.5 cm thick. After gel has set, final gelling carried out at 4 °C for 30 minutes. There should not be any air bubbles in the gel.
5. Remove the tapes and keep the gel plate in the buffer tank. Add 1X TAE buffer into the reservoirs until it covers the surface of gel at a depth of 3-4 mm.
6. Slowly remove the sample comb and load the samples into the wells (Mix 1-20µl of RNA or DNA with 6X gel loading buffer; loading volume depends on the sample and make sure gel loading buffer get diluted to 1X with sample).

7. Voltage 70V for 2-3 hours (95V for 45-60 minutes) or until the first band has migrated at least 2.5 inches away from the wells. The voltage must never exceed 100V. For low melt Agarose use low voltage (70V). Always run the gel in constant voltage.
8. Stain gel in ethidium bromide, letting it sit for 5-10 min. Destain gel by placing in deionized distilled water for 5 min.
9. Transfer the gel onto a UV light source. Usually a trans illuminator is used to facilitate this step. Place a piece of plastic wrap between the gel and surface of the illuminator. Use a face shield, gloves, and body shield to minimize the UV exposure. Take a picture for records.
10. Locate the DNA or RNA bands and excise by using a sharp scalpel blade (e.g. to obtain the desired band)

Note: Range of separation in gels containing different concentrations of agarose.

% of agarose (%[w/v])	**Efficient range of separation of linear** DNA molecules (Kb)
0.3	5-60
0.6	1-20
0.7	0.8-10
0.9	0.5-7
1.2	0.4-6
1.5	0.2-3
2.0	0.1-2

REAL TIME RT-PCR MEASURING EQUINE CYTOKINE GENE EXPRESSION
PREPARATION OF COMPETENT BACTERIA CELLS - DH5α

Materials

1. Large, autoclave tray with ice for the ice/water bath.
2. 40 sterile microcentrifuge tubes.
3. Glycerol
4. LB agar plates without ampicillin.
5. Autoclave centrifuge bottles, microcentrifuge tubes. Dry cycle. 30 min.
6. Chill these: centrifuge bottle, 15 ml conical tube, 0.1 M $MgCl_2$ and $CaCl_2$ solutions.

Perform all procedures using sterile plasticware and solutions.

Solutions

1. 100 ml of 0.1 M $MgCl_2$ prepared from 1 M $MgCl_2$ stock.
2. 100 ml of 0.1 M $CaCl_2$ prepared from 1 M $CaCl_2$ stock.
3. Stock solutions can be sterilized by autoclaving and stored at room temperature. 0.1M solutions should be prepared fresh.
4. LB (10g Bacto-tryptone, 5g yeast extract, 5g NaCl for 1000 ml LB) supplemented with 1 g/L glucose. Autoclave.

Preparation of solutions

1. Glucose-supplemented LB medium (500 ml)

Bacto-tryptone		5.0 g
Bacto-yeast extract		2.5 g
NaCl		2.5 g
Glucose		0.5 g
dH_2O	to	500 ml

Autoclave. Liquid cycle 30 min. Store at 4C.

2. Glycerol 100 ml
Autoclave. Liquid cycle 30 min. Store at 4C.

3. 1 M $MgCl_2$ stock (100 ml)
   $MgCl_2 \cdot 6H_2O$ (FW 203.30) 20.33 g
   dH2O to 100 ml
   Autoclave. Liquid cycle 30 min. Store at Room temperature.

4. 1 M $CaCl_2$ stock (100 ml)
   $CaCl_2 \cdot 2H_2O$ (FW 47.02) 14.70 g
   dH2O to 100 ml
   Autoclave. Liquid cycle 30 min. Store at Room temperature.

5. 0.1 M $MgCl_2$ working solution (100 ml) and 0.1 M $CaCl_2$ working solution (100 ml)

Method

1. Streak out bacteria (DH5α or other strain) on an LB agar plate (without antibiotics). Allow to grow overnight at 37 °C.
2. The next day, pick a single colony and grow in 2 ml of LB medium (without antibiotics), shaking (250 rpm) at 37 °C overnight. Best to do this in the late afternoon.
3. Take 0.5 ml of the prepared LB medium to use as a blank for the OD. Transfer overnight bacterial prep to a 2L flask containing 500 ml of **glucose-supplemented LB medium**. Incubate at 37 °C with vigorous shaking. During this time chill all solutions and centrifuge bottles on ice and turn on spectrophotometer, set wavelength at 550. After several hours (2.5-3 h), remove 0.5 ml of bacteria using a sterile pipet and check OD_{550} (use LB/glucose as blank). Continue to check the culture until the OD_{550} reaches 0.5 (bacteria double about every 20 min). As soon as the correct OD is achieved immediately transfer the culture flask from the shaker to an ice/water bath. Constantly swirl flask for 5 min until the whole sample is uniformly chilled. Pour the bacteria into the chilled centrifuge bottle and spin at 4000 rpm, 4 °C for 20 min.
4. Decant supernatant and place bottle with bacteria pellet on ice. Resuspend in 10 ml of ice cold 0.1 M $MgCl_2$ using sterile 10 ml pipet. Once resuspended, add the remaining 90 ml of chilled 0.1 M $MgCl_2$. Sit on ice for 5 min and spin for 20 min at 4000 rpm 4 °C.
5. While spinning, transfer 8.6 ml of 0.1 M $CaCl_2$ to a 15 ml conical tube. Add 1.4 ml glycerol. Mix well and let sit on ice.
6. Decant supernatant and place bottle on ice. Resuspend in 10 ml of ice cold 0.1 M $CaCl_2$ using sterile 10 ml pipet. Once resuspended, add the remaining 81.4 ml of ice cold 0.1 M $CaCl_2$. Sit on ice for 20 min and spin in the centrifuge for 20 min at 4000 rpm 4 °C.
7. Decant supernatant well and place bottle on ice. Resuspend bacteria in a chilled solution of 8.6 ml 0.1 M $CaCl_2$ /1.4 ml glycerol. Mix well and transfer 0.25 ml aliquots to microcentrifuge tubes that have been placed in dry ice or drop tubes into liquid nitrogen. Quick freeze and store bacteria at -80 °C until use. Once thawed, the cells should not be frozen

TRANSFORMATION OF DH5α

Materials

1. Water bath at 42 °C
2. Warm SOC medium to RT
3. Warm 3 LB plates w/ampicillin
4. Thaw **on ice** 1 vial of competent cells (DH5α) for each transformation

Methods

1. Thaw on ice, one vial of competent cells per transformation.
2. Add all ligated product to 100ul of competent cell and mix by stirring gently with the pipette. Do not mix by pipetting up and down.

3. Incubate on ice for 30 min
4. Heat-shock the cells for 45 seconds at 42 °C without shaking
5. Immediately transfer the tubes on ice 2min
6. Add 900ul of RT SOC medium
7. Cap the tube tightly and shake the tube horizontally at 37 °C for 1 h (240rpm)
8. After incubation at 37C for 1h. Transfer the culture to microcentrifuge tube. Decant the supernatant leaving about 100ul of media. Resuspend the bacterial pellet.
9. Spread 100ul from each transformation on a prewarmed LB agar plate (w/ampicillin) and incubate overnight at 37°

BCA PROTEIN ASSAY (adapted for Nanodrop use)

The BCA Assay requires a standard curve to be generated each time it is run

Materials
BCA protein assay (Pierce; Cat# 23225)

Method
1. Prepare diluted albumin (BSA) standards.
- Dilute the contents of one BSA ampule into several clean vials. Preferably use the same diluent as the sample(s). Each 1 ml ampule of 2.0 mg/ml BSA is sufficient to prepare a set of diluted standards.

Working range = 20-2,000 ug/ml

Vial	Volume of Diluent	Volume and Source of BSA	Final BSA concentration
A	0	300ul of Stock	2,000 ug/ml *
B	125ul	375ul of Stock	1,500 ug/ml *
C	325ul	325ul of Stock	1,000 ug/ml *
D	175ul	175ul of vial B dilution	750 ug/ml
E	325ul	325ul of vial C dilution	500 ug/ml *
F	325ul	325ul of vial E dilution	250 ug/ml
G	325ul	325ul of vial F dilution	125 ug/ml *
H	400ul	100ul of vial G dilution	25 ug/ml
I	400ul	0	0ug/ml= Blank

If nanodrop allows only 5 standard points use these concentrations (*) to make the standard curve

2. Prepare the BCA Working Reagent (WR)
- Use the following formula to determine the total volume of WR required:
(# standards + # unknowns) × (# replicates) × (volume of WR per sample) = total volume WR required

3. Prepare WR
- Mix 50 parts of BCA reagent A with 1 part of BCA reagent B (50:1, Reagent A:B)

4. Regular assay (using a 20:1 reagent/sample volume ratio).
- Pipet 4 ul of sample in 80 ul of BCA reagent into a 1.7 ml centrifuge tube and mix well.
- Incubate tubes at 37 °C for 30 minutes (working range = 20- 2,000 ug/ml). It is better to use water bath.
- Cool all tubes to RT.

5. Measure protein concentration using Nanodrop.
- A blank must be measured before the standard curve may be generated.
- Step 1: Measure the blank (BCA reagent – a “0” standard)
- Step 2: Up to 5 standards can be measured
- Step 3: Measure samples

ANTIBODY PURIFICATION FROM ASCITES

Materials

1. Zeba Desalt Spin Columns (2ml, Thermo Scientific #89889; 5ml #89891)
2. Melon Gel IgG Spin Purification Kit (Thermo Scientific # 45206)
3. Ascites Conditioning Reagent (Thermo Scientific #45219)
4. Variable-speed centrifuge
5. 15 ml conical tubes
6. Buffer for exchange
7. Serum samples
8. Pipettes and tips

Methods

A. Ascites Conditioning

1. Measure the volume of the sample and transfer to a centrifuge tube
2. Place one half the sample volume of 1 X Gel Purification Buffer into a tube and add 40 µl of the Ascites Conditioning Reagent for every 1 ml of original sample volume. Pulse vortex for 10 sec.
3. While mixing the sample, slowly add the buffer containing the Ascites Conditioning Reagent.
4. Rock or rotate sample for 10 min at RT. (Mixture appears opaque after conditioning)
5. Centrifuge sample at 5,000 ×g for 10 min. Take the supernatant and discard the pellet.
6. Desalt sample using Zeba Desalt Spin Columns pre-equilibrated with 1X Melon Gel Purification Buffer. (For best results, use a sample volume less than 10% of the total Zeba Column volume) Follow the manufacter's instructions about "Procedure for Protein Desalting".

B. IgG Purification from Ascites

1. Equilibrate the Melon Gel IgG Purification Support and Buffer to RT
2. Swirl bottle containing the Purification Support (don't vortex) to obtain an even suspension. Dispense 500µl of slurry into a Spin Column placed in a microcentrifuge tube. Swirl the bottle of gel slurry before pipetting each sample to maintain the gel suspension.
3. Centrifuge the uncapped column/tube for 1 min at 2,000-6,000 × g, then remove the spin column and discard flow-through.
4. Add 10 µl of 5X Regenerant per 1 ml of sample to the conditioned ascites and mix. Add 100 µl of the mixture to the gel, cap column, and incubate for 5 min at RT with end-over-end mixing.
5. Remove the bottom cap from the column, loosen top cap and re-insert spin column in the collection tube.
6. Centrifuge for 1 min to collect the purified antibody in the microcentrifuge tube. Repeat steps 5-7 for the second batch.
7. The antibody may be directly used or stored at -20 °C

NOTE: Discard or regenerate the gel. For gel regeneration, perform the following steps:

1. Add 1.5 times the gel-bed volume of Melon Gel 1X Regenerant, mix for 5 min with end-over-end mixing, centrifuge and discard flow-through. Repeat this process a total of three times.
2. Wash gel with 10 times the gel-bed volume of water.
3. For storage, wash column with 10 times the gel-bed volume of 1X Melon Gel Purification Buffer. For storage longer than 1 week, add a final concentration of 0.02% sodium azide to the buffer used to wash the column.

IgG ANTIBODY PURIFICATION FROM SERUM

Materials

1. Zeba Desalt Spin Columns (2ml, Thermo Scientific #89889; 5ml #89891)

2. Melon Gel IgG Spin Purification Kit (Thermo Scientific # 45206)
3. Variable-speed centrifuge
4. 15 ml conical tubes
5. Buffer for exchange
6. Serum samples
7. Pipettes and tips

Methods

A. Procedure for buffer exchange

1. Twist off the column's bottom closure and loosen cap. Place column in a collection tube.
2. Centrifuge column at 1,000 × g for 2 min to remove storage solution. Place a mark on the side of the column where the compacted resin is slanted upward. Place column in centrifuge with the mark facing outward in all subsequent centrifugation step.
3. Add 1ml of Melon Gel Purification Buffer to the column. Centrifuge at 1,000 × g for 2 min to remove buffer.
4. Repeat step 3 two additional times, discarding buffer from the collection tube.
5. Place column in a new collection tube, remove cap and slowly apply 200-700 µl sample to the center of the compact resin bed.
6. To ensure maximal protein recovery from low-volume samples, apply a stacker of ultrapure water or buffer to the resin bed after the sample has fully absorbed (40 µl stacker for samples <350µl)
7. Centrifuge at 1,000 × g for 2 min to collect the sample. Discard column after use.

B. Spin-column procedure for antibody purification

1. Equilibrate the Melon Gel IgG Purification Support and Purification Buffer to RT (~ 15 min)
2. Swirl bottle containing the Purification Support (don't vortex) to obtain an even suspension. Dispense 500µl of slurry into a Spin Column placed in a microcentrifuge tube. Swirl the bottle of gel slurry before pipetting each sample to maintain the gel suspension.
3. Centrifuge the uncapped column/tube for 1 min at 2,000-6,000 × g, then remove the spin column and discard flow-through.
4. Add 300 µl of Purification Buffer to the column, pulse centrifuge for 10 sec and discard flow-through. Repeat this wash once. Place the bottom cap on the column.
5. Add 10-100 µl of buffer exchanged serum to the column. Cap column and incubate for 5 min at RT with end-over-end mixing.
6. Remove the bottom cap from the column, loosen top cap and re-insert spin column in the collection tube.
7. Centrifuge for 1 min to collect the purified antibody in the microcentrifuge tube. Repeat steps 5-7 for the second batch.
8. The antibody may be directly used or stored at -20 °C.

NOTE: Discard the used gel support. If the gel must be used again, it can be regenerated by adding 500µl of 5M NaCl or 0.5N NaOH, mix for 5 min, centrifuge, and discard flow-through. Wash gel five times by adding 500µl Purification Buffer, centrifuge and discard flow-through. Add 500µl Purification Buffer and store at 4 °C. The gel may be regenerated three times without significant loss of selectivity.

BIOTINYLATION OF EAV RECOMBINANT VIRUSES

Materials

1. Amersham ECL Protein Biotinylation Module (RPN2203)
2. Orbital shaker
3. PBS, pH 7.5
4. PBS containing 1% BSA
5. Distilled water

Methods

1. Determine the concentration of protein to be biotinylated (see BCA method using nanodrop)
2. Prepare a 40 mM working concentration of bicarbonate buffer (BB) by diluting 1:20 in distilled water. (prepare always fresh)
3. Place the biotinylation reagent at RT and ensure the vial has equilibrated to RT prior to opening.
4. Dilute the protein to 1mg/ml in the diluted bicarbonate buffer. The maximum volume suitable for loading on to the column is 2.5 ml (the minimum volume is 2.0 ml). Add 40ul of biotinylation reagent for each mg of protein.
5. Incubate at RT for 1 h with constant agitation.
6. Discard the buffer at the top of the Sephadex G25 column, and cut 1-2 mm off the tip seal. Equilibrate the column with 5 ml of PBS-1% BSA (pH 7.5) followed by 20 ml of PBS. Discard the column washings. **Do not allow the column to run dry.**
7. Allow the buffer level in the top of the column to fall to the level of the plastic sinter at the top of the gel bed.
8. Apply the protein sample (in 2.0-2.5 ml) to the column. Allow the sample volume to enter the column before eluting with PBS and collecting fractions.
9. Elute the sample in 5 ml of PBS (use 2-3 mls of PBS to wash the tubes containing virus). **Collect 1 ml fractions (total 5 fractions)**. Measure protein concentration of 1-5 fractions to determine the eluted protein containing fractions.
10. Measure either protein concentration or UV absorbance at 280nm to verify the fraction number containing the eluted protein.
11. Aliquot in 0.5ml/tube. Make one tube with 110 µl of biotinylated EAV for titration. Store at -80C

VIRUS BINDING ASSAY

Keep everything at 4 °C during the whole experiment

1. See EEC in 6 well plates and wait to grow 100% confluent.
2. Place cells at 4 °C for 30 min to cool down.
3. Wash cells with cold PBS-2%FBS (PBS-F) 3 times before adding biotinylated VBS into each well.
4. Incubate the virus and cell mixtures at 4 °C on a shaker for 60 min.
5. Remove the inocula and wash the unbound cells extensively (3X) with cold PBS-F
6. Add the non-enzymatic cell dissociation solution (Sigma, #C-5914, 1X, 1 ml/25cm^2 flask), 400ul/well and mix on a shaker.
7. Incubate at 4 °C until cells are dissociated form the plates.
8. Add 1ml PBS-F to each well to the cells and pipet repeatedly to dissociate clumps. Transfer the cell suspension in 1.5ml eppendorf tube. Spin at 1000xg for 5 min (in real time PCR room, cool centrifuge at 4C prior to the experiment) and wash with 1ml PBS-F once to remove non-enzymatic buffer.
9. Incubate the washed cell pellets with 200ul 1:100 diluted streptavidin-FITC conjugated (Amersham, #RPN 1232) in PBS F for 60 min at 4C on a shaker
10. Wash cells once with ice cold PBS, and resuspend in 500 ul PBS F for immediate flow cytometric analysis.

Modified protocol for PBMC (EEC for control)

1. Prepare PBMC as for conventional flow cytometry staining. Process AD and NAD cells separately. Incubate on ice to keep it at 4C. Also resuspend EEC cells to use as control. Count the cells and place 10^6 cells into each well or tube.
2. Wash cells twice with ice cold PBS-2% FBS (PBS-F) at 4C
3. Incubate cells with anti-equine CD3 MAb (100ul) and biot-EAV (10ug protein, m.o.i. of 100? I am not sure how much difference is between these or which one will work better yet) in facs buffer (1% NGS; prepare newly and keep it sterile) for 45 min on ice.
4. Wash once with PBS-F
5. Incubate and anti-mouse IgG PE and streptavidin-FITC (total volume 100ul) for 45 min on ice
6. Wash twice with ice cold PBS-F followed by one wash with ice-cold PBS
7. Resuspend in 300ul of 2% paraformaldehyde.

INDIRECT IMMUNOFLUORESCENT ASSAY

Materials:

1. Chamber slides (Lab-Tek® [Chamber Slide™]; Nunc, Inc.) or coverslips for 24-well plate
2. Cover slips (large).
3. Confluent monolayer of cells (BHK21, RK13 etc.)
4. Cell medium (10% BCS-EMEM)
5. Fixative: **4% paraformaldehyde**
6. Wash buffer: **10mM glycine in PBS**
7. Permeabilization buffer: **PBS w/ 0.2% Triton-X 100**
8. Primary antibody dilution: **PBS w/ 5% FBS**
9. Secondary antibody dilution buffer: **PBS w/ 5% FBS or 0.02% evans blue in PBS**
10. FITC-conjugated goat anti-mouse IgG F(ab')2 (Caltag)
11. Mounting medium (Vector, Vectashield H-1000)

Method:

1. Trypsinize cells (T-75 flask) and resuspend into 60 mls of growth media. Plate 0.3 ml per well on to 8-well chamber slides (in this case, usually cells in chamber slides will be ready for infection in 24 hours). Incubate at 37 °C. **OR** T-25 flask of cells were resuspended into 12 ml of growth medium. Plate 300µl cells per well on to eight chamber slides. Incubate at 37°C
2. Twenty four hours later or when cells are subconfluent aspirate media and infect with EAV at a m.o.i. of 5 (100 µl of diluted VBS53 EAV). Adsorb for 1 hour at 37 ºC. Add 0.3 ml of fresh medium and incubate for 24 hours.
3. Aspirate cell media.
4. Wash one time with **cold** PBS (0.6 ml per well).
5. Fix with 4% paraformaldehyde in PBS for at least 30 min at room temperature.
6. Rinse 3X in PBS/10mM glycine. 0.5-0.6ml/well. Leave the cells in your last PBS-glycine wash and store them at 4 °C until labeling
7. Permeablize with PBS containing 0.2% Triton-X 100, leave at RT 5-10min.
8. Wash 3X with PBS/10mM glycine with slides on a shaker.
9. Dilute mouse MAb 12A4 against EAV nsp1
   Make 1:250 dilutions for unconjugated 12A4 (3.5µg/ml)
   Make 1:100 dilutions for AF488 conjugated 12A4 (1mg/ml)
10. Place 100µl drops of diluted Ab to each well. Incubate at RT for 1 hour. Leave slides on a shaker.
11. Wash 3X with PBS/10mM glycine 3 times with slides on a shaker.
12. Dilute secondary Ab [FITC-conjugated goat anti-mouse IgG F(ab')2 (Cat # 31543, Pierce Biotechnology) and FITC-conjugated goat anti-rabbit IgG(H+L) F(ab')2 (Cat # 31573, Pierce Biotechnology)]
    Make 1:100 dilutions
13. Incubate in dark for 1h at RT with slides on a shaker.
14. Wash 3X with PBS/10mM glycine with slides on a shaker.
15. Remove gaskets. Peel off the plastic stickers. Add a drop of mounting medium with DAPI (Vector, Vectashield H-1500) on each well of the chamber slides. Then place a coverslip over the stained slide. Store at 4 °C in dark.

FLOW PROTOCOL FOR SURFACE AND INTRACELLULAR LABELING of AD and NAD PBMCs

Materials

1. 4% paraformaldehyde fixation

2. FACS buffer (DPBS with 0.1% (w/v) sodium azide. Filter 0.2 μm pore membrane. Store at 4 °C. Add 1% NGS when needed)
3. Permeabilization buffer: DPBS, 1% heat-inactivated NGS, 0.1% (w/v) sodium azide, 0.1% saponin (w/v) and sterile filter (0.2 μm pore membrane)
4. Antibodies with appropriate dilution (All intracellular antibody dilutions will be performed in permeabilization buffer/ surface marker Abs are diluted in FACS buffer)
5. Secondary antibodies
6. Blocking solution (Flow buffer with 10% FBS)

Methods

Virus infection

1. Plate cells in each 150 mm culture dish and infect with virus at m.o.i. of 5. Dilute the virus in minimum volume of plain media (7 ml of plain RPMI is enough to cover 150 mm dish) Note: Include control cells (e.g. equine endothelial cells T-75 has approx. 1.5×10^7 cells)
2. Adsorb virus for 1 h and add 18 ml of 10% cRPMI media into each dish. Incubate for 12, 18, 36 h.
3. Cell collection.
4. Non-adherent cells: collect TCF. Wash twice with PBS (10 ml each time) and pull them together with TCF.
   Adherent cells: discard TCF and wash with PBS (10 ml each time) and discard the washed fluid. After washing, collect adherent cells using a scrapper and wash the dish with PBS and collect the PBS wash.
5. Pellet cells and count them.

Surface staining

1. Dilute the surface markers in facs buffer. Dilute cell pellet in facs buffer and equally aliquot ~1.0 $x10^6$ cells into each of V-bottomed 96 well plate.
2. Label cells with 100ul of cell surface marker. Mix by pipetting and incubate for 30 minutes at 4 °C (ice-bucket).
3. Wash once with 200ul facs buffer, centrifuge at 500 *g* for 5 minutes.
4. Label cells with 100ul of 2° Ab (goat anti-mouse IgG-PE conjugated diluted 1:200 in facs buffer). Incubate for 30 minutes at 4 °C covered with aluminum foil
5. Wash once with 200ul facs buffer, centrifuge at 500 *g* for 5 min. Flick off excess

E. INTRACELLULAR EAV STAINING

6. Fix the cells with 200μl 4% paraformaldehyde for 30 minutes at RT in dark. Centrifuge at 500 *g* for 5 minutes.
7. Wash once with 200ul facs buffer.
8. Permeabilize membrane with permeabilization buffer (200 μl /tube) for 5 minutes.
9. Centrifuge at 500 *g* for 5 minutes.
10. Block Fc receptors with 10% FBS in FACS buffer for 30 minutes at RT in dark.
11. Dilute the intracellular labeling antibody in permeabilization buffer.
12. Label with fluorochrome- conjugated intracellular antibody for 30 minutes at RT in dark.
13. Wash 1X with 200 ul FACS buffer.
14. Resuspend in 200 ul of 0.5% paraformaldehyde/PBS and store at 4 °C for next day acquisition.

SDS-PAGE and WESTERN BLOTTING

A. SDS-PAGE

Materials

1. BIO-RAD minigel apparatus

2. Glass plates with 1.5 mm spacers (Bio-Rad Cat #1653312)
3. Glass plates (short plates; Bio-Rad Cat#1653308)
4. 1.5 mm combs, 10 lanes (Bio-Rad Cat #1653365) or 15 lanes (Bio-Rad Cat#1653366)
5. Gaskets (Bio-Rad Cat #1653305)
6. Casting frames (Bio-Rad Cat#1653304)
7. 1.5 M Tris HCl pH 8.8, ml (Bio-Rad #161-0798)
8. 0.5 M Tris HCl pH 6.8, ml (Bio-Rad #161-0799)
9. Acrylamide/Bis, 30%/0.8% (Bio-Rad Cat #161-0158)
10. 10% SDS, µl (Bio-Rad Cat #161-0416)
11. TEMED, µl (Bio-Rad Cat #161-0801)
12. 10% Ammonium persulfate (APS; Bio-Rad Cat #161-0700)
13. Dissolve 1g of APS in 10ml of DW
14. Prepare 1 ml aliquots and store at -20 °C
15. Laemmli sample buffer (Bio-Rad Cat #161-0737)
16. No-Weigh™ Dithiothreitol (DTT; Pierce Cat # 20291)
17. BenchMark Pre-stained protein ladder (Invitrogen, Cat #10748-010)
18. MagicMark XP (Invitrogen, Cat #LC5602)
19. Molecular grade water

<Gel Recipes: to make 2 mini-gels of 1.5mm thickness>

	Resolving (lower) gel		Stacking (upper) gel
	10%	12%	4%
30% AA	4.9	6 ml	0.675 ml
1.5 M Tris HCl pH 8.8	3.75	3.75 ml	-
0.5 M Tris HCl pH 6.8	-	-	1.25 ml
dH2O	6	4.95 ml	3 ml
10% SDS	150 µl	150 ul	50 µl
10% AP	75 µl	75 µl	30 µl
TEMED	15 µl	15 µl	5.5 µl

Buffers (See below for buffer recipe)

1. 1X TGS Running Buffer

Methods

1. Assemble the minigel apparatus: Wash glass plates and spacers with distilled water and detergent. Air-dry in a rack. The glass plates must be absolutely clean. Just before assembly wipe the glass plates with 70% ethanol.
2. Preparation of gel solutions using following table: Make up 12% resolving gels for viral proteins. Make up 10% resolving gel if looking for heavy (50,000 kDa) and light (25,000 kDa) of purified immunoglobulins. This will give best separation and resolution of heavy and light chains. Make up 5% stacking gel at the same time.
3. Prepare both gel solutions according to the recipe. Do not add TEMED until just before pouring the gel into the apparatus.
4. Pour the gel solution between the glass plates. Leave enough space for the stacking gel (comb depth + 1 cm approx). Overlay the gel with dH_2O.
5. Let the gel to polymerize (approx. 30 min), pour off the overlay and wash the top of gel several times with dH_2O. Remove any remaining H_2O with the edge of a paper towel.
6. Add TEMED to the prepared stacking gel solution, mix and immediately pour over top of resolving gel. Add close to the top. Place combs (before placing the combs should be washed with warm water and dried) in to the stacking gel (stop 3-5 mm above the inter phase of stacking and resolving gels). Avoid air bubbles. Allow 15 minutes for polymerization (during this time get the samples ready). Remove combs. Air bubbles should run in to replace combs.
7. Make up one liter of 1X SDS-PAGE running buffer (4X = 232 g glycine, 48 g Tris base, 16 g SDS made up to 4 liters) and pour 500 ml into the buffer tank.

8. Remove the gels (molds with the plexiglass holders) from the casting stand and lock into the central unit with thumbs pushing from the bottom. Small glass plate goes against the rubber gasket. Bottom clicks into place on base pate of the central unit.
9. Drop assemble unit into the buffer tank. Add running buffer to center compartment until gels get submerged. Do not allow inside buffer and buffer in the tank to communicate (not imperative). Flush out each well with pipette before loading the samples.
10. Preparation of Samples and Running the Gel: Denature protein in sample buffer (with the appropriate concentrations of DTT Pierce #20291) for 1-3 minutes. Can store the samples at -20^{0}C or -70^{0}C. Mix 1 tube of DTT (500mM) with 250ul of sample buffer. Mix with sample 1:1 dilution (e.g. 15ul of DTT in sample buffer + 15ul of sample)
11. Load 30-35 µl (10 lane combs) or 15 µl (15 lane combs) per lane. Use long slender pipette tips. Slip into space between two glass plates gently eject the sample into the well made by the comb. Load 1X sample buffer into lane 1 and 10 (or 15; do not load samples into these lanes and this will avoid the smiling effect). Load appropriate molecular weight markers to the second lane.
12. Add running buffer to the buffer tank until the level of the top of the gels.
13. Cover minigel unit (fits only one way) and fix red to red (positive), black to black (negative). Proteins are negatively charged and they migrate to the anode at the bottom. Run at 200 V, 30~40 min.
14. Stop when the dye front reaches the bottom. Turn off the power, pull off top and remove central gel unit and mark the left side of the glass plates with a "Sharpie" pen (this will indicate the lane one). Take apart the plates and cut the corner of the gel with a blade for identification (e.g. top left corner for gel).
15. Gels are ready for transfer (for western immunoblotting), autoradiography (for immunoprecipitation), or staining with Coomassie or silver stains. Proceed to appropriate protocol.

B. Gel transfer to PVDF membrane

Materials
1. Immun-Blot® PVDF membrane (7×8.4 cm; Bio-Rad Cat #162-0174)
2. Extra thick blot paper (cut to same size as blot membranes; Bio-Rad Cat#1703969)
3. Methanol (Fisher Cat#A412-4)
4. Clean forceps

Buffers (See below for buffer recipe)
1. Transfer buffer
2. TBS-T

Methods
1. Soak 2 filter papers for each gel in transfer buffer.
2. Pre-wet PVDF membrane in 100% methanol for 1-2 min and equilibrate the membrane in DW for 2 min and let it in transfer buffer.
3. Equilibrate the gel for 10 min in transfer buffer
4. For transfer, place one filter paper, PVDF membrane, SDS-PAGE and on top the second filter paper.
5. Assemble the transfer unit. Run at 15V for 1hr.
6. Rinse the transferred membrane in TBS-T buffer and proceed to western blotting step.

C. Western Blotting

Materials
1. Skim milk (Bio-Rad Cat#170-6404)
2. Antibody saver trays (Scienceware, small size)
3. Primary antibody (e.g. anti-EAV nsp1 [12A4] purified IgG)
4. Biotinylated goat anti-mouse IgG (Zymed Cat #81-6540) or biotinylated goat anti-rabbit IgG (Zymed Cat #81-6140)
5. Streptavidin-HRP (Zymed Cat #43-8323)
6. ECL™ Western blotting analysis system (GE Healthcare Cat #RPN2109)

7. Rad Tape (Midsci Cat #RAD-10)

Buffers (See below for buffer recipe)
1. TBS-T
2. Antibody dilution buffer (ADB)
3. 5% nonfat dry milk/PBS blocking buffer

Methods
1. Block the membrane in blocking buffer at 4 °C O/N on a shaker or 1-2 hr at RT.
2. Wash the membrane with TBS-T once.
3. Incubate with primary antibody (most of MAb work at 1µg/ml) 1 hr at RT.
4. Wash 3 times with TBS-T (10 min/each)
5. Incubate with 1:5,000 diluted secondary antibody (Biotin-conjugated anti-Ms or anti-Rb) in ADB 1hr at RT.
6. Wash 3 times with TBS-T (10 min/each)
7. Incubate with 1:2,000 diluted Stv-HRP in Stv-HRP dilution buffer 1hr at RT.
8. Wash 3 times with TBS-T (10 min/each)
9. Mix 1:1 components of ECL to develop the membrane.

COOMASSIE BLUE R PROTEIN STAINING FOR DETECTION OF PROTEIN IN SDS-PAGE GELS

1. Place the gels on a glass dish and add 100 ml of Coomassie blue stain and leave on the rocker for 4 hours or more (can stain over night) to allow staining.
2. Remove the Coomassie blue stain (save can reuse) and add 200-250 ml of gel destaining buffer (40% methanol, 10% acetic acid in distilled water). Leave on the rocker for 8 hours. Keep a sponge or kimwipes in the glass dish to absorb stain.
3. Dry the gels on cellophane/perspex frames. Get two 12'' x 10'' cellophane sheets and wet with distilled water (wet one at a time). Lay one wet cellophane sheet on the bottom frame (with center in place to support cellophane) and place the gels over that. Overlay with second wet cellophane, avoid air bubbles, make good contact between gels and the cellophane sheets. Place the top frame (no center needed). Clamp edges together with bulldog clips while pulling cellophane tight. Make small hole for drainage in bottom corner and leave upright. Allow to dry 8-12 hours and remove the frames and store the gels.

Reference

1. Traub-Dargatz JL, Salman MD, Voss JL. Medical problems of adult horses, as ranked by equine practitioners. *J Am Vet Med Assoc* 1991;198:1745-1747.
2. Fraipont A, Van Erck E, Ramery E, et al. Subclinical diseases underlying poor performance in endurance horses: diagnostic methods and predictive tests. *Vet Rec* 2011;169:154.
3. Mullis K, Faloona F, Scharf S, et al. Specific enzymatic amplification of DNA in vitro: the polymerase chain reaction. *Cold Spring Harb Symp Quant Biol* 1986;51 Pt 1:263-273.
4. Higuchi R, Fockler C, Dollinger G, et al. Kinetic PCR analysis: real-time monitoring of DNA amplification reactions. *Biotechnology* 1993;11:1026-1030.
5. Pusterla N, Madigan JE, Leutenegger CM. Real-time polymerase chain reaction: a novel molecular diagnostic tool for equine infectious diseases. *J Vet Intern Med* 2006;20:3-12.
6. Powell DG. Viral respiratory disease of the horse. *Vet Clin North Am Equine Pract* 1991;7:27-52.
7. Powell DG, Timoney PJ, Murphy T, et al. The application of advanced molecular techniques to investigate epizootics of infectious disease in the equine population. *Acta Vet Scand Suppl* 1988;84:337-339.
8. Pusterla N, Kass PH, Mapes S, et al. Surveillance programme for important equine infectious respiratory pathogens in the USA. *Vet Rec* 2011;169:12.
9. Diaz-Mendez A, Viel L, Hewson J, et al. Surveillance of equine respiratory viruses in Ontario. *Can J Vet Res* 2010;74:271-278.
10. Wright PF, Neumann G, Kawaoka Y. Orthomyxoviruses In: Knipe DM,Howley PM, eds. *Fields Virology*. 5th ed. Philedelphia, PA: Lippincott Williams and Wilkins, 2007;1691-1740.
11. Webster RG, Bean WJ, Gorman OT, et al. Evolution and ecology of influenza A viruses. *Microbiol Rev* 1992;56:152-179.
12. Chen W, Calvo PA, Malide D, et al. A novel influenza A virus mitochondrial protein that induces cell death. *Nat Med* 2001;7:1306-1312.
13. Webster RG. Are equine 1 influenza viruses still present in horses? *Equine Vet J* 1993;25:537-538.
14. Sovinova O, Tumova B, Pouska F, et al. Isolation of a virus causing respiratory disease in horses. *Acta Virol* 1958;2:52-61.
15. Waddell GH, Teigland MB, Sigel MM. A New Influenza Virus Associated with Equine Respiratory Disease. *J Am Vet Med Assoc* 1963;143:587-590.
16. van Maanen C, Cullinane A. Equine influenza virus infections: an update. *Vet Q* 2002;24:79-94.
17. Oxburgh L, Berg M, Klingeborn B, et al. Evolution of H3N8 equine influenza virus from 1963 to 1991. *Virus Res* 1994;34:153-165.
18. Oxburgh L, Berg M, Klingeborn B, et al. Equine influenza virus from the 1991 Swedish epizootic shows major genetic and antigenic divergence from the prototype virus. *Virus Res* 1993;28:263-272.

19. Endo A, Pecoraro R, Sugita S, et al. Evolutionary pattern of the H 3 haemagglutinin of equine influenza viruses: multiple evolutionary lineages and frozen replication. *Arch Virol* 1992;123:73-87.
20. Lai AC, Rogers KM, Glaser A, et al. Alternate circulation of recent equine-2 influenza viruses (H3N8) from two distinct lineages in the United States. *Virus Res* 2004;100:159-164.
21. Daly JM, Lai AC, Binns MM, et al. Antigenic and genetic evolution of equine H3N8 influenza A viruses. *J Gen Virol* 1996;77 (Pt 4):661-671.
22. Bryant NA, Rash AS, Russell CA, et al. Antigenic and genetic variations in European and North American equine influenza virus strains (H3N8) isolated from 2006 to 2007. *Vet Microbiol* 2009;138:41-52.
23. Yamanaka T, Niwa H, Tsujimura K, et al. Epidemic of equine influenza among vaccinated racehorses in Japan in 2007. *J Vet Med Sci* 2008;70:623-625.
24. Crawford PC, Dubovi EJ, Castleman WL, et al. Transmission of equine influenza virus to dogs. *Science* 2005;310:482-485.
25. Gerger H. Clinical features, sequelae and epidemiology of equine influenza. In: Bryans JT,Gerber H, eds. *Equine Infectious Diseases*. Karger, New York, 1969;63-80.
26. Powell DG. Equine infectious respiratory disease. *Vet Rec* 1975;96:30-34.
27. Li F, Drummer HE, Ficorilli N, et al. Identification of noncytopathic equine rhinovirus 1 as a cause of acute febrile respiratory disease in horses. *J Clin Microbiol* 1997;35:937-943.
28. Black WD, Wilcox RS, Stevenson RA, et al. Prevalence of serum neutralising antibody to equine rhinitis A virus (ERAV), equine rhinitis B virus 1 (ERBV1) and ERBV2. *Vet Microbiol* 2007;119:65-71.
29. Hartley CA, Ficorilli N, Dynon K, et al. Equine rhinitis A virus: structural proteins and immune response. *J Gen Virol* 2001;82:1725-1728.
30. Kriegshauser G, Deutz A, Kuechler E, et al. Prevalence of neutralizing antibodies to Equine rhinitis A and B virus in horses and man. *Vet Microbiol* 2005;106:293-296.
31. Studdert MJ, Gleeson LJ. Isolation and characterisation of an equine rhinovirus. *Zentralbl Veterinarmed B* 1978;25:225-237.
32. Plummer G. An equine respiratory virus with enterovirus properties. *Nature* 1962;195:519-520.
33. McCollum WH, Timoney PJ. Studies on the seroprevalence and frequencey of equine rhinovirus-I and -II infection in normal horse urine. In: Plowright W, Rossdale PD,Wade JF, eds. *Equine infectious diseases VI*. Cambridge, United Kingdom: R & W Publications, 1992;83-87.
34. Timoney PJ, McCollum WH. Equine viral arteritis. *Vet Clin North Am Equine Pract* 1993;9:295-309.
35. Balasuriya UB, Hedges JF, Smalley VL, et al. Genetic characterization of equine arteritis virus during persistent infection of stallions. *J Gen Virol* 2004;85:379-390.
36. MacLachlan NJ, Balasuriya UB. Equine viral arteritis. *Adv Exp Med Biol* 2006;581:429-433.
37. Crabb BS, Studdert MJ. Equine herpesviruses 4 (equine rhinopneumonitis virus) and 1 (equine abortion virus). *Adv Virus Res* 1995;45:153-190.
38. van Maanen C. Equine herpesvirus 1 and 4 infections: an update. *Vet Q* 2002;24:58-78.

39. Smith DJ, Iqbal J, Purewal A, et al. In vitro reactivation of latent equid herpesvirus-1 from CD5+/CD8+ leukocytes indirectly by IL-2 or chorionic gonadotrophin. *J Gen Virol* 1998;79 (Pt 12):2997-3004.
40. Browning GF, Ficorilli N, Studdert MJ. Asinine herpesvirus genomes: comparison with those of the equine herpesviruses. *Arch Virol* 1988;101:183-190.
41. Studdert MJ, Crabb BS, Ficorilli N. The molecular epidemiology of equine herpesvirus 1 (equine abortion virus) in Australasia 1975 to 1989. *Aust Vet J* 1992;69:104-111.
42. Agius CT, Studdert MJ. Equine herpesviruses 2 and 5: comparisons with other members of the subfamily gammaherpesvirinae. *Adv Virus Res* 1994;44:357-379.
43. Borchers K, Wolfinger U, Ludwig H, et al. Virological and molecular biological investigations into equine herpes virus type 2 (EHV-2) experimental infections. *Virus Res* 1998;55:101-106.
44. Galosi CM, de la Paz VC, Fernandez LC, et al. Isolation of equine herpesvirus-2 from the lung of an aborted fetus. *J Vet Diagn Invest* 2005;17:500-502.
45. Sledge DG, Miller DL, Styer EL, et al. Equine herpesvirus 2-associated granulomatous dermatitis in a horse. *Vet Pathol* 2006;43:548-552.
46. Fu ZF, Robinson AJ, Horner GW, et al. Respiratory disease in foals and the epizootiology of equine herpesvirus type 2 infection. *N Z Vet J* 1986;34:152-155.
47. Kershaw O, von Oppen T, Glitz F, et al. Detection of equine herpesvirus type 2 (EHV-2) in horses with keratoconjunctivitis. *Virus Res* 2001;80:93-99.
48. PN CO, O'Rielly JL, Ficorilli N, et al. Isolation of equine herpesvirus type 2 (equine gammaherpesvirus 2) from foals with keratoconjunctivitis. *J Am Vet Med Assoc* 1994;205:329-331.
49. Brault SA, Bird BH, Balasuriya UB, et al. Genetic heterogeneity and variation in viral load during equid herpesvirus-2 infection of foals. *Vet Microbiol* 2011;147:253-261.
50. Brault SA, Blanchard MT, Gardner IA, et al. The immune response of foals to natural infection with equid herpesvirus-2 and its association with febrile illness. *Vet Immunol Immunopathol* 2010;137:136-141.
51. Allen GP, Murray MJ. Equine herpesvirus-2 (EHV-2) and -5 (EHV-5) infections. In: Coetzer JAW,Tustin RC, eds. *Infectious Disease of LIvestock*: Oxford Press Cape Town, 2004;860-867.
52. Marenzoni ML, Passamonti F, Lepri E, et al. Quantification of Equid herpesvirus 5 DNA in clinical and necropsy specimens collected from a horse with equine multinodular pulmonary fibrosis. *J Vet Diagn Invest* 2011;23:802-806.
53. Nordengrahn A, Merza M, Ros C, et al. Prevalence of equine herpesvirus types 2 and 5 in horse populations by using type-specific PCR assays. *Vet Res* 2002;33:251-259.
54. Bell SA, Balasuriya UB, Gardner IA, et al. Temporal detection of equine herpesvirus infections of a cohort of mares and their foals. *Vet Microbiol* 2006;116:249-257.
55. Wang L, Raidal SL, Pizzirani A, et al. Detection of respiratory herpesviruses in foals and adult horses determined by nested multiplex PCR. *Vet Microbiol* 2007;121:18-28.
56. Todd JD. Comments on rhinoviruses and parainfluenza viruses of horses. *J Am Vet Med Assoc* 1969;155:387-390.

57. Petzoldt K, Schmidt R. Detection of adenovirus particles in the horse. *Arch Virol* 1971:392-294.
58. McChesney AE, England JJ, Adcock JL, et al. Adenoviral infection in suckling Arabian foals. *Pathol Vet* 1970;7:547-564.
59. Studdert MJ, Blackney MH. Isolation of an adenovirus antigenically distinct from equine adenovirus type 1 from diarrheic foal feces. *Am J Vet Res* 1982;43:543-544.
60. McGuire TC, Poppie MJ. Hypogammaglobulinemia and thymic hypoplasia in horses: a primary combined immunodeficiency disorder. *Infect Immun* 1973;8:272-277.
61. Thompson DB, Studdert MJ, Beilharz RG, et al. Inheritance of a lethal immunodeficiency disease of Arabian foals. *Aust Vet J* 1975;51:109-113.
62. Enders JF, Weller TH, Robbins FC. Cultivation of the Lansing Strain of Poliomyelitis Virus in Cultures of Various Human Embryonic Tissues. *Science* 1949;109:85-87.
63. Landry ML, Mayo DR, Hsiung GD. Rapid and accurate viral diagnosis. *Pharmacol Ther* 1989;40:287-328.
64. Blount RE, Jr., Morris JA, Savage RE. Recovery of cytopathogenic agent from chimpanzees with coryza. *Proc Soc Exp Biol Med* 1956;92:544-549.
65. Henrickson KJ. Advances in the laboratory diagnosis of viral respiratory disease. *Pediatr Infect Dis J* 2004;23:S6-10.
66. Gubareva LV, Webster RG, Hayden FG. Detection of influenza virus resistance to neuraminidase inhibitors by an enzyme inhibition assay. *Antiviral Res* 2002;53:47-61.
67. Wetherall NT, Trivedi T, Zeller J, et al. Evaluation of neuraminidase enzyme assays using different substrates to measure susceptibility of influenza virus clinical isolates to neuraminidase inhibitors: report of the neuraminidase inhibitor susceptibility network. *J Clin Microbiol* 2003;41:742-750.
68. Deyde VM, Nguyen T, Bright RA, et al. Detection of molecular markers of antiviral resistance in influenza A (H5N1) viruses using a pyrosequencing method. *Antimicrob Agents Chemother* 2009;53:1039-1047.
69. Coons AH, Creech HJ, Jones RN. Immunological properties of an antibody containing a fluorescent group. *Proc Soc Exp Biol Med* 1941;47:200-202.
70. Liu C. Rapid diagnosis of human influenza infection from nasal smears by means of fluorescein-labeled antibody. *Proc Soc Exp Biol Med* 1956;92:883-887.
71. Bell DM, Walsh EE, Hruska JF, et al. Rapid detection of respiratory syncytial virus with a monoclonal antibody. *J Clin Microbiol* 1983;17:1099-1101.
72. Wong DT, Welliver RC, Riddlesberger KR, et al. Rapid diagnosis of parainfluenza virus infection in children. *J Clin Microbiol* 1982;16:164-167.
73. Waner JL, Whitehurst NJ, Downs T, et al. Production of monoclonal antibodies against parainfluenza 3 virus and their use in diagnosis by immunofluorescence. *J Clin Microbiol* 1985;22:535-538.
74. Kalter SS, Armour V, Reinarz JA. Rapid diagnosis of respiratory disease due to adenovirus and mycoplasma. *Arch Gesamte Virusforsch* 1969;28:34-40.
75. Landry ML, Cohen S, Ferguson D. Prospective study of human metapneumovirus detection in clinical samples by use of light diagnostics direct immunofluorescence reagent and real-time PCR. *J Clin Microbiol* 2008;46:1098-1100.

76. Landry ML, Ferguson D. SimulFluor respiratory screen for rapid detection of multiple respiratory viruses in clinical specimens by immunofluorescence staining. *J Clin Microbiol* 2000;38:708-711.
77. Hornsleth A, Friis B, Andersen P, et al. Detection of respiratory syncytial virus in nasopharyngeal secretions by ELISA: comparison with fluorescent antibody technique. *J Med Virol* 1982;10:273-281.
78. McIntosh K, Hendry RM, Fahnestock ML, et al. Enzyme-linked immunosorbent assay for detection of respiratory syncytial virus infection: application to clinical samples. *J Clin Microbiol* 1982;16:329-333.
79. Harmon MW, Pawlik KM. Enzyme immunoassay for direct detection of influenza type A and adenovirus antigens in clinical specimens. *J Clin Microbiol* 1982;15:5-11.
80. Yasunaga S, Maeda K, Matsumura T, et al. Application of a type-specific enzyme-linked immunosorbent assay for equine herpesvirus types 1 and 4 (EHV-1 and -4) to horse populations inoculated with inactivated EHV-1 vaccine. *J Vet Med Sci* 2000;62:687-691.
81. Kriegshauser G, Kuechler E, Skern T. Aggregation-associated loss of antigenicity observed for denatured virion protein 1 of Equine rhinitis A virus in an enzyme-linked immunosorbent assay. *Virus Res* 2009;143:130-133.
82. Kriegshauser G, Cullinane A, Kuechler E, et al. Denatured virion protein 1 of equine rhinitis B virus 1 contains authentic B-cell epitopes recognised in an enzyme-linked immunosorbent assay--short communication. *Acta Vet Hung* 2008;56:265-270.
83. Casals J. Immunological techniques for animal viruses. In: Maramorosch K,Koprowski H, eds. *Methods in Virology*. New York: Academic Press, 1967;113-194.
84. OIE Manual of Diagnostic Tests and Vaccines for Terrestrial Animals. *OIE Manual of Diagnostic Tests and Vaccines for Terrestrial Animals*. 5th ed. Paris, France: Office International des Epizooties, 2004.
85. Zurhein G, Chou SM. Particles Resembling Papova Viruses in Human Cerebral Demyelinating Disease. *Science* 1965;148:1477-1479.
86. Epstein MA, Achong BG, Barr YM. Virus Particles in Cultured Lymphoblasts from Burkitt's Lymphoma. *Lancet* 1964;1:702-703.
87. Dane DS, Cameron CH, Briggs M. Virus-like particles in serum of patients with Australia-antigen-associated hepatitis. *Lancet* 1970;1:695-698.
88. Flewett TH, Bryden AS, Davies H. Letter: Virus diarrhoea in foals and other animals. *Vet Rec* 1975;96:JMM.
89. Feinstone SM, Kapikian AZ, Purceli RH. Hepatitis A: detection by immune electron microscopy of a viruslike antigen associated with acute illness. *Science* 1973;182:1026-1028.
90. Flewett TH, Bryden AS, Davies H. Letter: Virus particles in gastroenteritis. *Lancet* 1973;2:1497.
91. Kapikian AZ, Wyatt RG, Dolin R, et al. Visualization by immune electron microscopy of a 27-nm particle associated with acute infectious nonbacterial gastroenteritis. *J Virol* 1972;10:1075-1081.
92. Wolk D, Mitchell S, Patel R. Principles of molecular microbiology testing methods. *Infect Dis Clin North Am* 2001;15:1157-1204.

93. Saiki RK, Scharf S, Faloona F, et al. Enzymatic amplification of beta-globin genomic sequences and restriction site analysis for diagnosis of sickle cell anemia. *Science* 1985;230:1350-1354.
94. Mullis KB. The unusual origin of the polymerase chain reaction. *Sci Am* 1990;262:56-61, 64-55.
95. Eisenstein BI. The polymerase chain reaction. A new method of using molecular genetics for medical diagnosis. *N Engl J Med* 1990;322:178-183.
96. White TJ, Madej R, Persing DH. The polymerase chain reaction: clinical applications. *Adv Clin Chem* 1992;29:161-196.
97. Shibata D, Fu YS, Gupta JW, et al. Detection of human papillomavirus in normal and dysplastic tissue by the polymerase chain reaction. *Lab Invest* 1988;59:555-559.
98. Skerra A. Phosphorothioate primers improve the amplification of DNA sequences by DNA polymerases with proofreading activity. *Nucleic Acids Res* 1992;20:3551-3554.
99. Erlich HA, Gelfand D, Sninsky JJ. Recent advances in the polymerase chain reaction. *Science* 1991;252:1643-1651.
100. Persing DH. Polymerase chain reaction: trenches to benches. *J Clin Microbiol* 1991;29:1281-1285.
101. Wagar EA. Direct hybridization and amplification applications for the diagnosis of infectious diseases. *J Clin Lab Anal* 1996;10:312-325.
102. Mittermeier RA. Conservation International and biodiversity conservation. *Nature* 2000;405:255.
103. Qian K. Detection of HCV RNA in serum by reverse transcription polymerase chain reaction (rt-PCR). *Methods Mol Med* 1999;19:47-53.
104. Falus A, Hajnal A. Detection of hepatitis C virus (HCV) by reverse transcription-polymerase chain reaction (RT-PCR) (a note). *Acta Microbiol Immunol Hung* 1995;42:235-236.
105. Haqqi TM, Sarkar G, David CS, et al. Specific amplification with PCR of a refractory segment of genomic DNA. *Nucleic Acids Res* 1988;16:11844.
106. Dynon K, Varrasso A, Ficorilli N, et al. Identification of equine herpesvirus 3 (equine coital exanthema virus), equine gammaherpesviruses 2 and 5, equine adenoviruses 1 and 2, equine arteritis virus and equine rhinitis A virus by polymerase chain reaction. *Aust Vet J* 2001;79:695-702.
107. Zhang L, Pan Z, Geng S, et al. Sensitive, semi-nested RT-PCR amplification of fusion gene sequences for the rapid detection and differentiation of Newcastle disease virus. *Res Vet Sci* 2010;89:282-289.
108. Tuksinvaracharn R, Tanayapong P, Pongrattanaman S, et al. Prevalence of dengue virus in Aedes mosquitoes during dry season by semi-nested reverse transcriptase-polymerase chain reaction (semi-nested RT-PCR). *J Med Assoc Thai* 2004;87 Suppl 2:S129-133.
109. Kiatpathomchai W, Boonsaeng V, Tassanakajon A, et al. A non-stop, single-tube, semi-nested PCR technique for grading the severity of white spot syndrome virus infections in Penaeus monodon. *Dis Aquat Organ* 2001;47:235-239.
110. Apaire-Marchais V, Ferre-Aubineau V, Colonna F, et al. Development of RT-semi-nested PCR for detection of hepatitis A virus in stool in epidemic conditions. *Mol Cell Probes* 1994;8:117-124.

111. Elnifro EM, Ashshi AM, Cooper RJ, et al. Multiplex PCR: optimization and application in diagnostic virology. *Clin Microbiol Rev* 2000;13:559-570.
112. Chamberlain JS, Gibbs RA, Ranier JE, et al. Deletion screening of the Duchenne muscular dystrophy locus via multiplex DNA amplification. *Nucleic Acids Res* 1988;16:11141-11156.
113. Mishra B, Sharma M, Pujhari SK, et al. Clinical applicability of single-tube multiplex reverse-transcriptase PCR in dengue virus diagnosis and serotyping. *J Clin Lab Anal* 2011;25:76-78.
114. Mihaly I, Kolozsi T, Liptai Z, et al. [Experience with multiplex nested PCR and fluorescent antibody tests in the diagnosis of acute central nervous system infections with herpes simplex virus type 1 and 2]. *Orv Hetil* 2010;151:1896-1903.
115. Kuroiwa Y, Nagai K, Okita L, et al. Comparison of an immunochromatography test with multiplex reverse transcription-PCR for rapid diagnosis of respiratory syncytial virus infections. *J Clin Microbiol* 2004;42:4812-4814.
116. Cassinotti P, Mietz H, Siegl G. Suitability and clinical application of a multiplex nested PCR assay for the diagnosis of herpes simplex virus infections. *J Med Virol* 1996;50:75-81.
117. Piatak M, Jr., Luk KC, Williams B, et al. Quantitative competitive polymerase chain reaction for accurate quantitation of HIV DNA and RNA species. *Biotechniques* 1993;14:70-81.
118. Nakagawa H, Shimomura H, Hasui T, et al. Quantitative detection of hepatitis C virus genome in liver tissue and circulation by competitive reverse transcription-polymerase chain reaction. *Dig Dis Sci* 1994;39:225-233.
119. VanDevanter DR, Warrener P, Bennett L, et al. Detection and analysis of diverse herpesviral species by consensus primer PCR. *J Clin Microbiol* 1996;34:1666-1671.
120. Wellinghausen N, Kochem AJ, Disque C, et al. Diagnosis of bacteremia in whole-blood samples by use of a commercial universal 16S rRNA gene-based PCR and sequence analysis. *J Clin Microbiol* 2009;47:2759-2765.
121. Shang S, Chen G, Wu Y, et al. Rapid diagnosis of bacterial sepsis with PCR amplification and microarray hybridization in 16S rRNA gene. *Pediatr Res* 2005;58:143-148.
122. Persson A, Pettersson B, Bolske G, et al. Diagnosis of contagious bovine pleuropneumonia by PCR-laser- induced fluorescence and PCR-restriction endonuclease analysis based on the 16S rRNA genes of Mycoplasma mycoides subsp. mycoides SC. *J Clin Microbiol* 1999;37:3815-3821.
123. Kuimelis RG, Livak KJ, Mullah B, et al. Structural analogues of TaqMan probes for real-time quantitative PCR. *Nucleic Acids Symp Ser* 1997:255-256.
124. Cockerill FR, 3rd. Application of rapid-cycle real-time polymerase chain reaction for diagnostic testing in the clinical microbiology laboratory. *Arch Pathol Lab Med* 2003;127:1112-1120.
125. Espy MJ, Uhl JR, Sloan LM, et al. Real-time PCR in clinical microbiology: applications for routine laboratory testing. *Clin Microbiol Rev* 2006;19:165-256.
126. Cockerill FR, 3rd, Smith TF. Response of the clinical microbiology laboratory to emerging (new) and reemerging infectious diseases. *J Clin Microbiol* 2004;42:2359-2365.
127. Beck ET, Henrickson KJ. Molecular diagnosis of respiratory viruses. *Future Microbiol* 2010;5:901-916.

128. Nazarenko IA, Bhatnagar SK, Hohman RJ. A closed tube format for amplification and detection of DNA based on energy transfer. *Nucleic Acids Res* 1997;25:2516-2521.
129. Schweiger B, Zadow I, Heckler R, et al. Application of a fluorogenic PCR assay for typing and subtyping of influenza viruses in respiratory samples. *J Clin Microbiol* 2000;38:1552-1558.
130. Black EM, Lowings JP, Smith J, et al. A rapid RT-PCR method to differentiate six established genotypes of rabies and rabies-related viruses using TaqMan technology. *J Virol Methods* 2002;105:25-35.
131. Higuchi R, Fockler C, Dollinger G, et al. Kinetic PCR analysis: real-time monitoring of DNA amplification reactions. *Biotechnology (N Y)* 1993;11:1026-1030.
132. Ishiguro T, Saitoh J, Yawata H, et al. Homogeneous quantitative assay of hepatitis C virus RNA by polymerase chain reaction in the presence of a fluorescent intercalater. *Anal Biochem* 1995;229:207-213.
133. Tseng SY, Macool D, Elliott V, et al. An homogeneous fluorescence polymerase chain reaction assay to identify Salmonella. *Anal Biochem* 1997;245:207-212.
134. van der Velden VH, Hochhaus A, Cazzaniga G, et al. Detection of minimal residual disease in hematologic malignancies by real-time quantitative PCR: principles, approaches, and laboratory aspects. *Leukemia* 2003;17:1013-1034.
135. Wittwer CT, Ririe KM, Andrew RV, et al. The LightCycler: a microvolume multisample fluorimeter with rapid temperature control. *Biotechniques* 1997;22:176-181.
136. Morrison TB, Weis JJ, Wittwer CT. Quantification of low-copy transcripts by continuous SYBR Green I monitoring during amplification. *Biotechniques* 1998;24:954-958, 960, 962.
137. Helps C, Lait P, Tasker S, et al. Melting curve analysis of feline calicivirus isolates detected by real-time reverse transcription PCR. *J Virol Methods* 2002;106:241-244.
138. Nazarenko I. Homogeneous detection of nucleic acids using self-quenched polymerase chain reaction primers labeled with a single fluorophore (LUX primers). *Methods Mol Biol* 2006;335:95-114.
139. Kusser W. Use of self-quenched, fluorogenic LUX primers for gene expression profiling. *Methods Mol Biol* 2006;335:115-133.
140. Nuovo GJ, Alfieri ML. The In Situ Detection of PCR-Amplified Hepatitis C RNA. *Methods Mol Med* 1999;19:263-278.
141. Khripin Y. High-throughput genotyping with energy transfer-labeled primers. *Methods Mol Biol* 2006;335:215-240.
142. Cardullo RA, Agrawal S, Flores C, et al. Detection of nucleic acid hybridization by nonradiative fluorescence resonance energy transfer. *Proc Natl Acad Sci U S A* 1988;85:8790-8794.
143. Clegg RM. Fluorescence resonance energy transfer. *Curr Opin Biotechnol* 1995;6:103-110.
144. Wu P, Brand L. Resonance energy transfer: methods and applications. *Anal Biochem* 1994;218:1-13.
145. Selvin PR, Hearst JE. Luminescence energy transfer using a terbium chelate: improvements on fluorescence energy transfer. *Proc Natl Acad Sci U S A* 1994;91:10024-10028.

146. Livak KJ, Flood SJ, Marmaro J, et al. Oligonucleotides with fluorescent dyes at opposite ends provide a quenched probe system useful for detecting PCR product and nucleic acid hybridization. *PCR Methods Appl* 1995;4:357-362.
147. Heid CA, Stevens J, Livak KJ, et al. Real time quantitative PCR. *Genome Res* 1996;6:986-994.
148. Gibson UE, Heid CA, Williams PM. A novel method for real time quantitative RT-PCR. *Genome Res* 1996;6:995-1001.
149. Costa JM, Ernault P, Olivi M, et al. Chimeric LNA/DNA probes as a detection system for real-time PCR. *Clin Biochem* 2004;37:930-932.
150. Kutyavin IV, Afonina IA, Mills A, et al. 3'-minor groove binder-DNA probes increase sequence specificity at PCR extension temperatures. *Nucleic Acids Res* 2000;28:655-661.
151. de Kok JB, Wiegerinck ET, Giesendorf BA, et al. Rapid genotyping of single nucleotide polymorphisms using novel minor groove binding DNA oligonucleotides (MGB probes). *Hum Mutat* 2002;19:554-559.
152. Belousov YS, Welch RA, Sanders S, et al. Single nucleotide polymorphism genotyping by two colour melting curve analysis using the MGB Eclipse Probe System in challenging sequence environment. *Hum Genomics* 2004;1:209-217.
153. Itabashi T, Maesawa C, Uchiyama M, et al. Quantitative detection of mutant alleles of the K-ras gene with minor groove binder-conjugated fluorogenic DNA probes. *Int J Oncol* 2004;24:687-696.
154. Lyamichev V, Brow MA, Dahlberg JE. Structure-specific endonucleolytic cleavage of nucleic acids by eubacterial DNA polymerases. *Science* 1993;260:778-783.
155. Selvin PR. Fluorescence resonance energy transfer. *Methods Enzymol* 1995;246:300-334.
156. Tyagi S, Kramer FR. Molecular beacons: probes that fluoresce upon hybridization. *Nat Biotechnol* 1996;14:303-308.
157. Tyagi S, Bratu DP, Kramer FR. Multicolor molecular beacons for allele discrimination. *Nat Biotechnol* 1998;16:49-53.
158. Vet JA, Van der Rijt BJ, Blom HJ. Molecular beacons: colorful analysis of nucleic acids. *Expert Rev Mol Diagn* 2002;2:77-86.
159. Hu QH, Liu XL, Zhuang ZX, et al. [Modified molecular beacon-based dual real-time PCR for detection of SARS virus and its application]. *Wei Sheng Yan Jiu* 2005;34:416-418.
160. Sum SS, Wong DK, Yuen MF, et al. Real-time PCR assay using molecular beacon for quantitation of hepatitis B virus DNA. *J Clin Microbiol* 2004;42:3438-3440.
161. Whitcombe D, Theaker J, Guy SP, et al. Detection of PCR products using self-probing amplicons and fluorescence. *Nat Biotechnol* 1999;17:804-807.
162. Carters R, Ferguson J, Gaut R, et al. Design and use of scorpions fluorescent signaling molecules. *Methods Mol Biol* 2008;429:99-115.
163. Thelwell N, Millington S, Solinas A, et al. Mode of action and application of Scorpion primers to mutation detection. *Nucleic Acids Res* 2000;28:3752-3761.
164. Roberts L. Human genome research. SNP mappers confront reality and find it daunting. *Science* 2000;287:1898-1899.

165. Singh SK, Kumar R, Wengel J. Synthesis of Novel Bicyclo[2.2.1] Ribonucleosides: 2'-Amino- and 2'-Thio-LNA Monomeric Nucleosides. *J Org Chem* 1998;63:6078-6079.
166. Kumar R, Singh SK, Koshkin AA, et al. The first analogues of LNA (locked nucleic acids): phosphorothioate-LNA and 2'-thio-LNA. *Bioorg Med Chem Lett* 1998;8:2219-2222.
167. Latorra D, Arar K, Hurley JM. Design considerations and effects of LNA in PCR primers. *Mol Cell Probes* 2003;17:253-259.
168. Latorra D, Campbell K, Wolter A, et al. Enhanced allele-specific PCR discrimination in SNP genotyping using 3' locked nucleic acid (LNA) primers. *Hum Mutat* 2003;22:79-85.
169. Braasch DA, Corey DR. Locked nucleic acid (LNA): fine-tuning the recognition of DNA and RNA. *Chem Biol* 2001;8:1-7.
170. Henegariu O, Heerema NA, Dlouhy SR, et al. Multiplex PCR: critical parameters and step-by-step protocol. *Biotechniques* 1997;23:504-511.
171. Wittwer CT, Herrmann MG, Gundry CN, et al. Real-time multiplex PCR assays. *Methods* 2001;25:430-442.
172. Burucoa C, Garnier M, Silvain C, et al. Quadruplex real-time PCR assay using allele-specific scorpion primers for detection of mutations conferring clarithromycin resistance to Helicobacter pylori. *J Clin Microbiol* 2008;46:2320-2326.
173. Ng CT, Gilchrist CA, Lane A, et al. Multiplex real-time PCR assay using Scorpion probes and DNA capture for genotype-specific detection of Giardia lamblia on fecal samples. *J Clin Microbiol* 2005;43:1256-1260.
174. Qu XS, Wanner LA, Christ BJ. Multiplex real-time PCR (TaqMan) assay for the simultaneous detection and discrimination of potato powdery and common scab diseases and pathogens. *J Appl Microbiol* 2011;110:769-777.
175. Woods DF, Reen FJ, Gilroy D, et al. Rapid multiplex PCR and real-time TaqMan PCR assays for detection of Salmonella enterica and the highly virulent serovars Choleraesuis and Paratyphi C. *J Clin Microbiol* 2008;46:4018-4022.
176. Hymas WC, Hillyard DR. Evaluation of Nanogen MGB Alert Detection Reagents in a multiplex real-time PCR for influenza virus types A and B and respiratory syncytial virus. *J Virol Methods* 2009;156:124-128.
177. Hymas WC, Mills A, Ferguson S, et al. Development of a multiplex real-time RT-PCR assay for detection of influenza A, influenza B, RSV and typing of the 2009-H1N1 influenza virus. *J Virol Methods* 2010;167:113-118.
178. Shisong F, Jianxiong L, Xiaowen C, et al. Simultaneous detection of influenza virus type B and influenza A virus subtypes H1N1, H3N2, and H5N1 using multiplex real-time RT-PCR. *Appl Microbiol Biotechnol* 2011;90:1463-1470.
179. Chen Y, Cui D, Zheng S, et al. Simultaneous detection of influenza A, influenza B, and respiratory syncytial viruses and subtyping of influenza A H3N2 virus and H1N1 (2009) virus by multiplex real-time PCR. *J Clin Microbiol* 2011;49:1653-1656.
180. Beck ET, Jurgens LA, Kehl SC, et al. Development of a rapid automated influenza A, influenza B, and respiratory syncytial virus A/B multiplex real-time RT-PCR assay and its use during the 2009 H1N1 swine-origin influenza virus epidemic in Milwaukee, Wisconsin. *J Mol Diagn* 2010;12:74-81.

181. Tam S, Clavijo A, Engelhard EK, et al. Fluorescence-based multiplex real-time RT-PCR arrays for the detection and serotype determination of foot-and-mouth disease virus. *J Virol Methods* 2009;161:183-191.
182. Huang YL, Pang VF, Pan CH, et al. Development of a reverse transcription multiplex real-time PCR for the detection and genotyping of classical swine fever virus. *J Virol Methods* 2009;160:111-118.
183. Belak S, Thoren P. Molecular diagnosis of animal diseases: some experiences over the past decade. *Expert Rev Mol Diagn* 2001;1:434-443.
184. Tetzner R. Prevention of PCR cross-contamination by UNG treatment of bisulfite-treated DNA. *Methods Mol Biol* 2009;507:357-370.
185. Oleksiewicz MB, Donaldson AI, Alexandersen S. Development of a novel real-time RT-PCR assay for quantitation of foot-and-mouth disease virus in diverse porcine tissues. *J Virol Methods* 2001;92:23-35.
186. Korimbocus J, Coates D, Barker I, et al. Improved detection of Sugarcane yellow leaf virus using a real-time fluorescent (TaqMan) RT-PCR assay. *J Virol Methods* 2002;103:109-120.
187. Gorzelniak K, Janke J, Engeli S, et al. Validation of endogenous controls for gene expression studies in human adipocytes and preadipocytes. *Horm Metab Res* 2001;33:625-627.
188. Hussy D, Stauber N, Leutenegger CM, et al. Quantitative fluorogenic PCR assay for measuring ovine herpesvirus 2 replication in sheep. *Clin Diagn Lab Immunol* 2001;8:123-128.
189. Huggett J, Dheda K, Bustin S, et al. Real-time RT-PCR normalisation; strategies and considerations. *Genes Immun* 2005;6:279-284.
190. Kompalic-Cristo A, Frotta C, Suarez-Mutis M, et al. Evaluation of a real-time PCR assay based on the repetitive B1 gene for the detection of Toxoplasma gondii in human peripheral blood. *Parasitol Res* 2007;101:619-625.
191. Toussaint JF, Sailleau C, Breard E, et al. Bluetongue virus detection by two real-time RT-qPCRs targeting two different genomic segments. *J Virol Methods* 2007;140:115-123.
192. Muller J, Eis-Hubinger AM, Daumer M, et al. A novel internally controlled real-time reverse transcription-PCR assay for HIV-1 RNA targeting the pol integrase genomic region. *J Virol Methods* 2007;142:127-135.
193. Hoffmann B, Depner K, Schirrmeier H, et al. A universal heterologous internal control system for duplex real-time RT-PCR assays used in a detection system for pestiviruses. *J Virol Methods* 2006;136:200-209.
194. Olson VA, Laue T, Laker MT, et al. Real-time PCR system for detection of orthopoxviruses and simultaneous identification of smallpox virus. *J Clin Microbiol* 2004;42:1940-1946.
195. Drosten C, Seifried E, Roth WK. TaqMan 5'-nuclease human immunodeficiency virus type 1 PCR assay with phage-packaged competitive internal control for high-throughput blood donor screening. *J Clin Microbiol* 2001;39:4302-4308.
196. Niesters HG. Molecular and diagnostic clinical virology in real time. *Clin Microbiol Infect* 2004;10:5-11.

197. Stranska R, Schuurman R, de Vos M, et al. Routine use of a highly automated and internally controlled real-time PCR assay for the diagnosis of herpes simplex and varicella-zoster virus infections. *J Clin Virol* 2004;30:39-44.
198. Hodgson J, Zuckerman M, Smith M. Development of a novel internal control for a real-time PCR for HSV DNA types 1 and 2. *J Clin Virol* 2007;38:217-220.
199. King DP, Reid SM, Hutchings GH, et al. Development of a TaqMan PCR assay with internal amplification control for the detection of African swine fever virus. *J Virol Methods* 2003;107:53-61.
200. Hofmann MA. Construction of an infectious chimeric classical swine fever virus containing the 5'UTR of bovine viral diarrhea virus, and its application as a universal internal positive control in real-time RT-PCR. *J Virol Methods* 2003;114:77-90.
201. Lu Z, Branscum AJ, Shuck KM, et al. Comparison of two real-time reverse transcription polymerase chain reaction assays for the detection of Equine arteritis virus nucleic acid in equine semen and tissue culture fluid. *J Vet Diagn Invest* 2008;20:147-155.
202. Lu Z, Chambers TM, Boliar S, et al. Development and evaluation of one-step TaqMan real-time reverse transcription-PCR assays targeting nucleoprotein, matrix, and hemagglutinin genes of equine influenza virus. *J Clin Microbiol* 2009;47:3907-3913.
203. Lu Z, Dubovi EJ, Zylich NC, et al. Diagnostic application of H3N8-specific equine influenza real-time reverse transcription polymerase chain reaction assays for the detection of Canine influenza virus in clinical specimens. *J Vet Diagn Invest* 2010;22:942-945.
204. Quinlivan M, Dempsey E, Ryan F, et al. Real-time reverse transcription PCR for detection and quantitative analysis of equine influenza virus. *J Clin Microbiol* 2005;43:5055-5057.
205. Mori A, De Benedictis P, Marciano S, et al. Development of a real-time duplex TaqMan-PCR for the detection of Equine rhinitis A and B viruses in clinical specimens. *J Virol Methods* 2009;155:175-181.
206. Quinlivan M, Maxwell G, Lyons P, et al. Real-time RT-PCR for the detection and quantitative analysis of equine rhinitis viruses. *Equine Vet J* 2010;42:98-104.
207. Bergman AM. Beitrage zur kenntnis der virustrager bei rotlaufseuche, influenza erysipelatosa, des pferdes. *Z Infektionskrnkh* 1913;13:161-174.
208. Burki F, Gerber H. Ein virologisch gesicherter Grobausbruch von Equiner Arteritis. *Muench Tieraerztl Wochenschr* 1966;79.
209. Clark I. Transmission of pink-eye from appraently healthy stallions to mares. *J Comp Pathol* 1892;5.
210. Mumford JA. Preparing for equine arteritis. *Equine Vet J* 1985;17:6-11.
211. Plaateau E, Jacquet A. The propagation of influenza from stallion to mares. *J Comp Pathol* 1888;1:37-38.
212. Doll ER, Bryans JT, McCollum WH, et al. Isolation of a filterable agent causing arteritis of horses and abortion by mares; its differentiation from the equine abortion (influenza) virus. *Cornell Vet* 1957;47:3-41.
213. Bell SA, Balasuriya UBR, Maclachlan NJ. Equine Viral Arteritis. *Clinical Techniques in Equine Practice* 2006;5:233-238.
214. Echeverria MG, Pecoraro MR, Galosi CM, et al. The first isolation of equine arteritis virus in Argentina. *Rev Sci Tech* 2003;22:1029-1033.

215. Glaser AL, de Vries AA, Rottier PJ, et al. Equine arteritis virus: a review of clinical features and management aspects. *Vet Q* 1996;18:95-99.
216. Hullinger PJ, Gardner IA, Hietala SK, et al. Seroprevalence of antibodies against equine arteritis virus in horses residing in the United States and imported horses. *J Am Vet Med Assoc* 2001;219:946-949.
217. Huntington PJ, Forman AJ, Ellis PM. The occurrence of equine arteritis virus in Australia. *Aust Vet J* 1990;67:432-435.
218. Paweska JT, Binns MM, Woods PS, et al. A survey for antibodies to equine arteritis virus in donkeys, mules and zebra using virus neutralisation (VN) and enzyme linked immunosorbent assay (ELISA). *Equine Vet J* 1997;29:40-43.
219. St-Laurent G, Morin G, Archambault D. Detection of equine arteritis virus following amplification of structural and nonstructural viral genes by reverse transcription-PCR. *J Clin Microbiol* 1994;32:658-665.
220. Johnson B, Baldwin C, Timoney P, et al. Arteritis in equine fetuses aborted due to equine viral arteritis. *Vet Pathol* 1991;28:248-250.
221. Vaala WE, Hamir AN, Dubovi EJ, et al. Fatal, congenitally acquired infection with equine arteritis virus in a neonatal thoroughbred. *Equine Vet J* 1992;24:155-158.
222. Glaser AL, Chirnside ED, Horzinek MC, et al. Equine arteritis virus. *Theriogenology* 1997;47:1275-1295.
223. Timoney PJ, McCollum WH, Roberts AW, et al. Demonstration of the carrier state in naturally acquired equine arteritis virus infection in the stallion. *Res Vet Sci* 1986;41:279-280.
224. Neu SM, Timoney PJ, McCollum WH. Persistent infection of the reproductive tract in stallions experimentally infected with equine arteritis virus. 5th International Conference of Equine Infectious Diseases 1987;149-154.
225. Guthrie AJ, Howell PG, Hedges JF, et al. Lateral transmission of equine arteritis virus among Lipizzaner stallions in South Africa. *Equine Vet J* 2003;35:596-600.
226. Balasuriya UB, Hedges JF, Nadler SA, et al. Genetic stability of equine arteritis virus during horizontal and vertical transmission in an outbreak of equine viral arteritis. *J Gen Virol* 1999;80 1949-1958.
227. Hedges JF, Balasuriya UB, Timoney PJ, et al. Genetic divergence with emergence of novel phenotypic variants of equine arteritis virus during persistent infection of stallions. *J Virol* 1999;73:3672-3681.
228. Balasuriya UB, Evermann JF, Hedges JF, et al. Serologic and molecular characterization of an abortigenic strain of equine arteritis virus isolated from infective frozen semen and an aborted equine fetus. *J Am Vet Med Assoc* 1998;213:1586-1589, 1570.
229. Balasuriya UB, MacLachlan NJ. The immune response to equine arteritis virus: potential lessons for other arteriviruses. *Vet Immunol Immunopathol* 2004;102:107-129.
230. Balasuriya UB, MacLachlan NJ. Equine Viral Arteritis. *Equine infectious diseases, eds Sellon DCLong MT*. St. Louis, MO: Saunders/Elsevier, 2007;153-164.
231. Timoney PJ, McCollum WH, Murphy TW, et al. The carrier state in equine arteritis virus infection in the stallion with specific emphasis on the venereal mode of virus transmission. *J Reprod Fertil Suppl* 1987;35:95-102.

232. McCollum WH, Little TV, Timoney PJ, et al. Resistance of castrated male horses to attempted establishment of the carrier state with equine arteritis virus. *J Comp Pathol* 1994;111:383-388.
233. Holyoak GR, Giles RC, McCollum WH, et al. Pathological changes associated with equine arteritis virus infection of the reproductive tract in prepubertal and peripubertal colts. *J Comp Pathol* 1993;109:281-293.
234. MacLachlan NJ, Balasuriya UB, Rossitto PV, et al. Fatal experimental equine arteritis virus infection of a pregnant mare: immunohistochemical staining of viral antigens. *J Vet Diagn Invest* 1996;8:367-374.
235. Balasuriya UB, Snijder EJ. Arterivirus In: Mettenleiter TC,Sobrino F, eds. *Animal Viruses: Molecular Biology*. Norwich, United Kingdom: Caister Academic Press, 2008;97-148.
236. Moore BD, Balasuriya UB, Watson JL, et al. Virulent and avirulent strains of equine arteritis virus induce different quantities of TNF-alpha and other proinflammatory cytokines in alveolar and blood-derived equine macrophages. *Virology* 2003;314:662-670.
237. McCollum WH. Vaccination for equine viral arteritis. Proceeding of the 2ne international conference on equine infectious diseases 1969;143-151.
238. Fukunaga Y, McCollum WH. Complement-fixation reactions in equine viral arteritis. *Am J Vet Res* 1977;38:2043-2046.
239. Radwan AI, Burger D, Davis WC. The fate of sensitized equine arteritis virus following neutralization by complement of anti-IgG serum. *Virology* 1973;53:372-378.
240. Radwan AI, Burger D. The role of sensitizing antibody in the neutralization of equine arteritis virus by complement or anti-IgG serum. *Virology* 1973;53:366-371.
241. Radwan AI, Burger D. The complement-requiring neutralization of equine arteritis virus by late antisera. *Virology* 1973;51:71-77.
242. Radwan AI, Crawford TB. The mechanisms of neutralization of sensitized equine arteritis virus by complement components. *J Gen Virol* 1974;25:229-237.
243. Fukunaga Y, Imagawa H, Kanemaru T, et al. Complement-dependent serum neutralization with virulent and avirulent Bucyrus strains of equine arteritis virus. *Vet Microbiol* 1993;36:379-383.
244. Moraillon A, Moraillon R. Results of an epidemiological investigation on viral arteritis in France and some other European and African countries. *Ann Rech Vet* 1978;9:43-54.
245. Chirnside ED, Cook RF, Lock MW, et al. Monoclonal antibodies to equine arteritis virus The Fifth International Conference of Equine Infectious Diseases 1988;262-267.
246. Chirnside ED, de Vries AA, Mumford JA, et al. Equine arteritis virus-neutralizing antibody in the horse is induced by a determinant on the large envelope glycoprotein GL. *J Gen Virol* 1995;76 (Pt 8):1989-1998.
247. Chirnside ED, Francis PM, de Vries AA, et al. Development and evaluation of an ELISA using recombinant fusion protein to detect the presence of host antibody to equine arteritis virus. *J Virol Methods* 1995;54:1-13.
248. Chirnside ED, Francis PM, Mumford JA. Expression cloning and antigenic analysis of the nucleocapsid protein of equine arteritis virus. *Virus Res* 1995;39:277-288.

249. Hedges JF, Balasuriya UB, Ahmad S, et al. Detection of antibodies to equine arteritis virus by enzyme linked immunosorbant assays utilizing G(L), M and N proteins expressed from recombinant baculoviruses. *J Virol Methods* 1998;76:127-137.
250. Kheyar A, Martin S, St-Laurent G, et al. Expression cloning and humoral immune response to the nucleocapsid and membrane proteins of equine arteritis virus. *Clin Diagn Lab Immunol* 1997;4:648-652.
251. MacLachlan NJ, Balasuriya UB, Hedges JF, et al. Serologic response of horses to the structural proteins of equine arteritis virus. *J Vet Diagn Invest* 1998;10:229-236.
252. Balasuriya UB, Patton JF, Rossitto PV, et al. Neutralization determinants of laboratory strains and field isolates of equine arteritis virus: identification of four neutralization sites in the amino-terminal ectodomain of the G(L) envelope glycoprotein. *Virology* 1997;232:114-128.
253. Balasuriya UB, Dobbe JC, Heidner HW, et al. Characterization of the neutralization determinants of equine arteritis virus using recombinant chimeric viruses and site-specific mutagenesis of an infectious cDNA clone. *Virology* 2004;321:235-246.
254. Weiland E, Bolz S, Weiland F, et al. Monoclonal antibodies directed against conserved epitopes on the nucleocapsid protein and the major envelope glycoprotein of equine arteritis virus. *J Clin Microbiol* 2000;38:2065-2075.
255. Cavanagh D. Nidovirales: a new order comprising Coronaviridae and Arteriviridae. *Arch Virol* 1997;142:629-633.
256. Snijder EJ, Meulenberg JJ. The molecular biology of arteriviruses. *J Gen Virol* 1998;79:961-979.
257. Doll ER, Knappenberger RE, Bryans JT. An outbreak of abortion caused by the equine arteritis virus. *Cornell Vet* 1957;47:69-75.
258. Snijder EJ, Meulenberg JJ. The molecular biology of arteriviruses. *J Gen Virol* 1998;79:961-979.
259. Zhang J, Timoney PJ, Shuck KM, et al. Molecular epidemiology and genetic characterization of equine arteritis virus isolates associated with the 2006-2007 multi-state disease occurrence in the USA. *J Gen Virol*;91:2286-2301.
260. den Boon JA, Snijder EJ, Chirnside ED, et al. Equine arteritis virus is not a togavirus but belongs to the coronaviruslike superfamily. *J Virol* 1991;65:2910-2920.
261. van Dinten LC, den Boon JA, Wassenaar AL, et al. An infectious arterivirus cDNA clone: identification of a replicase point mutation that abolishes discontinuous mRNA transcription. *Proc Natl Acad Sci U S A* 1997;94:991-996.
262. Snijder EJ, van Tol H, Pedersen KW, et al. Identification of a novel structural protein of arteriviruses. *J Virol* 1999;73:6335-6345.
263. Firth AE, Zevenhoven-Dobbe JC, Wills NM, et al. Discovery of a small arterivirus gene that overlaps the GP5 coding sequence and is important for virus production. *J Gen Virol* 2011;92:1097-1106.
264. van Dinten LC, Rensen S, Gorbalenya AE, et al. Proteolytic processing of the open reading frame 1b-encoded part of arterivirus replicase is mediated by nsp4 serine protease and is essential for virus replication. *J Virol* 1999;73:2027-2037.
265. Ziebuhr J, Snijder EJ, Gorbalenya AE. Virus-encoded proteinases and proteolytic processing in the Nidovirales. *J Gen Virol* 2000;81:853-879.

266. de Vries AA, Post SM, Raamsman MJ, et al. The two major envelope proteins of equine arteritis virus associate into disulfide-linked heterodimers. *J Virol* 1995;69:4668-4674.
267. Snijder EJ, Dobbe JC, Spaan WJ. Heterodimerization of the two major envelope proteins is essential for arterivirus infectivity. *J Virol* 2003;77:97-104.
268. Wieringa R, de Vries AA, van der Meulen J, et al. Structural protein requirements in equine arteritis virus assembly. *J Virol* 2004;78:13019-13027.
269. Chirnside ED, de Vries AA, Mumford JA, et al. Equine arteritis virus-neutralizing antibody in the horse is induced by a determinant on the large envelope glycoprotein GL. *J Gen Virol* 1995;76:1989-1998.
270. Deregt D, de Vries AA, Raamsman MJ, et al. Monoclonal antibodies to equine arteritis virus proteins identify the GL protein as a target for virus neutralization. *J Gen Virol* 1994;75:2439-2444.
271. Glaser AL, de Vries AA, Dubovi EJ. Comparison of equine arteritis virus isolates using neutralizing monoclonal antibodies and identification of sequence changes in GL associated with neutralization resistance. *J Gen Virol* 1995;76:2223-2233.
272. Balasuriya UB, Heidner HW, Hedges JF, et al. Expression of the two major envelope proteins of equine arteritis virus as a heterodimer is necessary for induction of neutralizing antibodies in mice immunized with recombinant Venezuelan equine encephalitis virus replicon particles. *J Virol* 2000;74:10623-10630.
273. Balasuriya UB, Rossitto PV, DeMaula CD, et al. A 29K envelope glycoprotein of equine arteritis virus expresses neutralization determinants recognized by murine monoclonal antibodies. *J Gen Virol* 1993;74:2525-2529.
274. Balasuriya UB, Hedges JF, Nadler SA, et al. Genetic stability of equine arteritis virus during horizontal and vertical transmission in an outbreak of equine viral arteritis. *J Gen Virol* 1999;80 (Pt 8):1949-1958.
275. Konishi S, Akashi H, Sentsui H, et al. Studies on equine viral arteritis. I. Characterization of the virus and trial survey on antibody with vero cell cultures. *Nippon Juigaku Zasshi* 1975;37:259-267.
276. McCollum WH, Doll ER, Wilson JC, et al. Propagation of equine arteritis virus in monolayer cultures of equine kidney. *Am J Vet Res* 1961;22:731-735.
277. Harry TO, McCollum WH. Stability of viability and immunizing potency of lyophilized, modified equine arteritis live-virus vaccine. *Am J Vet Res* 1981;42:1501-1505.
278. Moore BD, Balasuriya UB, Nurton JP, et al. Differentiation of strains of equine arteritis virus of differing virulence to horses by growth in equine endothelial cells. *Am J Vet Res* 2003;64:779-784.
279. Wilson JC, Doll ER, Mc CW, et al. Propagation of equine arteritis virus previously adapted to cell cultures of equine kidney in monolayer cultures of hamster kidney. *Cornell Vet* 1962;52:200-205.
280. W.H. M, Doll ER, Wilson JC, et al. Isolation and propagation of equine arteritis virus in monolayer cell cultures of rabbit kidney. *Cornell Vet* 1962;52:452-458.
281. Hyllseth B. A plaque assay of equine arteritis virus in BHK-21 cells. *Arch Gesamte Virusforsch* 1969;28:26-33.
282. Zhang J, Timoney PJ, MacLachlan NJ, et al. Persistent equine arteritis virus infection in HeLa cells. *J Virol* 2008;82:8456-8464.

283. Nitschke M, Korte T, Tielesch C, et al. Equine arteritis virus is delivered to an acidic compartment of host cells via clathrin-dependent endocytosis. *Virology* 2008;377:248-254.
284. Fang Y, Snijder EJ. The PRRSV replicase: exploring the multifunctionality of an intriguing set of nonstructural proteins. *Virus Res* 2010;154:61-76.
285. Pedersen KW, van der Meer Y, Roos N, et al. Open reading frame 1a-encoded subunits of the arterivirus replicase induce endoplasmic reticulum-derived double-membrane vesicles which carry the viral replication complex. *J Virol* 1999;73:2016-2026.
286. Snijder EJ, van Tol H, Roos N, et al. Non-structural proteins 2 and 3 interact to modify host cell membranes during the formation of the arterivirus replication complex. *J Gen Virol* 2001;82:985-994.
287. van der Meer Y, van Tol H, Locker JK, et al. ORF1a-encoded replicase subunits are involved in the membrane association of the arterivirus replication complex. *J Virol* 1998;72:6689-6698.
288. van Dinten LC, Wassenaar AL, Gorbalenya AE, et al. Processing of the equine arteritis virus replicase ORF1b protein: identification of cleavage products containing the putative viral polymerase and helicase domains. *J Virol* 1996;70:6625-6633.
289. Asagoe T, Inaba Y, Jusa ER, et al. Effect of heparin on infection of cells by equine arteritis virus. *J Vet Med Sci* 1997;59:727-728.
290. Sano Y, Inaba Y, Uwatoko K, et al. Effect of heparin on hemagglutination by equine arteritis virus. *J Vet Med Sci* 1998;60:447-450.
291. Dobbe JC, van der Meer Y, Spaan WJ, et al. Construction of chimeric arteriviruses reveals that the ectodomain of the major glycoprotein is not the main determinant of equine arteritis virus tropism in cell culture. *Virology* 2001;288:283-294.
292. Verheije MH, Welting TJ, Jansen HT, et al. Chimeric arteriviruses generated by swapping of the M protein ectodomain rule out a role of this domain in viral targeting. *Virology* 2002;303:364-373.
293. Molenkamp R, van Tol H, Rozier BC, et al. The arterivirus replicase is the only viral protein required for genome replication and subgenomic mRNA transcription. *J Gen Virol* 2000;81:2491-2496.
294. Tian D, Wei Z, Zevenhoven-Dobbe JC, et al. Arterivirus minor envelope proteins are a major determinant of viral tropism in cell culture. *J Virol* 2012;86:3701-3712.
295. Nauwynck HJ, Duan X, Favoreel HW, et al. Entry of porcine reproductive and respiratory syndrome virus into porcine alveolar macrophages via receptor-mediated endocytosis. *J Gen Virol* 1999;80 (Pt 2):297-305.
296. Kreutz LC, Ackermann MR. Porcine reproductive and respiratory syndrome virus enters cells through a low pH-dependent endocytic pathway. *Virus Res* 1996;42:137-147.
297. van Dinten LC, van Tol H, Gorbalenya AE, et al. The predicted metal-binding region of the arterivirus helicase protein is involved in subgenomic mRNA synthesis, genome replication, and virion biogenesis. *J Virol* 2000;74:5213-5223.
298. Snijder EJ, Wassenaar AL, Spaan WJ. The 5' end of the equine arteritis virus replicase gene encodes a papainlike cysteine protease. *J Virol* 1992;66:7040-7048.
299. Snijder EJ, Wassenaar AL, Spaan WJ, et al. The arterivirus Nsp2 protease. An unusual cysteine protease with primary structure similarities to both papain-like and chymotrypsin-like proteases. *J Biol Chem* 1995;270:16671-16676.

300. den Boon JA, Faaberg KS, Meulenberg JJ, et al. Processing and evolution of the N-terminal region of the arterivirus replicase ORF1a protein: identification of two papainlike cysteine proteases. *J Virol* 1995;69:4500-4505.
301. Snijder EJ, Wassenaar AL, van Dinten LC, et al. The arterivirus nsp4 protease is the prototype of a novel group of chymotrypsin-like enzymes, the 3C-like serine proteases. *J Biol Chem* 1996;271:4864-4871.
302. Wassenaar AL, Spaan WJ, Gorbalenya AE, et al. Alternative proteolytic processing of the arterivirus replicase ORF1a polyprotein: evidence that NSP2 acts as a cofactor for the NSP4 serine protease. *J Virol* 1997;71:9313-9322.
303. Gorbalenya AE, Koonin EV, Donchenko AP, et al. Coronavirus genome: prediction of putative functional domains in the non-structural polyprotein by comparative amino acid sequence analysis. *Nucleic Acids Res* 1989;17:4847-4861.
304. Gorbalenya AE, Blinov VM, Donchenko AP, et al. An NTP-binding motif is the most conserved sequence in a highly diverged monophyletic group of proteins involved in positive strand RNA viral replication. *J Mol Evol* 1989;28:256-268.
305. van Hemert MJ, de Wilde AH, Gorbalenya AE, et al. The in vitro RNA synthesizing activity of the isolated arterivirus replication/transcription complex is dependent on a host factor. *J Biol Chem* 2008;283:16525-16536.
306. Baric RS, Stohlman SA, Lai MM. Characterization of replicative intermediate RNA of mouse hepatitis virus: presence of leader RNA sequences on nascent chains. *J Virol* 1983;48:633-640.
307. Lai MM, Baric RS, Brayton PR, et al. Characterization of leader RNA sequences on the virion and mRNAs of mouse hepatitis virus, a cytoplasmic RNA virus. *Proc Natl Acad Sci U S A* 1984;81:3626-3630.
308. Spaan W, Delius H, Skinner M, et al. Coronavirus mRNA synthesis involves fusion of non-contiguous sequences. *Embo J* 1983;2:1839-1844.
309. Sawicki SG, Sawicki DL. Coronaviruses use discontinuous extension for synthesis of subgenome-length negative strands. *Adv Exp Med Biol* 1995;380:499-506.
310. Pasternak AO, Spaan WJ, Snijder EJ. Nidovirus transcription: how to make sense...? *J Gen Virol* 2006;87:1403-1421.
311. Pasternak AO, van den Born E, Spaan WJ, et al. Sequence requirements for RNA strand transfer during nidovirus discontinuous subgenomic RNA synthesis. *Embo J* 2001;20:7220-7228.
312. Pasternak AO, van den Born E, Spaan WJ, et al. The stability of the duplex between sense and antisense transcription-regulating sequences is a crucial factor in arterivirus subgenomic mRNA synthesis. *J Virol* 2003;77:1175-1183.
313. van Marle G, Dobbe JC, Gultyaev AP, et al. Arterivirus discontinuous mRNA transcription is guided by base pairing between sense and antisense transcription-regulating sequences. *Proc Natl Acad Sci U S A* 1999;96:12056-12061.
314. van den Born E, Posthuma CC, Gultyaev AP, et al. Discontinuous subgenomic RNA synthesis in arteriviruses is guided by an RNA hairpin structure located in the genomic leader region. *J Virol* 2005;79:6312-6324.
315. de Vries AA, Chirnside ED, Bredenbeek PJ, et al. All subgenomic mRNAs of equine arteritis virus contain a common leader sequence. *Nucleic Acids Res* 1990;18:3241-3247.

316. den Boon JA, Kleijnen MF, Spaan WJ, et al. Equine arteritis virus subgenomic mRNA synthesis: analysis of leader-body junctions and replicative-form RNAs. *J Virol* 1996;70:4291-4298.
317. de Vries AAF, Horzinek, M.C., Rottier, P.J.M., de Groot, R.J. The genome organization of the *Nidovirales*: similarities and differences between arteri-, toro-, and coronaviruses. *Semin Virol* 1997;8:33-47.
318. Sawicki D, Wang T, Sawicki S. The RNA structures engaged in replication and transcription of the A59 strain of mouse hepatitis virus. *J Gen Virol* 2001;82:385-396.
319. Sawicki SG, Sawicki DL, Siddell SG. A contemporary view of coronavirus transcription. *J Virol* 2007;81:20-29.
320. Snijder EJ, Meulenberg JJ. Arteriviruses In: Knipe DM, Howley, Peter M., Griffin, Diane E., Lamb, Robert A., Martin, Malcolm A., Roizman, B., Straus, S.E., ed. *Fields Virology*. Fourth ed. Philadelphia, PA, USA: Lippincott Williams & Wilkins, 2001;1205-1220.
321. Helenius A. Virus Entry and Uncoating In: Knipe DM, Howley, Peter M., Griffin, Diane E., Lamb, Robert A., Martin, Malcolm A., Roizman, B., Straus, S.E., ed. *Fields Virology*. 5th ed. Philadelphia, PA, USA: Lippincott Williams and Wilkins, 2007;99-118.
322. Berger EA, Murphy PM, Farber JM. Chemokine receptors as HIV-1 coreceptors: roles in viral entry, tropism, and disease. *Annu Rev Immunol* 1999;17:657-700.
323. Zhang Y, Bergelson JM. Adenovirus receptors. *J Virol* 2005;79:12125-12131.
324. Mondor I, Ugolini S, Sattentau QJ. Human immunodeficiency virus type 1 attachment to HeLa CD4 cells is CD4 independent and gp120 dependent and requires cell surface heparans. *J Virol* 1998;72:3623-3634.
325. Sattentau QJ, Weiss RA. The CD4 antigen: physiological ligand and HIV receptor. *Cell* 1988;52:631-633.
326. Choe H. Chemokine receptors in HIV-1 and SIV infection. *Arch Pharm Res* 1998;21:634-639.
327. Su CM, Liao CL, Lee YL, et al. Highly sulfated forms of heparin sulfate are involved in japanese encephalitis virus infection. *Virology* 2001;286:206-215.
328. Skehel JJ, Wiley DC. Receptor binding and membrane fusion in virus entry: the influenza hemagglutinin. *Annu Rev Biochem* 2000;69:531-569.
329. Haywood AM. Characteristics of Sendai virus receptors in a model membrane. *J Mol Biol* 1974;83:427-436.
330. Spillmann D. Heparan sulfate: anchor for viral intruders? *Biochimie* 2001;83:811-817.
331. Gorbalenya AE, Enjuanes L, Ziebuhr J, et al. Nidovirales: evolving the largest RNA virus genome. *Virus Res* 2006;117:17-37.
332. Dveksler GS, Dieffenbach CW, Cardellichio CB, et al. Several members of the mouse carcinoembryonic antigen-related glycoprotein family are functional receptors for the coronavirus mouse hepatitis virus-A59. *J Virol* 1993;67:1-8.
333. Dveksler GS, Pensiero MN, Cardellichio CB, et al. Cloning of the mouse hepatitis virus (MHV) receptor: expression in human and hamster cell lines confers susceptibility to MHV. *J Virol* 1991;65:6881-6891.
334. Nedellec P, Dveksler GS, Daniels E, et al. Bgp2, a new member of the carcinoembryonic antigen-related gene family, encodes an alternative receptor for mouse hepatitis viruses. *J Virol* 1994;68:4525-4537.

335. Baric RS, Sullivan E, Hensley L, et al. Persistent infection promotes cross-species transmissibility of mouse hepatitis virus. *J Virol* 1999;73:638-649.
336. Benbacer L, Kut E, Besnardeau L, et al. Interspecies aminopeptidase-N chimeras reveal species-specific receptor recognition by canine coronavirus, feline infectious peritonitis virus, and transmissible gastroenteritis virus. *J Virol* 1997;71:734-737.
337. Lai MM, Cavanagh D. The molecular biology of coronaviruses. *Adv Virus Res* 1997;48:1-100.
338. Li W, Moore MJ, Vasilieva N, et al. Angiotensin-converting enzyme 2 is a functional receptor for the SARS coronavirus. *Nature* 2003;426:450-454.
339. Gramberg T, Hofmann H, Moller P, et al. LSECtin interacts with filovirus glycoproteins and the spike protein of SARS coronavirus. *Virology* 2005;340:224-236.
340. Jeffers SA, Tusell SM, Gillim-Ross L, et al. CD209L (L-SIGN) is a receptor for severe acute respiratory syndrome coronavirus. *Proc Natl Acad Sci U S A* 2004;101:15748-15753.
341. Delputte PL, Vanderheijden N, Nauwynck HJ, et al. Involvement of the matrix protein in attachment of porcine reproductive and respiratory syndrome virus to a heparinlike receptor on porcine alveolar macrophages. *J Virol* 2002;76:4312-4320.
342. Vanderheijden N, Delputte PL, Favoreel HW, et al. Involvement of sialoadhesin in entry of porcine reproductive and respiratory syndrome virus into porcine alveolar macrophages. *J Virol* 2003;77:8207-8215.
343. Vanderheijden N, Delputte P, Nauwynck H, et al. Effects of heparin on the entry of porcine reproductive and respiratory syndrome virus into alveolar macrophages. *Adv Exp Med Biol* 2001;494:683-689.
344. Delputte PL, Costers S, Nauwynck HJ. Analysis of porcine reproductive and respiratory syndrome virus attachment and internalization: distinctive roles for heparan sulphate and sialoadhesin. *J Gen Virol* 2005;86:1441-1445.
345. Calvert JG, Slade DE, Shields SL, et al. CD163 expression confers susceptibility to porcine reproductive and respiratory syndrome viruses. *J Virol* 2007;81:7371-7379.
346. Van Gorp H, Van Breedam W, Delputte PL, et al. Sialoadhesin and CD163 join forces during entry of the porcine reproductive and respiratory syndrome virus. *J Gen Virol* 2008;89:2943-2953.
347. Delputte PL, Nauwynck HJ. Porcine arterivirus infection of alveolar macrophages is mediated by sialic acid on the virus. *J Virol* 2004;78:8094-8101.
348. Delputte PL, Nauwynck HJ. Porcine arterivirus entry in macrophages: heparan sulfate-mediated attachment, sialoadhesin-mediated internalization, and a cell-specific factor mediating virus disassembly and genome release. *Adv Exp Med Biol* 2006;581:247-252.
349. Delputte PL, Van Breedam W, Delrue I, et al. Porcine arterivirus attachment to the macrophage-specific receptor sialoadhesin is dependent on the sialic acid-binding activity of the N-terminal immunoglobulin domain of sialoadhesin. *J Virol* 2007;81:9546-9550.
350. Delputte P, Van Gorp H, Van Breedam W, et al. Porcine reproductive and respiratory syndrome virus (PRRSV) entry in macrophages. *XIth Nidovirus Symposium*. Oxford, United Kingdom, 2008.
351. Kowalchyk K, Plagemann PG. Cell surface receptors for lactate dehydrogenase-elevating virus on subpopulation of macrophages. *Virus Res* 1985;2:211-229.

352. Inada T, Mims CA. Ia antigens and Fc receptors of mouse peritoneal macrophages as determinants of susceptibility to lactic dehydrogenase virus. *J Gen Virol* 1985;66 (Pt 7):1469-1477.
353. Inada T, Mims CA. Mouse Ia antigens are receptors for lactate dehydrogenase virus. *Nature* 1984;309:59-61.
354. Buxton IK, Chan SP, Plagemann PG. The IA antigen is not the major receptor for lactate dehydrogenase-elevating virus on macrophages from CBA and BALB/c mice. *Virus Res* 1988;9:205-219.
355. Yamada S, Suzuki Y, Suzuki T, et al. Haemagglutinin mutations responsible for the binding of H5N1 influenza A viruses to human-type receptors. *Nature* 2006;444:378-382.
356. Moore JP. Coreceptors: implications for HIV pathogenesis and therapy. *Science* 1997;276:51-52.
357. Kwong PD, Wyatt R, Robinson J, et al. Structure of an HIV gp120 envelope glycoprotein in complex with the CD4 receptor and a neutralizing human antibody. *Nature* 1998;393:648-659.
358. Olshevsky U, Helseth E, Furman C, et al. Identification of individual human immunodeficiency virus type 1 gp120 amino acids important for CD4 receptor binding. *J Virol* 1990;64:5701-5707.
359. Cordonnier A, Montagnier L, Emerman M. Single amino-acid changes in HIV envelope affect viral tropism and receptor binding. *Nature* 1989;340:571-574.
360. Crublet E, Andrieu JP, Vives RR, et al. The HIV-1 envelope glycoprotein gp120 features four heparan sulfate binding domains, including the co-receptor binding site. *J Biol Chem* 2008;283:15193-15200.
361. Howitt J, Anderson CW, Freimuth P. Adenovirus interaction with its cellular receptor CAR. *Curr Top Microbiol Immunol* 2003;272:331-364.
362. Hogle JM, Chow M, Filman DJ. Three-dimensional structure of poliovirus at 2.9 A resolution. *Science* 1985;229:1358-1365.
363. Filman DJ, Syed R, Chow M, et al. Structural factors that control conformational transitions and serotype specificity in type 3 poliovirus. *EMBO J* 1989;8:1567-1579.
364. Crocker PR, Mucklow S, Bouckson V, et al. Sialoadhesin, a macrophage sialic acid binding receptor for haemopoietic cells with 17 immunoglobulin-like domains. *EMBO J* 1994;13:4490-4503.
365. Faaberg KS, Even C, Palmer GA, et al. Disulfide bonds between two envelope proteins of lactate dehydrogenase-elevating virus are essential for viral infectivity. *J Virol* 1995;69:613-617.
366. Das PB, Dinh PX, Ansari IH, et al. The minor envelope glycoproteins GP2a and GP4 of porcine reproductive and respiratory syndrome virus interact with the receptor CD163. *J Virol* 2010;84:1731-1740.
367. Go YY, Cook RF, Fulgencio JQ, et al. Assessment of correlation between in vitro CD3(+) T cell susceptibility to EAV infection and clinical outcome following experimental infection. *Vet Microbiol* 2011.
368. Huntington PJ, Ellis PM, Forman AJ, et al. Equine viral arteritis. *Aust Vet J* 1990;67:429-431.
369. Carman S, Rae C, Dubovi E. Ontario. Equine arteritis virus isolated from a Standardbred foal with pneumonia. *Can Vet J* 1988;29:937.

370. Wieringa R, De Vries AA, Post SM, et al. Intra- and intermolecular disulfide bonds of the GP2b glycoprotein of equine arteritis virus: relevance for virus assembly and infectivity. *J Virol* 2003;77:12996-13004.
371. World Organization for Animal Health (OIE). *OIE Manual of Diagnostic Tests and Vaccines for Terrestrial Animals*. 5th ed. Paris, France: Office International des Epizooties, 2004.
372. Glaser AL, de Vries AA, Dubovi EJ. Comparison of equine arteritis virus isolates using neutralizing monoclonal antibodies and identification of sequence changes in G_L associated with neutralization resistance. *J Gen Virol* 1995;76 2223-2233.
373. Balasuriya UB, Leutenegger CM, Topol JB, et al. Detection of equine arteritis virus by real-time TaqMan reverse transcription-PCR assay. *J Virol Methods* 2002;101:21-28.
374. Belak S. The molecular diagnosis of porcine viral diseases: a review. *Acta Vet Hung* 2005;53:113-124.
375. Belak S. Molecular diagnosis of viral diseases, present trends and future aspects A view from the OIE Collaborating Centre for the Application of Polymerase Chain Reaction Methods for Diagnosis of Viral Diseases in Veterinary Medicine. *Vaccine* 2007;25:5444-5452.
376. Gilbert SA, Timoney PJ, McCollum WH, et al. Detection of equine arteritis virus in the semen of carrier stallions by using a sensitive nested PCR assay. *J Clin Microbiol* 1997;35:2181-2183.
377. Leutenegger CM, Higgins J, Matthews TB, et al. Real-time TaqMan PCR as a specific and more sensitive alternative to the branched-chain DNA assay for quantitation of simian immunodeficiency virus RNA. *AIDS Res Hum Retroviruses* 2001;17:243-251.
378. McKillen J, Hjertner B, Millar A, et al. Molecular beacon real-time PCR detection of swine viruses. *J Virol Methods* 2007;140:155-165.
379. Westcott DG, King DP, Drew TW, et al. Use of an internal standard in a closed one-tube RT-PCR for the detection of equine arteritis virus RNA with fluorescent probes. *Vet Res* 2003;34:165-176.
380. Chirnside ED, Spaan WJ. Reverse transcription and cDNA amplification by the polymerase chain reaction of equine arteritis virus (EAV). *J Virol Methods* 1990;30:133-140.
381. Ramina A, Dalla Valle L, De Mas S, et al. Detection of equine arteritis virus in semen by reverse transcriptase polymerase chain reaction-ELISA. *Comp Immunol Microbiol Infect Dis* 1999;22:187-197.
382. Sekiguchi K, Sugita S, Fukunaga Y, et al. Detection of equine arteritis virus (EAV) by polymerase chain reaction (PCR) and differentiation of EAV strains by restriction enzyme analysis of PCR products. *Arch Virol* 1995;140:1483-1491.
383. Starick E. Rapid and sensitive detection of equine arteritis virus in semen and tissue samples by reverse transcription-polymerase chain reaction, dot blot hybridisation and nested polymerase chain reaction. *Acta Virol* 1998;42:333-339.
384. Balasuriya UB, Snijder EJ, van Dinten LC, et al. Equine arteritis virus derived from an infectious cDNA clone is attenuated and genetically stable in infected stallions. *Virology* 1999;260:201-208.

385. Balasuriya UB, Timoney PJ, McCollum WH, et al. Phylogenetic analysis of open reading frame 5 of field isolates of equine arteritis virus and identification of conserved and nonconserved regions in the GL envelope glycoprotein. *Virology* 1995;214:690-697.
386. Bell SA, Balasuriya UB, Nordhausen RW, et al. Isolation of equine herpesvirus-5 from blood mononuclear cells of a gelding. *J Vet Diagn Invest* 2006;18:472-475.
387. Glaser AL, Renshaw RW, Trock SC, et al. Isolation of Salem virus, a novel equine paramyxovirus, and assessment of its etiologic role in a disease outbreak. *Vet Microbiol* 2002;87:205-212.
388. Balasuriya UB, Snijder EJ, Heidner HW, et al. Development and characterization of an infectious cDNA clone of the virulent Bucyrus strain of Equine arteritis virus. *J Gen Virol* 2007;88:918-924.
389. Clopper C, Pearson S. The use of confidence or fiducial limits illustrated in the case of the binomial. *Biometrika* 1934;26:404-413.
390. Bustin SA. Absolute quantification of mRNA using real-time reverse transcription polymerase chain reaction assays. *J Mol Endocrinol* 2000;25:169-193.
391. Klein D, Janda P, Steinborn R, et al. Proviral load determination of different feline immunodeficiency virus isolates using real-time polymerase chain reaction: influence of mismatches on quantification. *Electrophoresis* 1999;20:291-299.
392. Klein D, Leutenegger CM, Bahula C, et al. Influence of preassay and sequence variations on viral load determination by a multiplex real-time reverse transcriptase-polymerase chain reaction for feline immunodeficiency virus. *J Acquir Immune Defic Syndr* 2001;26:8-20.
393. Nakayama T, Mori T, Yamaguchi S, et al. Detection of measles virus genome directly from clinical samples by reverse transcriptase-polymerase chain reaction and genetic variability. *Virus Res* 1995;35:1-16.
394. Murphy FA, Gibbs EPJ, Horzinek MC, et al. *Veterinary Virology*. 3rd ed. San Diego: Veterinary Virology Academic Press, 1999.
395. Brown LE, Hinshaw VS, Webster RG. Antigenic variation in the influenza A virus nonstructural protein, NS1. *Virology* 1983;130:134-143.
396. Daniels RS, Skehel JJ, Wiley DC. Amino acid sequences of haemagglutinins of influenza viruses of the H3 subtype isolated from horses. *J Gen Virol* 1985;66 (Pt 3):457-464.
397. Klingeborn B, Rockborn G, Dinter Z. Significant antigenic drift within the influenza equi 2 subtype in Sweden. *Vet Rec* 1980;106:363-364.
398. Ozaki H, Shimizu-Nei A, Sugita S, et al. Antigenic variation among equine H 3 N 8 influenza virus hemagglutinins. *Jpn J Vet Res* 2001;48:177-186.
399. van Oirschot JT, Masurel N, Huffels AD, et al. Equine influenza in the Netherlands during the winter of 1978-1979; antigenic drift of the A-equi 2 virus. *Vet Q* 1981;3:80-84.
400. Wilson WD. Equine influenza. *Vet Clin North Am Equine Pract* 1993;9:257-282.
401. Office International des Epizooties (OIE). Equine Influenza. *Manual of Diagnostic Tests and Vaccines for Terrestrial Animals*. Paris, France: OIE, 2000;546-557.
402. Chambers TM, Shortridge KF, Li PH, et al. Rapid diagnosis of equine influenza by the Directigen FLU-A enzyme immunoassay. *Vet Rec* 1994;135:275-279.
403. Donofrio JC, Coonrod JD, Chambers TM. Diagnosis of equine influenza by the polymerase chain reaction. *J Vet Diagn Invest* 1994;6:39-43.

404. Fouchier RA, Bestebroer TM, Herfst S, et al. Detection of influenza A viruses from different species by PCR amplification of conserved sequences in the matrix gene. *J Clin Microbiol* 2000;38:4096-4101.
405. Munch M, Nielsen LP, Handberg KJ, et al. Detection and subtyping (H5 and H7) of avian type A influenza virus by reverse transcription-PCR and PCR-ELISA. *Arch Virol* 2001;146:87-97.
406. Oxburgh L, Hagstrom A. A PCR based method for the identification of equine influenza virus from clinical samples. *Vet Microbiol* 1999;67:161-174.
407. Yamanaka T, Tsujimura K, Kondo T, et al. Evaluation of antigen detection kits for diagnosis of equine influenza. *J Vet Med Sci* 2008;70:189-192.
408. Quinlivan M, Cullinane A, Nelly M, et al. Comparison of sensitivities of virus isolation, antigen detection, and nucleic acid amplification for detection of equine influenza virus. *J Clin Microbiol* 2004;42:759-763.
409. Foord AJ, Selleck P, Colling A, et al. Real-time RT-PCR for detection of equine influenza and evaluation using samples from horses infected with A/equine/Sydney/2007 (H3N8). *Vet Microbiol* 2008;137:1-9.
410. Donofrio JC, Coonrod JD, Davidson JN, et al. Detection of influenza A and B in respiratory secretions with the polymerase chain reaction. *PCR Methods Appl* 1992;1:263-268.
411. Spackman E, Senne DA, Myers TJ, et al. Development of a real-time reverse transcriptase PCR assay for type A influenza virus and the avian H5 and H7 hemagglutinin subtypes. *J Clin Microbiol* 2002;40:3256-3260.
412. Cahill J. Biosecurity Austrlia Advice 2008/22. Department of Agriculture, Fisheries and Forestry. http://www/daff.gov.au/, 2008.
413. Hoffmann E, Stech J, Guan Y, et al. Universal primer set for the full-length amplification of all influenza A viruses. *Arch Virol* 2001;146:2275-2289.
414. Branscum AJ, Gardner IA, Johnson WO. Estimation of diagnostic-test sensitivity and specificity through Bayesian modeling. *Prev Vet Med* 2005;68:145-163.
415. Lunn DJ, Thomas, A., Best, N., Spiegelhalter, D. WinBUGS - a Bayesian modelling framework: concepts, structure, and extensibility. *Statistics and Computing* 2000;10:325-337.
416. R Development Core Team. *A language and environment for statistical computing*. Vienna, Austria: R Foundation for Statistical Computing, 2008.
417. Yao Y, Nellaker C, Karlsson H. Evaluation of minor groove binding probe and Taqman probe PCR assays: Influence of mismatches and template complexity on quantification. *Mol Cell Probes* 2006;20:311-316.
418. Ito T, Kawaoka Y, Ohira M, et al. Replacement of internal protein genes, with the exception of the matrix, in equine 1 viruses by equine 2 influenza virus genes during evolution in nature. *J Vet Med Sci* 1999;61:987-989.
419. Bean WJ. Correlation of influenza A virus nucleoprotein genes with host species. *Virology* 1984;133:438-442.
420. Gorman OT, Bean WJ, Kawaoka Y, et al. Evolution of the nucleoprotein gene of influenza A virus. *J Virol* 1990;64:1487-1497.
421. Ismail TM, Sami AM, Youssef HM, et al. An outbreak of equine influenza type 1 in Egypt in 1989. *Vet Med J Giza* 1990;38:195-206.

422. Madic J, Martinovic S, Naglic T, et al. Serological evidence for the presence of A/equine-1 influenza virus in unvaccinated horses in Croatia. *Vet Rec* 1996;138:68.
423. Singh G. Characterization of A/eq-1 virus isolated during the equine influenza epidemic in India. *Acta Virol* 1994;38:25-26.
424. Webster RG. Influenza: an emerging disease. *Emerg Infect Dis* 1998;4:436-441.
425. Amonsin A, Songserm T, Chutinimitkul S, et al. Genetic analysis of influenza A virus (H5N1) derived from domestic cat and dog in Thailand. *Arch Virol* 2007;152:1925-1933.
426. Songserm T, Amonsin A, Jam-on R, et al. Fatal avian influenza A H5N1 in a dog. *Emerg Infect Dis* 2006;12:1744-1747.
427. Maas R, Tacken M, Ruuls L, et al. Avian influenza (H5N1) susceptibility and receptors in dogs. *Emerg Infect Dis* 2007;13:1219-1221.
428. Giese M, Harder TC, Teifke JP, et al. Experimental infection and natural contact exposure of dogs with avian influenza virus (H5N1). *Emerg Infect Dis* 2008;14:308-310.
429. Kilbourne ED, Kehoe JM. Demonstration of antibodies to both hemagglutinin and neuraminidase antigens of H3N2 influenza A virus in domestic dogs. *Intervirology* 1975;6:315-318.
430. Song D, Kang B, Lee C, et al. Transmission of avian influenza virus (H3N2) to dogs. *Emerg Infect Dis* 2008;14:741-746.
431. Song D, Lee C, Kang B, et al. Experimental infection of dogs with avian-origin canine influenza A virus (H3N2). *Emerg Infect Dis* 2009;15:56-58.
432. Fraser C, Donnelly CA, Cauchemez S, et al. Pandemic potential of a strain of influenza A (H1N1): early findings. *Science* 2009;324:1557-1561.
433. Garten RJ, Davis CT, Russell CA, et al. Antigenic and genetic characteristics of swine-origin 2009 A(H1N1) influenza viruses circulating in humans. *Science* 2009;325:197-201.
434. ProMED-mail. Influenza Pandemic (H1N1) 2009, Animal (30): China, Canine, 2009.
435. Dubovi EJ, Njaa BL. Canine influenza. *Vet Clin North Am Small Anim Pract* 2008;38:827-835, viii.
436. Payungporn S, Crawford PC, Kouo TS, et al. Influenza A virus (H3N8) in dogs with respiratory disease, Florida. *Emerg Infect Dis* 2008;14:902-908.
437. Yoon KJ, Cooper VL, Schwartz KJ, et al. Influenza virus infection in racing greyhounds. *Emerg Infect Dis* 2005;11:1974-1976.
438. Spindel ME, Lunn KF, Dillion S, et al. Detection and Quantification of canine influenza virus by one-step real-time reverse transcription PCR. *J Vet Intern Med* 2007;21:576.
439. Vander Veen R, Kamrud K, Mogler M, et al. Rapid Development of an Efficacious Swine Vaccine for Novel H1N1. *PLoS Curr Influenza* 2009:RRN1123.
440. Dong H, Zhang Y, Xiong H, et al. Detection of human novel influenza A (H1N1) viruses using multi-fluorescent real-time RT-PCR. *Virus Res* 2009;147:85-90.
441. Stanway G, Brown F, Christian P. Family Picornaviridae. In: Fauquet CM, Mayo MA, Maniloff J, et al., eds. *Virus Taxonomy: Eighth Report of the International Committee on Taxonomy of Viruses*. San Diego: Elsevier Academic Press, 2005;757–778.
442. Steil BP, Barton DJ. Cis-active RNA elements (CREs) and picornavirus RNA replication. *Virus Res* 2009;139:240-252.

443. Paul AV. Possible unifying mechanism of picornavirus genome replication In: Semler BL,Wimmer E, eds. *Molecular biology of picornaviruses*. Washington, D.C.: ASM Press, 2002;227-246.
444. Kok CC, McMinn PC. Picornavirus RNA-dependent RNA polymerase. *Int J Biochem Cell Biol* 2009;41:498-502.
445. Li F, Browning GF, Studdert MJ, et al. Equine rhinovirus 1 is more closely related to foot-and-mouth disease virus than to other picornaviruses. *Proc Natl Acad Sci U S A* 1996;93:990-995.
446. Wutz G, Auer H, Nowotny N, et al. Equine rhinovirus serotypes 1 and 2: relationship to each other and to aphthoviruses and cardioviruses. *J Gen Virol* 1996;77 (Pt 8):1719-1730.
447. Steck F, Hofer B, Schaeren B, et al. Equine rhinoviruses : new serotypes. the Fourth International Conference on Equine Infectious Diseases 1978;321-328.
448. Black WD, Hartley CA, Ficorilli NP, et al. Sequence variation divides Equine rhinitis B virus into three distinct phylogenetic groups that correlate with serotype and acid stability. *J Gen Virol* 2005;86:2323-2332.
449. Black WD, Studdert MJ. Formerly unclassified, acid-stable equine picornaviruses are a third equine rhinitis B virus serotype in the genus Erbovirus. *J Gen Virol* 2006;87:3023-3027.
450. Huang JA, Ficorilli N, Hartley CA, et al. Equine rhinitis B virus: a new serotype. *J Gen Virol* 2001;82:2641-2645.
451. Burrell MH, Wood JL, Whitwell KE, et al. Respiratory disease in thoroughbred horses in training: the relationships between disease and viruses, bacteria and environment. *Vet Rec* 1996;139:308-313.
452. Carman S, Rosendal S, Huber L, et al. Infectious agents in acute respiratory disease in horses in Ontario. *J Vet Diagn Invest* 1997;9:17-23.
453. Fukunaga Y, Kumanomido T, Kamada M, et al. Equine picornavirus: isolation of virus from the oral cavity of healthy horses. *Bull Equine Res Inst* 1983;20:103-109.
454. Johnson DJ, Ostlund EN, Palmer TJ, et al. Isolation of equine rhinitis A virus from horse semen contaminated with urine. *J Vet Diagn Invest* 2012;In press.
455. Plummer G, Kerry JB. Studies on an equine respiratory virus. *Veterinary record* 1962;74:967-970.
456. Hoffer B, Steck F, Gerber H, et al. An investigation of the etiology of viral respiratory disease in a remount depot. 3rd International Conference of Equine Infectious Disease 1972;527-545.
457. Black WD, Hartley CA, Ficorilli NP, et al. Reverse transcriptase-polymerase chain reaction for the detection equine rhinitis B viruses and cell culture isolation of the virus. *Arch Virol* 2007;152:137-149.
458. Burrows R. Laboratory diagnosis of some virus infections of the upper respiratory tract of the horse. *Equine Vet J* 1968;1:32-36.
459. Klaey M, Sanchez-Higgins M, Leadon DP, et al. Field case study of equine rhinovirus 1 infection: clinical signs and clinicopathology. *Equine Vet J* 1998;30:267-269.
460. McCollum WH. In: Balasuriya UB, ed, 2008.
461. Willoughby R, Ecker G, McKee S, et al. The effects of equine rhinovirus, influenza virus and herpesvirus infection on tracheal clearance rate in horses. *Can J Vet Res* 1992;56:115-121.

462. Powell DG, Burrows R, Spooner PR, et al. A study of infectious respiratory disease among horses in Great Britain, 1971-1976. 4th International Conference on Equine Infectious Disease 1978;451-459.
463. Faaberg KS, Balasuriya UB, Brinton MA, et al. Family - Arteriviridae In: Andrew MQK, Elliot L, Michael JA, et al., eds. *Virus Taxonomy*. San Diego: Elsevier, 2012;796-805.
464. Snijder EJ, Meulenberg JJ. The molecular biology of arteriviruses. *J Gen Virol* 1998;79 (Pt 5):961-979.
465. Russell P, Atkinson K, Krishnan L. Recurrent reproductive failure due to severe placental villitis of unknown etiology. *J Reprod Med* 1980;24:93-98.
466. Wensvoort G, Terpstra C, Pol JM, et al. Mystery swine disease in The Netherlands: the isolation of Lelystad virus. *Vet Q* 1991;13:121-130.
467. Johnson CR, Griggs TF, Gnanandarajah J, et al. Novel structural protein in porcine reproductive and respiratory syndrome virus encoded by an alternative ORF5 present in all arteriviruses. *J Gen Virol* 2011;92:1107-1116.
468. Snijder EJ, Spaan WJ. Arteriviruses In: Knipe DM, Howley, Peter M., Griffin, Diane E., Lamb, Robert A., Martin, Malcolm A., Roizman, B., Straus, S.E., ed. *Fields Virology*. 5th ed. Philadelphia: Lippincott Williams & Wilkins, 2006;1337-1355.
469. Mardassi H, Massie B, Dea S. Intracellular synthesis, processing, and transport of proteins encoded by ORFs 5 to 7 of porcine reproductive and respiratory syndrome virus. *Virology* 1996;221:98-112.
470. Balasuriya UB, Heidner HW, Davis NL, et al. Alphavirus replicon particles expressing the two major envelope proteins of equine arteritis virus induce high level protection against challenge with virulent virus in vaccinated horses. *Vaccine* 2002;20:1609-1617.
471. Ostrowski M, Galeota JA, Jar AM, et al. Identification of neutralizing and nonneutralizing epitopes in the porcine reproductive and respiratory syndrome virus GP5 ectodomain. *J Virol* 2002;76:4241-4250.
472. Jiang Y, Xiao S, Fang L, et al. DNA vaccines co-expressing GP5 and M proteins of porcine reproductive and respiratory syndrome virus (PRRSV) display enhanced immunogenicity. *Vaccine* 2006;24:2869-2879.
473. Faaberg KS. Arterivirus structural proteins and assembly In: Perlman S, Gallagher T,Snijder EJ, eds. *Nidovirus*. Washington, DC: AMS Press, 2008;211-234.
474. Faaberg KS, Plagemann PG. The envelope proteins of lactate dehydrogenase-elevating virus and their membrane topography. *Virology* 1995;212:512-525.
475. de Vries AA, Chirnside ED, Horzinek MC, et al. Structural proteins of equine arteritis virus. *J Virol* 1992;66:6294-6303.
476. Meulenberg JJ, Petersen-den Besten A, De Kluyver EP, et al. Characterization of proteins encoded by ORFs 2 to 7 of Lelystad virus. *Virology* 1995;206:155-163.
477. de Vries AF, Chirnside ED, Horzinek MC, et al. Equine arteritis virus contains a unique set of four structural proteins. *Adv Exp Med Biol* 1993;342:245-253.
478. Wu WH, Fang Y, Farwell R, et al. A 10-kDa structural protein of porcine reproductive and respiratory syndrome virus encoded by ORF2b. *Virology* 2001;287:183-191.
479. Wu WH, Fang Y, Rowland RR, et al. The 2b protein as a minor structural component of PRRSV. *Virus Res* 2005;114:177-181.

480. Wissink EH, Kroese MV, van Wijk HA, et al. Envelope protein requirements for the assembly of infectious virions of porcine reproductive and respiratory syndrome virus. *J Virol* 2005;79:12495-12506.
481. Kim HS, Kwang J, Yoon IJ, et al. Enhanced replication of porcine reproductive and respiratory syndrome (PRRS) virus in a homogeneous subpopulation of MA-104 cell line. *Arch Virol* 1993;133:477-483.
482. Duan X, Nauwynck HJ, Pensaert MB. Effects of origin and state of differentiation and activation of monocytes/macrophages on their susceptibility to porcine reproductive and respiratory syndrome virus (PRRSV). *Arch Virol* 1997;142:2483-2497.
483. Lawson SR, Rossow KD, Collins JE, et al. Porcine reproductive and respiratory syndrome virus infection of gnotobiotic pigs: sites of virus replication and co-localization with MAC-387 staining at 21 days post-infection. *Virus Res* 1997;51:105-113.
484. Rossow KD. Porcine reproductive and respiratory syndrome. *Vet Pathol* 1998;35:1-20.
485. Plagemann PG, Moennig V. Lactate dehydrogenase-elevating virus, equine arteritis virus, and simian hemorrhagic fever virus: a new group of positive-strand RNA viruses. *Adv Virus Res* 1992;41:99-192.
486. Hedges JF, Demaula CD, Moore BD, et al. Characterization of equine E-selectin. *Immunology* 2001;103:498-504.
487. Maess J, Reczko E, Bohm HO. [Equine arteritis virus: multiplication in BHK 21-cells buoyant density and electron microscopical demonstration]. *Arch Gesamte Virusforsch* 1970;30:47-58.
488. Konishi S, Akashi H, Sentsui H, et al. Studies on equine viral arteritis. I. Characterization of the virus and trial survey on antibody with Vero cell cultures. *Nihon Juigaku Zasshi* 1975;37:259-267.
489. Van Breedam W, Delputte PL, Van Gorp H, et al. Porcine reproductive and respiratory syndrome virus entry into the porcine macrophage. *J Gen Virol* 2010;91:1659-1667.
490. Das PB, Vu HL, Dinh PX, et al. Glycosylation of minor envelope glycoproteins of porcine reproductive and respiratory syndrome virus in infectious virus recovery, receptor interaction, and immune response. *Virology* 2011;410:385-394.
491. Pirzadeh B, Gagnon CA, Dea S. Genomic and antigenic variations of porcine reproductive and respiratory syndrome virus major envelope GP5 glycoprotein. *Can J Vet Res* 1998;62:170-177.
492. Zhang J, Go Y, Meade BJ, et al. Development and characterization of an infectious cDNA clone of the modified live virus vaccine strain of equine arteritis virus and its potential as a vaccine vector. *Submitted* 2012.
493. de Vries AA, Glaser AL, Raamsman MJ, et al. Genetic manipulation of equine arteritis virus using full-length cDNA clones: separation of overlapping genes and expression of a foreign epitope. *Virology* 2000;270:84-97.
494. Zhang J, Go YY, MacLachlan NJ, et al. Amino acid substitutions in the structural or nonstructural proteins of a vaccine strain of equine arteritis virus are associated with its attenuation. *Virology* 2008;378:355-362.
495. Nelson EA, Christopher-Hennings J, Drew T, et al. Differentiation of U.S. and European isolates of porcine reproductive and respiratory syndrome virus by monoclonal antibodies. *J Clin Microbiol* 1993;31:3184-3189.

496. de Vries AA, Glaser AL, Raamsman MJ, et al. Recombinant equine arteritis virus as an expression vector. *Virology* 2001;284:259-276.
497. Van Breedam W, Van Gorp H, Zhang JQ, et al. The M/GP(5) glycoprotein complex of porcine reproductive and respiratory syndrome virus binds the sialoadhesin receptor in a sialic acid-dependent manner. *PLoS Pathog* 2010;6:e1000730.
498. Weingartl HM, Sabara M, Pasick J, et al. Continuous porcine cell lines developed from alveolar macrophages: partial characterization and virus susceptibility. *J Virol Methods* 2002;104:203-216.
499. Balasuriya UB, MacLachlan NJ, De Vries AA, et al. Identification of a neutralization site in the major envelope glycoprotein (GL) of equine arteritis virus. *Virology* 1995;207:518-527.
500. Plagemann PG. The primary GP5 neutralization epitope of North American isolates of porcine reproductive and respiratory syndrome virus. *Vet Immunol Immunopathol* 2004;102:263-275.
501. Plagemann PG, Rowland RR, Faaberg KS. The primary neutralization epitope of porcine respiratory and reproductive syndrome virus strain VR-2332 is located in the middle of the GP5 ectodomain. *Arch Virol* 2002;147:2327-2347.
502. Han W, Wu JJ, Deng XY, et al. Molecular mutations associated with the in vitro passage of virulent porcine reproductive and respiratory syndrome virus. *Virus Genes* 2009;38:276-284.
503. Snijder EJ, Wassenaar AL, Spaan WJ. Proteolytic processing of the replicase ORF1a protein of equine arteritis virus. *J Virol* 1994;68:5755-5764.
504. van Aken D, Zevenhoven-Dobbe J, Gorbalenya AE, et al. Proteolytic maturation of replicase polyprotein pp1a by the nsp4 main proteinase is essential for equine arteritis virus replication and includes internal cleavage of nsp7. *J Gen Virol* 2006;87:3473-3482.
505. Zevenhoven-Dobbe JC, Greve S, van Tol H, et al. Rescue of disabled infectious single-cycle (DISC) equine arteritis virus by using complementing cell lines that express minor structural glycoproteins. *J Gen Virol* 2004;85:3709-3714.
506. Rostand KS, Esko JD. Microbial adherence to and invasion through proteoglycans. *Infect Immun* 1997;65:1-8.
507. Bhavanandan VP, Davidson EA. Proteoglycans: structure, synthesis, function. In: Allen HJ,Kisailus EC, eds. *Glycoconjugates: composition, structure, and function*. New York, NY.: Marcel Dekker, 1991;167-202.
508. Prydz K, Dalen KT. Synthesis and sorting of proteoglycans. *J Cell Sci* 2000;113 Pt 2:193-205.
509. Sasisekharan R, Venkataraman G. Heparin and heparan sulfate: biosynthesis, structure and function. *Curr Opin Chem Biol* 2000;4:626-631.
510. Park PW, Reizes O, Bernfield M. Cell surface heparan sulfate proteoglycans: selective regulators of ligand-receptor encounters. *J Biol Chem* 2000;275:29923-29926.
511. Esko JD, Selleck SB. Order out of chaos: assembly of ligand binding sites in heparan sulfate. *Annu Rev Biochem* 2002;71:435-471.
512. Byrnes AP, Griffin DE. Binding of Sindbis virus to cell surface heparan sulfate. *J Virol* 1998;72:7349-7356.
513. Chen Y, Maguire T, Hileman RE, et al. Dengue virus infectivity depends on envelope protein binding to target cell heparan sulfate. *Nat Med* 1997;3:866-871.

514. Compton T, Nowlin DM, Cooper NR. Initiation of human cytomegalovirus infection requires initial interaction with cell surface heparan sulfate. *Virology* 1993;193:834-841.
515. Klimstra WB, Ryman KD, Johnston RE. Adaptation of Sindbis virus to BHK cells selects for use of heparan sulfate as an attachment receptor. *J Virol* 1998;72:7357-7366.
516. Krusat T, Streckert HJ. Heparin-dependent attachment of respiratory syncytial virus (RSV) to host cells. *Arch Virol* 1997;142:1247-1254.
517. Laquerre S, Argnani R, Anderson DB, et al. Heparan sulfate proteoglycan binding by herpes simplex virus type 1 glycoproteins B and C, which differ in their contributions to virus attachment, penetration, and cell-to-cell spread. *J Virol* 1998;72:6119-6130.
518. WuDunn D, Spear PG. Initial interaction of herpes simplex virus with cells is binding to heparan sulfate. *J Virol* 1989;63:52-58.
519. Liu J, Thorp SC. Cell surface heparan sulfate and its roles in assisting viral infections. *Med Res Rev* 2002;22:1-25.
520. Conrad HE. *Heparin-binding proteins*. San Diego: Academic, 1998.
521. Cardin AD, Weintraub HJ. Molecular modeling of protein-glycosaminoglycan interactions. *Arteriosclerosis* 1989;9:21-32.
522. Huntington JA, Olson ST, Fan B, et al. Mechanism of heparin activation of antithrombin. Evidence for reactive center loop preinsertion with expulsion upon heparin binding. *Biochemistry* 1996;35:8495-8503.
523. Moore BD, Balasuriya UB, Hedges JF, et al. Growth characteristics of a highly virulent, a moderately virulent, and an avirulent strain of equine arteritis virus in primary equine endothelial cells are predictive of their virulence to horses. *Virology* 2002;298:39-44.
524. McCollum WH, Timoney PJ. Experimental observation on the virulence of isolates of equine arteritis virus. 8th International Conference on Equine Infectious Diseases 1999;558-559.
525. McCollum WH, Doll, E.R., Wilson, J.C., Cheatham, J. Isolation and propagation of equine arteritis virus in monolayer cell cultures of rabbit kidney. *Cornell Vet* 1962;52:452-458.
526. Balasuriya UB, Rossitto PV, DeMaula CD, et al. A 29K envelope glycoprotein of equine arteritis virus expresses neutralization determinants recognized by murine monoclonal antibodies. *J Gen Virol* 1993;74 (Pt 11):2525-2529.
527. Thompson JD, Gibson TJ, Plewniak F, et al. The CLUSTAL_X windows interface: flexible strategies for multiple sequence alignment aided by quality analysis tools. *Nucleic Acids Res* 1997;25:4876-4882.
528. Jones DT. Improving the accuracy of transmembrane protein topology prediction using evolutionary information. *Bioinformatics* 2007;23:538-544.
529. Jones DT, Taylor WR, Thornton JM. A model recognition approach to the prediction of all-helical membrane protein structure and topology. *Biochemistry* 1994;33:3038-3049.
530. Krogh A, Larsson B, von Heijne G, et al. Predicting transmembrane protein topology with a hidden Markov model: application to complete genomes. *J Mol Biol* 2001;305:567-580.

531. Claros MG, von Heijne G. TopPred II: an improved software for membrane protein structure predictions. *Comput Appl Biosci* 1994;10:685-686.
532. Zhang J, Timoney PJ, Maclachlan NJ, et al. Identification of an additional neutralization determinant of equine arteritis virus. *Virus Res* 2008;138:150-153.
533. Van Gorp H, Van Breedam W, Van Doorsselaere J, et al. Identification of the CD163 protein domains involved in infection of the porcine reproductive and respiratory syndrome virus. *J Virol* 2010;84:3101-3105.
534. Welch SK, Calvert JG. A brief review of CD163 and its role in PRRSV infection. *Virus Res* 2010;154:98-103.
535. Connolly SA, Jackson JO, Jardetzky TS, et al. Fusing structure and function: a structural view of the herpesvirus entry machinery. *Nat Rev Microbiol* 2011;9:369-381.
536. Liu N, Brown DT. Transient translocation of the cytoplasmic (endo) domain of a type I membrane glycoprotein into cellular membranes. *J Cell Biol* 1993;120:877-883.
537. Swameye I, Schaller H. Dual topology of the large envelope protein of duck hepatitis B virus: determinants preventing pre-S translocation and glycosylation. *J Virol* 1997;71:9434-9441.
538. Lambert C, Prange R. Dual topology of the hepatitis B virus large envelope protein: determinants influencing post-translational pre-S translocation. *J Biol Chem* 2001;276:22265-22272.

VITA

Zhengchun Lu

PERSONAL INFORMATION:

Date of Birth: Feburary 10, 1979 (Zhenjiang, People's Republic of China)

ACADEMIC DEGREES:

M.S., 2005 Leiden University Medical Center, Leiden Univeristy, Leiden, the Netherlands (Major in Biomedical Science)

M.D., 2002 School of Medicine, Jiangsu University, Zhenjiang, China

PROFESSIONAL EXPERIENCE:

2006 - 2012 Graduate Research Assistant, Department of Veterinary Science, Maxwell H. Gluck Equine Research Center, University of Kentucky

2003 - 2005 M.S. Research Assistant, Leiden University Medical Center Graduate Program of Biomedical Science, Leiden University, Leiden, the Netherlands. **Thesis Title: The role of non-structural proteins 2 and 3 in arterivirus replication complex formation**

2003 - 2002 Intern, Department of Internal Medicine, Affilicated Hospital of Jiangsu Univeristy, Zhenjiang, China

HONORS/AWARDS AND FELLOWSHIPS:

1. Trainee Travel Award, the American Association of Veterinary Laboratory Diagnosticians, 2009, San Diego, CA, USA
3. Conference/Research Student Support Funding, the Graduate School, University of Kentucky (2007, 2009)
4. Geoffrey C. Hughes Foundation Fellowship, University of Kentucky (2006-Present)
5. Graduate Study Scholarships, Chinese Scholarship Council, Beijing, China (2003-2005)
6. Merit Scholarships, Jiangsu University, Zhenjiang, China (1997-2002)

PEER-REVIEWED PUBLICATIONS:

1. *__Lu Z.,__ Branscum A., Shuck KM., Zhang J., Dubovi E., Timoney PJ., and Balasuriya UBR. Comparison of 2 real-Time RT-PCR assays for the detection of equine arteritis virus nucleic acid in equine semen and tissue culture fluid. J Vet Diagn Invest. 2008 Mar;20(2):147-55.

2. Posthuma CC., Pedersen KW., __Lu Z.,__ Joosten RG., Roos N., Zevenhoven-Dobbe JC., and Snijder EJ. Formation of the arterivirus replication/transcription complex: a key role for nonstructural protein 3 in the remodeling of intracellular membranes. J Virol. 2008 May;82(9):4480-91.

3. *Lu Z., Chambers TM., Boliar, S., Branscum, AJ., Timoney PJ., Dubovi EJ., Reedy SE., Tudor L., Sells S., Vickers ML., and Balasuriya UBR. Development and evaluation of one-step TaqMan® real-time reverse transcription-PCR assays targeting NP, M and HA genes of equine influenza virus. J Clin Microbiol. 2009 Dec;47(12):3907-13.

4. Zhang J., Timoney PJ., Shuck KM., Powell DG., Seoul G, Go YY., Lu Z., Meade BJ., and Balasuriya UBR. Molecular Epidemiology and Genetic Characterization of Equine Arteritis Virus Isolates Associated with the 2006/2007 Multi-State Disease Occurrence in the USA. J Gen Virol. 2010 Sep;91(Pt 9):2286-301.

5. *Lu Z., Dubovi EJ., Zylich N., Crawford PC., Sells S., Go YY., Loynachan AT., Timoney PJ., Chambers TM., and Balasuriya UBR. Diagnostic application of H3N8 specific equine influenza real-time RT-PCR assays for the detection of canine influenza virus in clinical specimens. J Vet Diagn Invest. 2010 Nov;22(6):942-5.

6. Summers A., Go YY., Lu Z., Timoney PJ., McCue PM., Zhang J., Shuck KM., and Bruemmer J. Response of stallions to primary immunization with a modified live equine viral arteritis vaccine. J Equine Vet Sci. 2011 Mar;31(3):129-38.

7. Miszczak F., Shuck KM., Lu Z., Go YY., Zhang J., Sells S., Vabret A., Pronost S., Fortier G., Timoney PJ., and Balasuriya UBR. Evaluation of two magnetic-bead-based viral nucleic acid purification kits and three real-time reverse transcription-PCR reagent systems in two TaqMan assays for equine arteritis virus detection in semen. J Clin Microbiol. 2011 Oct;49(10):3694-6.

8. Smith K., Li Y., Breheny P., Cook RF., Henney P., Sells S., Pronost S., Lu Z., Crossley B., Timoney P., Balasuriya UBR. A New Allelic Discrimination Real-Time PCR Assay for Detection and Differentiation of A2254 and G2254 Strains of Equine Herpesvirus-1. J Clin Microbiol. 2012 (In press)

9. *Lu Z., Zhang J., Huang CM., Faaberg KS., Rowland RRR., Timoney PJ., and Balasuriya UBR. Chimeric viruses containing the ectodomains of GP5 and M proteins of porcine reproductive and respiratory syndrome do not change the cellular tropism of equine arteritis virus. 2012 (Submitted to Virology)

10. Zhang J., Go YY., Lu Z., Meade B., Timoney PJ., and Balasuriya UBR. Development and characterization of an infectious cDNA clone of the modified live virus vaccine strain of equine arteritis virus and its potential as a vaccine vector. 2012. (Submitted to Virology)

11. *Lu Z., White J., Timoney PJ., and Balasuriya UBR. Development of one-step TaqMan® real-time reverse transcription-PCR and conventional reverse transcription PCR assay for the detection of equine rhinitis A and B viruses. 2012 (Submitted to

BMC Veterinary Research)

**Publications from PhD dissertation research project*

PUBLICATIONS IN PREPARATION:

1. ***Lu Z.,** Zhang J., Timoney PJ., Heidner HW., Williams JC., and Balasuriya UBR. Conserved arginine residues in the E protein of equine arteritis virus may play a role in heparin binding. (in final preparation)

**Publications from PhD dissertation research project*

ABSTRACTS/PRESENTATIONS:

1. **Lu Z.**, Branscum A., Shuck KM., Zhang J., Dubovi E., Timoney PJ, and Balasuriya UBR. 2007. Comparison of 2 real-time RT-PCR assays for the detection of equine arteritis virus nucleic acid in equine semen and tissue culture fluid. *Annual Meeting of American Association of Veterinary Laboratoy Diagnosticians, Reno, NV.*

2. **Lu Z.**, Branscum A., Shuck KM., Zhang J., Dubovi E., Timoney PJ., and Balasuriya UBR**.** 2008. Comparison of two real-time reverse transcription polymerase chain reaction assays for the detection of equine arteritis virus nucleic acid in equine semen and tissue culture fluid. *XIth Nidovirus Symposium, University of Oxford, Oxford, United Kingdom.*

3. **Lu Z.**, Branscum A., Shuck KM., Zhang J., Dubovi E., Timoney PJ., and Balasuriya UBR**.** 2008. Comparison of two real-time reverse transcription polymerase chain reaction assays for the detection of equine arteritis virus nucleic acid in equine semen and tissue culture fluid. *Second International Workshop on Equine Viral Arteritis, Lexington, KY.*

4. Zhang J., Shuck KM., Seoul G., Go YY., **Lu Z.,** Meade BJ., Powell DG., Timoney PJ., and Balasuriya UBR. 2008. Molecular characterization of equine arteritis virus isolates associated with 2006/2007 multi-state disease occurrence in the USA. *Second International Workshop on Equine Viral Arteritis, Lexington, KY*

5. **Lu Z.,** Chambers TM., Boliar S., Branscum AJ., Timoney PJ., Dubovi E., Reedy SE., Tudor L., Sells S., Vickers ML., and Balasuriya UBR**.** 2009. Development and evaluation of one-step TaqMan® real-time reverse transcription-PCR assays targeting NP, M and HA genes of equine influenza virus. *Annual Meeting of American Association of Veterinary Laboratory Diagnosticians, October 8-14, 2009, San Diego, CA.*

6. **Lu Z.,** Timoney PJ., Heidner HW., Williams JC., Zhang J., and Balasuriya UBR. Heparin-dependent attachment of equine arteritis virus to equine endothelial cells. 2010. *The 9th International Symposium on Plus-strand RNA Virus, May 17-22, 2010, Atlanta, GA.*

7. Zhang J., Go YY., **Lu Z.,** Meade B., Timoney PJ., and Balasuriya UBR. Development and characterization of an infectious cDNA clone of the modified live virus vaccine strain of equine arteritis virus and its potential as a vaccine vector. 2010 *9th International Symposium on Plus-strand RNA Virus, May 17-22, 2010, Atlanta, GA.*

8. Miszczak F., **Lu Z.,** Shuck KM., Timoney PJ., Go YY., Zhang J., Sells SS., Branscum AJ., Legrand L., Vabret A., Pronost S., and Balasuriya UBR. 2010. Comparison of commercial nucleic acid purification and real-time RT-PCR amplification kits for the detection of equine arteritis virus in equine semen using two previously described one-step real-time RT-PCR assays**.** *1st Congress of the European Association of Veterinary Laboratory Diagnosticians, September 15-17, 2010, Lelystad, the Netherlands.*